

Pectin degradation by *Botrytis cinerea*:  
recognition of endo-polygalacturonases by an Arabidopsis  
receptor and utilization of D-galacturonic acid

Lisha Zhang

## **Thesis committee**

### **Promoter**

Prof. dr. ir. P.J.G.M. de Wit  
Professor of Phytopathology  
Wageningen University

### **Co-promoter**

Dr. J.A.L. van Kan  
Assistant professor, Laboratory of Phytopathology  
Wageningen University

### **Other members**

Prof. dr. ir. J. Bakker, Wageningen University  
Prof. dr. ing. J.J.B. Keurentjes, Wageningen University / University of  
Amsterdam  
Dr. A.F.J.M. van den Ackerveken, Utrecht University  
Dr. A.F.J. Ram, Leiden University

This research was conducted under the auspices of the Graduate School of  
Experimental Plant Sciences

Pectin degradation by *Botrytis cinerea*:  
recognition of endo-polygalacturonases by an Arabidopsis  
receptor and utilization of D-galacturonic acid

Lisha Zhang

**Thesis**

submitted in fulfilment of the requirements for the degree of doctor  
at Wageningen University  
by the authority of the Rector Magnificus  
Prof. dr. M.J. Kropff,  
in the presence of the  
Thesis Committee appointed by the Academic Board  
to be defended in public  
on Wednesday 5 June 2013  
at 1.30 p.m. in the Aula

Lisha Zhang

Pectin degradation by *Botrytis cinerea*: recognition of endopolygalacturonases by an Arabidopsis receptor and utilization of D-galacturonic acid, 192 pages

PhD thesis, Wageningen University, Wageningen, NL (2013)

With references, with summaries in English and Dutch

ISBN 978-94-6173-540-9

# Contents

<b>Chapter 1</b>	General introduction	7
<b>Chapter 2</b>	Fungal endo-polygalacturonases are recognized as MAMPs in Arabidopsis by the Receptor-Like Protein RBPG1	23
<b>Chapter 3</b>	The D-galacturonic acid catabolism in <i>Botrytis cinerea</i>	59
<b>Chapter 4</b>	<i>Botrytis cinerea</i> mutants deficient in D-galacturonic acid catabolism have a perturbed virulence on <i>Nicotiana benthamiana</i> and Arabidopsis, but not on tomato	83
<b>Chapter 5</b>	Functional analysis of putative D-galacturonic acid transporters in <i>Botrytis cinerea</i>	107
<b>Chapter 6</b>	Pectate-induced gene expression in <i>Botrytis cinerea</i> and the identification and functional analysis of cis-regulatory D-galacturonic acid responsive elements	129
<b>Chapter 7</b>	General discussion	161
	References	171
	Summary	181
	Samenvatting	183
	Acknowledgements	185
	Curriculum vitae	187
	Publications	188
	Education statement of the graduate school	189



# CHAPTER 1

## General introduction

Lisha Zhang

This chapter is published as part of:

Zhang, L., and van Kan, J.A.L. The contribution of cell wall degrading enzymes to virulence of fungal plant pathogen. In: Kempken, F. (Ed.), *The Mycota XI (2nd Edition), Agricultural Applications*. Springer-Verlag, Berlin, in press.



## Introduction

Many fungi feed in or on plant tissues, either as saprotrophs, endophytes, symbionts or as pathogens. Saprotrophs grow on dead plant tissue and participate in its biological decomposition and recycling. The other three types of fungi, however, proliferate in or on living plants and often have intricate interactions with their host. These fungi must in many cases actively pass the plant surface through the cuticle and/or the cell wall, which collectively form a physical and chemical barrier between the environment and the internal tissues of the plant. Cell walls not only provide plant tissues strength and structure, but also protect against microbial invasion. Plants therefore invest substantial resources in constructing the cell wall and maintaining its integrity. Cell wall material makes up 50-80% of the total plant dry weight, and the vast majority of cell wall polymers consist of carbohydrates. The large amount of carbon deposited in cell walls on the other hand offers opportunities for fungi to utilise plant cell walls as a nutrient resource. Regardless of their trophic lifestyle in an ecosystem (saprotrophic, endophytic, symbiotic or pathogenic), many fungi indeed have the genetic potential to grow on plant cell wall carbohydrates as a saprotroph (Aro et al., 2005). There are only very few fungi which are known to have an extremely small number of genes encoding carbohydrate-degrading enzymes, including the biotroph *Ustilago maydis* and the obligate powdery mildew pathogen *Blumeria graminis* (Kämper et al., 2006; Spanu et al., 2010).

This chapter discusses the chemical structures of plant cell wall polysaccharides, the cell wall-associated resistance mechanisms that plants display against pathogens, and the microbial enzymes that are involved in cell wall decomposition. I will subsequently focus on the plant cell wall degrading enzymes of pathogenic fungi, and illustrate with case studies how the grey mould *Botrytis cinerea* decomposes pectins deposited in plant cell walls. Finally, I will present an outline of the research described in this thesis.

## Structure of plant cell walls

Plant cell walls are highly dynamic in chemistry and architecture. Their structure and composition vary between plant species and depend on the type of cell they surround, the stage of differentiation of the cell and the developmental stage of the plant itself. Plant cell walls consist mainly of polysaccharides which, together with lignin and proteins, form a complex 3-dimensional network. The main components of plant cell wall polysaccharides are cellulose, hemicellulose and pectin. Cellulose accounts for 20-30% of the dry mass of most primary cell walls. It consists of  $\beta$ -1,4-linked D-glucose residues that form unbranched polymeric chains, which are associated by strong hydrogen bonds into

crystalline cellulose microfibrils (Nishiyama et al., 2002). Cellulose microfibrils interact with hemicelluloses by hydrogen bonds and the cellulose-hemicellulose complex is physically entangled with pectins (Cosgrove, 2001). Both hemicellulose and pectin are branched polysaccharides of varying composition.

Hemicelluloses are relatively complex polysaccharides, which have  $\beta$ -1,4-linked backbones with an equatorial configuration, including xyloglucans, xylans, mannans and glucomannans, and  $\beta$ -(1,3;1,4)-glucans. Xyloglucan is present both in dicot and monocot cell walls, but it is more abundant in the walls of dicots (~20%) than in those of monocots (~2%). Xyloglucan consists of  $\beta$ -1,4-linked D-glucose residues, where D-xylose is  $\alpha$ -1,6-linked to D-glucose chains and can be substituted at O-2 with  $\beta$ -D-galactose or  $\alpha$ -L-arabinose. Xylans constitute the major hemicellulose in the primary cell walls of monocots. They are a diverse group of polysaccharides with a backbone of  $\beta$ -1,4-linked xylose residues, which can be substituted with  $\alpha$ -1,2-linked glucuronosyl and 4-O-methyl glucuronosyl residues. Acetylation of xylose residues may occur at the O-2 and/or O-3 positions. The backbone of mannans consists of  $\beta$ -1,4-linked D-mannose residues, whereas the backbone of glucomannans consists of glucose and mannose in a non-alternating pattern.  $\beta$ -1,3;1,4-glucans consist of  $\beta$ -1,4-glucans with interspersed single  $\beta$ -1,3-linkages (Caffall and Mohnen, 2009; Scheller and Ulvskov, 2010).

Pectins are the structurally most complex polysaccharides in nature. Pectin is the collective name for a series of polymers that are rich in D-galacturonic acid, including homogalacturonan (HG), rhamnogalacturonan I (RGI), rhamnogalacturonan II (RGII), and xylogalacturonan (XGA) (Figure 1A). The most abundant type of pectin is HG, which comprises over 60% of total pectin in plant cell walls. HG is a linear polymer of  $\alpha$ -1,4-linked D-galacturonic acid, which can be modified to different degrees by methyl-esterification at the C-6 carboxyl group and acetylation at O-2 or O-3. RGI, making up 20~35% of pectin, has a different backbone, which consists of repeating units of  $\alpha$ -1,4-D-galacturonic acid- $\alpha$ -1,2-L-rhamnose. The L-rhamnose residues in the backbone can be modified with side chains consisting of  $\beta$ -1,4-galactan, branched arabinan, and/or arabinogalactan. The structure of the side chains of RGI greatly varies among plants. RGII consists of an HG backbone, which can be substituted at O-2 or O-3 with different side chains. These side chains are composed of 12 different types of sugars in over 20 different linkages. Although RGII is the most structurally complex pectin, its structure is remarkably conserved among vascular plants. XGA also consists of an HG backbone, which can be substituted at O-3 with  $\beta$ -1,4-linked xylose residues (Caffall and Mohnen, 2009; Mohnen, 2008).

Currently, there are two models that describe how pectic polysaccharides are linked: the ‘smooth and hairy region’ model and the ‘rhamnogalacturonan backbone’ model (Figure 1B). In the first model, pectin is composed of hairy regions, consisting of RGI decorated with neutral sugar side chains, which are interspersed with smooth regions of HG. The second model describes HG as a side chain of RGI, similar to the neutral sugar side chains (Schols et al., 2009).

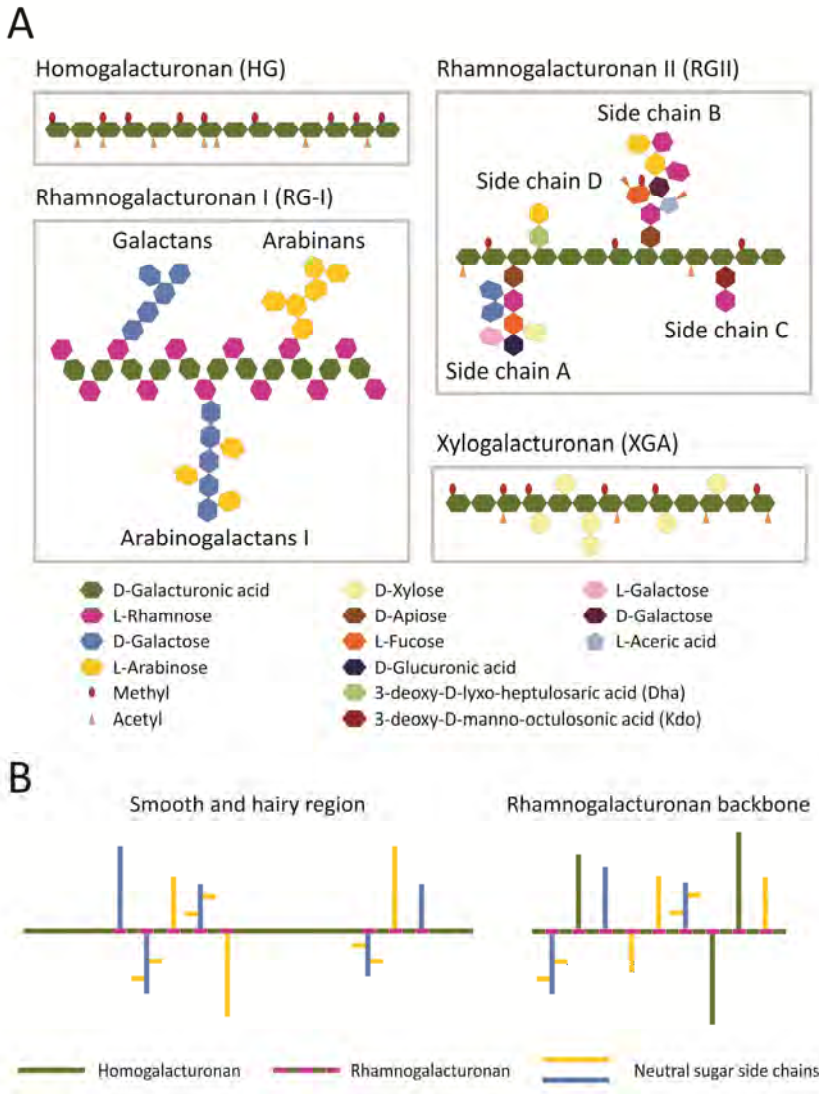


**Figure 1.** Schematic structure of pectin components in plant cell walls (A), adapted from Mohnen (2008); and two alternative models for the organization of the pectin network (B), adapted from Schols et al. (2009).

## Cell wall-associated resistance to plant pathogens

Plants protect their cell walls from penetration by pathogens in several ways: (i) inhibition of plant cell wall-degrading enzymes; (ii) remodelling of cell walls at the site of attempted penetration; (iii) perception of cell wall-derived molecules (damage-associated molecular patterns) followed by triggering of an immune response. I will focus on the first two aspects.

### A. Inhibition of cell wall degrading enzymes

Polygalacturonase-inhibiting proteins (PGIPs) are extracellular leucine-rich repeat (eLRR) proteins that physically interact with, and thereby inhibit, polygalacturonases (PGs) produced by fungi, bacteria and even insects (De Lorenzo et al., 2001; Federici et al., 2006; Juge, 2006). Secreted PGs are important virulence factors in several fungal pathogens, including *Aspergillus flavus* (Shieh et al., 1997), *Botrytis cinerea* (ten Have et al., 1998), *Alternaria citri* (Isshiki et al., 2001), and *Claviceps purpurea* (Oeser et al., 2002). Fungal PGs are able to decompose pectin and thus cause cell wall degradation and tissue maceration (see below). PGIPs are widely distributed in the plant kingdom, such as apple, bean, grape, pepper, raspberry, soybean, tomato, leek, and *Arabidopsis thaliana* (De Lorenzo et al., 2001). The potential of PGIPs to limit host tissue colonization by fungi was shown using overexpression and gene silencing. Specifically, the overexpression of a pear *PGIP* in tomato or grape plants, of bean *PvPGIP2* in tobacco, and of *AtPGIP1* and *AtPGIP2* in *A. thaliana* reduced *B. cinerea* infection (Aguero et al., 2005; Ferrari et al., 2003b; Powell et al., 2000). *A. thaliana* plants in which the *AtPGIP1* gene was silenced showed reduced PGIP accumulation and enhanced susceptibility to *B. cinerea* (Ferrari et al., 2006). Furthermore, overexpression of *Phaseolus vulgaris PvPGIP2* in wheat reduced the symptoms caused by *Fusarium moniliforme* and *Bipolaris sorokiniana* infection (Janni et al., 2008; Manfredini et al., 2005).

PGIPs are encoded by small gene families. The isoforms within a single plant species may exhibit differential *in vitro* inhibitory activities towards PGs from different fungi. The activity of several PGIP isoforms from bean and *A. thaliana* was tested *in vitro* towards PGs from saprotrophic and plant pathogenic fungi (Ferrari et al., 2003b), leading to hypotheses about differential inhibition and specificity in PG-PGIP interactions (Federici et al., 2006). It should however be noted that the *in vitro* interaction between PGs and PGIPs may not be representative for the situation *in planta*. Joubert et al. (2007) reported that the grapevine protein *VvPGIP1* was able to inhibit the activity of *B. cinerea* *BcPG2* *in planta*, even though the two proteins were not able to interact *in vitro*. Thus the failure of a given PGIP to inhibit a particular PG *in vitro* may not be informative about the potential

of this PGIP to interact with the PG *in planta* and thereby confer (partial) disease resistance.

Besides inhibitors of PGs, plants can also produce inhibitors of pectin methylesterases (PMEIs). The inhibition of PME activity results in a markedly higher degree of methylation of pectin, which impacts on cell wall properties and tissue texture (Jolie et al., 2010). Overexpression of a PMEI gene from kiwifruit in wheat was shown to increase resistance to fungal pathogens (Volpi et al., 2011). There is, however, an important conceptual difference between PGIPs and PMEIs. PGIPs only inhibit PGs of microbes and insects that attack the plant, but fail to inhibit endogenous plant PGs. On the contrary, PMEIs are active only against endogenous plant PMEs and presumably inactive against non-plant PMEs (Jolie et al., 2010).

### **B. Remodelling of cell walls at the site of attempted penetration**

Callose, the major constituent of papillae, is an important factor contributing to the resistance of plants against penetration and invasion by pathogenic fungi. Callose is present at low levels throughout a plant, especially in the sieve plates of phloem cells and in plasmodesmata. In response to biotic stress, plant cells rapidly synthesize callose in the vicinity of the site of pathogen penetration (Adie et al., 2007; Flors et al., 2008; Garcia-Andrade et al., 2011; Jacobs et al., 2003; Nishimura et al., 2003). The *A. thaliana* callose synthase GSL5/PMR4 is required for pathogen-induced callose deposition (Jacobs et al., 2003; Nishimura et al., 2003). *gsl5/pmr4* mutant plants lack callose and show enhanced susceptibility to the necrotrophic pathogens *Alternaria brassicicola*, *Plectosphaerella cucumerina* and *Pythium irregulare* (Adie et al., 2007; Flors et al., 2008; Garcia-Andrade et al., 2011). By contrast, *gsl5/pmr4* mutant plants show increased resistance to biotrophic pathogens *Erysiphe cichoracearum*, *Golovinomyces orontii* and *Hyaloperonospora parasitica*, due to a hyperstimulation of salicylic acid-dependent defence pathways, which remains to be understood (Jacobs et al., 2003; Nishimura et al., 2003).

Reactive oxygen species (ROS) are well known as signal molecules triggering plant defence response (Lamb and Dixon, 1997). H<sub>2</sub>O<sub>2</sub> is required for peroxidase-dependent lignification and for protein cross-linking in the cell wall (Hückelhoven, 2007). Rapid oxidative cross-linking of proline-rich proteins in the cell wall strengthens the wall, and thereby makes it more resistant to cell wall degrading enzymes (Jacobs et al., 2003; Nishimura et al., 2003).

## **Plant cell wall polysaccharide degradation**

The plant cuticle and cell wall are the first barriers to pathogen invasion. Fungal plant pathogens secrete a series of enzymes to decompose plant cell wall polysaccharides in order to facilitate the penetration, the subsequent maceration and the acquisition of carbon from decomposed plant tissues. Generally, these polysaccharide degrading enzymes can be divided into two classes: exo-acting enzymes and endo-acting enzymes. Exo-acting enzymes can be specific for the reducing end or the non-reducing end of polysaccharides. They release monomeric or dimeric glycosyl moieties during each catalytic event, providing the fungus with low molecular mass compounds that can be easily taken up. Endo-acting enzymes cleave polysaccharides randomly within the chain, resulting in a rapid decrease in the average chain length. The cleavage products, however, are generally too large to serve as nutrients for the fungus. It is commonly observed that any particular polysaccharide is degraded by a combination of endo-acting and exo-acting enzymes, acting synergistically on the substrate. The plant cell wall degrading enzymes that are secreted by fungi are all carbohydrate-active enzymes (Cantarel et al., 2009). Fungal cellulases, hemicellulases and pectinases can be assigned to CAZy families of glycoside hydrolases (GH), carbohydrate esterases (CE), and polysaccharide lyases (PL).

### **A. Cellulose degradation**

Three classes of enzymes, all belonging to GH families 6 and 7, are involved in cellulose degradation:  $\beta$ -1,4-endoglucanases, cellobiohydrolases and  $\beta$ -glucosidases. The  $\beta$ -1,4-endoglucanases hydrolyse the internal bonds to disrupt the crystalline cellulose microfibrils and expose individual cellulose polysaccharide chains. Cellobiohydrolases cleave two glucose units from the ends of the exposed chains, resulting in the release of the disaccharide cellobiose, which is subsequently hydrolysed by  $\beta$ -glucosidases into individual D-glucose monomers.

### **B. Hemicellulose degradation**

Hemicellulose consists of a group of relatively complex branched polysaccharides. The various backbones of hemicelluloses are hydrolysed by the corresponding set of GH family enzymes. Specifically, xyloglucan is decomposed by a combination of  $\beta$ -1,4-endoglucanases and  $\beta$ -glucosidases; xylan is decomposed by a combination of  $\beta$ -1,4-endoxylnases and  $\beta$ -xylosidases; mannan and galactomannan are decomposed by a combination of  $\beta$ -1,4-endomannanases and  $\beta$ -mannosidases. Various side chains of hemicelluloses are cleaved by different enzymes, which belong to GH and CE families. For example, the  $\alpha$ -linked D-xylose, D-galactose, D-glucuronic acid and L-arabinose residues are cleaved by  $\alpha$ -xylosidases,  $\alpha$ -galactosidases,  $\alpha$ -glucuronidases or  $\alpha$ -

arabinofuranosidases, respectively, whereas acetyl residues are cleaved by acetyl xylan esterases.

### **C. Pectin degradation**

Two types of backbones are present in pectin: the backbone of HG (smooth region) consisting of  $\alpha$ -1,4-linked D-galacturonic acid, and the backbone of RGI (hairy region) consisting of alternating  $\alpha$ -1,4 linked D-galacturonic acid and  $\alpha$ -1,2-linked rhamnose residues. Enzymes involved in degradation of the pectin backbone belong to the GH28 and PL1 and PL3 families. Smooth regions can be hydrolysed by endo-polygalacturonases (endo-PGs), exo-polygalacturonases (exo-PGs), pectin lyases and pectate lyases. Endo-PGs hydrolyse the (preferentially unmethylated) backbone of HG, releasing monomeric and/or oligomeric galacturonosyl fragments, whereas exo-PGs exclusively cleave at the non-reducing end of HG strands, thereby releasing D-galacturonic acid monomers. Pectin lyases and pectate lyases both cleave alternating  $\alpha$ -1,4 linked D-galacturonic acid linkages via  $\beta$ -elimination, resulting in a novel reducing end. Pectin lyases prefer substrates with a high degree of methylesterification, whereas pectate lyases prefer substrates with a low degree of methylesterification and require  $\text{Ca}^{2+}$ -ions for catalysis. The hairy regions of RGI can be hydrolysed by rhamnogalacturonan hydrolases and rhamnogalacturonan lyases, of which the former enzymes specifically cleave non-esterified galacturonosyl-rhamnosyl linkages.

Various substituents occur on the backbone of pectins, therefore diverse enzymes are involved in pectin side chain decomposition. Some of these enzymes cleave the entire side chains from the backbone, whereas others cleave the internal or terminal linkages of side chains. In addition, some of the enzymes not only act on pectin side chains, but also on hemicelluloses. Specifically,  $\alpha$ -arabinofuranosidases release L-arabinose, both from xylan, arabinoxylan and from side chains of rhamnogalacturonan; endo/exo-arabinanases hydrolyse  $\alpha$ -1,5 linked arabinose residues from the arabinan side chains of pectins;  $\beta$ -galactosidases release terminal D-galactose residues from the galactan side chains of pectins;  $\beta$ -xylosidases can hydrolyse  $\beta$ -1,4-linked xylose residues, both from xyloglucan and from side chains of xylogalacturonan. Finally, pectin acetylsterases and pectin methylesterases remove the acetyl and methyl residues, which are present in the smooth regions of pectins.

## **Cell wall degrading enzymes in plant pathogenic fungi: a case study of *Botrytis cinerea***

### **A. CAZymes in genomes of plant pathogenic fungi**

The number of genome sequences of fungi that have been released has rapidly grown in recent years (Martin et al., 2011). This provides opportunities to examine the repertoire of plant cell wall degrading enzymes secreted by plant pathogenic fungi and explore correlations between the CAZyme content in the genome, the CAZyme distribution over different enzyme families (GH, CE, PL) and the host range of the fungal pathogen.

Plant pathogens with different lifestyles appear to have different repertoires of the CAZymes that are involved in degrading plant cell walls. Necrotrophs and hemi-biotrophs (in the necrotrophic infection phase) secrete large amounts of cell wall degrading enzymes for host tissue decomposition and nutrient acquisition. The genomes of two closely related necrotrophs, *Botrytis cinerea* and *Sclerotinia sclerotiorum*, encode respectively 118 and 106 CAZymes associated with plant cell wall degradation (Amselem et al., 2011). These numbers are very similar to that in the saprotroph *Aspergillus niger*, but are lower than in other necrotrophs (*Phaeosphaeria nodorum* and *Pyrenophora teres f. teres*) and in the hemi-biotrophs *Fusarium graminearum* and *Magnaporthe oryzae* (Amselem et al., 2011). By contrast, many biotrophic pathogens and symbionts have a markedly lower content of CAZymes for cell wall degradation in their genome (Baxter et al., 2010; Duplessis et al., 2011; Martin et al., 2010), presumably to reduce the damage to the host and avoid the plant defence responses triggered by the release of cell wall fragments. The most extreme examples to date are the genomes of *Blumeria graminis* and *Ustilago maydis*, which contain only 10 and 33 genes encoding plant cell wall degrading enzymes (Amselem et al., 2011; Kämper et al., 2006; Spanu et al., 2010).

Plant pathogens with distinct host preference seem to use different approaches to decompose plant tissues. CAZyme analyses show that not only the contents, but also the distribution of CAZymes differ among plant pathogens. *B. cinerea* and *S. sclerotiorum* can both infect a wide range of dicot host plants, and prefer to infect soft plant tissues that are rich in pectin, such as flowers and fruits. This is reflected by the observation that both fungi grow better (*in vitro*) on pectic substrates than on xylan and cellulose. Their genomes contain larger proportions of CAZymes involved in decomposition of pectin (37% and 31%) and lower amounts of CAZymes involved in decomposition of cellulose (18% and 20%) and hemicellulose (40% and 41%). On the contrary, *P. nodorum*, *P. teres f. teres* and *M. oryzae* are pathogens of wheat, barley, and rice, which all belong to commelinoid monocots that contain less pectin in the cell wall. CAZyme analyses show that their

genomes contain smaller proportions of CAZymes involved in decomposition of pectin (18%, 17%, and 12%) and noticeably higher amounts of CAZymes involved in decomposition of cellulose (47%, 38%, and 37%) and hemicellulose (66%, 55%, and 68%), as compared to *B. cinerea* and *S. sclerotiorum* (Amselem et al., 2011).

## **B. Secretomes of plant pathogenic fungi**

Releasing nutrients from plant cell wall polysaccharides requires the secretion of an arsenal of plant cell wall degrading enzymes that act in synergy to decompose this complex structure. In culture filtrates of *Fusarium graminearum*, grown in medium containing hop cell wall material as sole carbon source, 17 different GH activities were detected, which could collectively hydrolyse crude plant material, with monosaccharide yields approaching 50% of the total sugars released by acid hydrolysis (Phalip et al., 2009).

Proteomics techniques are increasingly applied to study the secretomes of fungal pathogens, either *in vitro*, or during their interaction with plants. Besides being useful for annotating genomes, secretome analyses may enable to identify pathogen effectors (reviewed by (Koeck et al., 2011)) as well as (abundant) plant cell wall degrading enzymes. The latter information may provide leads to unravel the mechanisms that fungal pathogens utilise to decompose plant cell wall polysaccharides and acquire nutrients from their host. Several studies, including those in *B. cinerea* discussed below in detail, have revealed that plant cell wall degrading enzymes are abundant in fungal secretomes. In *S. sclerotiorum* culture filtrates, 18 secreted proteins were identified and 9 of them were plant cell wall degrading enzymes (Yajima and Kav, 2006). Studies on *F. graminearum* grown in medium containing various polysaccharide supplements, or in medium containing wheat or barley flour, resulted in the identification of 120 and 69 proteins, in which glycoside hydrolases represented approximately 25% of all identified proteins (Paper et al., 2007; Yang et al., 2011). In *M. oryzae*, 85 proteins were identified and 19 of them were annotated as plant cell wall hydrolases (Wang et al., 2011).

The secretome of *B. cinerea* has been analysed in different culture conditions (Espino et al., 2010; Fernandez-Acero et al., 2010; Shah et al., 2009a; Shah et al., 2009b). One study aimed to compare proteins secreted upon culturing *B. cinerea* in the presence of extracts of red tomato, ripe strawberry and *A. thaliana* leaves. Overall, 89 *B. cinerea* proteins were identified by LC-MS/MS, of which 60 contained a signal peptide in the (predicted) protein sequence. 30 of these 60 proteins are involved in carbohydrate metabolism and transport, and these proteins were more abundant in cultures grown in the presence of tomato and strawberry extract, as compared to cultures containing *A. thaliana* leaf extract (Shah et al., 2009a). The second study aimed to compare *B. cinerea* proteins induced by pectins with different degrees of methyl esterification. A total of 126 secreted proteins were identified

in cultures containing highly or partially esterified pectin, or sucrose. The abundance of proteins with functions in pectin degradation was similar in both pectin containing media, but higher as compared to sucrose containing medium (Shah et al., 2009b). In a similar study, proteins were sampled from *B. cinerea* cultures grown in presence of either glucose, starch, cellulose, pectin or tomato cell walls and submitted to two-dimensional gel electrophoresis. 57 unique proteins were identified, of which more than 50% are involved in plant cell wall polysaccharide decomposition (Fernandez-Acero et al., 2010). Finally, Espino et al. (2010) focused on the early secretome of *B. cinerea* because the early stages of development *in planta* are crucial in establishment of a successful infection. Conidia were inoculated in minimal medium, supplemented with extracts of tomato, strawberry or kiwifruit, and proteins were sampled after 16 h. A total of 105 proteins were identified, of which 36 are involved in plant cell wall polysaccharide degradation; proteins involved in pectin degradation were highly abundant (Espino et al., 2010). The lists of proteins identified in these studies show substantial overlap, as the methodology used was often comparable. Other culture methods, more sensitive protein identification methods and more reliable gene models will be required to generate a more comprehensive list of proteins identified as being secreted by *B. cinerea*.

### **The contribution of cell wall degrading enzymes to virulence of *Botrytis cinerea***

*Botrytis cinerea* is able to infect over 200 host plant species and different tissue types: stems, leaves, flowers and fruit. The pathogen can cause a variety of symptoms ranging from dry, necrotic areas to water-soaked, fully macerated lesions. The ability to cause disease on such different tissues and plant species suggests that *B. cinerea* has a large weaponry to kill and invade its hosts (Choquer et al., 2007). The ultimate purpose of a necrotrophic pathogen is not to kill its host, but to decompose the plant tissue and utilize host-derived nutrients for its own growth. As discussed above, *B. cinerea* secretes a spectrum of cell wall decomposing enzymes (including pectinases, cellulases, and hemicellulases) to facilitate plant tissue colonization and release carbohydrates for consumption (van Kan, 2006; Williamson et al., 2007).

#### **A. Pectinases**

*B. cinerea* often penetrates host leaf tissue at the anticlinal cell wall and subsequently grows into and through the middle lamella, which consists mostly of low-methylesterified pectin. Effective pectin degradation thus is important for virulence of *B. cinerea*. Several pectinases have been found to be abundant during host infection, including pectin and

pectate lyases, pectin methylesterases (PMEs), exo-polygalacturonases (exo-PGs), and endo-polygalacturonases (endo-PGs) (Cabanne and Doneche, 2002; Kars et al., 2005b; Kars and van Kan, 2004; Rha et al., 2001; ten Have et al., 2001). Especially the roles of endo-PGs and PMEs in virulence have been intensively investigated.

### **1. Endo-polygalacturonases**

The *B. cinerea* genome contains six genes encoding endo-PGs (Wubben et al., 1999). All gene family members are differentially expressed *in vitro* and *in planta* (ten Have et al., 2001; Wubben et al., 2000). Four regulatory mechanisms were proposed based on *in vitro* analysis: basal, constitutive expression was observed for *Bcpg1*; expression of *Bcpg3* was induced by low ambient pH, irrespective of the carbon source present; expression of *Bcpg4* and *Bcpg6* was induced by D-galacturonic acid; catabolite repression by glucose was observed for *Bcpg4* only. Other monosaccharides present in cell wall polymers, such as rhamnose, arabinose, and galactose did not notably regulate the expression of *Bcpg* genes. Regulation of the expression of *Bcpg2* and *Bcpg5* remained unclear (Wubben et al., 2000).

Altogether this endo-PG gene family equips the fungus with a flexible pectin degrading machinery, which provides a potential advantage for a fungus with such a broad range of hosts and tissue types. All gene family members display various expression patterns during infection, depending on the stage of infection and on the host (ten Have et al., 2001).

The endo-PG family members not only display diversity in their expression patterns but also in enzymatic characteristics. Five BcPGs were produced in *Pichia pastoris* and their biochemical properties were analysed (Kars et al., 2005a). All enzymes display optimal activity at low ambient pH, which is consistent with the acidification of the environment during the early stages of colonization by *B. cinerea* (Billon-Grand et al., 2012; Verhoeff et al., 1988). BcPG1, BcPG2 and BcPG4 prefer the non-methylesterified substrate polygalacturonic acid (PGA) to pectin, however, they show differences in substrate affinities and hydrolysis rates. BcPG3 and BcPG6 were shown to behave as processive endo-hydrolases, releasing monomers of D-galacturonate instead of oligomers (Kars et al., 2005a).

The function of endo-PG gene family members in virulence has been studied by deleting each single gene in *B. cinerea*. Knockout mutants  $\Delta Bcpg1$  and  $\Delta Bcpg2$  were reduced in virulence by 25% and > 50%, respectively (Kars et al., 2005a; ten Have et al., 1998).

### **2. Pectin methylesterases**

The degree of methylation (DM) of pectin in plant cell walls can range from 13% to approximately 80% (Voragen et al., 1986). Pectin methylesterases (PMEs) catalyse the

hydrolysis of methyl esters, releasing methanol and pectate. Pectate is a preferred substrate for many of the BcPGs (Kars et al., 2005b). This predicts that PME s are important for virulence on plant tissues with high DM pectin (such as in leaves), but not on tissues with low DM pectin (such as in fruit). However, the role of PME s in virulence of *B. cinerea* is controversial. The phenotype of a *Bcpme1* knockout mutant in one strain of *B. cinerea* supported this hypothesis (Valette-Collet et al., 2003). However, results in a different strain with single and double knockout mutants in two *Bcpme* genes, including the same *Bcpme1* gene, did not support this hypothesis (Kars et al., 2005b). In addition, the *Bcpme* mutants and the wild-type strain displayed better growth on 75% methylesterified pectin than on non-methylesterified polygalacturonic acid, suggesting that pectin de-methylation by PME s is not important for depolymerisation *in vivo* (Kars et al., 2005b). The profuse growth of *B. cinerea* on high DM pectin suggests that the biochemical properties of endo-PGs determined *in vitro* may not reflect their behaviour *in vivo*, or that accessory enzymes participate in the pectin degradation mediated by endo-PGs.

### **B. Other cell wall degrading enzymes**

Other cell wall degrading enzymes produced by *B. cinerea*, such as cellulases and hemicellulases, have also been studied. Deletion of a cellulase gene *Bcce15A*, encoding an endo- $\beta$ -1,4-glucanase, did not affect virulence (Espino et al., 2005), whereas the deletion of a hemicellulase gene *Bcxyn11A*, encoding an endo-  $\beta$ -1,4-xylanase, delayed lesion formation and reduced lesion size by more than 70% (Brito et al., 2006). The contribution of the *Bcxyn11A* gene in virulence was, however, not dependent on xylanase enzyme activity, but rather required the necrosis-inducing elicitor activity of the xylanase protein (Noda et al., 2010).

## Outline of the thesis

Pectin degradation plays an important role in the virulence of *Botrytis cinerea*. The aims of this thesis were on the one hand, to characterize a genetic locus in *Arabidopsis thaliana* that controls a necrotic response upon infiltration with BcPGs, and on the other hand, to unravel whether the role of BcPGs in virulence (Kars et al., 2005a; ten Have et al., 1998) relates only to a function in tissue disintegration and colonization, or also to a function in the release of an abundant source of monosaccharide (i.e. D-galacturonic acid) nutrients from pectic polymers. At the onset of this PhD thesis research, nothing was known about the pathways that *B. cinerea* exploits to utilize D-galacturonic acid released from pectic polymers.

**Chapter 2** describes a study on the natural genetic variation in responsiveness of *A. thaliana* to treatment with BcPG proteins. Among the many accessions tested, accession Col-0 was responsive to BcPGs (resulting in a necrotic response to protein infiltration), whereas accession Br-0 was unresponsive to BcPGs. A map-based cloning approach, in combination with functional genomics and comparative genomics strategies, revealed that the gene *RBPG1*, encoding a Receptor-Like Protein, determines the responsiveness to BcPGs in Col-0. Furthermore, chapter 2 describes that several fungal endo-PGs act as MAMPs and their recognition involves the formation of a complex with the receptor protein RBPG1 and the subsequent signal transduction leading to a necrotic response is mediated by the Receptor-Like Kinase SOBIR1.

**Chapter 3** describes the functional genetic and biochemical characterization of the D-galacturonic acid catabolic pathway in *B. cinerea*. The enzymatic activity of recombinant proteins was characterized, and the function of the genes in *B. cinerea* was studied by generating single and double knockout mutants and testing the mutants *in vitro* and *in planta*. In **Chapter 4**, the virulence of D-galacturonic acid catabolism-deficient mutants was further investigated on *Solanum lycopersicum*, *Nicotiana benthamiana* and *A. thaliana*. The mutants displayed a reduced virulence on *N. benthamiana* and *A. thaliana*. This phenotype was not only due to the inability of the mutants to utilize D-galacturonic acid as nutrient, but also due to the growth inhibition by catabolic intermediates.

**Chapter 5** describes the functional genetic characterization and cellular location of two putative D-galacturonic acid transporters in *B. cinerea*. **Chapter 6** describes an RNA sequencing study, performed to compare genome-wide transcriptional profiles in *B. cinerea* grown in media containing glucose and pectate as sole carbon sources. Conserved sequence motifs were identified in the promoters of genes involved in pectate decomposition and D-galacturonic acid utilization. The role of these motifs in regulating D-galacturonic acid-induced expression was functionally analysed.

**Chapter 7** presents a general discussion of the results in **Chapters 2-6** and puts them in a broader perspective. A model is proposed for the ways in which *B. cinerea* degrades pectin and subsequently consumes the released D-galacturonic acid, and for the co-regulation of genes involved in this process.

# CHAPTER 2

Fungal endo-polygalacturonases are recognized as MAMPs in Arabidopsis by the Receptor-Like Protein RBPG1

Lisha Zhang, Ilona Kars, Lia Wagemakers, Thomas W. H. Liebrand, Panagiota Tagkalaki, Devlin Tjoitang, Bert Essenstam, Joyce Elberse, Guido van den Ackerveken, Jan A. L. van Kan

## Abstract

Plants perceive microbial invaders using pattern recognition receptors (PRRs) that recognize microbe-associated molecular patterns (MAMPs). Two well-characterised MAMP receptors are the leucine-rich repeat receptor-like kinases (LRR-RLKs) FLS2 and EFR that recognize bacterial flagellin and translation elongation factor EF-Tu, respectively. In this study, we identified RBPG1, an *Arabidopsis thaliana* LRR receptor-like protein (LRR-RLP) that recognizes fungal endo-polygalacturonases (endo-PGs) and thus acts as a novel MAMP receptor. RBPG1 in particular recognizes the *Botrytis cinerea* BcPG3 protein. Infiltration of the BcPG3 protein into *A. thaliana* accession Col-0 induced a necrotic response, whereas accession Br-0 showed no symptoms. Heat-inactivated protein and a catalytically inactive mutant protein retained the ability to induce necrosis. An 11-amino acid peptide stretch was identified that is conserved among many fungal but not plant endo-PGs. A synthetic peptide comprising this sequence was unable to induce necrosis. A map-based cloning strategy, combined with comparative and functional genomics, led to the identification of the RBPG1 gene, and showed that this gene is essential for responsiveness of *A. thaliana* to the BcPG3 protein. Co-immunoprecipitation experiments demonstrated that RBPG1 and BcPG3 form a complex in *Nicotiana benthamiana*, which also involves the *A. thaliana* LRR-RLK SOBIR1. The *sobir1* mutant plants were unresponsive to BcPG3. Although transformation of RBPG1 in accession Br-0 resulted in gain of BcPG3 responsiveness, it did not alter the level of resistance to several microbial pathogens.

## Introduction

Microbe-associated molecular patterns (MAMPs) are molecular signatures of entire groups of microbes and have key roles in activation of defence response in plants (Boller and Felix, 2009; Jones and Dangl, 2006). Well characterized proteinaceous MAMPs are bacterial flagellin, EF-Tu and Ax21, fungal xylanase, and oomycete pep13, an epitope of a secreted transglutaminase (Boller and Felix, 2009; Monaghan and Zipfel, 2012). Plants recognize MAMPs by means of pattern recognition receptors (PRRs), comprising a group of leucine-rich repeat receptor-like kinases (LRR-RLKs) or leucine-rich repeat receptor-like proteins (LRR-RLPs) located in the plasma membrane (Greeff et al., 2012; Monaghan and Zipfel, 2012). The LRR-RLKs FLS2 and EFR recognize flg22 (the 22-amino-acid eliciting epitope from the conserved flagellin domain) and elf18/elf26 (peptides derived from the N-terminus of the translation elongation factor EF-Tu), respectively (Chinchilla et al., 2006; Gomez-Gomez and Boller, 2000; Kunze et al., 2004; Zipfel et al., 2006). The fungal protein ethylene-inducing xylanase (EIX) is recognized by the tomato LRR-RLPs LeEix1 and LeEix2, of which only the latter mediates a necrotic response (Ron and Avni, 2004).

BRI1-associated kinase-1/Somatic embryogenesis receptor kinase-3 (BAK1/SERK3) is an LRR-RLK acting as a common component in many RLK signalling complexes (Monaghan and Zipfel, 2012). Although it was originally identified as a protein that interacts with the brassinosteroid (BR) receptor BRI1 (Li et al., 2002; Nam and Li, 2002), BAK1 also forms ligand-induced complexes with FLS2 and EFR, and contributes to disease resistance against the pathogens *Pseudomonas syringae*, *Hyaloperonospora arabidopsidis* and *Phytophthora infestans* (Chaparro-Garcia et al., 2011; Chinchilla et al., 2007; Heese et al., 2007; Roux et al., 2011). Tomato BAK1 interacts in a ligand-independent manner with LeEix1 but not with LeEix2, and the BAK1-LeEIX1 interaction is required for the ability of LeEix1 to attenuate the signalling of LeEix2 (Bar et al., 2010). BAK1 has also been shown to interact with another LRR-RLK, BIR1 (BAK1-interacting receptor-like kinase 1). The *bir1* mutant showed extensive cell death, activation of constitutive defence responses, and impairment in the activation of the MAP kinase MPK4 (Gao et al., 2009). SOBIR1 mutants suppress BIR1 phenotypes and over-expression of SOBIR1 triggers cell death and defence responses (Gao et al., 2009). SOBIR1 does not physically interact with BIR1 suggesting that SOBIR1 mediates an alternative signal transduction route.

Fungal endopolygalacturonases (endo-PGs) are a class of pectinases that decompose plant cell walls by hydrolysing the homogalacturonan domain of pectic polysaccharides (van den Brink and de Vries, 2011). One of the pathogenic fungi for which the role of endo-PGs has been studied is *Botrytis cinerea*, the cause of grey mould disease on a wide range of plant species and tissues (Dean et al., 2012; van Kan, 2006; Williamson et al., 2007). The *B.*

*cinerea* genome (Amselem et al., 2011; Staats and van Kan, 2012) contains six genes encoding endo-PGs (Wubben et al., 1999), of which *BcPG1* and *BcPG2* are required for full virulence of *B. cinerea* (Kars et al., 2005a; ten Have et al., 1998). BcPGs, produced heterologously in *Pichia pastoris*, were capable of causing necrotic responses when infiltrated in leaves of several plant species (Kars et al., 2005a). The massive and prompt tissue collapse and necrotic response caused by BcPG2 in broad bean leaves depends on its enzymatic activity, since catalytically inactive mutant protein did not cause any tissue damage (Kars et al., 2005a). In a different study, BcPG1 was reported to induce defence responses in grapevine cell suspensions, and the defence inducing activity of BcPG1 was independent of enzymatic activity (Poinssot et al., 2003). These two studies with seemingly opposing conclusions were conducted with different endo-PG isozymes and on distinct tissues of different plant species. Therefore it remained inconclusive whether the plant responses observed after exposure to BcPGs are due to recognition of the protein, or by the sheer structural damage resulting from hydrolysis of pectin.

Oligogalacturonides (OGAs) are hydrolytic products released upon cleavage of homogalacturonan by endo-PGs (Caffall and Mohnen, 2009; Mohnen, 2008; van den Brink and de Vries, 2011). OGAs have been reported to function as damage-associated molecular patterns (DAMPs). Similar to MAMPs, DAMPs are able to activate plant defence responses, such as an oxidative burst, cell wall lignification, phytoalexin accumulation and changes in ion fluxes (Denoux et al., 2008; Galletti et al., 2008). The biological activity of OGAs is related to their molecular weight and the formation of Ca<sup>2+</sup>-dependent egg-box confirmation (Cabrera et al., 2008; Hematy et al., 2009; Vorwerk et al., 2004). Wall-associated kinases (WAKs), a family of cell wall-associated receptors, are able to bind OGAs *in vitro* (Decreux et al., 2006; Kohorn et al., 2009; Wagner and Kohorn, 2001). The extracellular domain of WAK1 serves as a receptor that perceives pectin damage caused by endo-PGs, and subsequently activates intracellular kinase signalling processes (Brutus et al., 2010). Overexpression of WAK1 in *Arabidopsis thaliana* enhances resistance to *B. cinerea* (Brutus et al., 2010).

Here, we describe the identification of natural variation in the responsiveness of *A. thaliana* to BcPGs. The accession Col-0 responded strongly to BcPGs, whereas accession Br-0 was unresponsive to BcPGs. Cloning and functional characterization demonstrated that the gene determining this dominant trait, which we designated *RBPG1*, encodes an LRR-RLP that mediates the responsiveness of Col-0 to BcPGs. Furthermore, we demonstrated that an endo-PG of another, non-pathogenic, fungal species can also act as MAMPs through recognition by the receptor protein RBPG1. The LRR-RLK SOBIR1 was found to interact with RBPG1 and is essential for responsiveness to fungal endo-PGs.

## Results

### Map-based cloning of *RBPG1*

In order to study the responsiveness of *Arabidopsis thaliana* to *Botrytis cinerea* endopolygalacturonases (BcPGs), leaves of 47 accessions (Table S1) were infiltrated with BcPG2, BcPG3, BcPG4 and BcPG6. Considerable variation in responsiveness was observed among these accessions, ranging from no visible symptoms to full necrosis of the infiltrated area (not shown). Eleven of the 47 accessions, representing the spectrum of phenotypic variation, were selected for further study (Table S1). The responses were scored in five classes ranging from 0 (no visible symptom) to 4 (full necrosis of the infiltrated area) (Figure S1A). The accessions Col-0, Kas-1, and Kas-2 showed the most severe symptoms in response to BcPGs, whereas the accessions Br-0 and Est-0 showed no symptoms (Figure 1A and Figure S1B). Plants from accessions Col-0 and Br-0 were crossed and F<sub>1</sub> progeny were responsive to BcPGs, indicating that responsiveness is a dominant trait. F<sub>1</sub> plants were selfed to obtain a segregating F<sub>2</sub> population (n > 350). 183 F<sub>2</sub> progeny were tested for their responsiveness to BcPGs in a quantitative manner and used for AFLP analysis. Quantitative trait locus (QTL) mapping identified a single locus governing the responsiveness to all BcPGs tested (Figure S2). The QTL is designated *RBPG1* (*R*esponsiveness to *B*otrytis *P*oly*G*alacturonase 1) and is positioned on chromosome 3 at a distance of ~10 cM from the *Glabrous1* (*gl1*) locus (Hauser et al., 2001), which also segregated in this cross. The primary mapping showed that the *RBPG1* locus is in a 1.6 Mbp region between AFLP markers E11/M62-F-131<F>-P1 and E11/M50-F-184<F>-P2 (Figure 1B and Figure S2A). Additional SNP markers were designed in this region based on sequence polymorphisms between Col-0 and Br-0 (<http://signal.salk.edu/atg1001/3.0/gebrowser.php>). Further mapping was performed with F<sub>8</sub> Recombinant Inbred Lines (RILs), obtained by single seed descent of the F<sub>2</sub> population (n =310), and placed the *RBPG1* locus in a smaller region of ~500 kb between SNP markers 6.7-1 and 9.10-2 (Figure 1B). To further narrow down the interval, fine mapping of the *RBPG1* locus was performed on a backcross F<sub>2</sub> population of *pad3* (a camalexin biosynthesis-deficient mutant in Col-0; (Zhou et al., 1999)) x BC41 (an F<sub>8</sub> RIL containing *rbpg1* as well as the *gl1* mutation). The *RBPG1* locus could be pinpointed to a region of ~85 kb delimited by SNP markers 7.8-7 and 7.8-5 (Figure 1B), which contains 21 candidate genes (Table S2).

As responsiveness is a dominant trait, a homozygous *RBPG1* T-DNA mutant in the Col-0 background would be unresponsive to BcPGs. To find out which of the 21 candidate genes is *RBPG1*, the available T-DNA insertion mutants of these candidate genes in a Col-0 background were investigated (Table S2). The homozygosity of the T-DNA mutants was checked by PCR and the mutants were phenotyped by infiltrating with BcPG3. All of the T-

DNA mutants tested were equally responsive to BcPG3 as Col-0 (Table S2). According to these results, the 17 genes of which the homozygous T-DNA mutants were responsive to BcPG3 could be eliminated as candidates. No T-DNA mutants were available for the genes *At3g24770*, *At3g24890* and *At3g25020*, whereas the T-DNA mutant in the *At3g24800* gene could not be made homozygous. Therefore, these four genes remained candidates.

The genome sequences of several *A. thaliana* accessions were released by the Arabidopsis 1001 genomes project (Cao et al., 2011), including Br-0, Eden-2, Est-1, and Gy-0. Among these accessions, Eden-2 was equally unresponsive to BcPG3 as Br-0, while Est-1 and Gy-0 were equally responsive to BcPG3 as Col-0. The different responsiveness of *A. thaliana* accessions to BcPGs could be due to amino acid substitutions in RBPG1. Thus SNPs in the 21 candidate genes were compared between accessions in order to identify SNPs that are associated with the responsive phenotype. In the 21 genes in the region, there were SNPs in 4 genes (from *At3g24770* to *At3g24860*) that lead to amino acid substitutions between Col-0 and Br-0. However, none of these substitutions was specifically associated with the phenotype in accessions Eden-2, Est-1, and Gy-0 (<http://signal.salk.edu/atg1001/3.0/gebrowser.php>). Surprisingly, the sequences in the *RBPG1* locus downstream of *At3g24890* were very poorly represented in accessions Br-0, Eden-2, and Gy-0, but also in many other accessions (<http://signal.salk.edu/atg1001/3.0/gebrowser.php>); especially, the region that comprises four highly homologous RLP paralogs in Col-0 is barely covered by mappable sequence reads in the other accessions. In combination with the results of T-DNA mutant analysis, *At3g24890* and *At3g25020* were considered to be the remaining candidates for being the *RBPG1* gene (Table S2).

To determine the function of *At3g24890* and *At3g25020*, both genes (under the control of the 35S promoter) were transformed into the BcPG-unresponsive accession Br-0. Transgenic plants expressing *At3g25020* displayed the BcPG-responsive phenotype (Figure 1A), whereas transgenic plants containing *At3g24890* constructs remained equally unresponsive to BcPG3 as the recipient accession Br-0 (Figure S3). The *At3g25020* gene encodes an LRR-RLP and is one of a family of four RLP-encoding genes that occur in a cluster within this region of the Col-0 genome (Figure 1B). The four genes are *At3g24900*, *At3g24982*, *At3g25010*, and *At3g25020* and correspond to the genes *RLP39-42* according to the classification of Wang et al. (2008). Genome reassembly of raw sequence data showed that this region in accession Br-0 contains only two RLP-encoding genes, *rbpg1-1* and *rbpg1-2* (Figure 1B), with over 80% identity to each other (Figure S4). Phylogenetic analysis shows that *RLP39* and *RLP41* cluster with *rbpg1-1*, whereas *RLP40* and *RLP42* cluster with *rbpg1-2* (Figure 1C). To determine whether the three Col-0 paralogs, *RLP39*, *RLP40*, and *RLP41* also confer responsiveness to BcPGs, these genes (under the control of the 35S promoter) were transformed into BC41 (an F<sub>8</sub> RIL of Col-0 x Br-0, unresponsive to

BcPG3). None of the transgenic plants carrying *RLP39*, *RLP40*, and *RLP41* constructs showed a BcPG-responsive phenotype (Figure S5). These data demonstrate that *RLP42* is the only gene in this region that confers responsiveness to BcPG3 and it is hereafter referred to as the *RBPG1* gene.

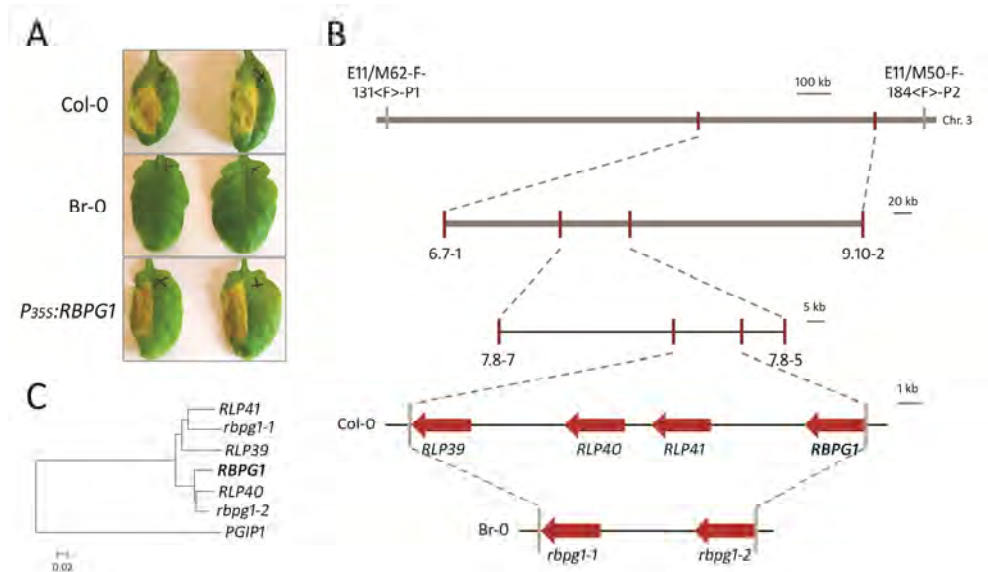


**Figure 1.** Map-based cloning of *RBPG1*. **A**, responsiveness of *Arabidopsis thaliana* accessions Col-0 and Br-0, and Br-0 transgenic plants expressing *P<sub>35S</sub>:RBPG1* to BcPG3. Photographed 7 days after infiltration with BcPG3. **B**, map of *RBPG1* locus. **C**, phylogenetic tree of *RBPG1* homologs in Col-0 and Br-0. The amino acid sequences were aligned by Clustal\_X 1.83 and the phylogenetic tree was generated by using Mega 4 by the Neighbor-Joining (NJ) method with 1000 bootstrap replicates.

### **RBPG1 confers responsiveness to catalytically inactive BcPG3, but not to oligogalacturonides**

Plant cell wall fragments such as oligogalacturonides (OGAs) can serve as DAMPs (Boller and Felix, 2009; D'Ovidio et al., 2004; Hematy et al., 2009; Rasul et al., 2012). To distinguish whether the RBPG1-dependent responsiveness to BcPG3 is through the recognition of the BcPG3 protein itself (acting as a MAMP) or through recognition of cell wall fragments released *in planta* (acting as DAMPs), heat-inactivated BcPG3 and catalytically inactive BcPG3 (D353E/D354N) were infiltrated into leaves of Col-0, Br-0, and Br-0 transgenic plants expressing *P<sub>35S</sub>:RBPG1*. Both the heat-inactivated and the catalytically inactive BcPG3 protein induced necrosis in Col-0 and in *P<sub>35S</sub>:RBPG1* transgenic plants, but not in Br-0 (Figure 2). Furthermore, the alcohol-insoluble residue (AIR) fraction consisting mainly of cell wall polysaccharides, was extracted from leaves of Col-0 and Br-0

and hydrolysed with active BcPG3. After 42 h incubation, the solubilised cell wall fragments released from the AIR were infiltrated into Col-0 and Br-0. However, they did not induce any visible symptom in Col-0 or Br-0. In addition, a set of distinct, partially purified OGAs with a degree of polymerization (DP) ranging from 3 to 20, at a concentration range from 10  $\mu\text{M}$  up to 1 mM, did not induce any visible symptom upon infiltration into leaves of Col-0 or Br-0. These results show that RBPG1 recognizes the BcPG3 protein as a MAMP and that the response to BcPG3 does not depend on its catalytic activity.

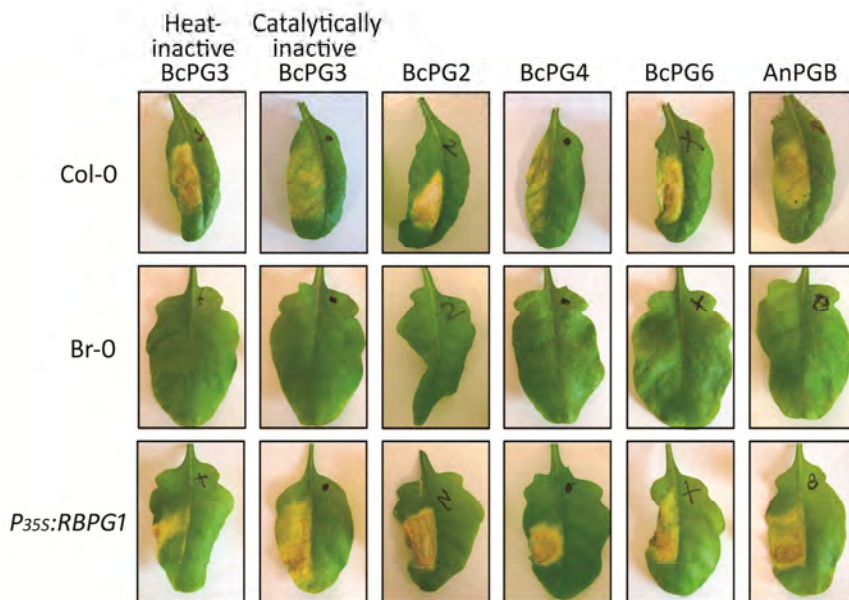


**Figure 2.** Responsiveness of *Arabidopsis thaliana* accessions Col-0 and Br-0, and Br-0 transgenic plants expressing *P<sub>35S</sub>:RBPG1* to fungal endo-PGs. Col-0 and *P<sub>35S</sub>:RBPG1* transgenic plants are responsive to heat-inactive BcPG3 (1.5  $\mu\text{M}$ ), catalytically inactive BcPG3, BcPG2 (0.1  $\mu\text{M}$ ), BcPG4 (3  $\mu\text{M}$ ), BcPG6 (1  $\mu\text{M}$ ) and AnPGB (0.3  $\mu\text{M}$ ). Photographed 7 days after infiltration.

### An 11-amino acid peptide stretch is conserved among fungal endo-PGs but fails to induce necrosis

Plants that are responsive to BcPG3 (Col-0, as well as Br-0 transgenes expressing *RBPG1*) were also responsive to BcPG2, BcPG4 and BcPG6, as well as to AnPGB from the saprotrophic fungus *Aspergillus niger* (Figure 2). In the case of flagellin and EF-Tu, conserved short peptide motifs are sufficient to trigger plant defence responses (Brunner et al., 2002; Felix et al., 1999; Kunze et al., 2004). To avoid self-recognition these conserved motifs should not be present in plants. Since multiple BcPGs and AnPGB were

able to induce necrosis (Figure 2), we considered the possibility that a peptide motif conserved among fungal endo-PGs, but absent in *A. thaliana*, might act as an epitope that is recognized by RBPG1. Amino acid sequence alignments of several fungal endo-PGs and three *A. thaliana* endo-PGs (Ogawa et al., 2009) showed that an 11-amino acid peptide stretch, adjacent to the catalytic site, is highly conserved among the fungal endo-PGs (fpg11). The homologous region in *A. thaliana* endo-PGs contains a glycine to proline substitution (Figure 3). To investigate whether fpg11 is able to induce necrosis, a synthetic 22-amino acid peptide corresponding to BcPG3 residues 367-388 (with fpg11 in the middle) was infiltrated in leaves of Col-0 and Br-0. In concentrations ranging from 0.01 mM to 1 mM, the peptide did not induce any symptoms till 7 days after infiltration.

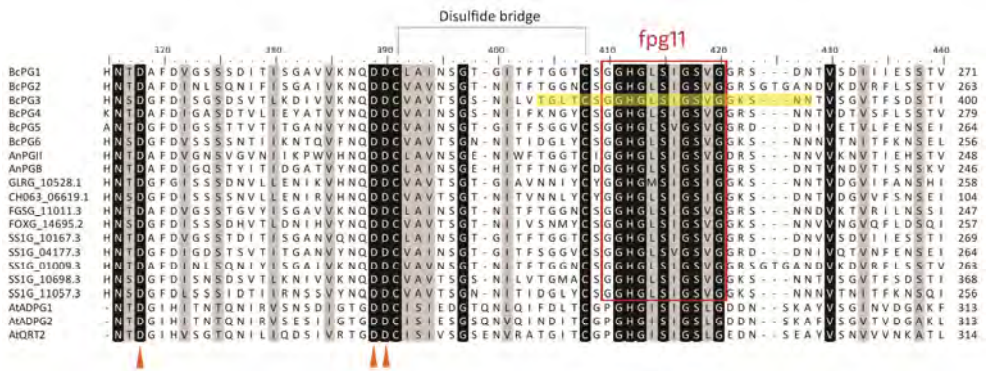


**Figure 3.** Amino acid sequence alignment of fungal endo-PGs and *Arabidopsis thaliana* endo-PGs. The red frame indicates the conserved fungal 11-amino acid peptide (fpg11). The triangles indicate the catalytic site residues. The sequence highlighted in yellow represents the 22-amino acid synthetic peptide used for infiltration. The numbers on the right hand side of sequences from each protein indicate the coordinate of the last amino acid in the alignment. Accession numbers: BcPG1 (AAV84613), BcPG2 (AAV84614), BcPG3 (AAV84615), BcPG4 (AAV84616), BcPG5 (AAV84617), BcPG6 (AAV84618), AnPG1 (1701294A), AnPG8 (Q9P4W3); AtADPG1 (At3g57510), AtADPG2 (At2g41850), AtQRT2 (At3g07970). The gene locus for other species: GLRG\_10528 (*Colletotrichum graminicola*), CH063\_06619 (*Colletotrichum higginsianum*), FGSG\_11011 (*Fusarium graminearum*), FOXG\_14695.2 (*Fusarium oxysporum*), SS1G (*Sclerotinia sclerotiorum*).

### The C-terminal intracellular domain of RBPG1 is not required for the responsiveness

One striking difference between RBPG1 and the three homologs from accession Col-0 (RLP39-41) and two homologs from accession Br-0 (rbpg1-1 and rbpg1-2) is the presence of an extended C-terminal intracellular domain of 9 amino acid residues (Figure 4 and S3). To investigate whether this domain is required for the responsiveness, two constructs were generated in which the C-terminal domain of RBPG1 is truncated: RBPG1\_Trunc1 lacking the C-terminal 18 amino acids, and RBPG1\_Trunc2 lacking the C-terminal 10 amino acids. Also a construct was generated in which the C-terminal residue of rbpg1-2 is

replaced with the C-terminal 10 amino acids of *RBPG1* (*rbpg1-2\_Swap1*; Figure 4). These three gene constructs (under the control of the 35S promoter) were transformed into BC41 (an F<sub>8</sub> RIL of Col-0 x Br-0, unresponsive to BcPG3). *RBPG1\_Trunc1* and *RBPG1\_Trunc2* conferred responsiveness of BC41 to BcPG3 similar to that of the full-length *RBPG1* construct, whereas the recipient line BC41 and the plants that were transformed with *rbpg1-2\_Swap1* constructs were unresponsive to BcPG3 (Figure 4). These results show that the C-terminal intracellular domain of RBPG1 is not required for the responsiveness.

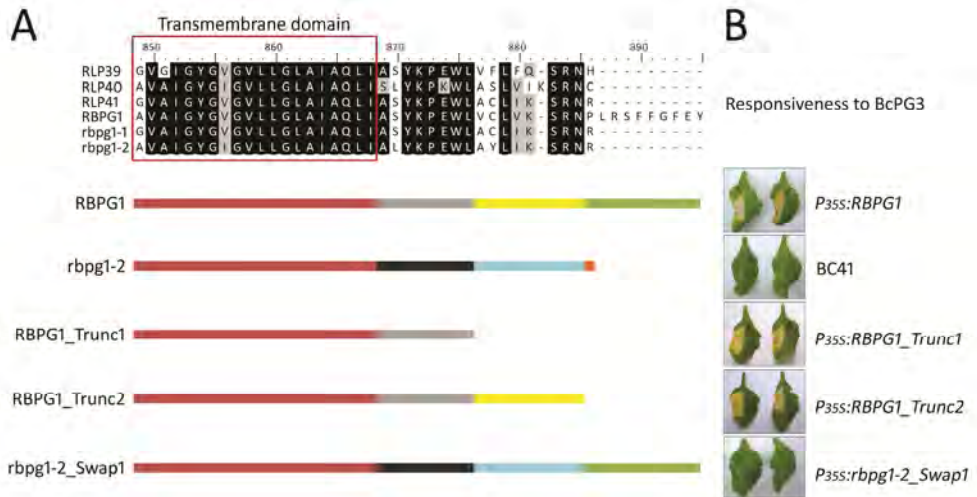


**Figure 4.** The C-terminal intracellular domain of RBPG1 is not required for the responsiveness to BcPG3. A, schematic representation of the design of truncated RBPG1 and swapped *rbpg1-2* constructs. B, responsiveness of BC41 plants containing different constructs to BcPG3. Photographed 7 days after infiltration with BcPG3.

### BcPG3 interacts with RBPG1 in *Nicotiana benthamiana*

To determine whether BcPG3 physically interacts with RBPG1, immunoprecipitation analysis was performed by transient co-expression of 10xMyc-tagged BcPG3 together with RBPG1-GFP in *N. benthamiana*. Two days after agro-infiltration, RBPG1-GFP proteins were immunoprecipitated using GFP Trap beads, and the purified proteins were analysed by Western blot. BcPG3 was co-immunoprecipitated with RBPG1-GFP, but not with the GFP beads alone (Figure 5A). GFP-tagged EFR was used as an additional negative control, to exclude that BcPG3 interacts non-specifically with extracellular LRR-domain-containing proteins (Figure 5B). To further confirm the interaction between BcPG3 and RBPG1, we swapped the epitope tags and co-expressed 10xMyc-tagged RBPG1 and GFP-tagged BcPG3 in *N. benthamiana*. BcPG3-GFP was equally capable of immunoprecipitating RBPG1-myc (Figure 5A).

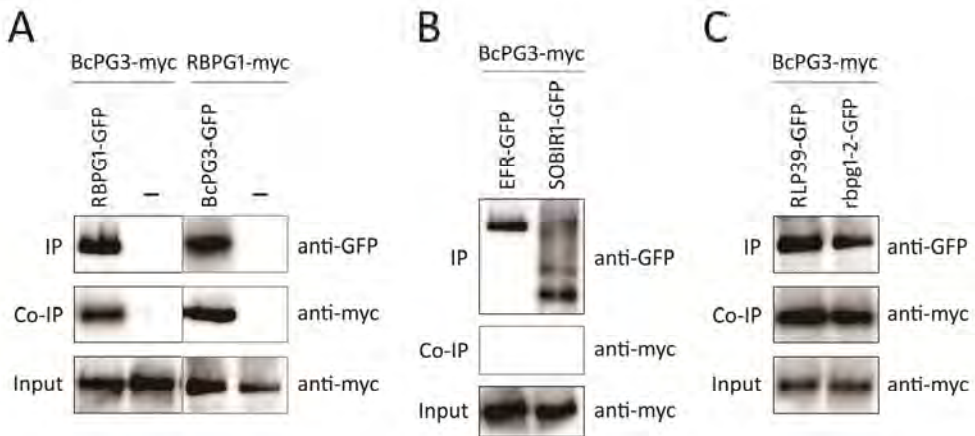


**Figure 5.** BcPG3 forms a complex with RBPG1 and its homologs in *Nicotiana benthamiana*. Coimmunoprecipitation of (A) BcPG3 and RBPG1, (B) BcPG3 and EFR or SOBIR1, (C) BcPG3 and RLP39 or *rbpg1-2*. Total proteins expressed in *N. benthamiana* leaves were subjected to immunoprecipitation with GFP Trap beads followed by immunoblot analysis with anti-myc antibodies to detect BcPG3-myc and RBPG1-myc; and anti-GFP antibodies to detect RBPG1-GFP, EFR-GFP, SOBIR1-GFP, RLP39-GFP, *rbpg1-2*-GFP and BcPG3-GFP.

### SOBIR1 is required for the RBPG1 dependent responsiveness to BcPG3

BAK1/SERK3 and other SERK family members play important roles in plant defence responses by forming complexes with a number of LRR-receptor-like kinases (LRR-RLKs), e.g. FLS2 and EFR (Chinchilla et al., 2009; Roux et al., 2011). Recently, the tomato LRR-RLK SOBIR1 was shown to interact specifically with a number of LRR-RLPs (Liebrand et al., 2013). Furthermore, overexpression of SOBIR1 in *A. thaliana* activates defence responses (Gao et al., 2009). To test whether LRR-RLKs are involved in the response of RBPG1 to BcPG3, *A. thaliana* plants carrying mutations in different LRR-RLK genes were analysed. The *efr* mutant and all the *serk* mutants tested were unaltered in their responsiveness to BcPG3 (Figure 6A). Interestingly, the *sobir1-1* mutant did not show any symptoms following infiltration with BcPG3 (Figure 6A). Co-immunoprecipitation analysis showed that RBPG1 physically interacts with SOBIR1, but not with SERK2, BAK1/SERK3 or EFR (Figure 6B). In addition, GFP-tagged SOBIR1 was incapable to immunoprecipitate 10xMyc-tagged BcPG3 (Figure 5B).

### RBPG1 homologs physically interact with BcPG3 and SOBIR1

Among the six homologs of RBPG1 from Col-0 and Br-0, RBPG1 is the only receptor protein that confers the responsiveness to BcPG3. To test whether the specificity is determined by the interaction of the ligand (BcPG3) with the receptor, co-immunoprecipitation analysis was also performed with RBPG1 homologs by transient co-expression of 10xMyc-tagged BcPG3 with GFP-tagged RLP39, RLP40, RLP41, and *rbpg1-2* in *N. benthamiana* (cloning of the *rbpg1-1* construct was unsuccessful). RLP39 and *rbpg1-2* were able to co-immunoprecipitate BcPG3 (Figure 5C). Moreover, GFP-tagged SOBIR1 was able to co-immunoprecipitate 10xMyc-tagged RLP39 and *rbpg1-2* (Figure 6C). Due to the very low expression level of either GFP-tagged or 10xMyc-tagged RLP40 and RLP41 proteins (not shown), their interaction with BcPG3 or SOBIR1 could not be studied.

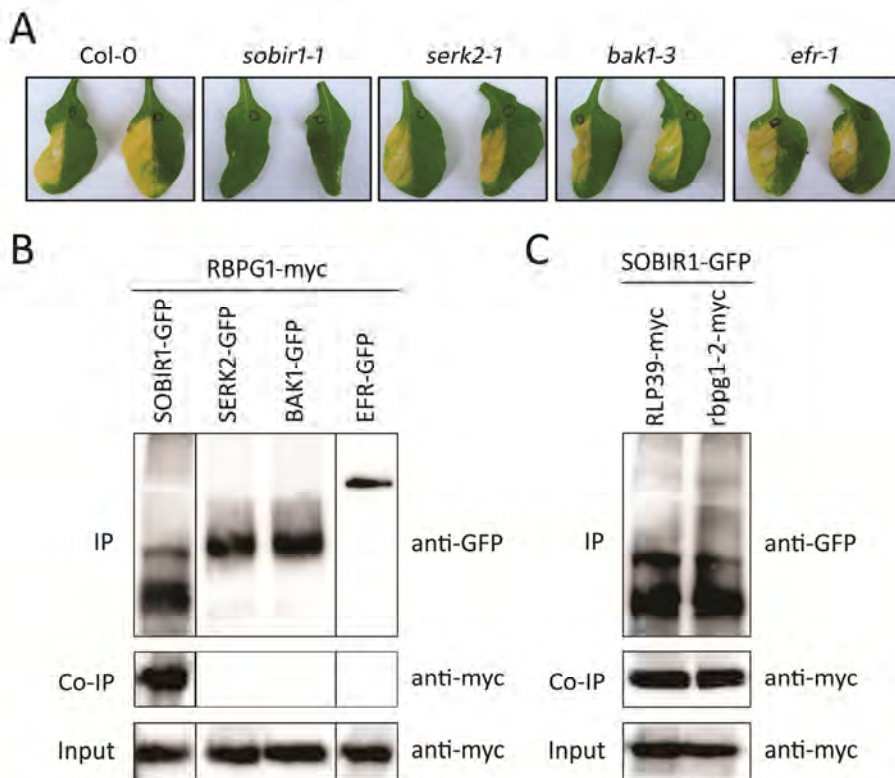


**Figure 6.** SOBIR1 is required for RBPG1 dependent responsiveness. **A**, responsiveness of *Arabidopsis thaliana* mutants to BcPG3. Photographed 7 days after infiltration with BcPG3. **B**, co-immunoprecipitation of RBPG1 and SOBIR1, SERK2, BAK1, or EFR. **C**, co-immunoprecipitation of SOBIR1 and RLP39 or *rbpg1-2*. Total proteins expressed in *N. benthamiana* leaves were subjected to immunoprecipitation with GFP Trap beads followed by immunoblot analysis with anti-myc antibodies to detect RBPG1-myc, RLP39-myc, and *rbpg1-2-myc*; and with anti-GFP antibodies to detect SOBIR1-GFP, SERK2-GFP, BAK1-GFP and EFR-GFP.

### RBPG1 does not contribute to disease resistance

To determine whether RBPG1 contributes to disease resistance, three independent *P<sub>35S</sub>:RBPG1* T3 transgenic Br-0 lines (homozygous T2 lines with single copy integration) and the recipient accession Br-0 were inoculated with the necrotrophic fungal pathogen *B. cinerea*, the biotrophic oomycete pathogen *Hyaloperonospora arabidopsidis*, the hemibiotrophic oomycete pathogen *Phytophthora capsici*, and the bacterium *Pseudomonas syringae* pv. tomato DC3000. All three transgenic lines were equally susceptible as Br-0 to these tested pathogens (not shown). Despite the fact that Col-0 responds to BcPG3 and *sobir1-1* mutants show loss of responsiveness, susceptibility of the *sobir1-1* mutant to pathogen infection is not altered as compared to Col-0.

### Discussion

Genetic variation in response of *Arabidopsis thaliana* to BcPGs was studied and a single locus, designated *RBPG1*, was identified by QTL mapping on the F<sub>2</sub> population of Col-0 x Br-0. The *RBPG1* gene in the locus was identified by further map-based cloning and a combination of functional and comparative genomics analysis. *RBPG1* (*RLP42*) encodes an LRR receptor-like protein (LRR-RLP) and is one of a family of four LRR-RLP-encoding genes (*RLP39*, *RLP40*, *RLP41*, *RLP42*) that occur in a cluster (Wang et al., 2008) within the *RBPG1* locus of the Col-0 genome. By contrast, accession Br-0 contains only two LRR-RLP-encoding genes (*rbpg1-1* and *rbpg1-2*) in this region (Figure 1B). Phylogenetic analysis shows that *RLP39* and *RLP41* cluster with *rbpg1-2*, whereas *RLP40* and *RBPG1* cluster with *rbpg1-1* (Figure 1C). Among these six paralogs, *RBPG1* is the only gene that confers the responsiveness to BcPG3. It is likely that a duplication of a gene-cluster with two paralogs occurred in the lineage to Col-0 and subsequently *RBPG1* gained the responsiveness to BcPG3. This region in the *A. thaliana* genome shows great diversity, which cannot easily be unravelled. Accession Col-0 contains four paralogs with high nucleotide identity, however, in many other accessions the region is barely covered by mappable sequence reads (Cao et al., 2011) (<http://signal.salk.edu/atg1001/3.0/gebrowser.php>). In order to determine the structure of this region in the Br-0 genome, it appeared essential to perform a *de novo* assembly of Br-0 sequence reads, and manually validate the assembled contigs. Likewise, genome assembly is probably required to study the genetic variation of these LRR-RLPs in many different *A. thaliana* accessions.

Besides BcPG2, BcPG3, BcPG4, and BcPG6, also AnPGB produced by the saprotroph *Aspergillus niger* induces necrosis in Col-0 (Figure 2), suggesting that fungal endo-PGs act as microbe-associated molecular patterns (MAMPs) instead of specific pathogen-

associated molecular patterns (PAMPs). Nevertheless, there have been controversies whether the enzymatic activity of fungal endo-PGs is required for triggering plant responses (Boudart et al., 2003; Kars et al., 2005a; Poinssot et al., 2003). Our data show that catalytically inactive BcPG3 and heat-inactive BcPG3 were able to induce necrosis similar to active BcPG3 (Figure 2). This observation suggests that RBPG1 recognizes the BcPG3 protein itself rather than the oligogalacturonides (OGAs), hydrolytic products released from pectin by endo-PGs (Caffall and Mohnen, 2009; Mohnen, 2008; van den Brink and de Vries, 2011). OGAs have been reported to act as DAMPs that activate defence responses following recognition by WAK1 (Brutus et al., 2010; Denoux et al., 2008; Kohorn and Kohorn, 2012). We did not observe any visible symptoms upon infiltration with several OGAs of different size ranges at concentrations up to 1 mM, however, we did not monitor whether these OGAs induced any stress or defence response at the transcriptional level. Our hypothesis that the BcPG3 protein itself is recognized as a MAMP was further corroborated by a co-immunoprecipitation assay which provided evidence that RBPG1 forms a complex with BcPG3 (Figure 5A). These data collectively suggest that fungal endo-PGs act as MAMPs that are recognized by LRR-RLP RBPG1.

Multiple fungal endo-PGs were capable of inducing necrosis, suggesting that a conserved motif might be involved in the recognition by RBPG1. Amino acid sequence alignment identified an 11-amino acid peptide (fpg11) that is the longest conserved stretch among fungal endo-PGs; other conserved sequence stretches were 7 amino acids (the catalytic site) or shorter than 4 amino acids. However, a synthetic peptide covering fpg11 was not capable of inducing necrosis. Either the structure of fpg11 could differ between the full-length protein and the synthetic peptide, or the peptide is unstable after infiltration in the plant. Notably, the corresponding region in the sequence of *A. thaliana* endo-PGs contains a proline residue instead of glycine at position 1. This proline likely alters the 3-dimensional structure of plant endo-PGs in this region, which would enable them to escape recognition by the plant itself. Further studies are required to elucidate which amino acid motifs in BcPG3 are crucial for the recognition.

Not only RBPG1 was able to physically interact with BcPG3, also RLP39 and *rbpg1-2* are able to form a complex with BcPG3 (Figure 5C), even though they did not confer the responsiveness to BcPG3. This situation is analogous to the tomato LRR-RLPs LeEix1 and LeEix2, encoded by two paralogous genes from a gene cluster, that act as receptors for fungal ethylene-inducing xylanase (EIX). Both receptors are able to bind EIX, whereas only LeEix2 mediates defence responses (Ron and Avni, 2004). We considered the possibility that differences in the cytoplasmic domain between RBPG1 and its paralogs may account for the ability of RBPG1 to transduce a signal. Genetic complementation studies, however, demonstrated that the extended C-terminal intracellular domain of RBPG1 is not required

for inducing necrosis. Several studies suggest that MAMP receptors must form a complex with interactors for proper signal transduction to occur (Chinchilla et al., 2007; Monaghan and Zipfel, 2012; Roux et al., 2011). An alternative reason for the inability of RLP39, RLP40, and RLP41 to respond to BcPG3 could be the lack of interaction with other membrane-associated proteins. We showed that the LRR-RLK SOBIR1 is an interactor of RBPG1 and is required for the responsiveness to BcPG3. RLP39 and *rbpg1-2* were also able to form a complex with SOBIR1 in the co-immunoprecipitation assay (Figure 6). It cannot be excluded that other (as yet unknown) components in the complex have the ability to bind RBPG1 to determine specificity.

BAK1 is an interactor involved in diverse signalling processes (Boller and Felix, 2009; Monaghan and Zipfel, 2012), and forms a ligand-induced complex with BRI1, FLS2 and EFR (Chinchilla et al., 2007; Li et al., 2002; Nam and Li, 2002; Roux et al., 2011). However, BAK1 and other SERK family members do not seem to be involved in the RBPG1 mediated signalling (Figure 6). SOBIR1 was initially identified as a suppressor of BIR1 (BAK1-interacting receptor-like kinase 1) that positively regulates cell death (Gao et al., 2009). More recent studies show that SOBIR1 particularly interacts with LRR-RLPs that play a role in plant defence against fungal pathogens (Liebrand et al., 2013). Our data showed that SOBIR1 interacts with RBPG1 in a ligand-independent manner (Figure 6).

The role of RBPG1 in disease resistance was investigated by inoculating transgenic plants expressing *RBPG1* with microbial pathogens with distinct lifestyles: the necrotrophic fungus *Botrytis cinerea*, the biotrophic oomycete *Hyaloperonospora arabidopsidis*, the hemibiotrophic oomycete *Phytophthora capsici*, and the bacterium *Pseudomonas syringae* pv. tomato DC3000. Overexpression of *RBPG1* did not notably enhance disease resistance. Since there is no T-DNA insertion mutant available in the coding sequence of *RBPG1*, we could not study whether knockout mutants in *RBPG1* are more susceptible to these pathogens. Since SOBIR1 is essential for RBPG1 mediated responsiveness, *sobir1-1* mutants could be used as a tool to indirectly test whether *RBPG1* influences disease susceptibility. The *sobir1-1* mutants showed similar susceptibility as Col-0 to the pathogens tested, which is consistent with the previous study that *sobir1* mutant did not enhance susceptibility to *Pst* DC3000 (Gao et al., 2009). We did observe that accession Col-0 is slightly less susceptible than Br-0 to these pathogens (except for *B. cinerea*), suggesting that other genes in Col-0, outside the RBPG1 locus, contribute to partial disease resistance.

Taken together, our studies provide evidence for a novel group of MAMPs (fungal endo-PGs), which are recognized by a novel PRR (RGP1) activating cell death through SOBIR1.

## Materials and methods

### Plant materials and growth conditions

The *Arabidopsis thaliana* plants used in this study were grown in a greenhouse at 20 °C or in a growth chamber at 20 °C and 70% relative humidity under a 12 h light/dark cycle (short-day conditions 8 h light/16 h dark). *A. thaliana* accessions were kindly provided by Maarten Koornneef, Corry Hanhart and Joost Keurentjes (Laboratory of Genetics of Wageningen University, The Netherlands). Transgenic seeds were grown on 1/2 Murashige and Skoog (MS) medium plates with 1% sucrose and 1% plant agar containing 20 µg/ml hygromycin or 50 µg/ml kanamycin for ~2 weeks. Antibiotic-resistant seedlings were transferred into soil and the copy number of the transgenes was determined by qRT-PCR. T-DNA insertion mutants were obtained from the Arabidopsis Biological Resource Centre (Columbus, Ohio, USA) or from the Nottingham Arabidopsis Stock Centre (Nottingham, UK). The homozygosity of the T-DNA mutants was checked by PCR using primers listed in Table S3.

### Phenotypic scoring

Six to eight-week old plants were infiltrated with BcPGs purified from culture filtrates of *Pichia pastoris* expressing BcPGs, as previously described (Kars et al., 2005a). In the initial screening, 47 *A. thaliana* accessions (Table S1) were infiltrated with BcPG2, BcPG3, BcPG4, and BcPG6 at 3 U/ml (diluted in 10 mM sodium acetate buffer, pH 4.2) in duplicate. Multiple rosette leaves per plant were infiltrated with one BcPG on either side of the mid-vein. Eleven selected accessions (Table S1) were subsequently infiltrated with BcPG2, BcPG3, and BcPG6 in duplicate with 3 U/ml. Plants of the F<sub>2</sub> population of Col-0 x Br-0 were infiltrated with BcPG2 in triplicate and with BcPG3, BcPG4, and BcPG6 in duplicate. Plants of the F<sub>2</sub> and F<sub>3</sub> population of BC41 x *pad3* were infiltrated with BcPG3 in duplicate.

The response to each infiltration was visually scored on a scale ranging from 0 to 4, as follows: 0, no symptoms; 1, chlorotic spots within the infiltrated zone; 2, chlorosis covering the infiltration zone; 3, abundant chlorosis with necrotic spots; and 4, complete necrosis (Figure S1A).

### Genotyping of F<sub>2</sub> population of Col-0 x Br-0

Genotypic data on the F<sub>2</sub> population of Col-0 x Br-0 were generated (Keygene N.V., Wageningen, The Netherlands) using amplified fragment length polymorphism (AFLP) markers (Vos et al., 1995) with the restriction enzymes *EcoRI* and *MseI*. AFLP markers were amplified using adapter specific primers containing two (E+2) or three (M+3) selective nucleotides. Five different E+2/M+3 primer combinations were used (Table S4).

AFLP amplification reactions were performed in a Perkin Elmer 9600 thermocycler (Perkin Elmer Corp., Norwalk, CT, USA). The amplified DNA products were separated on a MegaBACE 1000 capillary electrophoresis system (Amersham BioSciences). Proprietary AFLP marker analysis software (Keygene N.V.) was used to score the markers co-dominantly on the basis of peak intensities. Data that could not be scored co-dominantly unambiguously were scored dominantly. The genetic linkage map of the F<sub>2</sub> population was constructed using the JoinMap 3.0 program (Stam, 1993; van Ooijen and Voorrips, 2001), applying the Kosambi mapping function.

### **Quantitative trait loci analysis**

Quantitative trait locus (QTL) mapping was performed using the software packages MapQTL version 4.0 (van Ooijen et al., 2002) and WinQTLcart version 2.5 (Wang et al., 2006). For each BcPG, the QTL analysis was performed on the individual replicates and on the averages of the replicates. The data were analysed using the interval mapping method (IM), calculating the log-likelihood (LOD) values every 1 cM along the chromosome. QTL were significant when the LOD score exceeded the significance threshold ( $P = 0.05$ ), which represents 95% confidence intervals for normally distributed data. Empirical thresholds for interval mapping were obtained by permutations (10,000), as implemented in the package (Churchill and Doerge, 1994). The resulting genome-wide LOD threshold for all traits in the F<sub>2</sub> population was 3.3 (Figure S2B).

### **Further mapping with the F<sub>8</sub> RILs of Col-0 x Br-0**

Individuals of the F<sub>2</sub> population of Col-0 x Br-0 were propagated by single seed descent to generate an F<sub>8</sub> recombinant inbred line (RIL) population, comprising 310 RILs. Three recombinants between markers E11/M62-F-131<F>-P1 and E11/M50-F-184<F>-P2 (Figure S2A) were identified by PCR with SNP markers (Table S4), which were designed based on the single nucleotide polymorphisms between the sequences of Col-0 and Br-0 (<http://signal.salk.edu/atg1001/3.0/gebrowser.php>).

### **Fine mapping with the F<sub>2</sub> population of BC41 x *pad3* mutant**

To fine map *RBPG1*, BC41 (an F<sub>8</sub> RIL of Col-0 x Br-0, which is homozygous for the Br-0 allele in the *RBPG1* locus and unresponsive to BcPGs) was crossed with the *pad3* mutant in the Col-0 background (Zhou et al., 1999). BC41, alike accession Br-0, is glabrous and has the mutated *gl1* gene (*GL1* is involved in trichome synthesis; (Hauser et al., 2001)). The *RBPG1* locus, and the *GL1* locus are both located on chromosome 3. The genetic distance between *RBPG1* and *GL1* is estimated to be 6~10 cM, based on the RIL population. F<sub>2</sub> plants that had trichomes and were unresponsive to BcPG3 were putative recombinants and were used for linkage analysis with SNP markers (Table S5). In total, over 4000 F<sub>2</sub>

plants were grown and phenotyped; 400 of those plants were genotyped and 10 new recombinants were identified, reducing the *RBPG1* locus to a region delimited by SNP markers 7.8-7 and 7.8-5 (Figure 1B).

### **Genome sequence reassembly of accession Br-0 in *RBPG1* locus**

The raw sequencing data of Br-0 were kindly provided by Dr. R. Schmitz (SALK Institute, La Jolla, USA). The reads were mapped on the genome of accession Col-0 (version TAIR10), however subtracting the sequences between coordinates 9,090,000 and 9,250,000 on chromosome 3, which spans the region from about 8 kb upstream of *At3g24890* to 100 kb downstream of *At3g25060*, using Bowtie 2 version 2.0.0-beta4 (Langmead and Salzberg, 2012). Unmapped Br-0 reads were sorted and filtered accordingly using SAMtools version 0.1.18 (Li et al., 2009) and FastQC (<http://www.bioinformatics.babraham.ac.uk/projects/fastqc/>; version 0.10.0). Filtered reads were assembled with Velvet version 1.1.07 (Zerbino and Birney, 2008) using the K-mer setting as 57. Six assembled nodes were mapped to the *RBPG1* locus and 14 pairs of primers (Table S6) were used to fill in gaps between the nodes, enabling to assemble them into one contig. The entire contig was finally confirmed by sequencing.

### **AIR digestion with BcPG3 and OGA preparation for infiltration in plants**

Leaves of 5-6-week-old plants were freeze dried and milled. AIR was extracted with 70% ethanol at 50 °C as described (Hilz et al., 2005). Twenty milligram of AIR was suspended in 10 mM sodium acetate pH 4.2 and incubated with 200 U BcPG3 at room temperature. After 42 h hydrolysis, the supernatant was obtained by centrifugation at 13,000 rpm for 10 min and filtrated through an Amicon ultra 0.5 ml centrifugal filter with 3 K membrane (Millipore), that eliminates OGAs with a degree of polymerization > 15. The collected filtrate containing hydrolysed cell wall fragments was infiltrated into *A. thaliana* leaves directly. The BcPG3 proteins that remained in the filter were also collected and diluted to 100 U/ml for leaf infiltration.

OGAs of defined length were prepared and quantified according to Kester and Visser (1990). Samples containing pure compounds (GalpA)<sub>3</sub> and (GalpA)<sub>4</sub>, as well as mixtures of (GalpA)<sub>4-5</sub>, (GalpA)<sub>2-6</sub>, (GalpA)<sub>4-10</sub> and (GalpA)<sub>7-9</sub> were each infiltrated in leaves at final concentrations of 0.1 mM, 0.3 mM and 1 mM. OGAs of various lengths were generated by incubating 200 mL of 1% (w/v) PGA in 10 mM sodium acetate buffer, pH 4.2, with 25 U of either *Aspergillus niger* PGII or BcPG2 for 10 min at 30°C. The partial digests were boiled for 5 min to stop digestion and treated three times with 3 g of Dowex 50W-X8 (H<sup>+</sup>) (Bio-Rad) to convert all pectic fragments into the acidic form. The PGA/AnPGII digest was separated by gel filtration using a 60 x 2.6 cm Superdex 200 column (Amersham

Biosciences). Elution was carried out with water and fractions containing reducing sugars were collected in six pools. Pool 1 contained (GalpA)<sub>6-20</sub> (~10 μM each); pool 2 contained mainly (GalpA)<sub>4-12</sub> (~20 μM each); pool 3 comprised primarily (GalpA)<sub>1-7</sub> (~10 μM each); pool 4 consisted especially of GA monomers (70 μM) and (GalpA)<sub>2-5</sub> (~10 μM each); pool 5 and 6 primarily contained (GalpA)<sub>1-4</sub> (~5 μM each).

### Plasmid construction and transformation

For complementation analysis in the Br-0 background, the genomic DNA sequence of *At3g24890* was amplified from Col-0 with primers AT174/176 and cloned into pDONR207 (Invitrogen) by Gateway cloning to obtain the entry vector pENTR-*At3g24890*. Due to the high sequence identity in the coding regions, we first amplified ~3.9 kb genomic DNA fragments encompassing *RLP39*, *RLP40*, *RLP41*, and *RBPG1* from Col-0 with primers AT188/189, AT170/171, AT190/191, and AT172/173, which are respectively specific for each gene fragment; a ~3.9 kb genomic DNA fragment containing *rbpg1-2* was amplified from Br-0 with primers AT219/204. The resulting fragments were used as templates to amplify *RLP39*, *RLP40*, *RLP41*, and *RBPG1*, and *rbpg1-2* with primers AT192/193, AT194/195, AT196/198, AT177/178, and AT196/250 respectively, which were subsequently cloned into pDONR207 to generate the entry vectors. Two C-terminally truncated *RBPG1* fragments (*RBPG1\_Trunc1* and *RBPG1\_Trunc2*) were amplified from pENTR-*RBPG1* with primers AT177/251 and AT177/252 respectively; and the swapped *rbpg1-2\_Swap1* fragment was amplified from pENTR-*rbpg1-2* with primers AT196/254. The resulting fragments were cloned into pDONR207 to obtain the entry vectors. All the genes in entry vectors were confirmed by sequencing. Expression vectors (35S promoter) were created by Gateway cloning of pMDC32 (Curtis and Grossniklaus, 2003) with the corresponding entry vectors, respectively; binary constructs were transformed into *Agrobacterium tumefaciens* GV3101 and subsequently into *A. thaliana* plants by floral dipping (Clough and Bent, 1998).

For transient expression in *Nicotiana benthamiana*, *Bcp3* with a plant PR1 signal peptide was amplified from pAT2-3 (Joubert et al., 2007) with primers At265/268 and cloned into donor vector pDONR207 to obtain the entry vector, which was checked by sequencing. Expression vectors were created by Gateway cloning of pSOL2095 (Liebrand et al., 2012) or pGWB20 (Nakagawa et al., 2007) with the corresponding entry vectors and transformed into *A. tumefaciens* C58C1, carrying helper plasmid pCH32 (Liebrand et al., 2012) or into *A. tumefaciens* GV3101 (only for SERK2 and BAK1 constructs).

The substitutions chosen for generating the catalytically inactive *Bcp3*<sup>D353E/D354N</sup> protein were designed based on studies of (Armand et al., 2000) on the catalytic residues of *Aspergillus niger* *pgB*. For mutant protein production in *Pichia pastoris*, site-directed

mutagenesis was carried out by amplifying two fragments of mutant allele *Bcpg3*<sup>D353E/D354N</sup> from pPIC3.5-*Bcpg3* (Kars et al., 2005a) with primers AT261/269 and AT270/262, which were linked by overlap-PCR with primers AT261/262. The resulting mutant allele *Bcpg3*<sup>D353E/D354N</sup> was cloned into pGEM-T easy vector (Promega) and checked by sequencing. To generate N-terminal Myc-tagged BcPG3, wild-type and mutant alleles of *Bcpg3* were amplified from pPIC3.5-*Bcpg3* and pGEMT-*Bcpg3*<sup>D353E/D354N</sup> respectively with primers AT261/262 and linked with 10xMyc (derived from pGWB20 with primers AT263/264) by overlap-PCR with primers AT261/264, and subsequently cloned into pGEM-T easy vector and checked by sequencing. The *EcoRI/NotI*-digested fragments of *Bcpg3-myc* and *Bcpg3*<sup>D353E/D354N</sup>-*myc* derived from pGEM-T constructs were subcloned into the corresponding sites of pPIC3.5K (Invitrogen), yielding the *P. pastoris* expression vectors. The *Sall* linearized pPIC3.5K-*Bcpg3* and pPIC3.5K-*Bcpg3*<sup>D353E/D354N</sup> were used to transform *P. pastoris* GS115 by electroporation (Kars et al., 2005a).

The constructs generated are listed in Table S7, and primers used for cloning are shown in Table S8.

### **Transient expression in *Nicotiana benthamiana***

*A. tumefaciens* strains C58C1 (except for SERK2 and BAK1 that were in GV3101) were grown in LB medium supplemented with appropriate antibiotics at 28 °C for overnight. Cultures were harvested and resuspended in MMA medium (2.0% sucrose, 0.5% Murashige and Skoog salts without vitamins, 0.2% MES, 0.2 mM acetosyringone, pH 5.6) to OD<sub>600</sub> = 2.0. Cultures carrying pGWB20-*Bcpg3* were resuspended at an OD<sub>600</sub> = 0.2 and cultures carrying pZP-SERK2 or pZP-BAK1 were resuspended at an OD<sub>600</sub> = 0.5. For co-expression, two cultures carrying appropriate constructs were mixed in a 1:1 ratio, incubated for 2h and infiltrated into 6-week-old *N. benthamiana* leaves. Samples were collected 2 days after *Agro*-infiltration for co-immunoprecipitation analysis.

### **Immunoprecipitation and immunoblotting**

Immunoprecipitation was performed as described previously (Liebrand et al., 2012). *N. benthamiana* membrane fractions were extracted in extraction buffer (150 mM NaCl, 1.0% IGEPAL CA-630 [NP-40], 0.5% sodium deoxycholate, 0.1% SDS, 50 mM Tris, pH 8.0). After centrifugation at 14,000 rpm for 15 min, 15 µl of GFPTrap\_A beads (Chromotek) was added to the supernatant and incubated for 1 h at 4 °C. After washing the beads five times with extraction buffer, immunoprecipitated proteins were separated by 8% SDS-PAGE gels and electroblotted onto Immun-Blot polyvinylidene difluoride membranes (Bio-Rad) at 22 V overnight. Membranes were rinsed in TBS and blocked for 1 h in 5% skimmed milk in TBS-Tween (0.1% [v/v]). GFP-tagged proteins were detected with 1:5000 diluted anti-GFP-

HRP (MACS antibodies); whereas myc-tagged proteins were detected with 1:2000 diluted anti-myc (cMyc 9E10, sc-40, Santa Cruz) and subsequently with 1:2000 diluted anti-Mouse Ig-HRP (Amersham). SuperSignal west femto chemiluminescent substrate (Thermo) was applied for signal development.

### **Infection assay**

*Botrytis cinerea* strain B05.10 was used for infection on 5-6-week-old plants as described previously (Zhang and van Kan, 2013).

*Hyaloperonospora parasitica* isolate Maks9 (kindly provided by Dr. E. Holub, Warwick HRI) was maintained on *A. thaliana* accession Br-0. *H. parasitica* maintenance and infection were performed as described previously (van Damme et al., 2005) with minor modification. Plants were inoculated with spores ( $5 \times 10^4$  spores/ml) by using of a spray gun (Holub et al., 1994), air-dried for ~30 min, and incubated under a sealed lid at 100% relative humidity in a growth chamber at 16 °C with 9 h of light per day. Sporulation levels were quantified at 6 days post inoculation (dpi) by counting the number of sporangiophores per seedling.

*Phytophthora capsici* strain LT3112 was cultured as described previously (Huitema et al., 2011). Each leaf of 3-4-week old plants was inoculated with 2 µl of *P. capsici* zoospore suspension ( $10^5$  zoospores/ml) under a sealed lid at 100% relative humidity. Infection symptoms were scored for each leaf at 4 dpi.

*Pseudomonas syringae* pv. tomato DC3000 was used for infection on 5-week-old plants as described previously (Cabral et al., 2011). Infected leaf discs were collected at 0 and 2 days after bacterial infiltration. A total of five biological replicates, of three leaf discs each, were harvested per sample per time point.

### **Accession numbers**

Sequence data from Col-0 can be found in the Arabidopsis Genome Initiative databases under the following accession numbers: RLP39, At3g24900; RLP40, At3g24982; RLP41, At3g25010; RBPG1, At3g25020; SOBIR1, At2g31880; EFR, At5g20480; SERK2, At1g34210; BAK1/SERK3, AT4g33430.

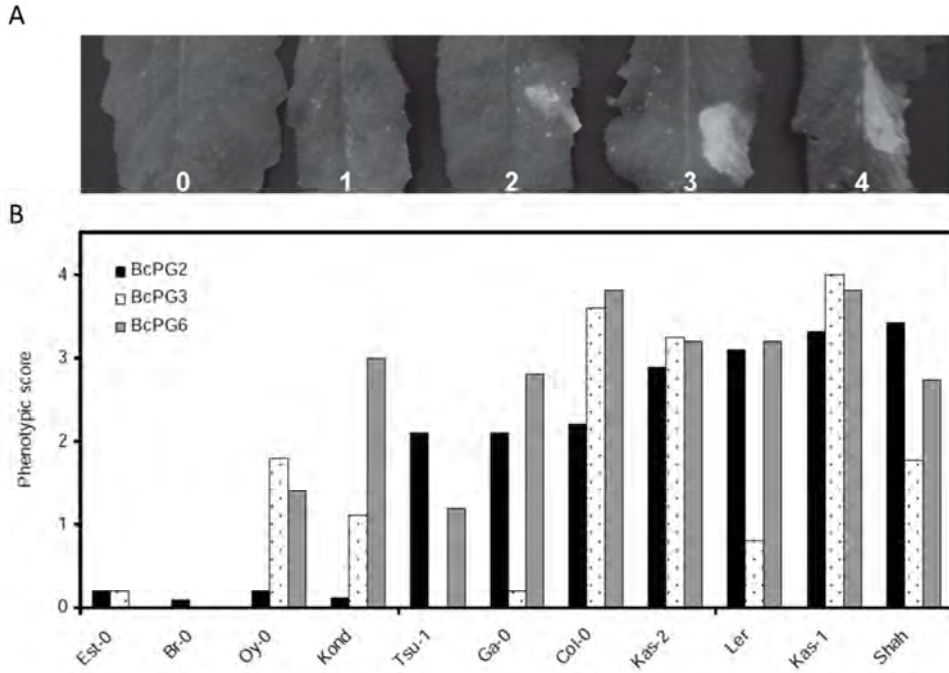
### **Supporting information**

Supplementary Figures S1, S2, S3, S4, S5 and Supplementary Table S1, S2, S3, S4, S5, S6, S7, S8.

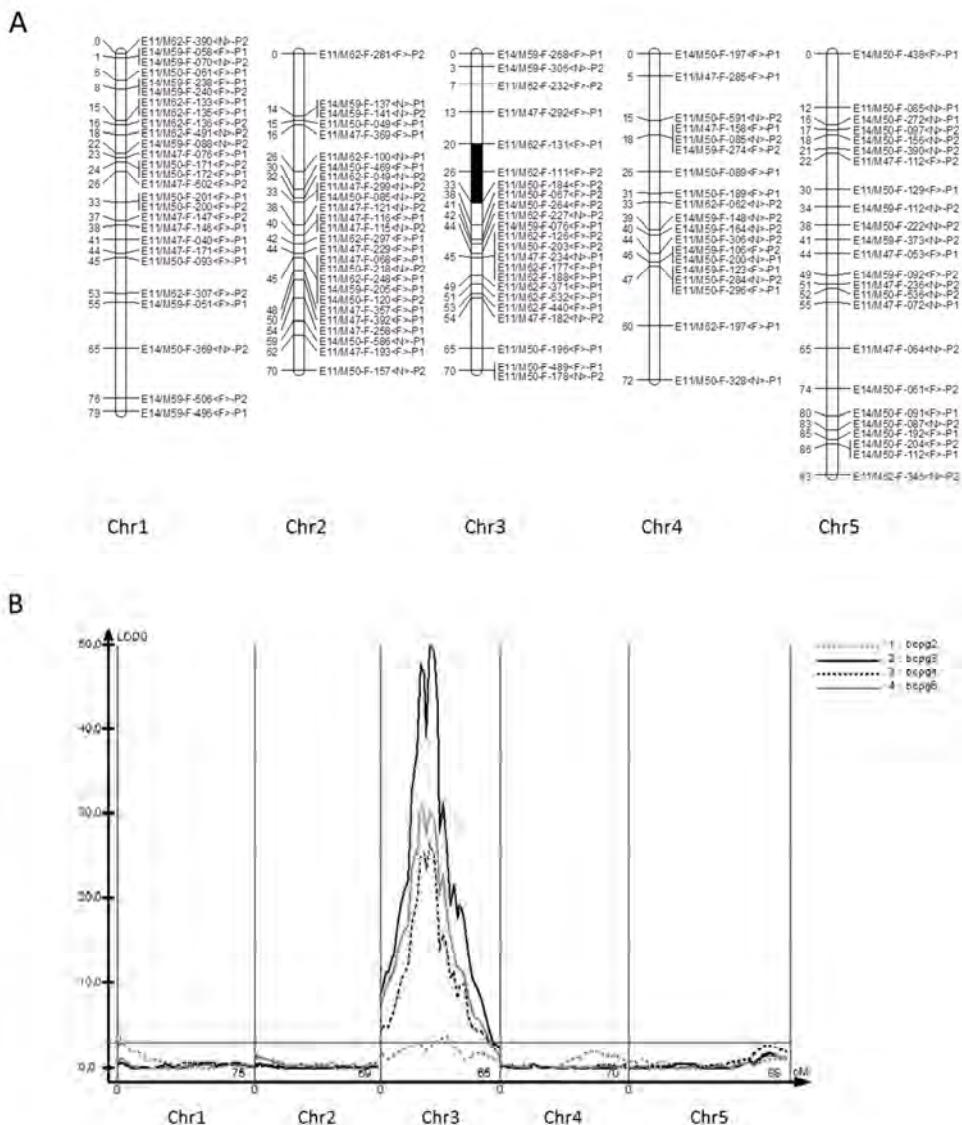
## Acknowledgments

We thank Maarten Koornneef, Corry Hanhart and Joost Keurentjens (WU Laboratory of Genetics) for providing *Arabidopsis thaliana* accessions; Geja Krooshof for providing the endo-PGs; Bob Schmitz and Joe Ecker (Salk Institute) for providing the Br-0 sequence reads; Catherine Albrecht and Sacco de Vries (WU Laboratory of Biochemistry) for providing SERK-GFP constructs; Silke Robatzek and Cyril Zipfel (Sainsbury Laboratory) for providing the EFR entry vector and *efr* mutant; Yuelin Zhang (University of British Columbia) for providing *sobir1-1* mutant; Ronnie de Jonge and Luigi Faino (WU Laboratory of Phytopathology) for assistance in genome sequence reassembly of accession Br-0; Rik van Wijk (currently at Nickerson-Zwaan Group) for assistance in QTL mapping analysis. Hanneke Witsenboer (Keygene N.V.) for facilitating the initial AFLP mapping. This research was partly funded by the Technology Foundation STW (project WGC05034), by the Technological Top Institute Green Genetics (TTI-GG, Project 2CC035RP), and the Netherlands Graduate School Experimental Plant Sciences.

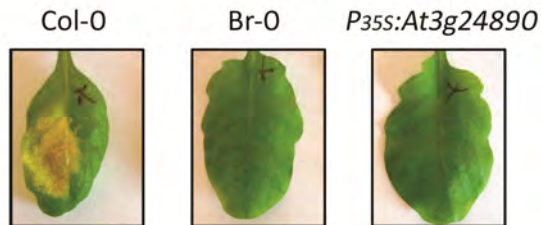
## Supporting information



**Supplementary Figure 1.** Responsiveness of *Arabidopsis thaliana* accessions to *Botrytis cinerea* endopolygalacturonases. A, the response was visually scored in five classes ranging from 0 to 4, with 0 = no symptoms, 1 = chlorotic spots within the infiltrated zone, 2 = chlorosis covering the infiltrated zone, 3 = abundant chlorosis with necrotic spots, 4 = complete necrosis. B, phenotypic score of the response of eleven selected *A. thaliana* accessions to *B. cinerea* endopolygalacturonases BcPG2, BcPG3, and BcPG6 (3 U/ml).

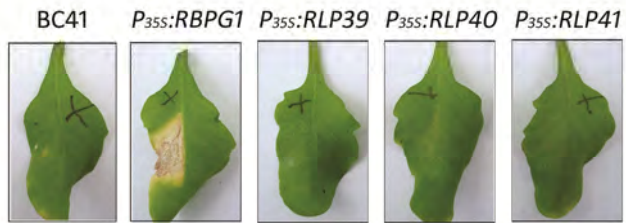


**Supplementary Figure 2.** QTL mapping of the *RBPG1* locus from the  $F_2$  population of Col-0 x Br-0. A, the AFLP linkage map showing the position of the QTL governing responsiveness to BcPG2, BcPG3, BcPG4, and BcPG6 (black bar). B, the log-likelihood (LOD) scores of the QTL. The grey horizontal line corresponds to the significance threshold of 3.3. The LOD scores per trait are: LOD=4 (BcPG2), LOD=52 (BcPG3), LOD=27 (BcPG4), LOD=31 (BcPG6).



**Supplementary Figure 3.** Responsiveness of *Arabidopsis thaliana* accessions Col-0 and Br-0, and Br-0 transgenic plants expressing  $P_{35S}:At3g24890$  to BcPG3. Photographed 7 days after infiltration with BcPG3.





**Supplementary Figure 5.** Responsiveness of *Arabidopsis thaliana* F<sub>8</sub> RIL line BC41 and BC41 transgenic plants expressing *P<sub>35s</sub>:RBPG1*, *P<sub>35s</sub>:RLP39*, *P<sub>35s</sub>:RLP40* and *P<sub>35s</sub>:RLP41* to BcPG3. Photographed 7 days after infiltration with BcPG3.

**Supplementary Table 1.** *Arabidopsis thaliana* accessions used in this study.

Accessions	Origin	Stock centre number
Br-0 <sup>a</sup>	Brno (Czech Republic)	N6626
Bs-1	Basel (Switzerland)	N6627
Cnt-1	Canterbury (UK)	N1635
Co-0	Coimbra (Portugal)	N6669
Col-0 <sup>a</sup>	Columbia (USA)	N907
Col-4	Columbia (USA)	N933
Ct-1	Catania (Italy)	N1094
Cvi	Cape Verdi Islands	N8580
Cvi-1 (bas)	Cape Verdi Islands	N8580
Di (Dijon-G)	Dijon (France)	N10159
Eden-2 <sup>b</sup>	Eden, N Sweden (Sweden)	CS76125
Ei-2	Eifel (Germany)	N6689
Ema-1	East Malling (UK)	N1637
En-2	Enkheim (Germany)	N1138
Eri	Eriengboda (Sweden)	N10042
Est-0 <sup>a</sup>	Estonia (Russia)	N6700
Est-1 <sup>b</sup>	Estonia (Russia)	CS76127
Ga-0 <sup>a</sup>	Gabelstein (Germany)	N6714
Ga-2	Gabelstein (Germany)	N10209
Gy-0	La Miniere (France)	N6732
Ka-0	Karnten (Austria)	N6752
Kas-1 <sup>a</sup>	Kashmir (India)	N903
Kas-2 <sup>a</sup>	Kashmir (India)	N1264
Kond <sup>a</sup>	Kondara (Tadjikistan)	N9175
Kyoto	Kyoto (Japan)	N10231
Ler <sup>a</sup>	Landsberg (Germany)	NW20
Ler Koornneef	Landsberg (Germany)	N8581
Li-0	Limburg (Germany)	N6775
Lip-0	Lipowiec/Chrzanow (Poland)	N6780
Lm-2	Le Mans (France)	N6784
Lz-0	Lezoux/Puy-de-Dome (France)	N6788
Ma-0	Marburg/Lahn (Germany)	N6789
Nd-0	Niederzenz (Germany)	N6803
Nd-1	Niederzenz (Germany)	N1636
No-0	Halle (Germany)	N1394
Nok-1	Noordwijk (Netherlands)	N6807
Oy-0 <sup>a</sup>	Oystese (Norway)	N6824
Pi-0	Pitztal Tirol (Austria)	N6832
Rld-1	Netherlands	N913
Rsch-0	Rschew/Starize (Russia)	N6848
Shah <sup>a</sup>	Pamiro-Alay (Tadjikistan)	N929

## Recognition of fungal endo-polygalacturonases by RBPG1

Stw-0	Stobowa (Poland)	N6865
Ts-1	Tossa del Mar (Spain)	N1552
Tsu-1 <sup>a</sup>	Tsu (Japan)	N1640
Wei-0	Weiningen (Switzerland)	N6182
Wei-1	Weiningen (Switzerland)	N1639
Wi-0	Wildbad (Germany)	N6920
Ws-1	Wassilewskija (Russia)	N2223
Wt-1	Wietze (Germany)	N1604

<sup>a</sup> Accessions representing the spectrum of variation in the responsiveness that were used in further studies.

<sup>b</sup> Accessions that were not included in the first screening.

**Supplementary Table 2.** Candidate genes in the *RBPG1* locus.

Gene	T-DNA mutant				Amino acid substitutions ( between Col-0 and Br-0)
	Number	Location	Genotype <sup>a</sup>	Phenotype <sup>b</sup>	
At3g24770	n.a.	-	-	-	Yes
At3g24780	SALK_082006	Exon	HM	Responsive	No
At3g24790	SALK_152499	Exon	HM	Responsive	No
At3g24800	SALK_049244	Exon	HT	Responsive	No
At3g24810	SALK_089717	5'-UTR	HM	Responsive	Yes
At3g24820	SALK_103742	5'-UTR	HM	Responsive	No
At3g24840	SAIL_1168_C04	Intron	HM	Responsive	Yes
	SALK_122535	Exon	HM	Responsive	
At3g24850	SALK_036306	Exon	HM	Responsive	Yes
At3g24860	SALK_038594	Exon	HM	Responsive	No
At3g24890	n.a.	-	-	-	n.i.
At3g24900	SALK_126505	Exon	HM	Responsive	n.i.
At3g24927	SAIL_544_G05	Exon	HM	Responsive	n.i.
At3g24982	GABI_564D03	Exon	HM	Responsive	n.i.
At3g25010	SALK_024020	Exon	HM	Responsive	n.i.
At3g25013	SALK_045377	Intron	HM	Responsive	n.i.
At3g25014	SALK_045377	5'-UTR	HM	Responsive	n.i.
At3g25020	n.a.	-	-	-	n.i.
At3g25030	SALK_091158	Exon	HM	Responsive	n.i.
At3g25040	GABI_044G01	5'-UTR	HM	Responsive	n.i.
At3g25050	SALK_106019	5'-UTR	HM	Responsive	n.i.
	SALK_032898	Exon	HM	Responsive	
At3g25060	SALK_083673	Exon	HM	Responsive	n.i.

n.a. No T-DNA insertion mutant available.

<sup>a</sup> T-DNA mutants are homozygous (HM) mutants or heterozygous (HT) mutants.

<sup>b</sup> The responsiveness of T-DNA mutants to BcPG3.

n.i. Sequence in Br-0 is not informative.

Recognition of fungal endo-polygalacturonases by RBPG1

**Supplementary Table 3.** Primers used in analysis of *Arabidopsis thaliana* homozygous T-DNA mutants.

Primer No.	Targeted gene	Sequence (5' - 3')	T-DNA mutant number
AT05	At3g24780 F	CTGCATCTACAAAGTATTCTAAC	SALK_082006
AT06	At3g24780 R	CTCGTGAGGTAACACAGCAC	
AT07	At3g24790 F	TGATCCTCCAGTGATTACCG	SALK_152499
AT08	At3g24790 R	CCCTATCGAACGACGAGGC	
AT11	At3g24800 F	GCAGTAAGGTTCCAGAAAACGCT	SALK_049244
AT12	At3g24800 R	CAAGCCTGTGGTCAGGAGTG	
AT13	At3g24810 F	GAGAGGGCCTTTGACACCTT	SALK_089717
AT14	At3g24810 R	TCTCTGTTGTTGCTGTTCTGC	
AT17	At3g24820 F	GACGACCACACATATGGTGAC	SALK_103742
AT18	At3g24820 R	TCGATCCATTCTCAAGCTATTC	
AT21	At3g24840 F	GATGATTATCATACCATGTTGAG	SAIL_1168_C04
AT22	At3g24840 R	GTCAGGATAGTTGTCACCGTC	
AT23	At3g24840 F	TCAGGACCTTGTAAATGCGAATG	SALK_122535
AT24	At3g24840 R	CTCCATCAGGTGATGACATATC	
AT27	At3g24850 F	GACTGATTCTGAGATCGAAGAC	SALK_036306
AT28	At3g24850 R	TGGACTCCACAGACGTCAAGA	
AT29	At3g24860 F	GCATCAACCTCCGCCGTCG	SALK_038594
AT30	At3g24860 R	ACAATCCTCCACCAACTCCAG	
AT91	At3g24900 F	AGTTCCTAACTCCTTTGTGCG	SALK_126505
AT92	At3g24900 R	CCATAGAAGTTGTTGAATGGAG	
AT39	At3g24927 F	GACTTGCCACGTGCTCTTTG	SAIL_544_G05
AT40	At3g24927 R	CAACAACGCAATAGGCTGCAC	
AT103	At3g24982 F	GTATTCCTGACAAGTATTATGAG	GABI_564D03
AT76	At3g24982 R	CAGAGAAGCTAGCCACTTCGG	
AT43	At3g25013/14 F	CGTTGTTGCGGCAGATTCTC	SALK_045377
AT44	At3g25013/14 R	TGAGAATTAACGCGATGATGAC	
AT77	At3g25010 F	GTCTATCTATGGAGCAAAAGTG	SALK_024020
AT78	At3g25010 R	TGCTCTTAATCAGACAAGCTAG	
AT47	At3g25030 F	GATGGTGGAGATAGGCTGAGA	SALK_091158
AT48	At3g25030 R	TCTTCCAACAACCTCCATCAATG	
AT49	At3g25040 F	TGGTCGGGCTAGAGGTGAAC	GABI_044_G01
AT50	At3g25040 R	GAACACTGGCTAGGTGAGTC	
AT53	At3g25050 F	CGGTTAGGCAGCAATCTAGAG	SALK_106019
AT54	At3g25050 R	AGAATGGAGTGTAGAAACATGAC	
AT53	At3g25050 F	CGGTTAGGCAGCAATCTAGAG	SALK_032898
AT90	At3g25050 R	GGCGTCCTTGGATTGAACC	
AT81	SALK line T-DNA	TGGTTCACGTAGTGGCCATCG	
AT82	SAIL line T-DNA	TTCATAACCAATCTCGATACAC	
AT83	GABI line T-DNA	CCCATTGGACGTGAATGTAGACAC	

## Chapter 2

**Supplementary Table 4.** The number of polymorphic AFLP markers found between the *Arabidopsis thaliana* accessions Col-0 and Br-0 using five primer combinations. The polymorphic markers were used to genetically analyse the Col-0 x Br-0 F<sub>2</sub> population. Selective nucleotides are given between brackets.

<i>EcoRI</i>	<i>MseI</i>			
	M47 (CAA)	M50 (CAT)	M59 (CTA)	M62 (CTT)
E11 (AA)	27	26	-	25
E14 (AT)	-	20	22	-

**Supplementary Table 5.** Primers used in genetic mapping.

Primer No.	SNP marker	Sequence (5'-3')*	Target allele
LZ6.7-1CF	6.7-1	GAGGAACAGTACCACAGAATCG	Col-0
LZ6.7-1CR		TTCGGTGACCGTGGTGAGAAT	Col-0
LZ6.7-1BF		GAGGAACAGTACCACAGAATCT	Br-0
LZ6.7-1BR		TTCGGTGACCGTGGTGAGAAA	Br-0
LZ 7.8-5 CF	7.8-5	CTTCATGTGGACGAATCGGT	Col-0
LZ 7.8-5 CR		CCAGCCTGTGCAAACCTG	Col-0
LZ 7.8-5 BF		CTTCATGTGGACGAATCGGC	Br-0
LZ 7.8-5 BR		CCAGCCTGTGCAAACCTA	Br-0
LZ7.8-7 CF	7.8-7	GGAACGGACGAACGGTTAGTC	Col-0
LZ7.8-7 BF		GGAACGGACGAACGGTTAGTG	Br-0
LZ7.8-7 R		GAATGGTAAGTACCAGTAACGTG	Col-0/Br-0
LZ9.10-2CF	9.10-2	CCCTCCATTACTTACTGAAGT	Col-0
LZ9.10-2CR		CCTCGCTACTTGGTTCGGCA	Col-0
LZ9.10-2BF		CCCTCCATTACTTACTGAAGC	Br-0
LZ9.10-2BR		CCTCGCTACTTGGTTCGGCC	Br-0

\* Letters in bold represent the polymorphic nucleotides between Col-0 and Br-0 alleles.

**Supplementary Table 6.** Primers used for Br-0 sequence assembly and confirmation.

Primer No.	Targeted fragment	Sequence (5'-3')*
AT199	assembleBrseq1 F	<b>GTTTTCCAGTCACGAC</b> GGATTTATAGTTCCAGTGAAGTG
AT200	assembleBrseq1 R	<b>CAGGAAACAGCTATGAC</b> GTTAGCTAAAACCATCATCTTCTC
AT201	assembleBrseq2 F	<b>GTTTTCCAGTCACGAC</b> GGCATAAGGACAAACACATTGG
AT202	assembleBrseq2 R	<b>CAGGAAACAGCTATGAC</b> AGGCACCACTGTGCAGTGAC
AT203	assembleBrseq3 F	<b>GTTTTCCAGTCACGAC</b> GCCGAGGAAGCCACTACTTG
AT204	assembleBrseq3 R	<b>CAGGAAACAGCTATGAC</b> CACTTAGCCACATACTCTTCTC
AT235	assembleBrseq4 F	<b>GTTTTCCAGTCACGAC</b> TACGCAATTCGGATCGAGTCC
AT206	assembleBrseq4 R	<b>CAGGAAACAGCTATGAC</b> TTCACTTCCGTTTAAAGCAAAGAC
AT207	assembleBrseq5 F	<b>GTTTTCCAGTCACGAC</b> TTCTTACTAACAACCTTCTAGTG
AT208	assembleBrseq5 R	<b>CAGGAAACAGCTATGAC</b> CTCAGTCAGTTTCGCAGAAGTG
AT209	assembleBrseq6 F	<b>GTTTTCCAGTCACGAC</b> TGCTAAGGTTAAGGCTCTAGTG
AT210	assembleBrseq6 R	<b>CAGGAAACAGCTATGAC</b> GAAGGAAATGCAGGGCTTTGTG
AT211	assembleBrseq7 F	<b>GTTTTCCAGTCACGAC</b> CTATTGCCAATCCAAGTAACAC
AT212	assembleBrseq7 R	<b>CAGGAAACAGCTATGAC</b> TCGGTGAGATCTTAGATTTGG
AT213	assembleBrseq8 F	<b>GTTTTCCAGTCACGAC</b> TGGACCGGTAAGTTGTTGTAG
AT214	assembleBrseq8 R	<b>CAGGAAACAGCTATGAC</b> TAAAGCATGCTTCTGAGTTAGAC
AT215	assembleBrseq9 F	<b>GTTTTCCAGTCACGAC</b> TCAAACGTACGGAAAATCTAGAC
AT216	assembleBrseq9 R	<b>CAGGAAACAGCTATGAC</b> CTCGGATTTGTCCACTAGAAG
AT217	assembleBrseq10 F	<b>GTTTTCCAGTCACGAC</b> CCCTTGAATTTTCAATGCTCCTTG
AT218	assembleBrseq10 R	<b>CAGGAAACAGCTATGAC</b> TGCCTACTGTCTATTGGAAGAC
AT219	assembleBrseq11 F	<b>GTTTTCCAGTCACGAC</b> GGTTTTGTATGAGTTGAAACAAGG
AT220	assembleBrseq11 R	<b>CAGGAAACAGCTATGAC</b> AAGTGTTAAACTGGAAGCAGTG
AT221	assembleBrseq12 F	<b>GTTTTCCAGTCACGAC</b> AAAGATCTTAACGGTTTCTGCTC
AT222	assembleBrseq12 R	<b>CAGGAAACAGCTATGAC</b> TCGGTGAGATCTTAGATTTGG
AT223	assembleBrseq13 F	<b>GTTTTCCAGTCACGAC</b> ATTACAGATTGAAAGAGGTATGTC
AT224	assembleBrseq13 R	<b>CAGGAAACAGCTATGAC</b> TACCTCCTCTTCAATTCCTTC
AT225	assembleBrseq14 F	<b>GTTTTCCAGTCACGAC</b> GGAGCCCAAATTGACTTGAGAG
AT226	assembleBrseq14 R	<b>CAGGAAACAGCTATGAC</b> GTTAAAAGAGTTCTTGTGGAAATC

\* Sequences in bold are M13 forward and reverse sequences for sequencing the amplified fragments, respectively.

Supplementary Table 7. Plasmids used in this study.

Plasmid name	Vector backbone	Application	Reference
pENTR-At3g24890	pDONR207	Entry vector for gateway clone	This study
pENTR-RLP39	pDONR207	Entry vector for gateway clone	This study
pENTR-RLP40	pDONR207	Entry vector for gateway clone	This study
pENTR-RLP41	pDONR207	Entry vector for gateway clone	This study
pENTR-RBPG1	pDONR207	Entry vector for gateway clone	This study
pENTR-rbpg1-2	pDONR207	Entry vector for gateway clone	This study
pENTR-RBPG1_Trunc1	pDONR207	Entry vector for gateway clone	This study
pENTR-RBPG1_Trunc2	pDONR207	Entry vector for gateway clone	This study
pENTR-rbpg1-2_Swap1	pDONR207	Entry vector for gateway clone	This study
pENTR-Bcpg3	pDONR207	Entry vector for gateway clone	This study
pMDC32-At3g24890	pMDC32	Overexpression in <i>Arabidopsis thaliana</i> (35S Pro)	This study
pMDC32-RLP39	pMDC32	Overexpression in <i>Arabidopsis thaliana</i> (35S Pro)	This study
pMDC32-RLP40	pMDC32	Overexpression in <i>Arabidopsis thaliana</i> (35S Pro)	This study
pMDC32-RLP41	pMDC32	Overexpression in <i>Arabidopsis thaliana</i> (35S Pro)	This study
pMDC32-RBPG1	pMDC32	Overexpression in <i>Arabidopsis thaliana</i> (35S Pro)	This study
pMDC32-rbpg1-2	pMDC32	Overexpression in <i>Arabidopsis thaliana</i> (35S Pro)	This study
pMDC32-RBPG1_Trunc1	pMDC32	Overexpression in <i>Arabidopsis thaliana</i> (35S Pro)	This study
pMDC32-RBPG1_Trunc2	pMDC32	Overexpression in <i>Arabidopsis thaliana</i> (35S Pro)	This study
pMDC32-rbpg1-2_Swap1	pMDC32	Overexpression in <i>Arabidopsis thaliana</i> (35S Pro)	This study
pBin-RLP39	psOL2095	Transient expression in <i>Nicotiana benthamiana</i> (35S Pro, C-eGFP)	This study
pBin-RLP40	psOL2095	Transient expression in <i>Nicotiana benthamiana</i> (35S Pro, C-eGFP)	This study
pBin-RLP41	psOL2095	Transient expression in <i>Nicotiana benthamiana</i> (35S Pro, C-eGFP)	This study
pBin-RBPG1	psOL2095	Transient expression in <i>Nicotiana benthamiana</i> (35S Pro, C-eGFP)	This study
pBin-rbpg1-2	psOL2095	Transient expression in <i>Nicotiana benthamiana</i> (35S Pro, C-eGFP)	This study
pBin-Bcpg3	psOL2095	Transient expression in <i>Nicotiana benthamiana</i> (35S Pro, C-eGFP)	This study
pBin-SOBIR1	psOL2095	Transient expression in <i>Nicotiana benthamiana</i> (35S Pro, C-eGFP)	Liebrand et al., submitted
pBin-EFR	psOL2095	Transient expression in <i>Nicotiana benthamiana</i> (35S Pro, C-eGFP)	This study
pZP-SERK2	pZP	Transient expression in <i>Nicotiana benthamiana</i> (35S Pro, C-eGFP)	Albrecht et al., 2008
pZP-BAK1	pZP	Transient expression in <i>Nicotiana benthamiana</i> (35S Pro, C-eGFP)	Albrecht et al., 2008
pgWB20-RLP39	pgWB20	Transient expression in <i>Nicotiana benthamiana</i> (35S Pro, C-10xMyc)	This study
pgWB20-RLP40	pgWB20	Transient expression in <i>Nicotiana benthamiana</i> (35S Pro, C-10xMyc)	This study
pgWB20-RLP41	pgWB20	Transient expression in <i>Nicotiana benthamiana</i> (35S Pro, C-10xMyc)	This study

pGWB20-RBPG1	pGWB20	Transient expression in <i>Nicotiana benthamiana</i> (35S Pro, C-10xMyc)	This study
pGWB20-rbpg1-2	pGWB20	Transient expression in <i>Nicotiana benthamiana</i> (35S Pro, C-10xMyc)	This study
pGWB20-Bcpg3	pGWB20	Transient expression in <i>Nicotiana benthamiana</i> (35S Pro, C-10xMyc)	This study
pGEM-Bcpg3 <sup>D353E/D354N</sup>	pGEM-T easy	Confirmation of sequence	This study
pGEM-Bcpg3-myc	pGEM-T easy	Confirmation of sequence	This study
pGEM-Bcpg3 <sup>D353E/D354N</sup> -myc	pGEM-T easy	Confirmation of sequence	This study
pPIC3.5K-Bcpg3-myc	pPIC3.5K	Protein production in <i>Pichia pastoris</i>	This study
pPIC3.5K-Bcpg3 <sup>D353E/D354N</sup> -myc	pPIC3.5K	Protein production in <i>Pichia pastoris</i>	This study

**Supplementary Table 8.** Primers used for plasmid construction.

Primer No.	Targeted gene	Sequence (5'-3')*
AT174	At3g24890 F	<i>GGGGACAAGTTTGTACAAAAAAGCAGGCTTCA</i> TGTTGGTGGATAGGAATGGC
AT176	At3g24890 R	<i>GGGGACCACCTTTGTACAAGAAAGCTGGGTCA</i> CGTAATCTTCTTCTTTCCAGT
AT188	RLP39 F	CTATATAATGCCAAATTAGATAGAC
AT189	RLP39 R	ATTAGGTCCTTTGTGATGATATGG
AT170	RLP40 F	TGGGGAGAGACGAAACATCTG
AT171	RLP40 R	AAAGAGTTATATTGTTTCAGTG
AT190	RLP41 F	GTTTCGTCAAATGATACGGTGG
AT191	RLP41 R	CAGTTTCAGATGTTTCGTCTC
AT172	RBPG1 F	GCATCTCCAATAATGATCATCAC
AT173	RBPG1 R	GTATAAGCAAATTAGATATGCTACG
AT192	RLP39 F	<i>GGGGACAAGTTTGTACAAAAAAGCAGGCTTCA</i> TGTTCTGAATTTGCTTTCCGTTTTG
AT193	RLP39 R	<i>GGGGACCACCTTTGTACAAGAAAGCTGGGTCA</i> TGGTTTCTGCTGAAACAGAA
AT194	RLP40 F	<i>GGGGACAAGTTTGTACAAAAAAGCAGGCTTCA</i> TGTTCTGAATTTGCTTTCCAGTTTTG
AT195	RLP40 R	<i>GGGGACCACCTTTGTACAAGAAAGCTGGGTCA</i> CAAGTTTCTGCTTTAATTACCAG
AT196	RLP41/rbpg1-2 F	<i>GGGGACAAGTTTGTACAAAAAAGCAGGCTTCA</i> TGTTCTGAATTTGCTTTCCGTTTT
AT198	RLP41 R	<i>GGGGACCACCTTTGTACAAGAAAGCTGGGTCA</i> CGGTTTCTGCTTTAATCAGAC
AT177	RBPG1 F	<i>GGGGACAAGTTTGTACAAAAAAGCAGGCTTCA</i> TGTTCTAAATCGCTTTGGGTTTTG
AT178	RBPG1 R	<i>GGGGACCACCTTTGTACAAGAAAGCTGGGTCA</i> TACTCAAACCAAAAAAAGATCGT
AT250	rbpg1-2 R	<i>GGGGACCACCTTTGTACAAGAAAGCTGGGTCA</i> CGGTTTCTGCTTTAATCAGAT
AT251	RBPG1 R	<i>GGGGACCACCTTTGTACAAGAAAGCTGGGTCA</i> CGCTGCTGGTTGATGAAG
AT252	RBPG1 R	<i>GGGGACCACCTTTGTACAAGAAAGCTGGGTCA</i> CGCTGCTTTAACCAACAATAAG
AT254	rbpg1-2 R	<i>GGGGACCACCTTTGTACAAGAAAGCTGGGTCA</i> TACTCAAACCAAAAAAAGATCGTAACGGGTTGTTTCTGCTTTAATCAGATAAGC
AT265	Bcpg3 F	<i>GGGGACAAGTTTGTACAAAAAAGCAGGCTTCA</i> TGGGATTTGTTCTCTTTTCACAA
AT268	Bcpg3 R	<i>GGGGACCACCTTTGTACAAGAAAGCTGGGTCA</i> TGATGGGCATCCAGTAGATGG
AT261	Bcpg3 F	<b>GAATTC</b> ATGCGTTCTGCGATCATCCTC
AT262	Bcpg3 R	CACCGTTAAITTAACCCGCTGTTCCATGGTGGATGGGCATCCAGTAGATGG
AT263	10xMyc F	CCATCTACTGGATGCCATCACCATGGAACAGCGGGTTAATAACGGTG
AT264	10xMyc R	<b>CGGGCCGCGGG</b> AAATTCGAGCTTAAGC
AT269	Bcpg3 R	CACCTTCCGTCGCCAAAATTGGCAACCCAGACCATGAT
AT270	Bcpg3 F	<i>GGGGACCACCTTTGTACAAGAAAGCTGGGTCA</i> TGGATGGGCATCCAGTAGATGG

\* Restriction sites for cloning are in bold; the *attB1* and *attB2* sites are indicated in italic, respectively.

# CHAPTER 3

## The D-galacturonic acid catabolic pathway in *Botrytis cinerea*

Lisha Zhang, Harry Thiewes and Jan A. L. van Kan

This chapter is published as:

Zhang, L., Thiewes, H. and van Kan, J.A.L. (2011) The D-galacturonic acid catabolic pathway in *Botrytis cinerea*. *Fungal Genet. Biol.* 48, 990-997.

## Abstract

D-galacturonic acid is the most abundant component of pectin, one of the major polysaccharide constituents of plant cell walls. D-galacturonic acid potentially is an important carbon source for microorganisms living on (decaying) plant material. A catabolic pathway was proposed in filamentous fungi, comprising three enzymatic steps, involving D-galacturonate reductase, L-galactonate dehydratase, and 2-keto-3-deoxy-L-galactonate aldolase. We describe the functional, biochemical and genetic characterization of the entire D-galacturonate-specific catabolic pathway in the plant pathogenic fungus *Botrytis cinerea*. The *B. cinerea* genome contains two non-homologous galacturonate reductase genes (*Bcgar1* and *Bcgar2*), a galactonate dehydratase gene (*Bclgd1*), and a 2-keto-3-deoxy-L-galactonate aldolase gene (*Bclga1*). Their expression levels were highly induced in cultures containing D-galacturonic acid, pectate, or pectin as the sole carbon source. The four proteins were expressed in *Escherichia coli* and their enzymatic activity was characterized. Targeted gene replacement of all four genes in *B. cinerea*, either separately or in combinations, yielded mutants that were affected in growth on D-galacturonic acid, pectate, or pectin as the sole carbon source. In *Aspergillus nidulans* and *A. niger*, the first catabolic conversion only involves the *Bcgar2* ortholog, while in *Hypocrea jecorina*, it only involves the *Bcgar1* ortholog. In *B. cinerea*, however, BcGAR1 and BcGAR2 jointly contribute to the first step of the catabolic pathway, albeit to different extent. The virulence of all *B. cinerea* mutants in the D-galacturonic acid catabolic pathway on tomato leaves, apple fruit and bell peppers was unaltered.

## Introduction

D-galacturonic acid is the major component of the plant cell wall polysaccharide pectin. Consequently, D-galacturonic acid potentially is an important carbon source for microorganisms living on plant material, either as a saprotroph or a pathogen (Richard and Hilditch, 2009). For bacteria, a catabolic pathway has been described in which five enzymes convert D-galacturonic acid to pyruvate and glyceraldehyde-3-phosphate, via the intermediate metabolites D-tagaturonate, D-altronate, 2-keto-3-deoxy-gluconate and 2-keto-3-deoxy-6-phospho-gluconate (Richard and Hilditch, 2009).

A different catabolic pathway occurs in filamentous fungi. Early studies in *Aspergillus nidulans* cultured on D-galacturonic acid as sole carbon source showed that mutants in pyruvate dehydrogenase or pyruvate carboxylase were unable to grow, whereas a pyruvate kinase mutant remained able to use this carbon source. These observations suggested that in *A. nidulans*, D-galacturonic acid is metabolized through a non-phosphorylating pathway which yields glyceraldehyde and pyruvate (Hondmann et al., 1991; Uitzetter et al., 1986; Visser et al., 1988). It was also shown that an NADPH-dependent glycerol dehydrogenase was induced on D-galacturonic acid (Sealy-Lewis and Fairhurst, 1992). The non-phosphorylating pathway in fungi was supported by more recent studies on *Hypocrea jecorina* (anamorph *Trichoderma reesei*). In *H. jecorina*, D-galacturonic acid is first converted to L-galactonate by GAR1, a galacturonate reductase (Kuorelahti et al., 2005). Deletion of the *gar1* gene in *H. jecorina* severely compromised the ability to grow on D-galacturonic acid as the sole carbon source (Mojzita et al., 2010). The second enzyme of the pathway is L-galactonate dehydratase (LGD1), which converts L-galactonate to 2-keto-3-deoxy-L-galactonate. The *H. jecorina* *lgd1* deletion mutant could not grow on D-galacturonic acid (Kuorelahti et al., 2006). The next enzyme in the pathway was identified as 2-keto-3-deoxy-L-galactonate aldolase (LGA1) which splits 2-keto-3-deoxy-L-galactonate into pyruvate and L-glyceraldehyde (Hilditch et al., 2007). Deletion of the *lga1* gene resulted in the intracellular accumulation of 2-keto-3-deoxy-L-galactonate (Wiebe et al., 2010). It was also reported that an NADPH-dependent glycerol dehydrogenase (GLD1) is involved in the conversion of L-glyceraldehyde to glycerol as the final step of this pathway (Liepins et al., 2006). The D-galacturonic acid catabolic pathway in filamentous fungi, as proposed by Richard and Hilditch (2009) is summarized in Figure 1.

Transcriptome analysis of *A. niger* grown in liquid medium containing pectic substrates showed that four genes, designated as *gaaA*, *gaaB*, *gaaC* and *gaaD*, were upregulated during growth on pectin or D-galacturonic acid (Martens-Uzunova and Schaap, 2008). Interestingly, the *A. niger* *gaaA* and *gaaC* genes are in the same locus, but transcribed in opposite direction, sharing the same promoter region. The *A. niger* *gaaA* gene was shown

to encode an active galacturonate reductase, yet the gene is not homologous to *H. jecorina gar1* and the *A. niger* GAAA protein has properties distinct from the *H. jecorina* GAR1 protein (Martens-Uzunova and Schaap, 2008). The *A. niger* genome contains an ortholog of *H. jecorina gar1*, designated *A. niger gar1*, located on a different scaffold and its expression is not strongly induced by D-galacturonic acid (Martens-Uzunova and Schaap, 2008). A gene that is orthologous to *A. niger gaaA* exists in *H. jecorina*, and is designated as *gar2* with unknown function (Richard and Hilditch, 2009).

*Botrytis cinerea*, a necrotrophic plant pathogenic fungus, is able to infect a wide range of plant species and tissues. It often penetrates host tissues at the anticlinal cell wall and subsequently grows into and through the middle lamella, which consists mostly of pectin. Throughout the infection process, *B. cinerea* secretes a series of cell wall-degrading enzymes (CWDEs) to break down plant cell wall polymers for plant surface penetration, tissue invasion and nutrient release (van Kan, 2006; Williamson et al., 2007). Among these CWDEs, several pectinases have been found to be abundant during infection, including pectin and pectate lyases, pectin methylesterases (PMEs), exopolygalacturonases (exo-PGs) and endopolygalacturonases (endo-PGs) (Cabanne and Doneche, 2002; Kars et al., 2005b; Kars and van Kan, 2004; Rha et al., 2001; ten Have et al., 2001). The *B. cinerea* genome contains six genes encoding endo-PGs (Wubben et al., 1999), of which *Bcpg1* and *Bcpg2* are important for virulence (Kars et al., 2005a; ten Have et al., 1998). Although the expression profiles of the *Bcpg* genes and the biochemical properties of the enzymes have been well studied and the importance of pectin degradation for virulence of *B. cinerea* has been documented (Kars et al., 2005a; ten Have et al., 1998), little is known about how *B. cinerea* utilizes the ultimate hydrolytic product of pectin (i.e. D-galacturonic acid) for its growth. We performed a genetic and biochemical characterization of the D-galacturonic acid catabolic pathway in *B. cinerea*. The genes were identified and their expression was investigated during growth on different carbon sources. The enzymatic activity of recombinant proteins was characterized, and the function of the genes in *B. cinerea* was studied by generating single and double deletion mutants and testing them *in vitro* and *in planta*.

## Results

### Identification of *B. cinerea* genes involved in D-galacturonic acid catabolism

Blast analysis of genome databases with *H. jecorina* GAR1 and *A. niger* GAAA, GAAB, GAAC, and GAAD protein sequences identified the homologous genes in *B. cinerea*, which were designated as *Bcgar1*, *Bcgar2*, *Bclgd1*, *Bclga1*, and *Bcglr1*, respectively. The gene names and locus tags are listed in Figure 1. The open reading frame (ORF) of *Bcgar1*, which is interrupted by three introns, is 933 bp and encodes a predicted protein of 310 aa with 68% identity to *A. niger* GAR1 and 66% identity to *H. jecorina* GAR1. The ORF of *Bcgar2*, which is interrupted by one intron, is 1266 bp and encodes a predicted protein of 421 aa with 73% identity to *A. niger* GAAA and 74% identity to *H. jecorina* GAR2. Sequence identity between BcGAR1 and BcGAR2 is lower than 5% (Figure S1). The ORF of *Bclgd1*, which is interrupted by two introns, is 1353 bp and encodes a predicted protein of 450 aa with 77% identity to *A. niger* GAAB and 84% identity to *H. jecorina* LGD1. The ORF of *Bclga1* lacks an intron, is 978 bp and encodes a predicted protein of 325 aa with 60% identity to *A. niger* GAAC and 71% identity to *H. jecorina* LGA1. The ORF of *Bcglr1*, which is interrupted by one intron, is 975 bp and encodes a predicted protein of 324 aa with 43% identity to *A. niger* GAAD and 44% identity to *H. jecorina* GLD1. *Bcgar2* and *Bclga1* are located in the same genomic locus sharing the same promoter region (Martens-Uzunova and Schaap, 2008), whereas *Bcgar1* is located elsewhere in the genome (Figure 1).

### Expression profile of *B. cinerea* genes involved in D-galacturonic acid catabolism

To investigate the expression profile of *Bcgar1*, *Bcgar2*, *Bclgd1*, *Bclga1* and *Bcglr1* in *B. cinerea*, their mRNA level was determined by real-time PCR in cultures containing glucose, D-galacturonic acid, pectate, or citrus fruit pectin as sole carbon source, respectively. Cultures were first grown in glucose-containing medium and transferred to fresh medium with the different carbon sources mentioned, and sampled at 3 h and 9 h after transfer for transcript analysis (Figure 2). *Bcgar1* was induced ~10 fold, while *Bcgar2*, *Bclgd1*, and *Bclga1* were strongly (30~100 fold) induced in cultures with D-galacturonic acid, pectate, and pectin as carbon source at 3 h after transfer, compared to continuous growth in glucose-containing culture. For every gene, the transcript level was higher at 3 h after transfer than that at 9 h after transfer (Figure 2). Also *Bcglr1* transcript was induced in cultures with D-galacturonic acid, pectate, and pectin as carbon source at 3 h compared to that in glucose-containing culture (Figure 2). Besides the BcGLR1 protein, there could be unspecific dehydrogenases that are active on L-glyceraldehyde, therefore we considered that *Bcglr1* is not specific for galacturonic acid catabolism, and we focused on *Bcgar1*, *Bcgar2*, *Bclgd1*, and *Bclga1* for further studies.

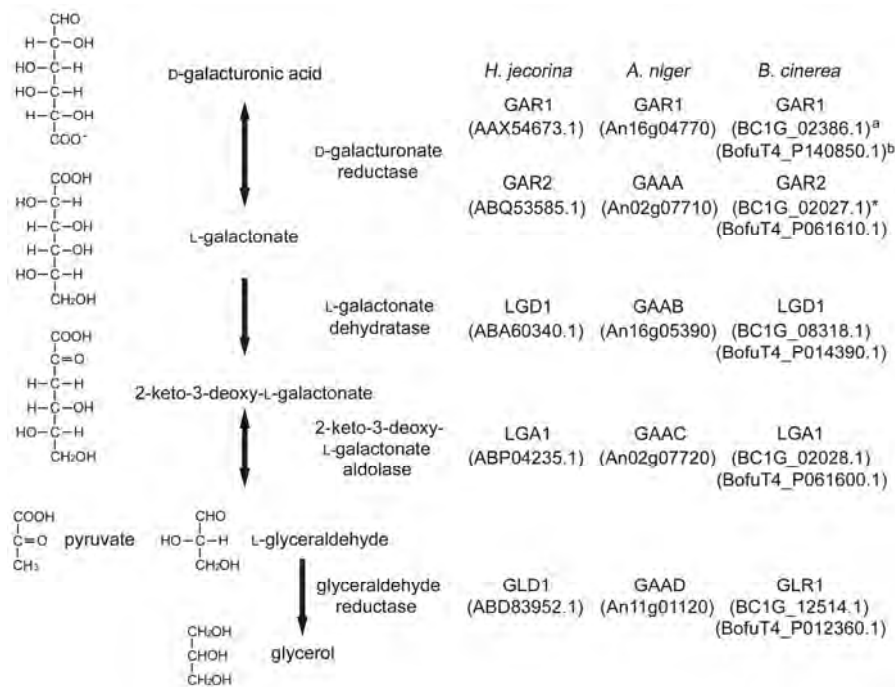


**Figure 1.** D-galacturonic acid catabolic pathway in fungi (proposed by Richard and Hilditch, 2009). *H. jecorina*, *A. niger*, and *B. cinerea* homologues for each step are listed. <sup>a</sup>Locus ID of *B. cinerea* strain B05.10. <sup>b</sup>Locus ID of *B. cinerea* strain T4. <sup>\*</sup>Structural misannotation.

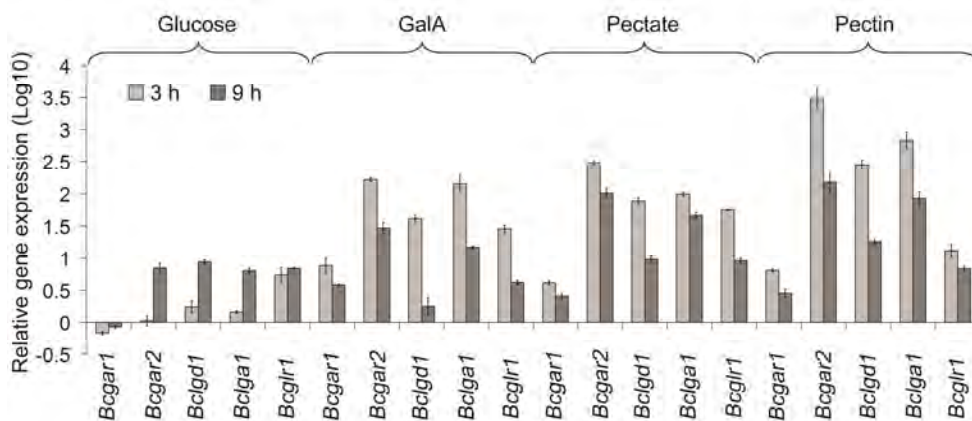


**Figure 2.** Relative transcript levels of D-galacturonic acid catabolism genes in different carbon sources as assessed by real-time PCR. Cultures were sampled for RNA extraction at 0, 3 or 9 h after transfer from a pre-culture with glucose as carbon source. mRNA levels of the genes were normalized to the constitutive reference gene *Bcrp15* and time point 0, according to the  $2^{-\Delta\Delta Ct}$  method. Data are represented as mean  $\pm$  standard error. Two independent biological repeats were performed and four technical replicates of each repeat were analysed.

### Biochemical characterization of BcGAR1, BcGAR2, BcLGD1 and BcLGA1

To investigate whether the proteins encoded by *Bcgar1*, *Bcgar2*, *Bclgd1* and *Bclga1* have the biochemical activities predicted from the sequence, the ORFs were cloned. The proteins were produced in *E. coli* with an N-terminal histidine tag and purified by affinity chromatography. Migration on SDS-PAGE gels of the purified BcGAR1, BcGAR2, BcLGD1 and BcLGA1 was slightly faster than expected based on the predicted molecular masses of 36.9 kDa, 49.2 kDa, 52.4 kDa and 38.5 kDa, respectively (Figure 3A). The activities of recombinant BcGAR1 and BcGAR2 were measured by monitoring the decrease of cofactor NADPH with D-galacturonic acid as substrate (Figure 3B and C). Similar enzyme activities of BcGAR1 and BcGAR2 were observed using either D-galacturonic acid (Figure 3B and C) or D-glucuronic acid (GlucA) as substrate (Figure S2A and S2B), respectively. The Michaelis-Menten constants of BcGAR1 and BcGAR2 for D-galacturonic acid are 2.5 mM and 0.12 mM, and for D-glucuronic acid they are 1.4 mM and 1.0 mM, respectively.

The enzyme activity of recombinant BcLGD1 was measured by coupling it with the reductase reaction (performed with BcGAR1) using either D-galacturonic acid or D-glucuronic acid as substrate (Figure 3D and S2C). BcLGD1 was able to use as substrates both L-galactonate and L-gulonate, originating from the conversion by BcGAR1 of D-galacturonic acid or D-glucuronic acid, respectively.

As the substrate for 2-keto-3-deoxy-L-galactonate aldolase (LGA) activity in the forward direction is not commercially available, the enzyme activity of recombinant BcLGA1 was measured in the reverse direction using pyruvate and DL-glyceraldehyde as substrates (Figure 3E). The BcLGA1 reaction reached equilibrium within 30 min with 5 µg protein (Figure 3E). No activity was observed in reactions without enzyme or with heat-inactivated enzyme for BcGAR1, BcGAR2, BcLGD1 and BcLGA1 (not shown).

### Effect of the deletion of *Bcgar1*, *Bcgar2*, *Bclgd1*, and *Bclga1* on D-galacturonic acid catabolism

To determine the functions of *Bcgar1*, *Bcgar2*, *Bclgd1*, and *Bclga1* on D-galacturonic acid catabolism in *B. cinerea*, deletion mutants were created by replacing the coding region of each gene with the hygromycin phosphotransferase resistance gene (*HPH*) in *B. cinerea* wild-type strain B05.10 background (Figure S3). *Bcgar1* and *Bcgar2* double-deletion mutants ( $\Delta Bcgar1/\Delta Bcgar2$ ) were created by replacing the coding region of *Bcgar1* with the nourseothricin resistance gene (*NAT*) in a  $\Delta Bcgar2$  mutant background (Figure S3). Since *Bcgar2* and *Bclga1* are located in the same locus, double-deletion mutants of both genes ( $\Delta Bcgar2/\Delta Bclga1$ ) were generated in a single step using *HPH* as selection marker, in a wild-type background (Figure S3E). Between 3 and 8 independent deletion mutants

were obtained for each target gene or combination of genes; in each case, two independent mutants were characterized in detail at molecular level and phenotypically. Figure S3F-G shows the verification by PCR of two independent mutants for each type of deletion that was generated. Southern blot hybridization showed that a single homologous integration event, without additional ectopic integration, occurred in all the mutants except for  $\Delta Bcgar2$ -6 and  $\Delta Bclgd1$ -4 (not shown).

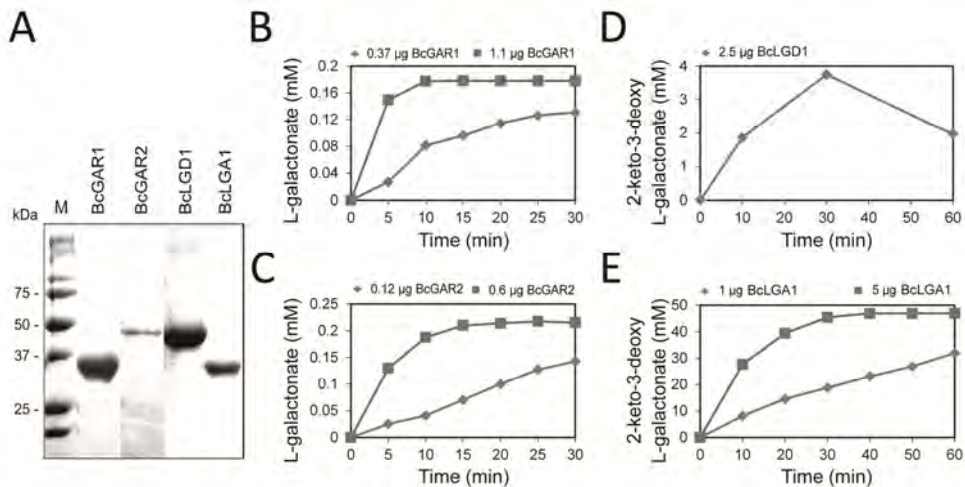


**Figure 3.** SDS-PAGE and enzymatic activity of purified proteins. A, SDS-PAGE showing Coomassie brilliant blue R250-stained purified proteins. B and C, recombinant BcGAR1 and BcGAR2 activities were determined by monitoring the decrease of NADPH absorbance at 340 nm. NADPH (0.25 mM) and D-galacturonic acid (50 mM) were added at t=0. The increase in L-galactonate was proportional to the decrease in NADPH. D and E, recombinant BcLGD1 and BcLGA1 activities were determined by monitoring the increase of 2-keto-3-deoxy-L-galactonate. For each enzyme activity, at least two independent measurements were performed with independently isolated and purified enzyme batches. Biological replicates showed similar curves, of which one is presented.

Radial growth assays revealed that all the deletion mutants grew almost equally as the wild-type strain B05.10 on glucose-containing medium. The  $\Delta Bclgd1$ ,  $\Delta Bclga1$ ,  $\Delta Bcgar1/\Delta Bcgar2$  and  $\Delta Bcgar1/\Delta Bclga1$  mutants were however completely unable to grow on D-galacturonic acid as the sole carbon source (Figure 4A).  $\Delta Bcgar1$  mutants showed similar growth to B05.10 and  $\Delta Bcgar2$  mutants showed a slight reduction of colony diameter compared to B05.10 on D-galacturonic acid as sole carbon source (Figure 4A). To confirm and independently quantify the growth reduction of the mutants, fungal biomass accumulation was monitored in liquid culture containing D-galacturonic acid as the sole carbon source. The  $\Delta Bcgar2$  mutants showed > 90% reduction of biomass after 3

days culture compared to B05.10, while  $\Delta Bclgd1$ ,  $\Delta Bclga1$ , and  $\Delta Bcgar2/\Delta Bclga1$  mutants showed no detectable biomass accumulation (Figure 4B). Complementation of the  $\Delta Bcgar2$ ,  $\Delta Bclgd1$ , and  $\Delta Bclga1$  mutants by a wild-type gene construct restored the growth both on D-galacturonic acid plates (Figure 4A) and in liquid culture (Figure 4B), respectively. These results indicate that there is only one D-galacturonic acid catabolism pathway in *B. cinerea*, which involves *Bcgar1*, *Bcgar2*, *Bclgd1*, and *Bclga1*; furthermore, *Bcgar1* and *Bcgar2* are both involved in the first step of the pathway, and they are able to (partially) complement each other's function.

#### **Growth of *Bcgar1*, *Bcgar2*, *Bclgd1*, and *Bclga1* deletion mutants on pectic substrates**

In order to assess whether the deletion of *Bcgar1*, *Bcgar2*, *Bclgd1*, and *Bclga1* affects the ability of *B. cinerea* to use pectin, we compared the growth of these mutants with the wild-type strain B05.10 on plates containing pectate (the linear polymer of D-galacturonic acid), apple pectin (with 61% D-galacturonic acid), or citrus fruit pectin (with 78% D-galacturonic acid) as the sole carbon source. The  $\Delta Bclgd1$ ,  $\Delta Bclga1$ ,  $\Delta Bcgar1/\Delta Bcgar2$  and  $\Delta Bcgar1/\Delta Bclga1$  mutants were unable to grow on pectate as the sole carbon source, whereas  $\Delta Bcgar1$  and  $\Delta Bcgar2$  single mutants showed similar growth to B05.10. Complementation of  $\Delta Bcgar2$ ,  $\Delta Bclgd1$ , and  $\Delta Bclga1$  mutants with the respective wild-type gene restored the impaired growth (Figure 4A). These results were in agreement with their growth on D-galacturonic acid (Figure 4A).  $\Delta Bclgd1$ ,  $\Delta Bclga1$ ,  $\Delta Bcgar1/\Delta Bcgar2$  and  $\Delta Bcgar1/\Delta Bclga1$  mutants showed about 50% and 75% reduced colony diameter on apple pectin and citrus pectin (Figure 4A), respectively. These results indicate that the deletion of *Bcgar1*, *Bcgar2*, *Bclgd1*, and *Bclga1* results in the impaired ability to use pectate and pectin. The extent of growth reduction of the mutants on pectic substrates was positively correlated to the proportion of D-galacturonic acid in the substrate. Apple pectin contains approximately 61% of D-galacturonic acid (and 27% of neutral sugars), whereas citrus pectin contains 78% of D-galacturonic acid (and 9% of neutral sugars), and growth of the mutants on apple pectin was consistently better than on citrus pectin. Growth of the mutants on sodium pectate, which contains no neutral sugars, was negligible.

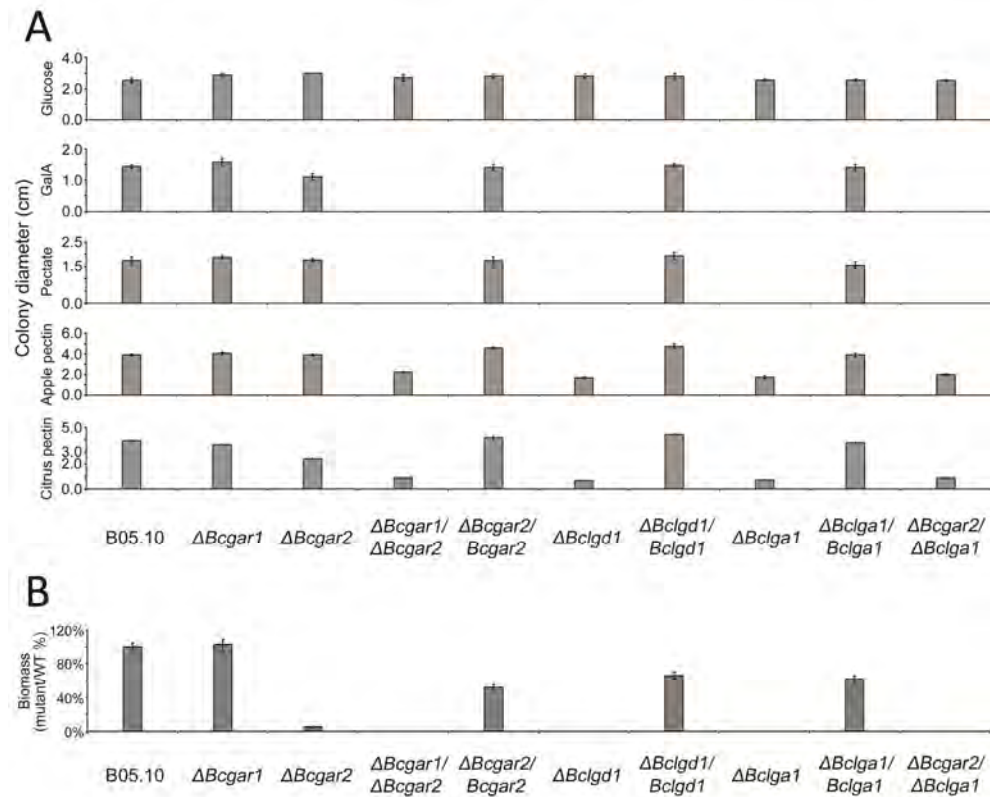


**Figure 4.** Effect of the deletion of *Bcgar1*, *Bcgar2*, *Bclgd1*, and *Bclga1* on growth of *B. cinerea* on agar medium containing various carbon sources. A, colony diameter of B05.10 and all the mutants strains on plates containing either glucose, D-galacturonic acid, pectate, apple pectin, or citrus pectin as the sole carbon source. B, the comparison of biomass of mutant strains and wild-type strain B05.10 in liquid culture containing D-galacturonic acid (D-GalA) as the sole carbon source. Two independent deletion mutants of each gene or gene-combinations were analysed and showed similar results, results of one mutant are presented.

### Virulence of mutants

The virulence of  $\Delta Bcgar1/\Delta Bcgar2$ ,  $\Delta Bclgd1$ ,  $\Delta Bclga1$ , and  $\Delta Bcgar1/\Delta Bclga1$  mutants was investigated on different plant species and tissues. There was no difference in lesion sizes between any of the tested mutants and the wild-type strain B05.10 on tomato leaves, apple fruit or bell peppers (not shown).

## Discussion

In this study, we have genetically and biochemically characterized the D-galacturonic acid catabolic pathway in *B. cinerea*, which consists of three steps involving 4 genes: *Bcgar1*, *Bcgar2*, *Bclgd1*, and *Bclga1*. Richard and Hilditch (2009) proposed that an L-glyceraldehyde reductase (GLR1) also is involved in the D-galacturonic acid catabolic pathway; however, since there might be unspecific dehydrogenases that are also active with L-glyceraldehyde, this step is not specifically dedicated to D-galacturonic acid catabolism. Hence, *Bcglr1* was not considered as part of the D-galacturonic acid-specific catabolic pathway in *B. cinerea* and we did not study it in detail. The expression of *Bcgar1*, *Bcgar2*, *Bclgd1*, and *Bclga1* is co-regulated by D-galacturonic acid, although transcript levels of *Bcgar1* following transfer to D-galacturonic acid-containing medium were (much) lower than of *Bcgar2*. These results are in agreement with the microarray data in *A. niger*, where *gaaA* to *gaaD* were reported to be highly expressed during growth on D-galacturonic acid, whereas *gar1* was not strongly induced by D-galacturonic acid (Martens-Uzunova and Schaap, 2008). Among the genes that were co-expressed in *A. niger* during growth on D-galacturonic acid are two hexose transporter genes, An14g04280 and An03g01620 (Martens-Uzunova and Schaap, 2008). It is plausible to suggest that these genes encode D-galacturonic acid transporters. We identified the *B. cinerea* orthologs of these *A. niger* genes, BC1G\_12561.1 (*Bchxt15*; (Dulermo et al., 2009)) and BC1G\_08389.1 (*Bchxt18*; our annotation), and observed that their transcript levels were induced by D-galacturonic acid as well (not shown). Further studies will need to elucidate whether BcHXT15 and BcHXT18 could be the *B. cinerea* D-galacturonic acid transporters involved in the uptake of D-galacturonic acid from the environment prior to its entry into the catabolic pathway.

*A. nidulans* mutant strain WG222 is unable to grow on D-galacturonic acid as sole carbon source, since it has a nonsense mutation in the *gaaA* gene (homologous to *Bcgar2*). The *A. nidulans* genome contains a gene homologous to *Bcgar1*, ANIA\_05986, but this gene is unable to compensate for the lack of D-galacturonic acid reductase activity in the *gaaA* mutant (Martens-Uzunova and Schaap, 2008). By contrast, deletion of the *gar1* gene in *H. jecorina* led to at least six-fold lower biomass accumulation during growth on D-galacturonic acid (Mojzita et al., 2010) and the *H. jecorina gar2* gene (Richard and Hilditch, 2009) is insufficient to support substantial growth on D-galacturonic acid. In the case of *B. cinerea*, however, two genes encoding non-homologous galacturonate reductases (Figure S2) collectively are required for the first step of D-galacturonic acid catabolism. Either  $\Delta Bcgar1$  or  $\Delta Bcgar2$  single mutants remained able to grow on D-galacturonic acid, while  $\Delta Bcgar1/\Delta Bcgar2$  double deletion mutants completely lost the ability to utilize D-galacturonic acid. These results unequivocally show that *Bcgar1* and *Bcgar2* are both

functional in the D-galacturonic acid catabolic pathway in *B. cinerea*, whereas a single galacturonate reductase gene operates in *A. nidulans* (Martens-Uzunova and Schaap, 2008), *H. jecorina* and *A. niger* (Mojzita et al., 2010).

In spite of the involvement of both *Bcgar1* and *Bcgar2* in the first step of the catabolic pathway, their roles are not equally important. BcGAR2 showed a 20-fold lower  $K_m$  for D-galacturonic acid as substrate as compared to BcGAR1. Moreover, *Bcgar2* transcript levels were induced by D-galacturonic acid to higher levels than those of *Bcgar1*. Collectively these data suggest that BcGAR2 plays a more important role in D-galacturonic acid catabolism than BcGAR1. This is consistent with the analysis of deletion mutants:  $\Delta Bcgar2$  mutants showed 90% reduction in biomass accumulation on D-galacturonic acid, while  $\Delta Bcgar1$  mutants did not display any biomass reduction. The second and third step in the catabolic pathway are performed by a single enzyme, alike in *H. jecorina* (Hilditch et al., 2007; Kuorelahti et al., 2006) and *A. niger* (Martens-Uzunova and Schaap, 2008). The  $\Delta Bclgd1$  and  $\Delta Bclga1$  mutants were entirely unable to grow on D-galacturonic acid, indicating that *B. cinerea* only has one L-galactonate dehydratase and 2-keto-3-deoxy-L-galactonate aldolase.

BcGAR1 and BcGAR2 showed similar enzymatic activity with either D-galacturonic acid or D-glucuronic acid as substrate, while BcLGD1 showed a slightly higher enzymatic activity on L-galactonate as substrate, as compared to L-gulonate. These results demonstrate that BcGAR1, BcGAR2 and BcLGD1 are not specific for D-galacturonic acid but also accept D-glucuronic acid as input to the pathway. One would expect that *B. cinerea* is able to catabolise D-glucuronic acid. However, wild-type *B. cinerea* is unable to grow on D-glucuronic acid as sole carbon source (not shown). This raises the possibility that D-glucuronic acid does not induce gene expression of the pathway genes equally effective as D-galacturonic acid. We supplemented medium containing 50 mM D-glucuronic acid as the major carbon source with a low amount of D-galacturonic acid (50  $\mu$ M), in order to induce expression of *Bcgar1*, *Bcgar2*, *Bclgd1*, and *Bclga1*, however, this did not allow the growth of *B. cinerea* on D-glucuronic acid (not shown). The alternative explanation could be that *B. cinerea* lacks specific transporters for uptake of D-glucuronic acid prior to entry into the catabolic pathway.

*B. cinerea* deletion mutants in the endoPG genes *Bcpg1* and *Bcpg2* show a severe reduction in virulence (Kars et al., 2005a; ten Have et al., 1998), indicating that decomposition of pectin in plant cell walls is important for *B. cinerea* infection. Experiments using such  $\Delta Bcpg$  mutants, however, do not permit to distinguish whether pectin decomposition by *B. cinerea* is important for the process of physical colonization of plant tissue (enabled by the destructive action of the enzymes on plant cell wall integrity)

or for providing nutrients for fungal growth. This distinction can be made by analysing *B. cinerea* mutants in the D-galacturonic acid catabolic pathway described here. Such mutants may be anticipated to express the full spectrum of pectin depolymerizing enzymes (endopolygalacturonases, exopolygalacturonases, pectin and pectate lyases), yet they are unable to consume the most abundant monosaccharide released upon pectin degradation, and utilize it for their growth. Indeed the growth rate of the D-galacturonic acid catabolic mutants on pectic substrates was severely reduced and was inversely correlated to the proportion on sugars other than D-galacturonic acid in the substrate (Figure 4). However, the lesion sizes caused by  $\Delta Bcgar1/\Delta Bcgar2$ ,  $\Delta Bclgd1$ ,  $\Delta Bclga1$ , and  $\Delta Bcgar1/\Delta Bclga1$  mutants on tomato leaves, apples and peppers were indistinguishable from the wild-type. The mutants expressed the endopolygalacturonase genes to levels that were similar to or even slightly higher than the wild-type *B. cinerea* (not shown). The presence in the plant tissues tested of simple sugars (especially sucrose) and/or non-pectic polysaccharides (starch, cellulose, and hemicellulose) probably provided sufficient nutrients to compensate for the inability of the mutants to utilize degradation products of pectic substrates for growth. These data suggest that, in the plant tissues tested, the function of pectin depolymerization in virulence of *B. cinerea* is primarily in the process of tissue colonization, whereas the contribution of pectic substrates to nutrition for hyphal growth seems limited. We currently investigate the growth of galacturonic acid catabolism-deficient mutants on other plant tissues, especially tissues with different pectin contents in the cell walls.

## Materials and Methods

### Fungal strain and growth conditions

*Botrytis cinerea* wild-type strain B05.10 and the mutant strains used in this study were grown and maintained as described (Wubben et al., 1999) and are indicated in Table 1. For radial growth assays, conidia of the strains were inoculated on Gamborg's B5 (Duchefa, Haarlem, The Netherlands) agarose medium supplemented with 10 mM  $(\text{NH}_4)_2\text{PO}_4$  and as carbon source either glucose (50 mM), D-galacturonic acid (50 mM), citrus fruit pectin (1 % w/v; Sigma), apple pectin (1 % w/v; Carl Roth KG) or sodium pectate (1% w/v; Sigma). The D-galacturonic acid content of citrus fruit pectin and apple pectin was 78% and 61%, respectively (Kravtchenko et al., 1992). Cultures were grown at 20 °C.

**Table 1.** Strains used in this study.

Strain	Description	Reference
B05.10		van Kan et al., 1997
$\Delta Bcgar1$ -2, 4	B05.10 $\Delta Bcgar1::HPH$	This study
$\Delta Bcgar2$ -5, 6	B05.10 $\Delta Bcgar2::HPH$	This study
$\Delta Bclgd1$ -4, 6	B05.10 $\Delta Bclgd1::HPH$	This study
$\Delta Bclga1$ -5, 18	B05.10 $\Delta Bclga1::HPH$	This study
$\Delta Bcgar2/\Delta Bclga1$ -22, 26	B05.10 $\Delta Bcgar2-\Delta Bclga1::HPH$	This study
$\Delta Bcgar1/\Delta Bcgar2$ -3, 7	B05.10 $\Delta Bcgar2::HPH \Delta Bcgar1::NAT$	This study
$\Delta Bcgar2$ -5/ <i>Bcgar2</i>	B05.10 $\Delta Bcgar2::HPH Bcgar2+NAT$	This study
$\Delta Bclgd1$ -6/ <i>Bclgd1</i>	B05.10 $\Delta Bclgd1::HPH Bclgd1+NAT$	This study
$\Delta Bclga1$ -5/ <i>Bclga1</i>	B05.10 $\Delta Bclga1::HPH Bclga1+NAT$	This study

### RNA extraction and RT-PCR

Gene expression was quantified by real-time PCR analysis on different carbon sources. The conidia of the wild-type strain B05.10 were incubated in Gamborg's B5 liquid culture supplemented with 10 mM  $(NH_4)_2PO_4$  and 30 mM glucose at 20 °C, 150 rpm. After 16 h of growth, the mycelium was harvested as described (Wubben et al., 1999) and transferred into fresh Gamborg's B5 medium supplemented with 10 mM  $(NH_4)_2PO_4$  and as carbon source either 50 mM glucose, 50 mM D-galacturonic acid, 0.5% (w/v) citrus fruit pectin (Sigma), or 0.5% (w/v) sodium pectate (Sigma). Mycelium was harvested from these cultures at 0, 3, and 9 h post transfer, freeze-dried and total RNA was isolated using the Nucleospin® RNA plant kit (Machery-Nagl, Düren, Germany), according to the manufacturer's instructions. First strand cDNA was synthesized from 1 µg total RNA with SuperScript® III Reverse Transcriptase (Invitrogen) according to the manufacturer's instructions.

Quantitative RT-PCR was performed using an ABI7300 PCR machine (Applied Biosystems, Foster City, U.S.A.) in combination with the qPCR SensiMix kit (BioLine, London, U.K.) with primers LZ101/102 (*Bcgar1*), LZ35/36 (*Bcgar2*), LZ37/38 (*Bclgd1*), LZ39/40 (*Bclga1*), LZ41/42 (*Bcglr1*), and LZ80/81 (*Bcrp15*), which are listed in Table S1. Real-time PCR conditions were as follows: an initial 95 °C denaturation step for 10 min followed by denaturation for 15 s at 95 °C and annealing/extension for 45 s at 60 °C for 40 cycles. The data were analysed on the 7300 System SDS software (Applied Biosystems, Foster City, U.S.A.). The gene expression values were normalized to the expression of the constitutively expressed gene *Bcrp15*.

### Gene cloning, expression and purification of the encoded proteins

The open reading frames (ORFs) of *Bcgar1*, *Bcgar2*, *Bclgd1* and *Bclga1* were amplified from cDNA synthesized on total RNA isolated from a *B. cinerea* culture grown on D-galacturonic acid with primer pairs LZ113/114, LZ25/26, LZ51/52, and LZ29/30 (Table S1),

which were designed according to the gene models of *B. cinerea* strain T4. The ORFs were cloned into a pGEM-T Easy vector (Promega) and confirmed by sequencing. The ORFs of *Bcgar2* and *Bclga1* were re-amplified from the pGEM-T constructs with primers LZ47/48 and LZ53/54 (Table S1), respectively; and cloned into expression vector pET16b (Novagen) by using the *NdeI* and *BamHI* restriction sites. Insert sequences were verified by DNA sequencing analysis (Macrogen). The *BamHI*-restricted ORFs of *Bcgar1* and *Bclgd1* derived from pGEM-T constructs were subcloned into the corresponding sites of pET16b. The orientations were confirmed by PCR with T7 promoter primer (Invitrogen) and LZ52 or LZ114.

For heterologous protein expression, the constructs were transformed into *E. coli* strain BL21. The overnight cultures were diluted 100-fold into fresh LB medium and grown further at 28 °C until OD<sub>600</sub> reached ~1.0. IPTG (0.5 mM) was added to induce protein expression and the culture was continued at 25 °C overnight. The induced cultures were harvested by centrifugation (4000 g) for 10 min. The cell extracts were obtained by using BugBuster™ Protein extraction reagent (Novagen). The histidine-tagged proteins were purified with Ni-NTA agarose beads (Qiagen) according to the manufacturer's instructions.

### Enzyme activity assays

D-galacturonic acid reductase activity was measured by monitoring the change of absorbance of NADPH at 340 nm in reaction buffer containing 0.37/1.1 µg BcGAR1 or 0.12/0.6 µg BcGAR2; 10 mM sodium phosphate, pH 7.0; 0.25 mM NADPH; and 50 mM D-galacturonic acid or 50 mM D-glucuronic acid, pH 5.2. Michaelis-Menten constants for D-galacturonic acid and D-glucuronic acid, of which the concentration was ranging from 1 mM to 75 mM (for BcGAR1), or from 0.1 mM to 2.5 mM (for BcGAR2), were determined at a NADPH concentration of 0.25 mM.

As L-galactonic acid is not commercially available, L-galactonate dehydratase activity was measured by starting with the D-galacturonic acid reductase reaction which contained 15 µg BcGAR1; 10 mM sodium phosphate, pH 7.0; 5 mM NADPH; and 50 mM D-galacturonic acid or 50 mM D-glucuronic acid, pH 5.2. After the overnight reaction, MgCl<sub>2</sub> was adjusted to a final concentration of 5 mM, and 2.5 µg BcLGD1 was added to the reaction and the mixture was further incubated at room temperature. The production of 2-keto-3-deoxy-L-galactonate was measured by the thiobarbituric acid method (Buchanan et al., 1999).

As 2-keto-3-deoxy-L-galactonate is not commercially available, 2-keto-3-deoxy-L-galactonate aldolase activity was measured in the reverse direction (Hilditch et al., 2007) by determining the production of 2-keto-3-deoxy-L-galactonate from pyruvate and glyceraldehyde as described above. The reaction buffer contained 1/5 µg BcLGA1; 10 mM

sodium phosphate, pH 7.0; 10 mM pyruvate; and 10 mM DL-glyceraldehyde. Reactions without enzyme and reactions with heat-inactivated enzyme (65 °C for 15 min) were included as negative controls. The assays were performed at room temperature.

#### **Deletion of *Bcgar1*, *Bcgar2*, *Bclgd1*, and *Bclga1* genes in *B. cinerea***

The gene replacement strategy for generating *B. cinerea* deletion constructs, *B. cinerea* protoplast transformation and PCR-based screening of transformants were described by Kars et al. (2005b). Primers used for amplification of gene replacement fragments are listed in Table S1. To generate *Bcgar2-Bclga1* double deletion mutant, primers LZ01, 02, and 03 were used to amplify the 5'-flanking fragment, and primers LZ10, 11, and 12 were used to amplify the 3'-flanking fragment. The hygromycin (*HPH*) and nourseothricin (*NAT*) cassette, derived from vector pLOB7 (Figure S4) and pNR3 (Figure S5) with primers 20/21, were used as selection marker to replace the target genes, as indicated in Table 1. Genomic DNA of transformants was screened for the presence of the wild-type target gene by PCR by amplifying the target genes *Bcgar1*, *Bcgar2*, *Bclgd1*, and *Bclga1* with primers LZ113/114, LZ25/26, LZ27/28, and LZ29/30, respectively. Deletion mutants were routinely double checked by PCR using the same method. Southern hybridization was performed to confirm the recombination, in accordance with the manufacturer's instructions for DIG nucleic acid detection kit (Roche, Germany). The primers for amplification of *Bcgar1*, *Bcgar2*, *Bclgd1*, and *Bclga1* probes are LZ110/111, LZ55/56, LZ16/17, and LZ95/96, respectively (Table S1). The probes for detecting the *HPH* or *NAT* cassettes were amplified using pLOB7 and pNR3 as templates with primers LZ92/93 and 21/LZ92, respectively.

#### **Complementation construct in *B. cinerea***

In order to obtain the complementation plasmids rapidly and efficiently, a gateway cloning vector pNR4 (Figure S6) was generated. The *attP1P2* cassette containing the chloramphenicol resistance gene (*CmR*) and *ccdB* gene was amplified with primers LZ60/94 using the pDONR207 vector (Invitrogen) as template. The *attP1P2* fragment was digested with *SacI/XbaI* and cloned into the corresponding sites of vector pNR3 (Figure S5), yielding the plasmid pNR4. The *attP1P2* sites of pNR4 were verified by sequencing. The complementation fragments of *Bcgar2*, *Bclgd1*, and *Bclga1*, including ~1500 bp upstream and ~300 bp downstream sequences of the coding region, were amplified with primers LZ97/98, LZ99/100, and LZ62/63 which contain *attB1* and *attB2* sites, respectively. The purified fragments were recombined with pNR4 in BP reactions (Invitrogen) in the appropriate concentration. The resulting plasmids were used for *B. cinerea* protoplast transformation.

### **Measurement of *B. cinerea* biomass**

Fungal biomass in liquid cultures was determined by using a lateral flow device (QuickStix™ kit for *B. cinerea*, Enviro-Logix, Portland, Maine; Dewey et al., 2008), which quantifies a stable water-soluble, extracellular epitope (Meyer and Dewey, 2000). Liquid cultures (Gamborg's B5 with 10 mM (NH<sub>4</sub>)H<sub>2</sub>PO<sub>4</sub> and 50 mM D-galacturonic acid) were set up in three replicates starting with 10<sup>4</sup> conidia in 20 ml of medium, and the culture filtrate was sampled for biomass measurement after three days of culturing. Signal intensity for mutant strains was determined with a QuickStix™ optical reader (Envirologix) and compared to that of the wild-type strain.

### **Virulence assays**

The virulence of mutants was evaluated on tomato leaves (ten Have et al., 1998). Droplets of a suspension of conidia of wild-type and mutants (2 µl, 10<sup>6</sup> conidia/ml in potato dextrose broth, 1.2 g/l) were inoculated on opposite sides of the central vein (3-4 droplets per leaf half). Each comparison of wild-type and mutant was performed on 4 leaflets of one composite tomato leaf, on two composite leaves per plant, and two plants per experiment, leading to a total of at least 50 lesions per experiment. Lesion sizes were measured with a digital caliper at 3 days post inoculation. Each mutant was tested in at least two independent experiments.

Apple fruit and bell peppers were purchased from a local grocery. Each fruit was inoculated cross-wise with two droplets of the wild-type and two droplets of the mutant (2 µl, 10<sup>6</sup> conidia/ml in potato dextrose broth, 1.2 g/l). The inoculation site was first punctured with a needle to prevent the inoculum from rolling off the surface. Ten apples and 15 peppers were used for each mutant in each experiment. Lesion sizes were measured with a digital caliper at 4-6 days post inoculation, depending on disease progression. Inoculation sites that did not result in expanding lesions were eliminated from measurements and quantification. Each mutant was tested in at least two independent inoculation experiments.

Lesion sizes were statistically analysed by a Student *t*-test, using two-tailed distribution and two-sample unequal variance.

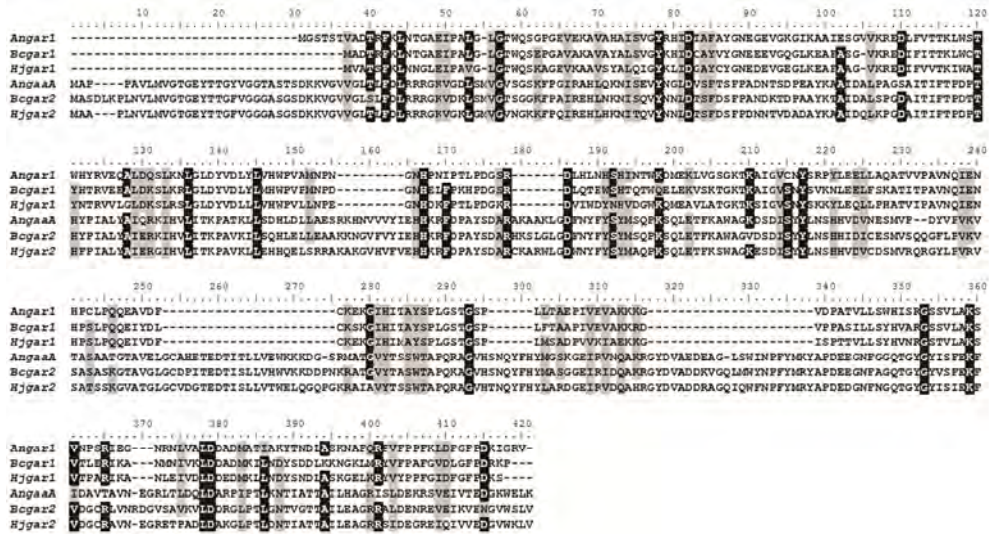
### **Supporting information**

Supplementary Figures S1, S2, S3, S4, S5, S6 and Supplementary Table S1.

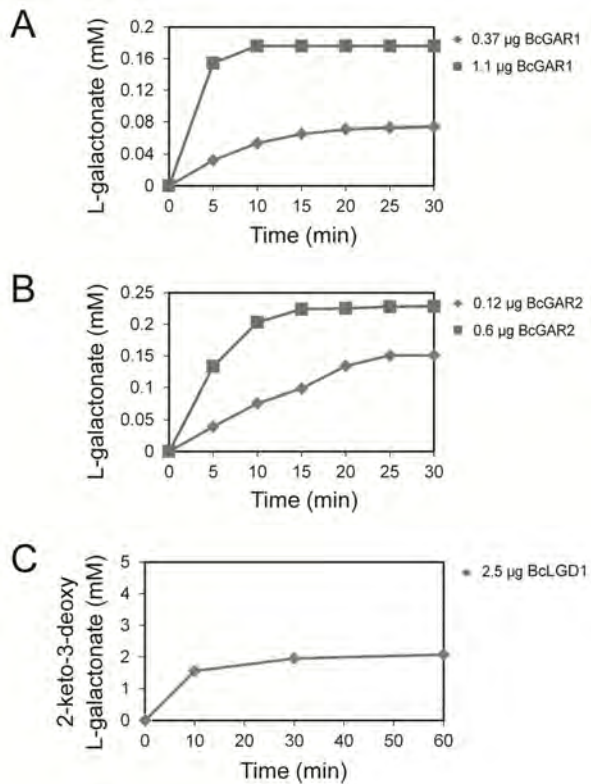
## **Acknowledgements**

The authors acknowledge funding by the Foundation Technological Top Institute Green Genetics (project 2CC035RP) and the Netherlands Graduate School Experimental Plant Sciences.

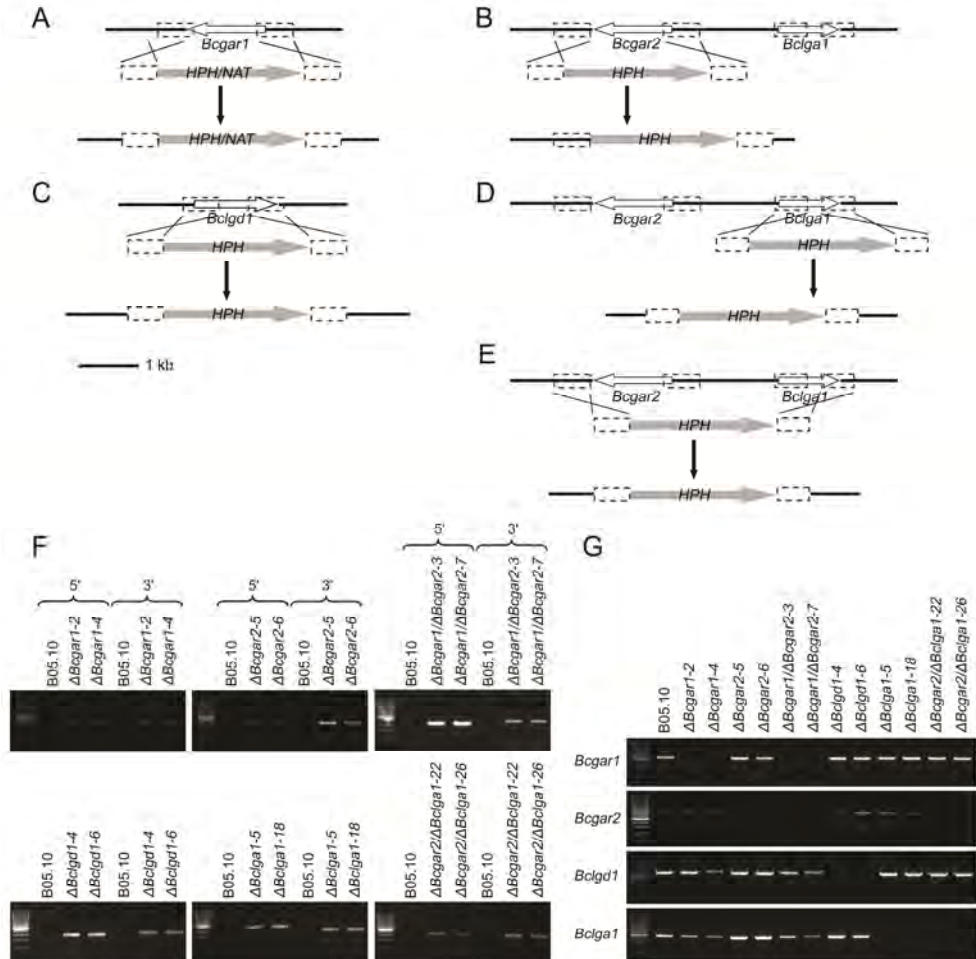
## Supporting information



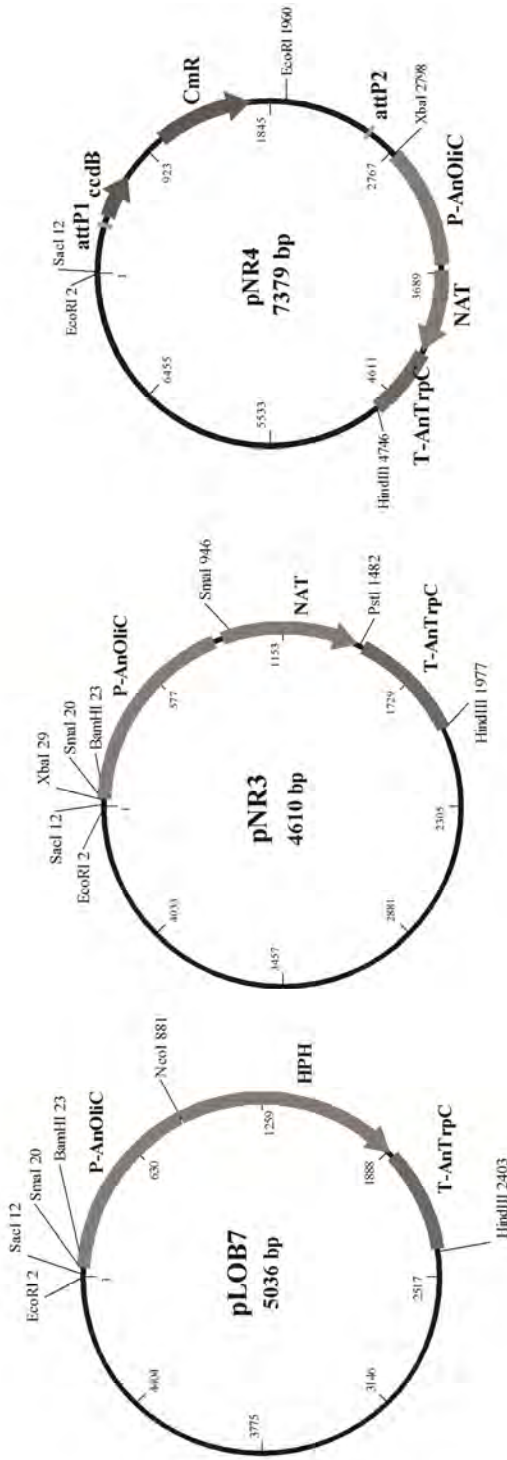
Supplementary Figure 1. Amino acid sequence alignment of *B. cinerea* GAR1 and GAR2, *A. niger* GAR1 and GAAA, and *H. jecorina* GAR1 and GAR2.



**Supplementary Figure 2.** Enzymatic activities of purified histidine-tagged proteins using D-glucuronic acid (GlucA) as substrate. A and B, recombinant BcGAR1 and BcGAR2 activities were determined by monitoring the decrease of NADPH absorbance at 340 nm, respectively. The initial concentration of NADPH was 0.25 mM. GlucA (50 mM) was added as substrate at  $t=0$ . C, recombinant BcLGD1 activity was determined by monitoring the production of 2-keto-3-deoxy-L-galactonate.



**Supplementary Figure 3.** Deletion of *Bcgar1*, *Bcgar2*, *Bclgd1*, and *Bclga1* by targeted gene replacement. A, organization of *Bcgar1* locus before and after homologous recombination in wild-type strain (HPH resistance cassette) or  $\Delta Bcgar2$  mutant (NAT resistance cassette). B-E, organization of *Bcgar2* (B), *Bclgd1* (C), *Bclga1* (D), and *Bcgar2-Bclga1* (E) locus before and after homologous recombination. Orientation of the target gene and HPH/NAT are indicated by white and grey arrows, respectively. Upstream and downstream flanks of target genes are shown with grey dashed-line frames. F and G, Polymerase chain reaction (PCR) analysis of wild-type strain B05.10 and knockout mutant strains. The genomic DNA of each strain was used to verify homologous recombination by using primer pairs 5.1/23 and 3.1/22 for 5' and 3' recombination (F) and absent of targeted genes in the corresponding knockout mutants (G), respectively.



Supplementary Figure 4. pLOB7 vector map.

Supplementary Figure 5. pNR3 vector map.

Supplementary Figure 6. pNR4 vector map.

**Supplementary Table 1.** Primers used in this study.

Target gene	Primer name	Sequence (5'-3') <sup>a</sup>	Purpose
<i>Bcgar1</i>	LZ101	GCTTAGTACCATGTTGCTCG	
	LZ102	TTCTTCTTCAGGTCGTCTGAG	
<i>Bcgar2</i>	LZ35	CCCAGCTATCCGTGAACATC	
	LZ36	CACCTGGGAAAGCGGCATC	
<i>Bclgd1</i>	LZ37	TGGTCATGGCATGACTTTCAC	Real-time RT-PCR
	LZ38	GTTGCGAATCGGAAACGAGATA	
<i>Bclga1</i>	LZ39	CAAGGTTTGGGAATTGTACAGAG	
	LZ40	GTATCTCCATATCCATAGTAGC	
<i>Bcglr1</i>	LZ41	GACAGGAAAGACATATATTTATCAC	
	LZ42	CAGTGGATAAGATAAAGGTCAAG	
<i>Bcrp15</i>	LZ80	GATGAGACCGTCAAATGGTTC	
	LZ81	CAGAAGCCCGTTACGACA	
<i>Bcgar1</i>	LZ113	CACACGGATCCGATGGCTGATACAAGATTCGAAGC	
	LZ114	CACACAGGATCCCTAAGGCTTTCTATCTGGGAAT	
<i>Bcgar2</i>	LZ25	TGATGGCTTCAGATTTGAAACCC	
	LZ26	TTAAACAAGAGACCAAAACACCA	
<i>Bcgar2</i>	LZ47	CACACACATATGGCTTCAGATTTGAAACCC	Gene cloning
	LZ48	CACACAGGATCCTTAAACAAGAGACCAAAACACCA	
<i>Bclgd1</i>	LZ51	CACACAGGATCCGATGGCTGAAGTTACAATCACAG	Protein expression
	LZ52	CACACAGGATCCTTAGATCTTGATACCCCTCCAAG	
<i>Bclga1</i>	LZ29	TGATGGCGGCAACCAACGGTTC	
	LZ30	CTATAAGCTGAACTCAACCTTC	
<i>Bclga1</i>	LZ53	CACACACATATGGCGGCAACCAACGGTTC	
	LZ54	CACACAGGATCCCTATAAGCTGAATCAACCTTC	
<i>Bcgar1</i>	LZ107 (5.1)	CGCTGCTTAAAGATCTTCG	
	LZ108 (5.2)	CAGTAGTCTTCCACGGGAAGTG	
<i>Bcgar1</i>	LZ109 (5.3)	GGGTACCGAGCTCGAATTCAGATTGCCATGTACCGAGTC	Gene replacement
	LZ110 (3.3)	CTCGCGCCGCAAGCTTTGGAGGATGGGGACATGAAG	
<i>Bcgar1</i>	LZ111 (3.2)	TGACTTTGCCGTCTCCAGTG	
	LZ112 (3.1)	AATTCATTCCTCGTCTACAG	
<i>Bcgar2</i>	LZ01 (5.1)	CTAAAGTGTAAGCCGGAGGTC	

	LZ02 (5.2)	CATACGCTTTCATTCAAGAACC	
	LZ03 (5.3)	GGGTACCGAGCTCGAATTCGGACGGTTAATATCTGGGTG	
	LZ55 (3.3)	CTCGGCGCGCGAAGCTTCACGTCTTCGCAGATCGAAC	
	LZ56 (3.2)	GTGGTAGTTGTTCTCGAAGTG	
	LZ57 (3.1)	GAAATCCATCAACTCGAGGAG	
	LZ13 (5.1)	CAATTGCCCCACTGTTGAGC	
	LZ14 (5.2)	CGATTATGCTCTCTTGACTGC	
	LZ15 (5.3)	GGGTACCGAGCTCGAATTCAGGAGGAAAGGGTGGCTC	
	LZ16 (3.3)	CTCGGCGCGCGAAGCTTGGAAATCGGTGTTGCCAACTGG	
	LZ17 (3.2)	GCCATCGTTGCCCTGCTGC	
	LZ18 (3.1)	CCCAACATGAAAAACCTCGAC	
	LZ07 (5.1)	AGGTCACCGGTCTCGGAC	
	LZ95 (5.2)	CCCACTTCTCTTCATCTACAC	
	LZ96 (5.3)	GGGTACCGAGCTCGAATTCATGTTGCGGTGTTTGGCGA	
	LZ10 (3.3)	CTCGGCGCGCGAAGCTTCGGTGGTGCAAAATGTCATGC	
	LZ11 (3.2)	CTGCATAACGTGTACGAATGAC	
	LZ12 (3.1)	CAAAAAGAGACGTGGACAACG	
	20 (cassette-5)	GAAATTCGAGCTCGGTACCCCGGGGA	
	21 (cassette-3)	CAAGCTTCGGCGCGCCGAG	
	22 (screen-3)	GTAACCATGCATGGTTGCCT	
	23 (screen-5)	GGGTACCGAGCTCGAATTC	
<i>attP</i> cassette	LZ60	CACACAAGAGCTCGCTTAGTTTGTGATGCCTGGCAG	
	LZ94	CACACAICTAGACGTTGAATGGCTCATAACAC	
<i>Bcgdr2</i>	LZ97	GGGGACAAGTTTGTACAAAAAAGCAGGCTTCCAGAAAAATCCTCGCTGAG	
	LZ98	GGGGACCACCTTTGTACAAGAAAGCTGGGTGTTTGGGGTTGAACGCGAG	
<i>Bclgd1</i>	LZ99	GGGGACAAGTTTGTACAAAAAAGCAGGCTACTTCTCGGGAAAGCCAAAGTG	
	LZ100	GGGGACCACCTTTGTACAAGAAAGCTGGGTGTTGAGATCAAGGACTTGGAC	
<i>Bclga1</i>	LZ62	GGGGACAAGTTTGTACAAAAAAGCAGGCTGGCAAGTAGAGATTTACCCA	
	LZ63	GGGGACCACCTTTGTACAAGAAAGCTGGGTCAAAAAGAGAACGTGGACAACG	

Gene complementation

<sup>a</sup>Restriction sites introduced for cloning are underlined, the *attB1* and *attB2* sites are indicated in italic, respectively.

# CHAPTER 4

*Botrytis cinerea* mutants deficient in D-galacturonic acid catabolism have a perturbed virulence on *Nicotiana benthamiana* and Arabidopsis, but not on tomato

Lisha Zhang and Jan A. L. van Kan

This chapter is published as:

Zhang, L. and van Kan, J.A.L. (2013) *Botrytis cinerea* mutants deficient in D-galacturonic acid catabolism have a perturbed virulence on *Nicotiana benthamiana* and Arabidopsis, but not on tomato. *Mol. Plant Pathol.* 14, 19-29.

## Abstract

D-galacturonic acid is the most abundant monosaccharide component of pectic polysaccharides that comprise a significant part of most plant cell walls. Therefore, it is potentially an important nutritional factor for *Botrytis cinerea* when it grows in and through plant cell walls. The D-galacturonic acid catabolic pathway in *B. cinerea* consists of three catalytic steps converting D-galacturonic acid to pyruvate and L-glyceraldehyde, involving two non-homologous galacturonate reductase genes (*Bcgar1* and *Bcgar2*), a galactonate dehydratase gene (*Bclgd1*), and a 2-keto-3-deoxy-L-galactonate aldolase gene (*Bclga1*). Knockout mutants in each step of the pathway ( $\Delta Bcgar1/\Delta Bcgar2$ ,  $\Delta Bclgd1$ , and  $\Delta Bclga1$ ) showed reduced virulence on *Nicotiana benthamiana* and *Arabidopsis thaliana* leaves, but not on *Solanum lycopersicum* leaves. The cell walls of *N. benthamiana* and *A. thaliana* leaves were shown to have a higher D-galacturonic acid content as compared to *S. lycopersicum*. The observation that mutants displayed a reduction in virulence, especially on plants with a high D-galacturonic acid content in cell walls, suggests that, in these hosts, D-galacturonic acid has an important role as carbon nutrient for *B. cinerea*. However, additional *in vitro* growth assays with the knockout mutants revealed that *B. cinerea* growth is reduced when D-galacturonic acid catabolic intermediates cannot proceed through the entire pathway, even when fructose is present as the major, alternative carbon source. These data suggest that the reduced virulence of D-galacturonic acid catabolism-deficient mutants on *N. benthamiana* and *A. thaliana* is not only a result of the inability of the mutants to utilize an abundant carbon source as nutrient, but also a result of the growth inhibition by catabolic intermediates.

## Introduction

*Botrytis cinerea* is a necrotrophic fungal plant pathogen infecting over 200 host plants and causing significant economic damage (pre- and post-harvest) to crops worldwide. The wide variety of symptoms on different tissues and plants suggests that *B. cinerea* possesses a large arsenal of weapons to invade its hosts (Choquer et al., 2007). The infection process includes the penetration of the host tissue, killing of the host cells and lesion expansion, followed by tissue maceration and sporulation (van Kan, 2006). *B. cinerea* produces a variety of compounds capable of killing plant cells, such as phytotoxic metabolites and proteins, oxalic acid and hydrogen peroxide (van Kan, 2006). However, the ultimate purpose of a necrotroph is not to kill its host, but to decompose the plant tissue and utilize the host-derived nutrients for its own growth. *B. cinerea* secretes multiple cell wall-degrading enzymes (including pectinases, cellulases and hemicellulases) to facilitate plant tissue colonization and to release carbohydrates for consumption; several of these enzymes have been demonstrated to be required for full virulence (Choquer et al., 2007).

*B. cinerea* often penetrates host leaf tissue at the anticlinal cell wall and subsequently grows into and through the middle lamella, which consists mostly of low-methyl-esterified pectin (ten Have et al., 2002). The importance of pectin degradation for the virulence of *B. cinerea* was demonstrated by targeted mutagenesis in endo-polygalacturonase (endo-PG) genes. Strains with mutations in endo-PG genes have a reduced capacity for pectin decomposition and, consequently, release reduced amounts of nutrients for the fungus to potentially catabolize. Strains with a mutation in the *Bcpg1* gene were reduced in virulence by 25% (ten Have et al., 1998), whereas mutants in the *Bcpg2* gene were reduced in virulence by > 50% (Kars et al., 2005a). These experiments, however, could not distinguish whether pectin decomposition during infection occurs for the purpose of plant tissue colonization or for the release of monosaccharides that serve as nutrients for fungal growth, or both. In order to distinguish between the relevance of pectin decomposition for plant tissue colonization or for nutrient acquisition by the fungus, it is imperative to obtain *B. cinerea* mutants that produce the full spectrum of plant cell wall-decomposing enzymes, but cannot catabolize the monosaccharides that are released from the cell wall polymers.

Current knowledge of monosaccharide utilization and catabolism by *B. cinerea* during plant infection is limited. NMR spectroscopy has suggested that, during colonization of sunflower cotyledons, *B. cinerea* converts glucose and fructose present in the host plant into mannitol via pathways involving the enzymes mannitol-1-phosphate dehydrogenase (BcMPD), mannitol-1-phosphate phosphatase and mannitol-2-dehydrogenase (BcMTDH)

(Dulermo et al., 2010; Dulermo et al., 2009). Transcript levels of *Bcmpd* and *Bcmtdh* as well as enzyme activities of BcMPD and BcMTDH increased during the progress of infection (Dulermo et al., 2009). Analysis of single- and double-knockout mutants in the *Bcmpd* and *Bcmtdh* genes, however, revealed that deletion of these genes did not abolish mannitol metabolism and did not affect virulence on sunflower (Dulermo et al., 2010). A different study showed that hexokinase is required for *B. cinerea* development and for virulence on apple and tomato fruit. The extent of reduction in virulence of a hexokinase-deficient mutant was correlated with the content of sugars in the fruit, in particular fructose (Rui and Hahn, 2007).

The monosaccharide D-galacturonic acid is the most abundant component of pectin polysaccharides (Caffall and Mohnen, 2009; Mohnen, 2008), and might constitute an important part of the nutrition of *B. cinerea* when it grows in and through plant cell walls. Recently, we have characterized the D-galacturonic acid catabolic pathway in *B. cinerea*, which consists of three catalytic steps converting D-galacturonic acid to pyruvate and L-glyceraldehyde. The pathway involves two nonhomologous galacturonate reductase genes (*Bcgar1* and *Bcgar2*), a galactonate dehydratase gene (*Bclgd1*) and a 2-keto-3-deoxy-Lgalactonate aldolase gene (*Bclga1*) (Zhang et al., 2011). Their transcript levels were induced substantially when the fungus was cultured in media containing D-galacturonic acid, pectate or pectin as the sole carbon source. BcGAR1 and BcGAR2 jointly contribute to the conversion of D-galacturonic acid to L-galactonate, albeit to a different extent. BcLGD1 converts L-galactonate to 2-keto-3-deoxy-L-galactonate, which is subsequently catalysed by BcLGA1 to pyruvate and L-glyceraldehyde. Targeted gene replacement of the four genes in *B. cinerea*, either separately or in combination, yielded mutants that were affected in growth on D-galacturonic acid or pectic substrates (pectate, apple pectin, citrus pectin) as the sole carbon source. The extent of growth reduction of the mutants on pectic substrates (as sole carbon source) was correlated with the proportion of D-galacturonic acid in the substrate. The growth of the mutants on apple pectin (containing only 61% D-galacturonic acid) was reduced by ~50%, whereas growth on citrus pectin (containing 78% D-galacturonic acid) was reduced by ~75%, and growth on sodium pectate (containing > 99%D-galacturonic acid) was negligible (Zhang et al., 2011).

In this study, we analysed the D-galacturonic acid content in leaf cell wall extracts of three plant species (*Solanum lycopersicum*, *Nicotiana benthamiana* and *Arabidopsis thaliana*) and analysed the expression profiles of *B. cinerea* D-galacturonic acid catabolic genes *in planta*, as well as the virulence of *B. cinerea* mutants in these genes.

## Results

### The D-galacturonic acid content in cell walls differs among plant species

The alcohol-insoluble residue (AIR) fraction, mainly consisting of cell wall polysaccharides, was extracted from leaves of *Solanum lycopersicum*, *Nicotiana benthamiana* and *Arabidopsis thaliana*. For all three plant species, AIR makes up ~70% of the leaf dry weight (not shown). The polysaccharides were hydrolysed and the monosaccharide composition and contents were quantified by chemical analysis (Figure 1). The contents of neutral sugars in the hydrolysed AIR fraction differed among the three plant species. The content of glucose (the most abundant neutral sugar) in the AIR polysaccharides of *S. lycopersicum* was significantly higher than that in *N. benthamiana* and *A. thaliana*. The content of uronic acids (> 95% of which is D-galacturonic acid) in the AIR polysaccharides of *S. lycopersicum* was 60–70% of the levels in *N. benthamiana* and *A. thaliana* (Figure 1). The contents of glucose, fructose and sucrose were measured in water-soluble leaf extracts of the three plant species. The contents of glucose and sucrose were higher in *N. benthamiana* than in *S. lycopersicum* and *A. thaliana*, whereas the content of fructose was higher in *S. lycopersicum* and *N. benthamiana* than in *A. thaliana* (Figure S1). The overall contents of free sugars in plant leaves were negligible relative to the sugars assimilated in the AIR extract from plant cell walls (Figure 1).

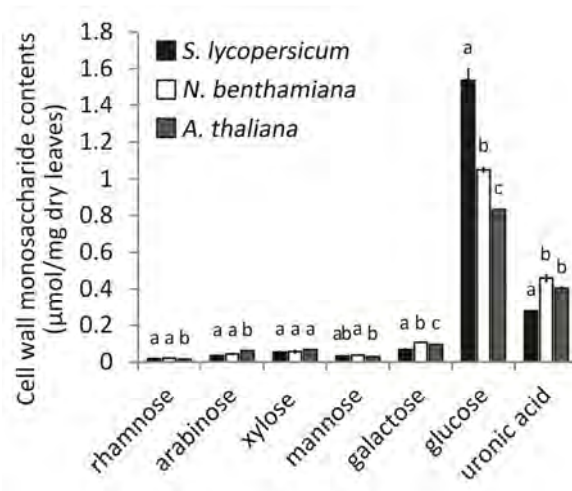


**Figure 1.** Cell wall monosaccharide contents of leaves of *Solanum lycopersicum*, *Nicotiana benthamiana*, and *Arabidopsis thaliana*. The monosaccharides analysed are given underneath the columns. Contents are given in  $\mu\text{mol}/\text{mg}$  dry weight. Bars indicate means  $\pm$  standard deviation. For each monosaccharide, letters above bars indicate statistical significance; bars not sharing letters represent significant mean differences at  $P < 0.05$  by Student's  $t$ -test.

### Transcript levels of D-galacturonic acid catabolic genes during infection

The expression profiles of the D-galacturonic acid catabolic genes *Bcgar1*, *Bcgar2*, *Bclgd1* and *Bclga1* were quantified during infection of wild-type *B. cinerea* on leaves of *S. lycopersicum*, *N. benthamiana* and *A. thaliana* at two time points (Figure 2). All four genes were expressed in each host plant and there were only marginal differences in transcript levels between 2 and 3 days post-inoculation (dpi) (relative to an internal standard transcript). The transcript levels of the four genes were all higher in *N. benthamiana* and *A. thaliana* than in *S. lycopersicum*, except for *Bcgar1* in *N. benthamiana* at 2 dpi. The relative transcript levels of *Bclgd1* were more than 2-fold higher in *N. benthamiana* and *A. thaliana* than in *S. lycopersicum*. The transcript levels observed *in planta* (higher in *N. benthamiana* and *A. thaliana* than in *S. lycopersicum*; Figure 2) correlate with the contents of D-galacturonic acid in the AIR polysaccharides, which were higher in *N. benthamiana* and *A. thaliana* than in *S. lycopersicum* (Figure 1).

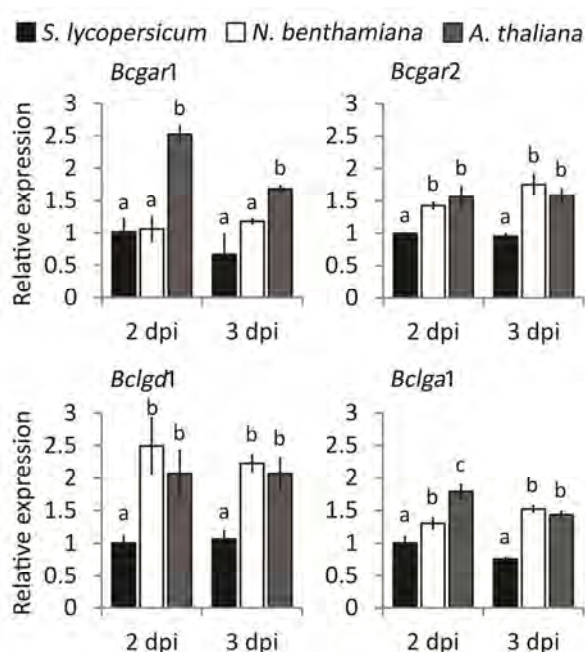


**Figure 2.** Relative transcript levels of D-galacturonic acid catabolic genes during infection on *Solanum lycopersicum*, *Nicotiana benthamiana*, and *Arabidopsis thaliana*. Infected plants were sampled at 2 and 3 days post-inoculation (dpi) for RNA extraction. mRNA levels of D-galacturonic acid catabolic genes were normalized to the levels of the constitutive reference gene *Bcrp15* and calibrated to the levels on *S. lycopersicum* at time point 2 dpi (set as 1), according to the  $2^{-\Delta\Delta Ct}$  method. Data are represented as means  $\pm$  standard deviation from one biological repeat. Three technical replicates of each repeat were analysed and three independent biological repeats performed, all with similar results. For each time point, letters above bars indicate statistical significance; bars not sharing letters represent significant mean differences at  $P < 0.05$  by Student's *t*-test.

**Virulence of D-galacturonic acid catabolism-deficient mutants on *Solanum lycopersicum*, *Nicotiana benthamiana* and *Arabidopsis thaliana* leaves**

To investigate to what extent D-galacturonic acid serves as an important carbon source for *B. cinerea* growth during infection, the virulence of  $\Delta Bcgar1/\Delta Bcgar2$ ,  $\Delta Bclgd1$ , and  $\Delta Bclga1$  mutants was tested on leaves of the three plant species. For each step in the D-galacturonic acid catabolic pathway, two independent mutants were tested and yielded essentially identical results.

On *S. lycopersicum* leaves, each mutant generated lesion sizes similar to that of the wild-type strain (Figure S2A). The fungal biomass on *S. lycopersicum* leaves was monitored at 2 dpi and 3 dpi, and each mutant showed a similar fungal biomass to that of the wild-type strain (Figure S2B).

On *N. benthamiana* leaves, mutants in all three steps of the catabolic pathway produced smaller lesions relative to those on the wild-type strain (Figure 3).  $\Delta Bcgar1/\Delta Bcgar2$  and  $\Delta Bclga1$  mutants displayed ~25% reduction in lesion size at 3 dpi, whereas  $\Delta Bclgd1$  mutants displayed ~45% reduction (Figure 3A and C). Immunological quantification indicated that the biomass of each mutant was similar to that of the wild-type strain at 2 dpi (not shown). At 3 dpi, however, the biomass of  $\Delta Bcgar1/\Delta Bcgar2$  and  $\Delta Bclga1$  mutants on *N. benthamiana* was ~71% of that of the wild-type strain, and the biomass of  $\Delta Bclgd1$  mutants was ~42% of that of the wild-type strain (Figure 3B). This suggests that the catabolism of D-galacturonic acid released from pectin in *N. benthamiana* leaves is important for the expansion of lesions, but not for the initial colonization. In addition to *N. benthamiana*, all mutants produced smaller lesions on *N. tabacum* leaves relative to those of the wild-type strain.  $\Delta Bclgd1$  mutants displayed a greater decrease in lesion size than did  $\Delta Bcgar1/\Delta Bcgar2$  and  $\Delta Bclga1$  mutants (not shown).

Finally, the virulence of  $\Delta Bcgar1/\Delta Bcgar2$ ,  $\Delta Bclgd1$  and  $\Delta Bclga1$  mutants was investigated on leaves of *A. thaliana* Columbia (Col-0). The *A. thaliana* leaf is much smaller than that of tomato and tobacco; thus, only one droplet of a suspension of conidia of wild-type or mutants was inoculated onto each detached leaf. Wild-type strain B05.10 caused extensive necrosis on Col-0, whereas the mutants showed a significant reduction in the extent of necrosis at 3 dpi (Figure 4A). As the shapes of expanding lesions on *A. thaliana* were not circular, it was not possible to determine the lesion diameter. The fungal biomass was quantified by immunodetection using pools of eight leaves sampled at different time points. Fungal biomass on Col-0 did not differ between the mutants and the wild-type strain at 2 dpi (not shown). However, at 3 dpi, the biomasses of  $\Delta Bcgar1/\Delta Bcgar2$ ,  $\Delta Bclgd1$  and  $\Delta Bclga1$  mutants on Col-0 were ~62%, ~50% and ~70% of

that of the wild-type strain, respectively (Figure 4B). These data are similar to the results on *N. benthamiana* (Figure 3B).

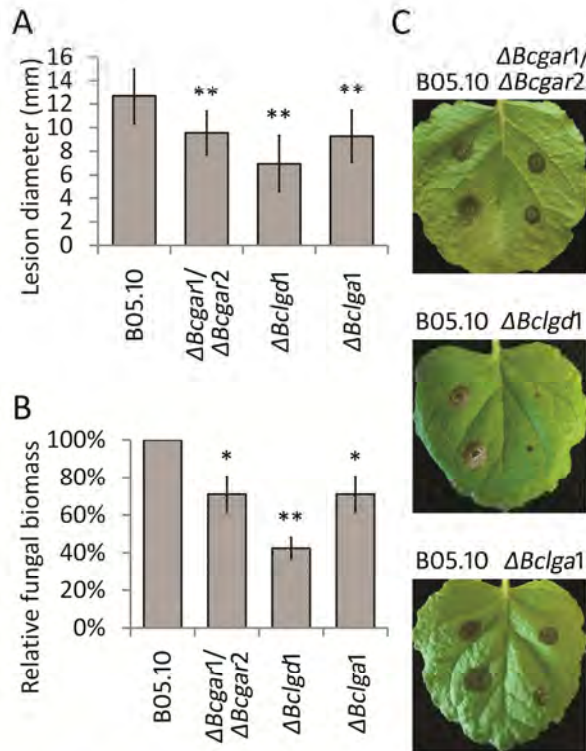


**Figure 3.** Virulence of D-galacturonic acid catabolism-deficient mutants on *Nicotiana benthamiana*. A, lesion development of *Botrytis cinerea* on *N. benthamiana* leaves was evaluated at 3 days post inoculation (dpi) by determining the average lesion diameter on 4 leaves from 8 plants each. Data represent means  $\pm$  standard deviation ( $n \geq 50$  independent lesions). B, *Botrytis cinerea* biomass by immunological detection at 3 dpi on *N. benthamiana*. Six discs (30 mm in diameter, containing the whole lesions in the centre) from 2 leaves of 3 plants were sampled as a pool for quantification. The fungal biomass of mutants was normalized to that of the wild-type strain. Experiments were repeated at least twice with similar results. \* $P < 0.05$ , \*\* $P < 0.01$  by Student's *t*-test. C, disease symptoms of *B. cinerea* on *N. benthamiana* leaves at 3 dpi.

### Transcript levels of endo-PG genes in D-galacturonic acid catabolism-deficient mutants

In plant tissues that are infected by *B. cinerea*, pectin is mainly depolymerized by secreted endo-PGs and exo-PGs (Kars et al., 2005a; Williamson et al., 2007; Wubben et al., 1999), releasing D-galacturonic acid that potentially serves as a nutrient for fungal growth. We considered the possibility that the reduced virulence in D-galacturonic acid catabolism-deficient mutants might be an indirect consequence of the altered regulation of endo-PG

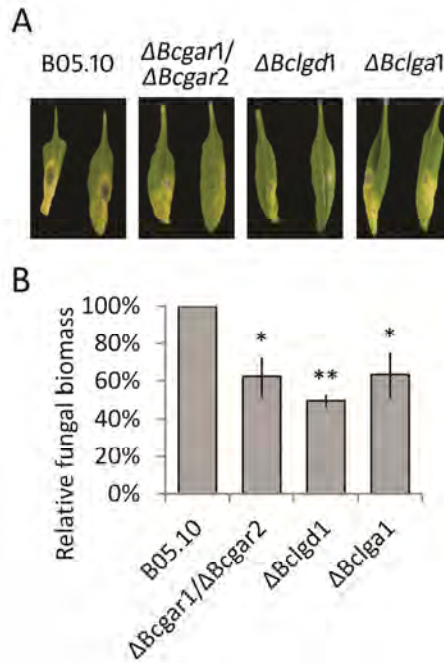


**Figure 4.** Virulence of D-galacturonic acid catabolism-deficient mutants on *Arabidopsis thaliana*. A, disease symptoms of *Botrytis cinerea* on *A. thaliana* leaves at 3 days post-inoculation (dpi). Two representative leaves are shown for each plant/strain combination. B, *Botrytis cinerea* biomass accumulation by immunological detection at 3 dpi. Eight detached leaves were sampled as a pool for quantification. The fungal biomass of mutants was normalized to that of the wild-type strain. Data represent means  $\pm$  standard deviation from two independent biological repeats. \* $P < 0.05$ , \*\* $P < 0.01$  by Student's *t*-test.

genes. To assess whether the expression profiles of endo-PG genes were affected in D-galacturonic acid catabolism-deficient mutants, the transcript levels of *Bcpg1*–*6* were investigated in the wild-type strain and in mutants during infection on *A. thaliana* at 2 and 3 dpi (Figure 5). *Bcpg1* showed similar transcript levels in the D-galacturonic acid catabolism-deficient mutants as in the wild-type strain at 2 and 3 dpi. Transcripts of *Bcpg2*, *Bcpg3* and *Bcpg5* were not detected under these experimental conditions. The transcript levels of *Bcpg4* and *Bcpg6* were higher in all the mutants relative to those in the wild-type strain at 2 and 3 dpi. These results are in agreement with reports indicating that transcript levels of *Bcpg4* and *Bcpg6* (but not *Bcpg1*, *Bcpg2*, *Bcpg3* and *Bcpg5*) are induced in cultures containing D-galacturonic acid as sole carbon source (Wubben et al., 2000). The expression profiles of *Bcpg4* and *Bcpg6* suggest that D-galacturonic acid (or catabolic pathway intermediates) accumulates in mutants during infection to a concentration sufficient to hyperinduce *Bcpg4* and *Bcpg6* transcripts.

During infection on *N. benthamiana*, higher transcript levels of *Bcpg4* and *Bcpg6* were also observed in the D-galacturonic acid catabolism-deficient mutants in comparison with those in the wild-type strain, especially at 3 dpi (Figure S3). By contrast, on *S. lycopersicum*, *Bcpg4* and *Bcpg6* exhibited similar transcript levels in the D-galacturonic acid catabolism-deficient mutants and in the wild-type, and their transcript levels were negligible compared with those on *N. benthamiana* and *A. thaliana* (Figure S3). These results indicate that the deficiency of D-galacturonic acid catabolism in *B. cinerea* does not impair the expression of endo-PG genes. Therefore, misregulation of endo-PG genes is not the cause for the reduced virulence of mutants.

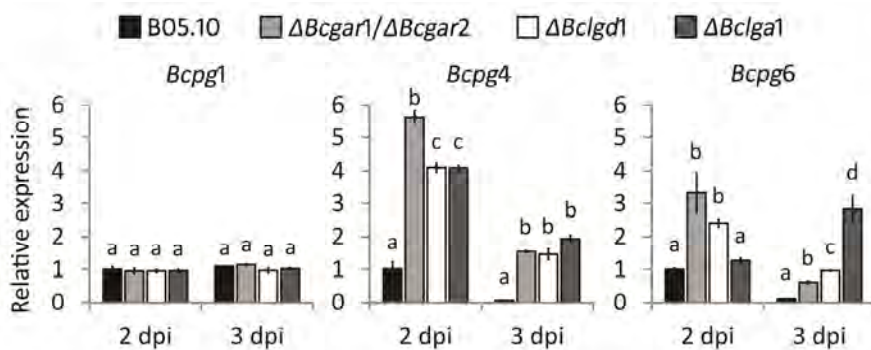


**Figure 5.** Relative transcript levels of *Bcpg1*, *Bcpg4*, and *Bcpg6* in wild-type *Botrytis cinerea* and D-galacturonic acid catabolism-deficient mutants during infection on *Arabidopsis thaliana* leaves. Infected plants were sampled at 2 and 3 days post-inoculation (dpi) for RNA extraction. mRNA levels of *Bcpg1*, *Bcpg4*, and *Bcpg6* genes were normalized to the levels of the constitutive reference gene *Bcrp15* and calibrated to wild-type strain B05.10 levels at time point 2 dpi (set as 1), according to the  $2^{-\Delta\Delta CT}$  method. Data are represented as means  $\pm$  standard deviation from one biological repeat. Three technical replicates of each repeat were analysed and three independent biological repeats were performed, which showed similar results. For each time point, letters above bars indicate statistical significance; bars not sharing letters represent significant mean differences at  $P < 0.01$  by Student's *t*-test.

### Defence responses in *Arabidopsis thaliana*

In order to test whether the reduced virulence of the *B. cinerea* mutants in *A. thaliana* could be explained by altered defence responses, the expression was monitored of several *A. thaliana* genes that are involved in basal resistance to pathogens, including *pad3*, required for the production of camalexin (Böttcher et al., 2009; Zhou et al., 1999), *PR1*, a marker gene for salicylic acid dependent defence (Cao et al., 1994; Delaney et al., 1994; Penninckx et al., 1996), and *PDF1.2*, a marker for jasmonic acid/ethylene-dependent defence (Penninckx et al., 1998; Thomma et al., 1998). Moreover, the expression was monitored of genes which contribute to partial resistance against *B. cinerea*, including *AtPGIP1*, *AtPME3* and *AtrbohD* (Ferrari et al., 2003a; Raiola et al., 2011; Torres et al., 2005;

van Baarlen et al., 2007). Transcript levels of these genes were determined following inoculation of *A. thaliana* with *B. cinerea* wild-type and D-galacturonic acid catabolism-deficient mutants. Most defence-related genes tested were induced to a similar extent by the wild-type and mutant *B. cinerea* strains; in a few cases, the defence genes showed lower expression levels in response to the mutants (Figure S4).

### **Growth inhibition by intermediates in the D-galacturonic acid catabolic pathway**

It was striking that the extent of virulence reduction of  $\Delta Bclgd1$  mutants on *N. benthamiana* and *A. thaliana* was higher than that of  $\Delta Bcgar1/\Delta Bcgar2$  and  $\Delta Bclga1$  mutants (Figure 3 and 4). If the reduction in virulence was merely caused by the inability of mutants to utilize D-galacturonic acid as carbon source for growth, one would expect that mutants in all three steps would show the same extent of reduction in virulence, which would reflect the contribution of D-galacturonic acid as a carbon source to the fungus. As the virulence of the  $\Delta Bclgd1$  mutants was reduced even more than that of  $\Delta Bcgar1/\Delta Bcgar2$  and  $\Delta Bclga1$  mutants, we hypothesized that the accumulation of the intermediate L-galactonate (substrate of the BcLGD1 protein) might result in growth inhibition to *B. cinerea*. To test this, the growth of D-galacturonic acid catabolism-deficient mutants was monitored on agar containing fructose as the most abundant carbon source, with or without a small amount of D-galacturonic acid. Unexpectedly, all three D-galacturonic acid catabolism-deficient mutants showed dose-dependent growth reduction when compared with the wild-type strain (Figure 6A). The growth of all three mutants was similar to that of the wild-type strain on medium with 0.05 mM D-galacturonic acid; however, growth was clearly reduced with 0.3 mM D-galacturonic acid between days 3 and 5 of incubation and severely reduced with 1 mM D-galacturonic acid within the first 3 days. Colony diameters of  $\Delta Bcgar1/\Delta Bcgar2$ ,  $\Delta Bclgd1$  and  $\Delta Bclga1$  mutants were 32%, 64% and 33% smaller on medium containing fructose + 0.3 mM D-galacturonic acid and 49%, 73% and 54% smaller on medium containing fructose + 1 mM D-galacturonic acid, respectively, when compared with the diameters on medium with fructose only. The wild-type strain did not show any growth reduction on medium with or without D-galacturonic acid. Transcripts of *Bcgar1*, *Bcgar2*, *Bclgd1* and *Bclga1* were repressed in the presence of glucose (Zhang et al., 2011). Therefore, we tested the growth of  $\Delta Bcgar1/\Delta Bcgar2$ ,  $\Delta Bclgd1$ , and  $\Delta Bclga1$  mutants on agar plates containing glucose as the major carbon source without or with 1 mM D-galacturonic acid. The growth of all three mutants was similar on agar plates containing 50 mM glucose with D-galacturonic acid as compared to growth without D-galacturonic acid. On agar plates containing 10 mM glucose with D-galacturonic acid, however, the growth of all three mutants was slightly reduced as compared to growth without D-galacturonic acid (Figure 6B).

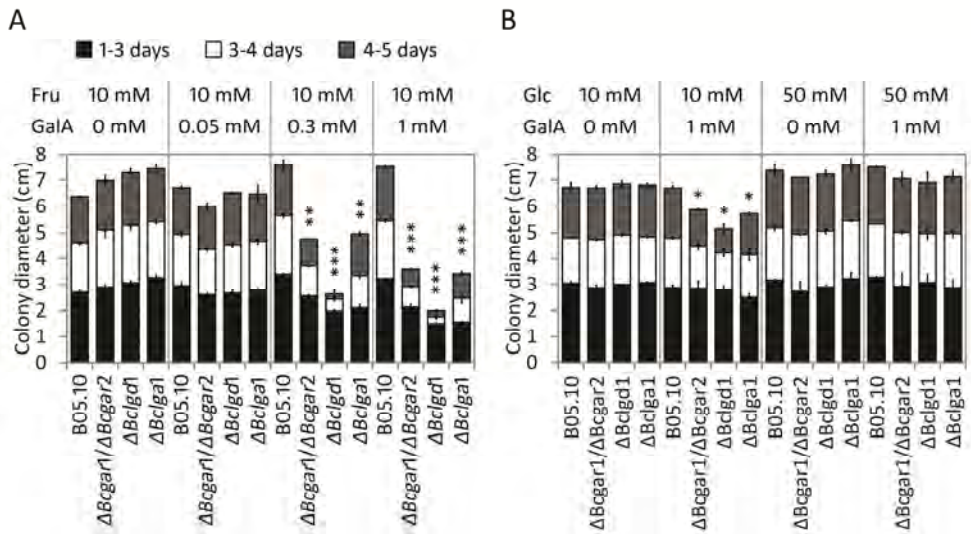


**Figure 6.** Radial growth of D-galacturonic acid catabolism-deficient mutants on agar medium containing fructose (A, Fru) or glucose (B, Glc) as the major carbon source, with different concentrations of D-galacturonic acid (GalA) as indicated at the top. Colony diameter was measured at 3, 4 and 5 days after incubation at 20 °C. Data presented are means  $\pm$  standard deviation from two biological repeats, with three technical replicates of each repeat. Asterisks indicate a significant difference to the wild-type strain based on Student's *t*-test (\* $P < 0.05$ , \*\* $P < 0.01$ , \*\*\* $P < 0.001$ ).

## Discussion

The fundamental question at the onset of this study was whether the important role of endo-PGs in virulence of *B. cinerea* (Kars et al., 2005a; ten Have et al., 1998) relates to a function in tissue disintegration and colonization, and/or to a function in the release of an abundant source of monosaccharide nutrients from pectic polymers. These functions might possibly be distinguished by analysing mutants with a normal set of pectinases, and thus fully able to decompose pectin, but unable to catabolise the D-galacturonic acid released by the action of these enzymes. If pectin degradation by *B. cinerea* is merely for the purpose of host tissue invasion and colonization, but does not contribute significantly to the release of nutrients for fungal growth, one would anticipate that the virulence of mutants in D-galacturonic acid catabolic genes would be unaltered when compared with that of the wild-type. If, however, D-galacturonic acid makes up a substantial proportion of the nutrition for the fungus, one would anticipate that the virulence of such mutants in D-galacturonic acid catabolic genes would be reduced. Furthermore, it could be expected that the extent of virulence reduction would be proportional to the D-galacturonic acid content in the host cell wall.

We analysed the D-galacturonic acid content in the cell wall extracts of leaves from three plant species that are commonly used for *B. cinerea* infection assays: *S. lycopersicum*, *N. benthamiana* and *A. thaliana*. Although substantial data are available on the leaf cell wall composition of *A. thaliana* (Harholt et al., 2006; Zablackis et al., 1995; Zandleven et al., 2007), only limited information is available on the composition of pectins and cell walls of leaves from *S. lycopersicum* (Curvers et al., 2010) and none on *N. benthamiana*. Although the latter two species are both Solanaceae and might be anticipated to have similar cell wall architecture, the composition of monosaccharides released from AIR in *N. benthamiana* was remarkably similar to that in *A. thaliana* and distinct from the composition in *S. lycopersicum*. The content of D-galacturonic acid in *S. lycopersicum* was only 60%–70% of that in the other two species, whereas the content of glucose was higher in *S. lycopersicum* leaves when compared with that in the other two plants. The amount of free monosaccharides in all three plants (on a mol/dry weight basis) was extremely low when compared with the monosaccharides assimilated in cell wall polysaccharides. The differences in D-galacturonic acid content between the three hosts might affect the nutrients available for *B. cinerea* growth when it colonizes the leaves of the respective hosts.

We have previously described a set of *B. cinerea* D-galacturonic acid catabolism-deficient mutants, which are blocked in one of three enzymatic steps in the catabolic pathway (Zhang et al., 2011). These mutants were unable to grow on polygalacturonic acid as sole carbon source, and showed severely reduced growth on apple pectin and citrus pectin, substrates that, in addition to D-galacturonic acid, contain neutral sugars. The extent of residual growth of the mutants correlated with the proportion of neutral sugars in these pectic substrates (Zhang et al., 2011). The *B. cinerea* D-galacturonic acid catabolism-deficient mutants showed a significant reduction in virulence on *N. benthamiana* and *A. thaliana* leaves when compared with the wild-type, but a similar virulence on *S. lycopersicum* leaves. The differential virulence was correlated with the content of D-galacturonic acid in the cell walls of the plants tested. The initial interpretation of the data was that, in *N. benthamiana* and *A. thaliana*, D-galacturonic acid makes up an important part of the nutrition for *B. cinerea*. The decomposition of pectin would release D-galacturonic acid monomers that cannot be utilized by the mutants for growth, thereby leading to significantly reduced lesion outgrowth. The observation that the virulence of the mutants on *S. lycopersicum* leaves was similar to that of the wild-type was tentatively explained by the low D-galacturonic acid content in this host, and the use of alternative carbon sources by the mutants.

The transcript levels of D-galacturonic acid catabolic genes during infection by wild-type *B. cinerea* correlated with the level of D-galacturonic acid in the leaf cell walls of the species

tested, with relatively high transcript levels in *N. benthamiana* and *A. thaliana*, as opposed to low transcript levels in *S. lycopersicum*. In individual mutant strains, the transcript levels of the other pathway genes were not altered during leaf infections, when compared with the levels in the wild-type. Specifically, there was no significant change in the transcript levels of *Bclgd1* and *Bclga1* in the  $\Delta Bcgar1/\Delta Bcgar2$  mutant, of *Bcgar1*, *Bcgar2* and *Bclga1* in the  $\Delta Bclgd1$  mutant, or of *Bcgar1*, *Bcgar2* and *Bclgd1* in the  $\Delta Bclga1$  mutant (not shown). These data suggest that D-galacturonic acid itself is responsible for the induction of the catabolic genes, and the catabolic intermediates derived from D-galacturonic acid are not required for induction of transcription. This finding is in agreement with the observation that, in an *Aspergillus niger* knockout mutant in the *gaaA* gene (orthologue of *Bcgar2*), transcript levels of genes downstream in the pathway were elevated in the presence of D-galacturonic acid, similar to that in the wild-type (Mojzita et al., 2010).

We tested whether a non-functional D-galacturonic acid catabolic pathway might affect the *in planta* expression of *B. cinerea* endo-PG genes, which could lead indirectly to reduction of virulence. Transcript levels of the *Bcpg1* gene, which is important for virulence of *B. cinerea* (Kars et al., 2005a; ten Have et al., 1998), were unaltered in the D-galacturonic acid catabolism-deficient mutants. By contrast, the expression of the *Bcpg4* and *Bcpg6* genes, which can be induced in the presence of D-galacturonic acid (Wubben et al., 2000), was elevated in the mutants relative to the wild-type strain. This suggests that the mutants sense elevated levels of D-galacturonic acid, when compared with the wild-type, presumably because the compound is catabolized in the wild-type strain, leading to lower intra- and/or extracellular D-galacturonic acid concentrations. The inability to catabolize D-galacturonic acid in the mutants leads to prolonged elevated levels of *Bcpg4* and *Bcpg6* transcripts. Expression analyses corroborated that the reduced virulence of D-galacturonic acid catabolism-deficient mutants was not a result of an indirect impact on the expression of *B. cinerea* endo-PG genes. Furthermore, we tested whether the reduced virulence of *B. cinerea* mutants on *A. thaliana* could be explained by an elevation in defence responses. All *A. thaliana* defence-related genes tested were induced to a similar extent by the wild-type and mutant *B. cinerea* strains; some defence genes even showed lower transcript levels in response to the mutants. The conclusion that the reduced virulence of D-galacturonic acid catabolism-deficient mutants was not caused by an altered regulation of *B. cinerea* endo-PG genes, or by a modulation of defence responses in the host, strengthened the initial hypothesis that D-galacturonic acid catabolism influences virulence directly, and therefore D-galacturonic acid may serve as an important nutritional component for the fungus. This hypothesis was challenged by the striking observation that the mutants did not all show the same reduction in virulence. The  $\Delta Bclgd1$  mutant (blocked in the second step in the pathway) showed markedly stronger

reduction in virulence than the mutants blocked in the first and third steps. This observation was indicative of growth inhibitory effects exerted by catabolic intermediates, which would partly or largely explain the differences between the  $\Delta Bclgd1$  mutant and the other mutants. As the catabolic pathway intermediates (L-galactonate and 2-keto-3-deoxy-L-galactonate, accumulating in the  $\Delta Bclgd1$  and  $\Delta Bclga1$  mutants, respectively) are not commercially available, it is not feasible to evaluate directly the growth-inhibiting effects of these compounds in *B. cinerea*. Therefore, experiments were performed in which *B. cinerea* wild-type and mutants were grown on agar, containing fructose as the most abundant carbon source, supplemented with different amounts of D-galacturonic acid. The growth of all three mutants was reduced on medium containing fructose supplemented with D-galacturonic acid when compared with growth on fructose alone. The growth reduction of the mutants in the presence of D-galacturonic acid occurred in a dose-dependent manner (Figure 6A). This suggests that the accumulation of all three intermediates in the D-galacturonic acid catabolic pathway is inhibitory to *B. cinerea*, with L-galactonate (product of the first step in the pathway, accumulating in the  $\Delta Bclgd1$  mutant) having the most severe growth-reducing effect. The mutants grew at a similar rate to the wild-type in the first 3 days, but then showed a severe decline in radial growth between days 3–4 and days 4–5. The  $\Delta Bclgd1$  mutant showed nearly complete growth cessation in the presence of 0.3 and 1 mM D-galacturonic acid. These observations provide support that the intermediates first need to be generated and accumulate before exerting their growth-reducing effect. Growth reduction was not observed when glucose (50 mM) was provided as the major carbon source, because the expression of D-galacturonic acid catabolic genes is repressed by glucose (Zhang et al., 2011). In addition, the expression of putative D-galacturonic acid transporter genes is repressed by glucose (Chapter 5 and 6). With 10 mM glucose and 1 mM D-galacturonic acid in the medium, the growth of mutants was reduced slightly between days 4 and 5 of incubation. This observation can be explained by the glucose being depleted after 3–4 days of incubation, leading to the release of repression of the D-galacturonic catabolic genes and putative D-galacturonic acid transporter genes. This enables the fungus to switch to D-galacturonic acid transport and consumption, resulting in the accumulation of pathway intermediates to levels sufficient to cause growth reduction. Future studies with knockout mutants of putative D-galacturonic acid transporter genes in the background of a  $\Delta Bclgd1$  mutant could confirm the growth-reducing effect of catabolic pathway intermediates both *in planta* and *in vitro*. Failure to import D-galacturonic acid would prevent the accumulation of the inhibitory intermediates and thereby alleviate the growth reduction. Such experiments were, however, beyond the scope of the present study. The D-galacturonic acid catabolic pathway has been characterized in *Hypocrea jecorina* and *Aspergillus niger*

(Martens-Uzunova and Schaap, 2008; Richard and Hilditch, 2009). In these fungi, there is no evidence of growth-reducing effects of catabolic pathway intermediates. Intracellular accumulation of 2-keto-3-deoxy-L-galactonate was observed in the *H. jecorina lga1* mutant and the *Aspergillus niger gaaC* mutant ( $\Delta Bclga1$  mutant in *B. cinerea*), but did not appear to affect hyphal viability or sporulation (Hilditch et al., 2007; Wiebe et al., 2010). In addition, the degradation of 2-keto-3-deoxy-L-galactonate was observed in *H. jecorina* and *Aspergillus niger* mutant cultures (Wiebe et al., 2010), suggesting that alternative mechanisms exist in these fungi, which prevent the accumulation of inhibitory compounds. Such alternative pathways are either less effective or missing in *B. cinerea*. The observed growth-reducing effects of catabolic pathway intermediates forced us to reconsider the interpretation of the virulence assays. It was particularly striking that the extent of reduction in virulence of the mutants in different steps of the catabolic pathway was strongly correlated with the extent of growth reduction *in vitro* (on fructose plus D-galacturonic acid). Furthermore, the reduced virulence was especially observed in host species with higher contents of D-galacturonic acid in their cell walls. *S. lycopersicum* has 30%–40% smaller amounts of D-galacturonic acid in its cell wall when compared with *N. benthamiana* and *A. thaliana*. This leads to less pronounced induction of the expression of D-galacturonic acid catabolic genes in *S. lycopersicum* than in the other two hosts, as corroborated by the observed expression profiles (Figure 2). The levels of glucose and sucrose in all three plants tested are negligible when compared with the monosaccharides deposited in cell walls. The concentrations of free monosaccharides in leaves are insufficient to cause catabolite repression of *B. cinerea* D-galacturonic acid catabolic genes (Figure S2). The consequence is that the growth-reducing effects of D-galacturonic acid catabolic intermediates during infection on *S. lycopersicum* leaves are negligible and lesions of the mutants are as large as those of the wild-type. By contrast, the higher D-galacturonic acid levels in *N. benthamiana* and *A. thaliana* leaves cause higher expression of D-galacturonic acid catabolic genes, and more rapid and greater accumulation of catabolic intermediates, leading to slower lesion outgrowth. Ideally, instead of comparing host species with distinct pectin composition, one might prefer to compare the virulence of *B. cinerea* on a single wild-type host species and on an isogenic mutant with an altered content of D-galacturonic acid in its cell wall. The *A. thaliana qua1* mutant is deficient in pectin synthesis and contains 25% less D-galacturonic acid in the cell wall (Bouton et al., 2002). However, this mutant is severely dwarfed and displays numerous features that would influence the interaction with *B. cinerea* in an unpredictable manner. Pectin is of such crucial relevance for plant cell architecture (Mohnen, 2008) that it is not feasible to compare the virulence of pathogens on genotypes from the same plant species with markedly different D-galacturonic acid contents. The question at the onset of this study

was whether the important role of endo-PGs in the virulence of *B. cinerea* relates to a function in tissue disintegration and colonization, and/or to a function in the release of an abundant source of monosaccharide nutrients from pectic polymers. The data presented here suggest that the reduced virulence of D-galacturonic acid catabolism deficient *B. cinerea* mutants on *N. benthamiana* and *A. thaliana* is only partly caused by the inability of mutants to utilize pectic monosaccharides that serve as an important nutrient source. The growth inhibitory effect of the D-galacturonic acid catabolic pathway intermediates might make a more significant contribution to the reduced virulence phenotype of the mutants.

## Materials and Methods

### Fungal strain and growth conditions

*Botrytis cinerea* wild-type strain B05.10 and the mutant strains  $\Delta Bcgar1/\Delta Bcgar2$ ,  $\Delta Bclgd1$ , and  $\Delta Bclga1$  used in this study were routinely grown on Malt Extract Agar (Oxoid; 50 gram/liter) in darkness at 20 °C for 3-4 days. The plates were placed for one night under near-UV light (350-400 nm) to promote sporulation, and were subsequently returned to darkness. Conidia were harvested 4-7 days later in 10-20 ml water, and the suspension was filtered over glass wool to remove mycelium fragments. The conidia suspension was centrifuged at 800 rpm (120 g) for 5 minutes. The supernatant was discarded and the conidia in the pellet resuspended at the desired density. For radial growth assays, conidia of the strains were inoculated on Gamborg's B5 (Duchefa, Haarlem, The Netherlands) agarose medium supplemented with 10 mM  $(NH_4)H_2PO_4$ , either fructose (10 mM) or glucose (10 or 50 mM) as carbon source and D-galacturonic acid (0.05, 0.3, or 1 mM). Cultures were grown at 20 °C and the colony diameter was measured after 3, 4, and 5 days of incubation.

### Plant material and growth conditions

*Solanum lycopersicum* (Moneymaker) and *Nicotiana benthamiana* plants were grown in a greenhouse at 20 °C. *Arabidopsis thaliana* wild-type Columbia (Col-0) plants were grown in a growth chamber at 20 °C and 70% relative humidity under a 12 h light/dark cycle.

### Plant infection

Leaves of 5-6 weeks-old *S. lycopersicum*, *N. benthamiana* and *A. thaliana* plants were inoculated with *B. cinerea*. Droplets of a suspension of conidia of wild-type and mutants (2  $\mu$ l,  $10^6$  conidia/ml in potato dextrose broth, 1.2 g/l) were inoculated on opposite sides of the central vein (for *S. lycopersicum* 3-4 droplets per leaf half, for *N. benthamiana* 1-2 droplets per leaf half). Each comparison of wild-type and mutant was performed on 4

leaflets of one composite tomato leaf, on two composite leaves per plant, and two plants per experiment; or on 3-4 leaves per *N. benthamiana* plant, and 6 plants per experiment; leading to a total of at least 50 lesions per experiment. Lesion diameters were measured with a digital calliper at 3 dpi. Six discs containing the infection lesions in the centre (30 mm in diameter) from 3 leaves of 3 plants were sampled at 2 and 3 days post inoculation (dpi) as a pool for RNA isolation and biomass quantification.

For *A. thaliana* infection, one droplet of a suspension of conidia of wild-type or mutants were inoculated on one side of each detached leaf. Eight leaves of each inoculation were sampled at 1, 2, and 3 dpi as a pool for RNA isolation and biomass quantification.

Each mutant was tested in at least two independent experiments. Lesion sizes and fungal biomass were analysed statistically by a Student's *t*-test, using two-tailed distribution and two-sample unequal variance.

### **RNA extraction and quantitative reverse transcription-polymerase chain reaction (qRT-PCR) analysis**

The infected plant material was freeze-dried and partially used for RNA extraction. Total RNA was isolated using a Nucleospin® RNA plant kit (Machery-Nagl, Düren, Germany), according to manufacturer's instructions. First strand cDNA was synthesized from 1 µg total RNA with SuperScript® III Reverse Transcriptase (Invitrogen) according to the manufacturer's instructions.

qRT-PCR was performed using an ABI7300 PCR machine (Applied Biosystems, Foster City, U.S.A.) in combination with the qPCR SensiMix kit (BioLine, London, U.K.). The primers to detect the transcripts of *B. cinerea* and *A. thaliana* genes are listed in Table S1 and S2, respectively. Real-time PCR conditions were as follows: an initial 95 °C denaturation step for 10 min followed by denaturation for 15 s at 95 °C and annealing/extension for 45 s at 60 °C for 40 cycles. The data were analysed on the 7300 System SDS software (Applied Biosystems, Foster City, U.S.A.). The transcript levels of target genes were normalized to the transcript levels of the constitutively expressed gene *Bcrp15* (for *B. cinerea* genes) and *Atactin* (for *A. thaliana* genes), according to the  $2^{-\Delta\Delta Ct}$  method.

### **Measurement of *B. cinerea* biomass**

The freeze-dried infected plant material was incubated in the extraction buffer (35 mg/ml), which is provided in the QuickStix™ kit for *B. cinerea* (Enviro-Logix, Portland, Maine). After 10 min incubation, the supernatants were used for fungal biomass quantification with a lateral flow device (Dewey et al., 2008), which quantifies a stable water-soluble, extracellular epitope (Meyer and Dewey, 2000). The signal intensity of the monoclonal antibody reaction was determined with an optical reader (Enviroligix) and converted into

fungal biomass ( $\mu\text{g}/\text{mg}$  plant tissue), which was calculated based on the standard curves generated by known amounts of dry mycelium diluted into extraction buffer. The fungal biomass of mutants was normalized to that of the wild-type strain.

### **Alcohol insoluble residues (AIR) preparation and sugar composition analysis**

Leaves of 5-6 weeks-old plants were freeze-dried and milled. AIR was extracted with 70% ethanol at 50 °C as described by Hilz et al. (2005). The obtained AIR was dissolved and pre-hydrolysed with 72% w/w sulphuric acid at 30 °C for 1 h followed by hydrolysis with additional ddH<sub>2</sub>O for 3 h at 100 °C. The uronic acid content of the hydrolysed samples was determined by m-hydroxydiphenyl assay (Blumenkranz and Asboe-Hansen, 1973; Kintner and Vanburen, 1982), using an auto-analyser (Skalar Analytical BV, Breda, The Netherlands). Galacturonic acid was used as a standard for quantification. After hydrolysis, the neutral sugars were converted into alditol acetates and determined by gas chromatography (Englyst and Cummings, 1984), using inositol as the internal standard.

### **Sugar extraction of plant leaves and sucrose, D-fructose, D-glucose determination**

Leaves of 5-6-week-old plants were freeze-dried and milled. Powered materials were extracted with 70% ethanol. The supernatant was filtered with a 0.2  $\mu\text{m}$  filter and evaporated to remove ethanol. The obtained sugar extracts were dissolved in water and purified with chloroform. The water phase was transferred to a fresh tube and incubated at 65 °C for 10 min to inactivate the enzymes in the samples. The sucrose, D-fructose, and D-glucose contents were measured with a sucrose, D-fructose, and D-glucose assay kit (Megazyme) according to the manufacturer's instruction.

## **Supporting information**

Supplementary Figures S1, S2, S3, S4 and Supplementary Tables S1, S2.

## **Acknowledgements**

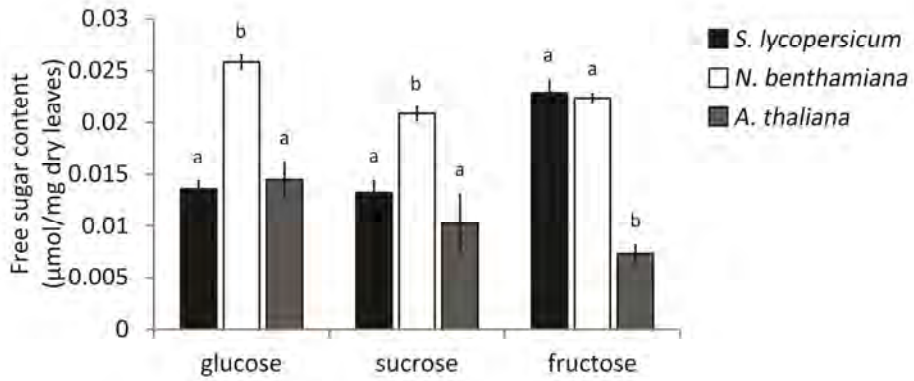
The authors are grateful to Yvonne Westphal and Henk Schols (Wageningen University, Laboratory of Food Chemistry) for providing facilities, advice and assistance for the determination of plant cell wall composition.

The authors are grateful to Barbara Blanco-Ulate and Ann Powell (Plant Sciences Department, University of California, Davis, USA), to Guido van den Ackerveken (Utrecht University, The Netherlands) and to Pierre de Wit (Wageningen University, Laboratory of

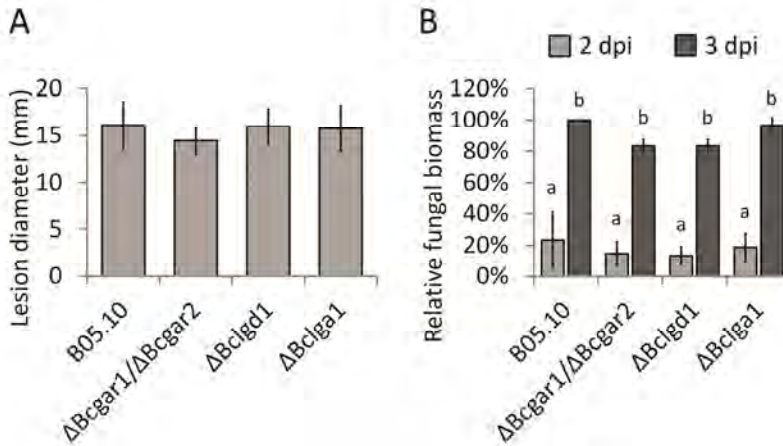
## Chapter 4

Phytopathology) for comments on a draft version of the manuscript and for fruitful discussion. The authors acknowledge funding by the Foundation Technological Top Institute Green Genetics (Project 2CC035RP) and the Netherlands Graduate School Experimental Plant Sciences.

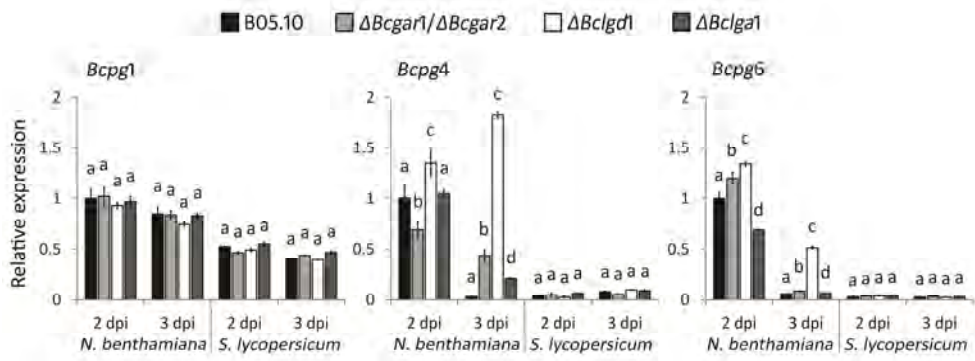
## Supporting information



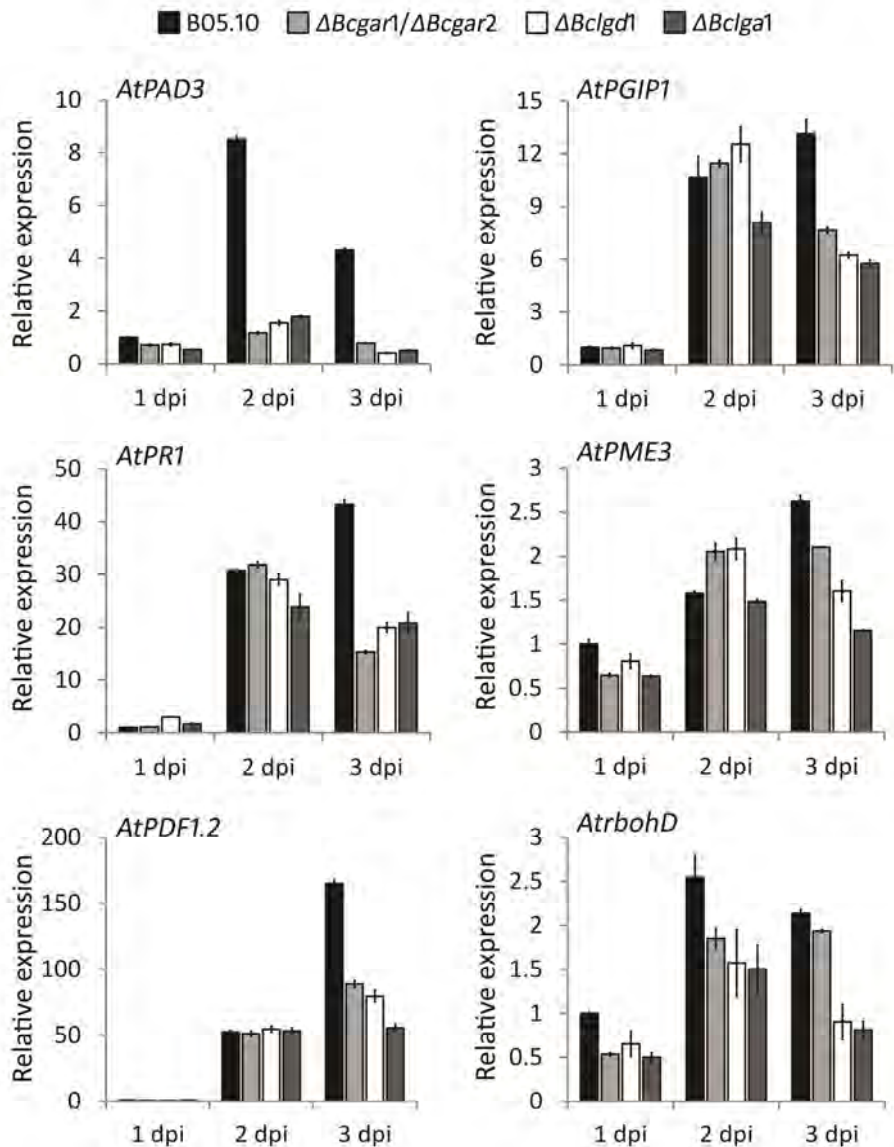
**Supplementary Figure 1.** Sugar contents in leaves of *Solanum lycopersicum*, *Nicotiana benthamiana*, and *Arabidopsis thaliana*. Bars indicate means  $\pm$  standard deviation. Letters above bars indicate statistical significance; bars not sharing letters represent significant mean differences at  $P < 0.05$  by Student's *t*-test.



**Supplementary Figure 2.** Virulence of D-galacturonic acid catabolism-deficient mutants on *Solanum lycopersicum* leaves. A, lesion sizes of *B. cinerea* wild-type and mutants were evaluated 3 days post-inoculation (dpi) by determining the average lesion diameter on 2 composite leaves from 2 plants each. Data represent means  $\pm$  standard deviation ( $n \geq 50$  independent lesions). B, *Botrytis cinerea* biomass accumulation by immunological detection at 2 and 3 dpi on *S. lycopersicum*. Six lesion discs (30 mm in diameter) from 3 leaves of 2 plants were sampled as a pool for quantification. Data represent means  $\pm$  standard deviation from two independent biological repeats. Letters above bars indicate statistical significance; bars not sharing letters represent significant mean differences at  $P < 0.05$  by Student's *t*-test.



**Supplementary Figure 3.** Relative transcript levels of *BcpG1*, *BcpG4*, and *BcpG6* in wild-type *Botrytis cinerea* and D-galacturonic acid catabolism-deficient mutants during infection on *Nicotiana benthamiana* and *Solanum lycopersicum* leaves. Infected plants were sampled at 2 and 3 days post-inoculation (dpi) for RNA extraction. mRNA levels of *BcpG1*, *BcpG4*, and *BcpG6* genes were normalized to the levels of the constitutive reference gene *Bcrp15* and calibrated to wild-type strain B05.10 levels at time point 2 dpi on *N. benthamiana* leaves (set as 1), according to the  $2^{-\Delta\Delta Ct}$  method. Data are represented as means  $\pm$  standard deviation from one biological repeat. Three technical replicates of each repeat were analysed and three independent biological repeats were performed, which showed similar results. For each time point on each plant leaves, letters above bars indicate statistical significance; bars not sharing letters represent significant mean differences at  $P < 0.05$  by Student's *t*-test.



**Supplementary Figure 4.** Relative transcript levels of *A. thaliana* defence-related genes during infection with *B. cinerea* wild-type strain and D-galacturonic acid catabolism-deficient mutants. Infected leaves were sampled at 1, 2, and 3 days post-inoculation (dpi) for RNA extraction. mRNA levels of *A. thaliana* genes were normalized to the levels of the constitutive reference gene *Atactin* and calibrated to the levels with *B. cinerea* wild-type at time point 1 dpi (set as 1), according to the  $2^{-\Delta\Delta Ct}$  method. Data are represented as means  $\pm$  standard deviation from one biological repeat. Three technical replicates of each repeat were analysed and three independent biological repeats were performed, which all showed similar results.

**Supplementary Table 1.** qRT-PCR primers of *Botrytis cinerea* genes used in this study.

Primer No.	Target gene	Sequence (5'-3')
LZ101	<i>Bcgar1</i> F	GCTTAGCTACCATGTTGCTCG
LZ102	<i>Bcgar1</i> R	TTCTTCTTCAGGTCGTCTGAG
LZ35	<i>Bcgar2</i> F	CCCAGCTATCCGTGAACATC
LZ36	<i>Bcgar2</i> R	CACCTGGGGAAAGCGCATC
LZ37	<i>Bclgd1</i> F	TGGTCATGGCATGACTTTCAC
LZ38	<i>Bclgd1</i> R	GTTGCGAATCGGAAACGAGATA
LZ39	<i>Bclga1</i> F	CAAGGTTTGGGAATTGTACAGAG
LZ40	<i>Bclga1</i> R	GTATCCTCCATATCCATAGTAGC
LZ66	<i>Bcpg1</i> F	CTGCCAACGGTGTCCGTATC
LZ67	<i>Bcpg1</i> R	GAACGACAACACCGTAGGATG
LZ68	<i>Bcpg2</i> F	GGAAGTCCCACTTTTGTTAC
LZ69	<i>Bcpg2</i> R	TCCATCCCACCATCTTGCTC
LZ70	<i>Bcpg3</i> F	TACTGTTGCGAAGAGCACAAAG
LZ71	<i>Bcpg3</i> R	GACTTGACGTAGGAGCTTCG
LZ72	<i>Bcpg4</i> F	CTTATTGAGTACGCCACTGTC
LZ73	<i>Bcpg4</i> R	AGTGTGCACGGTGTGTTGTC
LZ74	<i>Bcpg5</i> F	ATGATGGAACGTCCGGTGAG
LZ75	<i>Bcpg5</i> R	ATGTCCAATCGGTGCAAGAAC
LZ76	<i>Bcpg6</i> F	ATTTGATGTCAGCTCGTCCAG
LZ77	<i>Bcpg6</i> R	ACCTGAGCAATATAACCCGTC
LZ80	<i>Bcrp15</i> F	GATGAGACCGTCAAATGGTTC
LZ81	<i>Bcrp15</i> R	CAGAAGCCCACGTTACGACA

**Supplementary Table 2.** qRT-PCR primers of *Arabidopsis thaliana* genes used in this study.

Target gene	Sequence (5'-3')
<i>AtPAD3</i> F	GGCTGAAGCGGCATAAGAG
<i>AtPAD3</i> R	TCCAGGCTTAAGATGCTCGT
<i>AtPR1</i> F	TCGTCTTTGTAGCTCTGTAGGTGC
<i>AtPR1</i> R	ACCCAGGCTAAGTTTTCCC
<i>AtPDF1.2</i> F	CACCCTTATCTTCGCTGCTC
<i>AtPDF1.2</i> R	GTTGCATGATCCATGTTTGG
<i>AtPGIP1</i> F	GAACAAACTTACAGGTTCCATAC
<i>AtPGIP1</i> R	GATCCGGTTAAAGTCGATGTTG
<i>AtPME3</i> F	TTGTTGAAGGGGCAGATACAC
<i>AtPME3</i> R	CTTGAGCTTACGGTTGTTTGG
<i>AtrbohD</i> F	CGGCAAAGAATAGGAGTCTTC
<i>AtrbohD</i> R	GTTCTCTTGTGGAAGTCAAAC
<i>Atactin</i> F	CGAGCAGCATGAAGATTAAGG
<i>Atactin</i> R	GCCTGGACCTGCTTCATCATA

# CHAPTER 5

Functional analysis of putative D-galacturonic acid transporters  
in *Botrytis cinerea*

Lisha Zhang, Sayantani Chatterjee, Chenlei Hua, Jan A. L. van Kan

## Abstract

Plant pathogenic fungi use different strategies to acquire carbon sources from their host plants. *Botrytis cinerea* predominantly infects plant tissues and species that are rich in pectin, which is mainly composed of D-galacturonic acid. Effective utilization of D-galacturonic acid is important for virulence of *B. cinerea*. Transcriptome data showed that hexose transporter genes *Bchxt8*, *Bchxt11*, *Bchxt13* and *Bchxt15* are up-regulated in a culture with pectate as the sole carbon source, as compared to cultures with glucose. Additional qRT-PCR analysis showed that *Bchxt15* is highly (> 180 fold) and specifically induced by D-galacturonic acid, but not by five other carbon sources analysed, whereas *Bchxt13* is highly expressed in the presence of all carbon sources tested except for glucose. Subcellular location of BcHXT13-GFP and BcHXT15-GFP fusion proteins expressed under control of their native promoter was studied in a *B. cinerea* wild-type strain. Both genes are expressed during growth on D-galacturonic acid and the fusion proteins are localized in plasma membranes and intracellular vesicles. Mutants of *B. cinerea*, in which *Bchxt13* and *Bchxt15* genes were knocked out, were neither affected in their growth on D-galacturonic acid as the sole carbon source, nor in their virulence on tomato and *Nicotiana benthamiana* leaves.

## Introduction

The main sugar uptake system in fungi comprises hexose transporters, which are members of the major facilitator superfamily (MFS) and are membrane-bound proteins containing 12 putative transmembrane domains (Marger and Saier, 1993; Pao et al., 1998). The best characterised hexose transporters in fungi are from *Saccharomyces cerevisiae*, of which the genome contains 20 genes encoding hexose transporters (HXT1 to HXT17, GAL2, SNF3, and RGT2). None of these transporters are essential for growth on glucose due to their functional redundancy (Ozcan and Johnston, 1999). In *Aspergillus nidulans*, there are at least 17 putative hexose transporters and deletion of *hxtA* did not impair growth of the fungus on a variety of carbon sources (Wei et al., 2004).

Plant pathogenic fungi cause globally severe losses of crops during growth and after harvest every year (Fisher et al., 2012). Different fungi have developed different strategies to acquire nutrients from their host plants. The nutrition of biotrophic pathogens relies on living host cells, whereas necrotrophic pathogens kill plant cells and feed on dead or dying tissues. Other pathogens (hemi-biotrophs) employ both types of nutrition, starting with biotrophic growth and switching to necrotrophic invasion at a later stage.

A proton-dependent hexose symporter (UfHXT1) of the biotroph *Uromyces fabae*, the causal agent of broad bean rust, was shown to be involved in uptake of hexoses across the haustorial membrane (Voegelé et al., 2001). A study of five hexose transporters (CgHXT1-5) of the hemi-biotrophic pathogen *Colletotrichum graminicola* showed that these hexose transporters were functionally distinct: CgHXT1 to CgHXT3 are high affinity/low capacity transporters that accept several hexoses, whereas CgHXT5 is a low affinity/high capacity transporter with a narrow substrate specificity, involved in uptake of glucose and mannose only. Moreover, their expression was different at different stages of infection: *CgHXT1* and *CgHXT3* were transiently up-regulated during the biotrophic stage, and *CgHXT2* and *CgHXT5* were expressed exclusively during necrotrophic stages, while *CgHXT4* was expressed throughout the infection (Lingner et al., 2011).

The necrotrophic fungal plant pathogen *Botrytis cinerea* is able to infect over 200 host plants and causes severe damage to crops, both pre- and post-harvest (Dean et al., 2012). The broad range of host plants suggests that *B. cinerea* has adapted to various nutritional environments and possesses a complex sugar uptake system to acquire carbon nutrients from different hosts and during different infection stages (van Kan, 2006). Studies by Dulermo et al. (2009) on the expression profiles of 17 putative hexose transporter (*Bchxt*) genes in *B. cinerea* during infection of sunflower, showed four types of expression profiles for hexose transporters: (1) constitutive during the course of infection; (2) transient at a certain time point; (3) decreased during the course of infection; (4) increased at the late

stage of infection. Collectively, the data revealed that uptake of plant hexoses by *B. cinerea* is based on a multigenic transporter system. Doehlemann et al. (2005) specifically studied the biochemical properties of the high affinity fructose transporter BcFRT1, which is phylogenetically distinct from the 17 BcHXT proteins (Dulermo et al., 2009).

*B. cinerea* often penetrates host leaf tissue at the anticlinal cell wall and subsequently grows into and through the middle lamella, which consists mostly of low-methylesterified pectin. The monosaccharide D-galacturonic acid is the most abundant component of pectic polysaccharides (Caffall and Mohnen, 2009; Mohnen, 2008) and is the ultimate hydrolytic product released from pectin degradation. Recently, we have characterised the D-galacturonic acid catabolic pathway in *B. cinerea*, which consists of three catalytic steps converting D-galacturonic acid to pyruvate and L-glyceraldehyde. The pathway involves two non-homologous galacturonate reductase genes (*Bcgar1* and *Bcgar2*), a galactonate dehydratase gene (*Bclgd1*) and a 2-keto-3-deoxy-L-galactonate aldolase gene (*Bclga1*) (Zhang et al., 2011). Knockout mutants in each step of the pathway ( $\Delta Bcgar1/\Delta Bcgar2$ ,  $\Delta Bclgd1$ , and  $\Delta Bclga1$ ) were affected in growth on D-galacturonic acid, pectate, or pectin as the sole carbon source (Zhang et al., 2011) and in virulence on *Nicotiana benthamiana* and *Arabidopsis thaliana* leaves (Zhang and van Kan, 2013).

However, the D-galacturonic acid uptake system in *B. cinerea* during colonization and growth inside the host remains uncharacterized. Preliminary transcriptome data suggested that hexose transporter genes *Bchxt8*, *Bchxt11*, *Bchxt13* and *Bchxt15* (Dulermo et al., 2009) are up-regulated in a culture with pectate as the sole carbon source, as compared to cultures with glucose. In this study, their expression was further investigated by quantitative RT-PCR during growth on different carbon sources and during infection on different plants. Subcellular localization of BcHXT13-GFP and BcHXT15-GFP fusion proteins expressed under their native promoter was determined in a *B. cinerea* wild-type strain. In addition, the function of *Bchxt15* and *Bchxt13* in *B. cinerea* was studied by generating knockout mutants and testing them *in vitro* and *in planta*.

## Results

### Expression and phylogenetic analysis of four *Botrytis cinerea* hexose transporter genes

To determine whether *Bchxt8*, *Bchxt11*, *Bchxt13* and *Bchxt15* are specifically induced by D-galacturonic acid or not, their mRNA level was determined by quantitative RT-PCR (qRT-PCR) in cultures containing glucose, D-galacturonic acid, arabinose, rhamnose, galactose, or xylose as the sole carbon source. Cultures were first grown in glucose-containing medium and transferred to fresh medium with different carbon sources mentioned, and sampled at 3 h after transfer for transcript analysis. *Bchxt8* and *Bchxt13* were not only induced in the D-galacturonic acid-containing culture (~5-fold and ~20-fold respectively), but were also induced in cultures with other carbon sources tested. Especially *Bchxt8* was strongly (~230-fold) induced in cultures with galactose or xylose as carbon source, compared to a glucose-containing culture (Figure 1). Notably, *Bchxt15* was induced specifically and strongly (~180-fold) in the D-galacturonic acid-containing culture, compared to all other cultures (Figure 1). The expression of *Bchxt11* was similar among the different sugar-containing cultures (Figure 1).

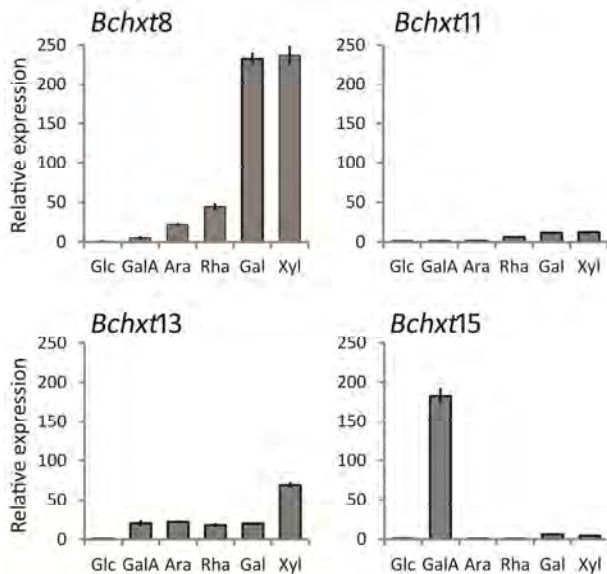


**Figure 1.** Relative transcript levels of hexose transporter genes in *Botrytis cinerea* during growth on different carbon sources (Glc, glucose; GalA, D-galacturonic acid; Ara, arabinose; Rha, rhamnose; Gal, galactose; Xyl, xylose) as assessed by qRT-PCR. Cultures of *B. cinerea* were sampled for RNA extraction at 3 h after transfer from a pre-culture with glucose as carbon source. mRNA levels of *Bchxt* genes were normalized to the levels of the constitutive reference gene *Bcrp15* and calibrated to the levels obtained in a glucose-containing culture (set as 1), according to the  $2^{-\Delta\Delta C_t}$  method. Data are represented as means  $\pm$  standard deviation from one biological repeat. Three technical replicates of each biological repeat were analysed and three independent biological repeats were performed, all with similar results.

Phylogenetic analysis was performed with BcHXT8, BcHXT11, BcHXT13, and BcHXT15, with 8 functionally characterised hexose transporters from pathogenic fungi differing in lifestyle (Doehlemann et al., 2005; Kim and Woloshuk, 2011; Lingner et al., 2011; Voegelé et al., 2001), and with 2 putative hexose transporters from the saprophytic fungus *Aspergillus niger* (Martens-Uzunova and Schaap, 2008). Figure 2 shows that three major clades of transporters were discriminated. BcHXT8 and BcHXT11 clustered with *Colletotrichum graminicola* and *Uromyces fabae* hexose transporters, and were most closely related to CgHXT3 and CgHXT1, respectively, both of which are transporters with high affinity for glucose (Lingner et al., 2011). By contrast, BcHXT13 and BcHXT15 clustered with the proteins encoded by An03g01620 and An14g04280, genes that were induced in *A. niger* grown on D-galacturonic acid or pectin (Kuivanen et al., 2012; Martens-Uzunova and Schaap, 2008). The third cluster contains BcFRT1, a fructose transporter from *B. cinerea* (Doehlemann et al., 2005), and FvFST1, a putative hexose transporter required by *Fusarium verticillioides* to colonize maize kernels (Kim and Woloshuk, 2011). Collectively, the expression and phylogenetic data suggest that BcHXT13 and BcHXT15 might play a role in D-galacturonic acid uptake; especially BcHXT15 might have a prominent role because of its strong and specific up-regulation by D-galacturonic acid. Thus, we focused on these two genes for further study.

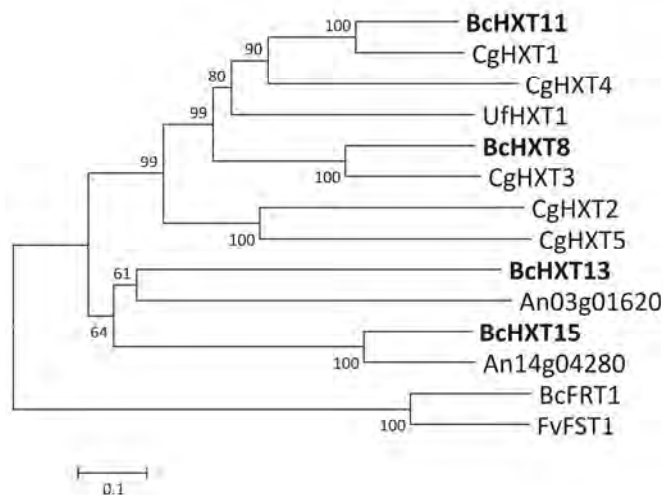


**Figure 2.** Phylogenetic analysis of fungal hexose transporters. Amino acid sequences of *B. cinerea* transporters were obtained from Broad institute *Botrytis cinerea* database ([http://www.broad-institute.org/annotation/genome/botrytis\\_cinerea/MultiHome.html](http://www.broad-institute.org/annotation/genome/botrytis_cinerea/MultiHome.html)) according to the locus ID (Staats and van Kan, 2012): BcHXT8: B0510\_7979; BcHXT11: B0510\_5073; BcHXT13: B0510\_9487; BcHXT15: B0510\_3996; BcFRT1: B0510\_8895; other fungal transporter sequences were obtained from GenBank according to the accession number: CgHXT1 to CgHXT5: FN433101 to FN433105; UfHXT1: AJ310209; FvFST1: EU152990. The amino acid sequences were aligned by Clustal\_X 1.83 and the phylogenetic tree was generated by using Mega 4 (Tamura et al., 2007) by the Neighbor-Joining (NJ) method with 1000 bootstrap replicates.

**Subcellular localization of BcHXT13 and BcHXT15**

To study the subcellular localization of BcHXT13 and BcHXT15, both genes were fused to GFP and transformed into *B. cinerea* wild-type strain B05.10 with their native promoters. The hyphae of transformants germinated in the presence of glucose, D-galacturonic acid, or xylose as carbon sources, were examined by epifluorescence microscopy. In the medium with D-galacturonic acid as carbon source, the BcHXT15-GFP expressing transformants showed fluorescence in the plasma membrane and septa, but also in vesicular structures which move inside the hyphae (Figure 3 and Figure 4). In most cases, fluorescence in the apical hyphal compartment is weaker than in the subapical hyphal region (Figure 3A). In the older hyphal region close to where the conidium germinated, the fluorescence was concentrated in immobile compartments which are larger than the mentioned vesicular structures (Figure 3B compared to 3A). No GFP fluorescence was detected in the hyphae of the BcHXT15-GFP expressing transformants, germinated in the presence of glucose or xylose (not shown). BcHXT13-GFP expressing transformants showed the same subcellular localization of fluorescence as the BcHXT15-GFP expressing transformants, when germinated in the medium with D-galacturonic acid or xylose as carbon source but not with glucose (Figure 3C and D). Under the same microscopic settings, the fluorescence of BcHXT13-GFP was in both cases weak as compared with BcHXT15-GFP in D-galacturonic acid (not shown). These results were consistent with the qRT-PCR data suggesting that *Bchxt13* is induced by both D-galacturonic acid and xylose, whereas *Bchxt15* is strongly induced solely by D-galacturonic acid (Figure 1).

To identify the nature of the vesicular structures and large compartments in which BcHXT15-GFP is located, the germinated hyphae of transformants were stained with fluorescent dyes DAPI, Mitotracker, and FM4-64, which specifically label nuclei, mitochondria and membrane structures, respectively. Figure 5 shows that the fluorescence of BcHXT15-GFP (green) does neither co-localize with DAPI-labelled nuclei (blue) nor with Mitotracker-labelled mitochondria (red). However, within 2 min of FM4-64 staining, the red dye is detected in the plasma membrane and in several small vesicles that overlapped with vesicles in which BcHXT15-GFP resided (Figure 6). After 2 h staining, FM4-64 signal was clearly observed in the membrane of the larger compartments where BcHXT15-GFP was located (Figure 6).

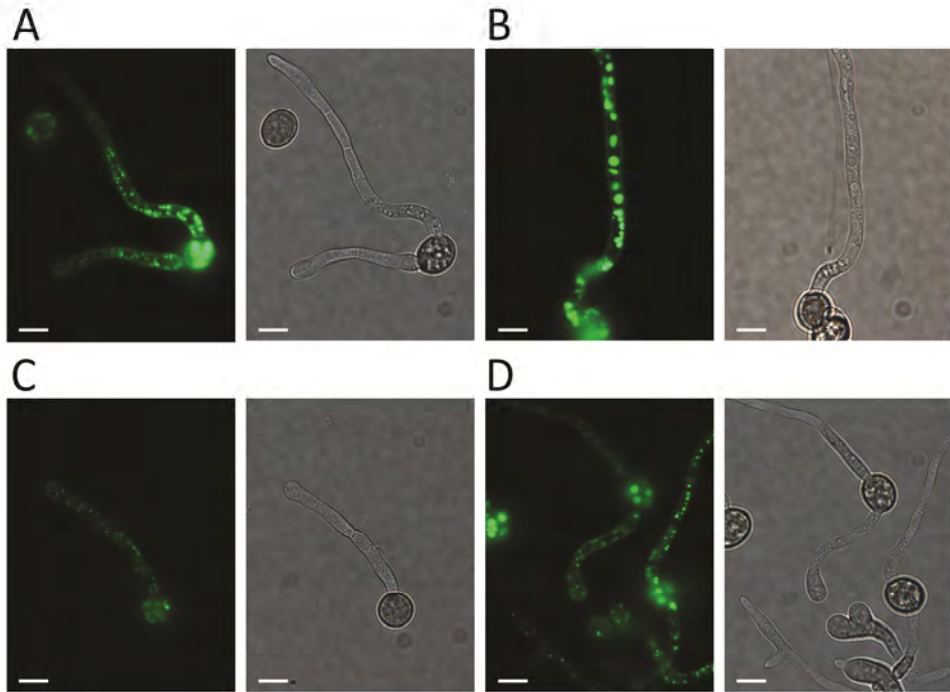


**Figure 3.** Subcellular localization of BcHXT15-GFP and BcHXT13-GFP in *Botrytis cinerea*. A and B, subcellular localization of BcHXT15-GFP during growth on medium with D-galacturonic acid at 20 h post incubation (hpi). C and D, subcellular localization of BcHXT13-GFP during growth on medium with D-galacturonic acid (C) or xylose (D) at 20 hpi. Fluorescence microscopic images are shown in the left panels and light microscope images are shown in the right panels (A to D). Scale bar = 10  $\mu$ m.

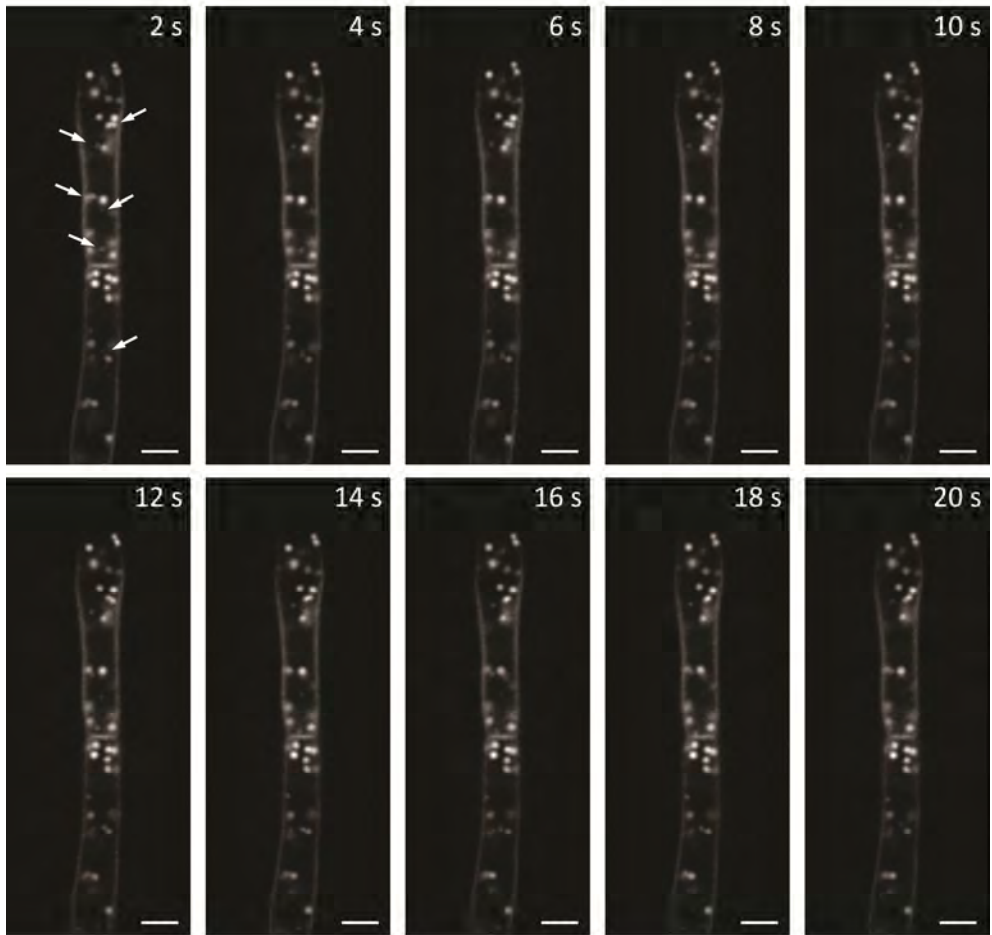


**Figure 4.** Time series imaging of subcellular localization of BcHXT15-GFP in *Botrytis cinerea*. Time interval of imaging is 2 s. Arrows indicate examples of moving vesicular structures. Scale bar = 5  $\mu$ m.

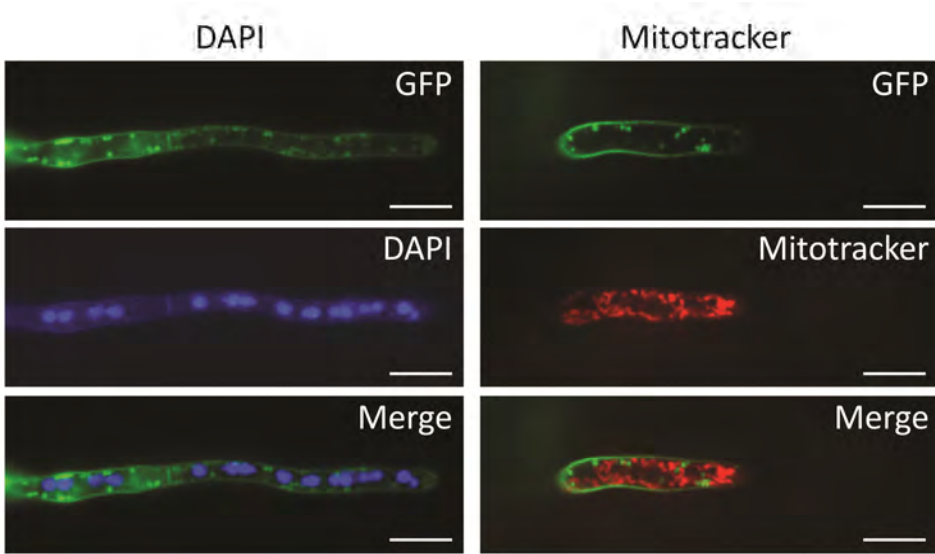


**Figure 5.** DAPI (blue) and Mitotracker (red) staining of BcHXT15-GFP expressing transformants. BcHXT15-GFP expressing transformant was stained with DAPI (blue) for 1 h or with Mitotracker (red) for 5 min before imaging. Scale bar = 10  $\mu$ m.

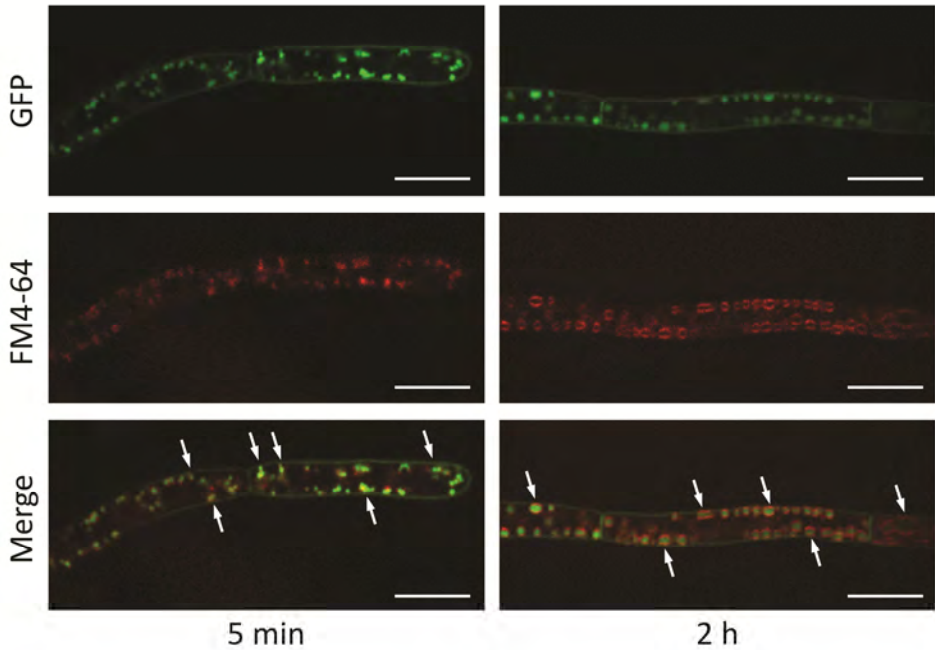


**Figure 6.** Co-localization of BcHXT15-GFP and FM4-64. FM4-64-stained BcHXT15-GFP-expressing transformant was imaged within 2 min and 2 h after staining, respectively. Arrows indicate examples of GFP and FM4-64 co-localization. Scale bar = 10  $\mu$ m.

### BcHXT13 and BcHXT15 are expressed during plant infection

The expression profiles of *Bchxt13* and *Bchxt15* were quantified during infection of wild-type *B. cinerea* on leaves of *S. lycopersicum* and *N. benthamiana* at 2 and 3 days post inoculation (dpi) (Figure 7A). Both genes were expressed in each host plant and there were only marginal differences in transcript levels between 2 and 3 dpi (relative to an internal standard transcript). The transcript levels of *Bchxt13* were only slightly different in *S. lycopersicum* and *N. benthamiana* between 2 and 3 dpi, whereas the transcript levels of *Bchxt15* were significantly higher in *N. benthamiana* than in *S. lycopersicum* at both time points. Furthermore, the expression of BcHXT13-GFP and BcHXT15-GFP was investigated on *N. benthamiana* leaves. At 2 dpi, fluorescence of BcHXT13-GFP and BcHXT15-GFP was visible throughout the mycelium in infected plant tissues (Figure 7B).

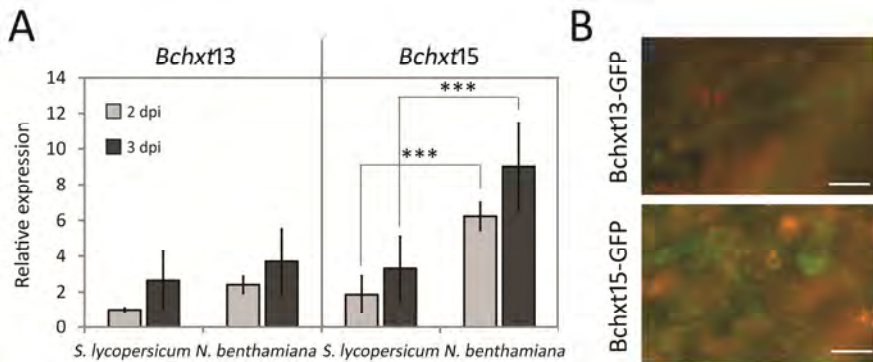


**Figure 7.** Expression of BcHXT13 and BcHXT15 during *Botrytis cinerea* infection on *Solanum lycopersicum* and *Nicotiana benthamiana* leaves. A, relative transcript levels of *Bchxt13* and *Bchxt15* as assessed by qRT-PCR. Infected plants were sampled at 2 and 3 days post-inoculation (dpi) for RNA extraction. mRNA levels of *Bchxt13* and *Bchxt15* were normalized to the levels of the constitutive reference gene *Bcrp15* and calibrated to the levels on *S. lycopersicum* at 2 dpi (set as 1), according to the  $2^{-\Delta\Delta C_t}$  method. Data are represented as means  $\pm$  standard deviation from one biological repeat. Three technical replicates of each biological repeat were analysed and three independent biological repeats were performed, all with similar results. B, subcellular localization of BcHXT15-GFP and BcHXT13-GFP in *B. cinerea* during infection on *N. benthamiana* leaves at 2 dpi. Scale bar = 50  $\mu$ m.

### Generation of *Bchxt13* and *Bchxt15* knockout mutants

To determine the function of *Bchxt13* and *Bchxt15* in D-galacturonic acid uptake in *B. cinerea*, knockout mutants were created by replacing the coding region of each gene by the hygromycin phosphotransferase resistance gene (*HPH*) in *B. cinerea* wild-type strain B05.10 background (Figure 8A). Two independent knockout mutants were characterized in detail at the molecular level (Figure 8B).

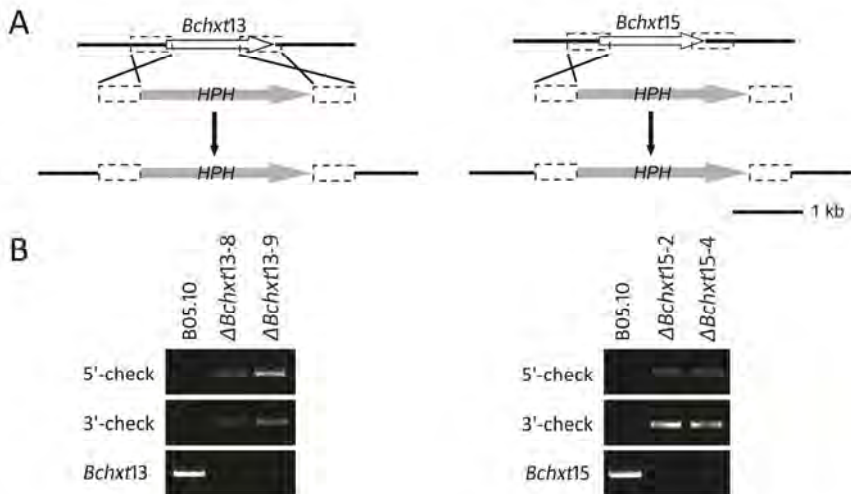


**Figure 8.** Knockout of *Bchxt13* and *Bchxt15* by targeted gene replacement. A, organization of *Bchxt13* and *Bchxt15* locus before and after homologous recombination in wild-type strain (*HPH* resistance cassette). Orientation of the target gene and *HPH* are indicated by white and grey arrows, respectively. Upstream and downstream flanks of target genes are shown with grey dashed-line frames. B, polymerase chain reaction (PCR) analysis of wild-type strain B05.10 and knockout mutant strains. The genomic DNA of each strain was used to verify 5' and 3' homologous recombination and absence of targeted genes in the corresponding knockout mutants, respectively.

### Growth of *Bchxt13* and *Bchxt15* knockout mutants on different carbon sources

Radial growth assays revealed that all the knockout mutants grew equally as the wild-type strain B05.10, on medium containing 50 mM glucose, as well as on medium with 50 mM D-galacturonic acid (not shown). To test whether D-galacturonic acid at a high concentration (50 mM) may be taken up by other BcHXTs in the  $\Delta Bchxt13$  and  $\Delta Bchxt15$  mutants, the radial growth was compared on medium containing 0.1 mM and 1 mM D-galacturonic acid.  $\Delta Bchxt13$  and  $\Delta Bchxt15$  mutants showed equal growth as the wild-type strain on medium with 1 mM D-galacturonic acid, whereas all the strains hardly grew on medium with 0.1 mM D-galacturonic acid (not shown). D-galacturonic acid is a strong acid and charged at the pH that is commonly used for the agar medium (pH 6-7). To test whether the medium pH influences the uptake of D-galacturonic acid, radial growth assays were also performed on strongly buffered medium (pH 4 and pH 5). However, all the mutants grew equally as the wild-type strain on both media, either with glucose or D-galacturonic acid as the sole carbon source (not shown). These results indicate that knockout of *Bchxt13* or *Bchxt15* does not impair the uptake of D-galacturonic acid in *B. cinerea*. In addition,  $\Delta Bchxt13$  and  $\Delta Bchxt15$  mutants showed the same growth as the

wild-type strain on medium with arabinose, rhamnose, galactose, or xylose as the sole carbon source (not shown).

#### **Virulence of $\Delta Bchxt13$ and $\Delta Bchxt15$ mutants**

The virulence of  $\Delta Bchxt13$  and  $\Delta Bchxt15$  mutants was investigated on *S. lycopersicum* and *N. benthamiana* leaves. There was no difference in lesion sizes between any of the tested mutants and the wild-type strain B05.10 (not shown).

## **Discussion**

In this study, the transcript levels of four *Botrytis cinerea* hexose transporter genes were investigated by qRT-PCR during *in vitro* growth in medium with different sugars as carbon source. *Bchxt15* is specifically up-regulated (~180-fold) by D-galacturonic acid while the other hexoses at most cause a ~5-fold transcript increase. The expression pattern of *Bchxt13* (Figure 1) might be considered to result from a high basal expression level on multiple hexoses, combined with specific induction (~3-fold) by xylose and catabolite repression in the presence of glucose. Furthermore, the expression of BcHXT13-GFP and BcHXT15-GFP controlled by their native promoter in *B. cinerea* is in agreement with the qRT-PCR analysis; BcHXT13-GFP is expressed in medium with D-galacturonic acid or xylose as the carbon source, whereas BcHXT15-GFP is expressed solely in D-galacturonic acid-containing medium (Figure 3). Moreover, the phylogenetic analysis (Figure 2) demonstrates that BcHXT13 and BcHXT15 closely grouped with the putative hexose transporters An03g01620 and An14g04280 from *Aspergillus niger*, respectively, two genes of which the expression was induced by D-galacturonic acid or pectin (Kuivanen et al., 2012; Martens-Uzunova and Schaap, 2008). It is plausible to suggest that BcHXT13 and BcHXT15 might be involved in D-galacturonic acid uptake with BcHXT15 likely playing a prominent role.

In *Saccharomyces cerevisiae* the transcriptional regulation of *HXT* genes in response to glucose is consistent with their function as low- or high-affinity transporters: for example, *HXT1* transcription is induced only by high concentrations of glucose and encodes a low-affinity glucose transporter, whereas *HXT6* and *HXT7* are expressed at low concentrations of glucose and encode high-affinity glucose transporters (Ozcan and Johnston, 1999). However, there is no systematic study in filamentous fungi demonstrating whether the substrate specificity of a hexose transporter is reflected in the profile of its gene expression.

The transcript level of *Bchxt15* was significantly higher in *Nicotiana benthamiana* than in *Solanum lycopersicum* (Figure 4A), which is correlated with the higher content of D-galacturonic acid in the cell walls of *N. benthamiana* as compared to *S. lycopersicum* (Zhang and van Kan, 2013). This observation is analogous to the transcript levels of D-galacturonic acid catabolic genes during infection on these plants, with relatively high transcript levels in *N. benthamiana* as opposed to low transcript levels in *S. lycopersicum* (Zhang and van Kan, 2013).

Functional analysis of *Bchxt13* and *Bchxt15* by characterising  $\Delta Bchxt13$  and  $\Delta Bchxt15$  knockout mutants did not reveal any phenotypic difference when compared with the wild-type strain. The *in vitro* growth of  $\Delta Bchxt13$  and  $\Delta Bchxt15$  mutants on medium with D-galacturonic acid as sole carbon source was indistinguishable from the wild-type strain B05.10. The presence of other hexose transporters probably facilitates sufficient uptake of D-galacturonic acid (at a relatively high concentration) for fungal growth. In order to reduce the contribution of the non-specific hexose transporters, the growth of  $\Delta Bchxt13$  and  $\Delta Bchxt15$  mutants was investigated on medium with D-galacturonic acid at a low concentration (1 mM). Nevertheless,  $\Delta Bchxt13$  and  $\Delta Bchxt15$  mutants grew equally to the wild-type strain. Lowering the concentration to 0.1 mM of D-galacturonic acid resulted in complete cessation of fungal growth, even in the wild-type recipient. These experiments were conducted in media that had a pH of 6. As D-galacturonic acid is an acid (pKa = 3.5), the ambient pH influences the charge of the molecule and might thereby influence its suitability as a substrate for the transporter. However,  $\Delta Bchxt13$  and  $\Delta Bchxt15$  mutants still showed similar growth as the wild-type strain on D-galacturonic acid-containing medium buffered to pH 4 and pH 5, at which the substrate is less charged. These experiments indicate that deletion of either *Bchxt13* or *Bchxt15* does not influence the uptake of D-galacturonic acid by *B. cinerea*, and the hexose uptake system in  $\Delta Bchxt13$  and  $\Delta Bchxt15$  mutants provides sufficient D-galacturonic acid for growth to the same extent as wild-type strain. Making  $\Delta Bchxt13/\Delta Bchxt15$  double mutants remains to be achieved, but even such mutants might still be able to grow on D-galacturonic acid, if other transporters can compensate for the absence of both BcHXT13 and BcHXT15.

This observation logically explains that  $\Delta Bchxt13$  and  $\Delta Bchxt15$  mutants were equally virulent as the wild-type strain on *S. lycopersicum* and *N. benthamiana* leaves, not only because the hexose uptake system transports sufficient D-galacturonic acid, but also because the fungus can utilize other sugars, present in host plant tissues as nutrients. Also a *B. cinerea* knockout mutant in a fructose transporter gene (*Bcfrt1*) showed normal growth on fructose and its virulence on bean and tomato leaves was indistinguishable from wild-type (Doehlemann et al., 2005).

Functional complementation in *Saccharomyces cerevisiae* is a convenient system to study fungal hexose transporter activity (Doehlemann et al., 2005; Kim and Woloshuk, 2011; Lingner et al., 2011). Transforming a candidate transporter gene into a *S. cerevisiae* strain, such as EBY.VW4000, which lacks 20 hexose transporters (Wieczorke et al., 1999) followed by investigating the growth of transformants on different hexoses can provide information about the substrate specificity of the transporter of interest. The ability of transformants expressing a candidate gene to grow on certain hexose(s) indicates that the protein encoded by this gene has the capacity to transport that/those specific hexose(s). However, there is no report of *S. cerevisiae* strains able to grow on D-galacturonic acid. Thus, we cannot use this method to analyse the D-galacturonic acid transporter activity of BcHXT13 and BcHXT15. Alternatively, *S. cerevisiae* can be used to quantify the uptake of hexoses by measuring the intracellular accumulation of radiolabeled substrates. A recent study demonstrated that *S. cerevisiae* has a high-capacity D-galacturonic acid uptake system (Souffriau et al., 2012), which suggests that it is not feasible to measure D-galacturonic acid uptake rate by BcHXT13 and BcHXT15 in *S. cerevisiae*. Surprisingly, none of more than 160 single and multiple *S. cerevisiae* deletion mutants in channels and transporters was affected in D-galacturonic acid uptake (Souffriau et al., 2012). In addition, genes with high homology to the genes of filamentous fungal D-galacturonic catabolic pathway (Martens-Uzunova and Schaap, 2008; Zhang et al., 2011) are absent in the *S. cerevisiae* genome. Altogether, it suggests that *S. cerevisiae* and filamentous fungi might have distinct D-galacturonic acid uptake systems and therefore the *S. cerevisiae* system is not suitable to perform functional analysis of filamentous fungal D-galacturonic acid transporters.

BcHXT13-GFP and BcHXT15-GFP are both located in the *B. cinerea* plasma membrane and in vesicular structures (Figure 3), in agreement with the reported location of other transporters, such as FvFST1 in *Fusarium verticillioides* (Kim and Woloshuk, 2011). Interestingly, the fluorescence of BcHXT15-GFP is weaker in the apical region (Figure 3B), suggesting that the uptake of D-galacturonic acid by BcHXT15 predominantly occurs in the subapical region rather than in the apical compartment. FM4-64 is a membrane-selective dye that is used as a marker to follow endocytosis in fungal cells (Fischer-Parton et al., 2000). The dye initially stains the plasma membrane and is subsequently internalized to small punctate vesicles, larger vesicles and eventually to the vacuolar membrane (Fischer-Parton et al., 2000; Hickey et al., 2004). The time courses of FM4-64 staining different cell components are variable among different fungi and also depend on the cell type and growth conditions tested (Hickey et al., 2004). In this study we observed the co-localization of BcHXT15-GFP with FM4-64 dye not only within 2 min after staining but also over a 2 h time lapse, suggesting that excess BcHXT15-GFP proteins are internalized by endocytosis and subsequently confined to vacuoles. It was reported that several *S.*

*cerevisiae* hexose transporters are internalized by endocytosis and degraded in vacuoles (Krampe and Boles, 2002; van Suylekom et al., 2007).

In summary, the data presented here suggest that BcHXT13 and BcHXT15 are both hexose transporters that localize in the plasma membrane. However, knockout mutants  $\Delta Bchxt13$  and  $\Delta Bchxt15$  were not impaired in their *in vitro* growth on D-galacturonic acid, likely due to functional redundancy of other hexose transporters. Genome-wide transcriptome analysis may be useful to identify the whole D-galacturonic acid uptake system in future.

## Materials and methods

### Fungal strain and growth conditions

*Botrytis cinerea* wild-type strain B05.10 and the mutant strains  $\Delta Bchxt13$  and  $\Delta Bchxt15$  used in this study were routinely grown on Malt Extract Agar (Oxoid, Basingstoke, UK; 50 g/L) in the dark at 20 °C for 3-4 days. The plates were placed for one night under near-UV light (350–400 nm) to promote sporulation, and were subsequently returned to darkness. Conidia were harvested 4-7 days later in 10–20 mL of water, and the suspension was filtered over glass wool to remove mycelium fragments. The conidia suspension was centrifuged at 1200 rpm for 5 min. The supernatant was discarded and the conidia in the pellet were resuspended at the desired density.

For radial growth assays, conidia of the strains were inoculated on Gamborg's B5 (Duchefa, Haarlem, The Netherlands) agarose medium supplemented with 10 mM  $(\text{NH}_4)_2\text{H}_2\text{PO}_4$  and as carbon source either D-glucose (50 mM), D-galacturonic acid (0.1, 1 or 50 mM), L-arabinose (50 mM), D-rhamnose (50 mM), D-galactose (50 mM), or D-xylose (50 mM). Cultures were grown at 20 °C and the colony diameter was measured after 3 to 5 days of incubation.

### RNA extraction and quantitative RT-PCR analysis

For *in vitro* gene expression analysis, the conidia of the wild-type strain B05.10 were incubated in Gamborg's B5 liquid culture supplemented with 10 mM  $(\text{NH}_4)_2\text{H}_2\text{PO}_4$  and 50 mM glucose at 20 °C, 150 rpm. After 16 h of growth, the mycelium was harvested as described (Wubben et al., 1999) and transferred into fresh Gamborg's B5 medium supplemented with 10 mM  $(\text{NH}_4)_2\text{H}_2\text{PO}_4$  and as carbon source either D-glucose, D-galacturonic acid, L-arabinose, D-rhamnose, D-galactose, or D-xylose (each at 50 mM). Mycelium was harvested from these cultures at 3 h post transfer and freeze dried.

For *in planta* gene expression analysis, six discs containing the infected lesions in the centre (30 mm in diameter) from three leaves of three plants were sampled at 2 and 3 dpi as a pool for RNA isolation.

Total RNA was isolated using the Nucleospin® RNA plant kit (Machery-Nagl, Düren, Germany), according to the manufacturer's instructions. First strand cDNA was synthesized from 1 µg total RNA with SuperScript® III Reverse Transcriptase (Invitrogen) according to the manufacturer's instructions.

Quantitative RT-PCR was performed using an ABI7300 PCR machine (Applied Biosystems, Foster City, U.S.A.) in combination with the qPCR SensiMix kit (BioLine, London, U.K.). The primers to detect the transcripts of *B. cinerea* genes are listed in Table S2. Real-time PCR conditions were as follows: an initial 95 °C denaturation step for 10 min followed by denaturation for 15 s at 95 °C and annealing/extension for 45 s at 60 °C for 40 cycles. The data were analysed on the 7300 System SDS software (Applied Biosystems, Foster City, U.S.A.). The transcript levels of target genes were normalized to the transcript levels of the constitutively expressed gene *Bcrp15*, according to the  $2^{-\Delta\Delta Ct}$  method.

#### **Knocking out of *Bchxt13* and *Bchxt15* genes in *B. cinerea***

The gene knockout strategy for generating *B. cinerea* knockout constructs, *B. cinerea* protoplast transformation and PCR-based screening of transformants were described by Kars et al. (2005). Primers used for amplification of gene knockout fragments are listed in Table S2. The hygromycin (HPH) cassette, derived from vector pLOB7 (Zhang et al., 2011) with primers 20/21, was used as selection marker to replace the target genes. Genomic DNA of transformants was screened for the presence of the wild-type target gene by PCR by amplifying the target genes *Bchxt13* and *Bchxt15* with primers LZ203/204 and LZ193/194, respectively. Knockout mutants were routinely double checked by PCR using the same method.

#### **Plant infection assay**

*Solanum lycopersicum* and *Nicotiana benthamiana* infection assay was performed as described previously (Zhang and van Kan, 2013, Chapter 4). Each mutant was tested in at least two independent experiments. Lesion sizes were analysed statistically by Student's *t*-test using a two-tailed distribution and two-sample unequal variance.

#### **Subcellular localization of BcHXT13 and BcHXT15 in *B. cinerea***

Primers used for construction of *Bchxt13-gfp* and *Bchxt15-gfp* are listed in Table S2. The gene fragments of *Bchxt13* and *Bchxt15*, including ~1000 bp upstream sequences of the coding region, were amplified with primers LZ205/241 and LZ195/239 using B05.10

genomic DNA as template. The *gfp* fragments were amplified from plasmid pNDH-GFP (Chapter 6) with primers LZ240/245 and LZ242/245, which were overlapping with the stop codons of *Bchxt13* and *Bchxt15*, respectively. The gene fragments and *gfp* fragments were fused by an overlap PCR with primers LZ205/245 and LZ195/245, respectively to generate *Bchxt13-gfp* and *Bchxt15-gfp*. The fused fragments were cloned into the pNR4 vector (Zhang et al., 2011) by a BP reaction (Invitrogen) in the appropriate concentration. The resulting plasmids were checked by sequencing (Macrogen) and subsequently transformed into *B. cinerea* wild-type strain B05.10 by protoplast transformation. The nourseothricin-resistant transformants were checked by PCR for the presence of the *gfp* gene and three independent transformants of each fusion were used for subcellular localization analysis.

For microscopic analysis, conidia of the BcHXT13-GFP and BcHXT15-GFP expressing strains were incubated at 20 °C on glass slides with Gamborg's B5 liquid medium supplemented with 10 mM (NH<sub>4</sub>)H<sub>2</sub>PO<sub>4</sub> and either 50 mM of D-glucose, D-galacturonic acid, or D-xylose as the carbon source. The glass slides were kept in a box with wet filter paper at the bottom to prevent evaporation of the liquid medium. The slides were covered with cover slips before investigation of GFP signal at 20 hpi. For DAPI, Mitotracker (red) and FM4-64 staining, all the stocks of dyes were diluted in liquid medium, at 1 µg/ml for DAPI, 1 µM for Mitotracker (red) and 10 µg/ml for FM4-64, respectively. The glass slides with germinated conidia were used directly for staining by washing with dye-containing liquid medium since after 20 h incubation most of germinated conidia were attached to the glass slides. Light and epifluorescence microscopy was done under a Nikon Eclipse 90i epifluorescence microscope (Nikon, Badhoevedorp, the Netherlands). DAPI fluorescence was investigated at least 1 h after adding the stain with DAPI filter (Ex 340-380, DM 400, BA 435-485). Mitotracker (red) and FM4-64 can be observed within 5 min after staining with TRITIC filter (Ex 540/25, DM 565, BA 605/55). GFP fluorescence was visualized by using a GFP-B filter (EX460-500, DM 505, BA510-560). The NIS-Elements software package was used to analyze digital pictures. For co-localization imaging, samples were prepared similarly but the fluorescence was imaged by using a Nikon Eclipse Ti inverted microscope connected to a Roper Scientific spinning disk system, consisting of a CSU-X1 spinning disk head (Yokogawa), QuantEM:512SC CCD camera (Roper Scientific) and a 100X magnifying lens between the spinning disk head and the camera. The DAPI, GFP and Mitotracker/FM4-64 fluorescences were excited using 405, 488 and 561nm laser lines, respectively. Metamorph software was used to analyse images.

## **Supporting information**

Supplementary Table S1.

## **Acknowledgements**

The authors are grateful to Pierre de Wit (Wageningen University, Laboratory of Phytopathology) for critical reading of the manuscript. The authors acknowledge funding by the Foundation Technological Top Institute Green Genetics (Project 2CC035RP) and the Netherlands Graduate School Experimental Plant Sciences.

## Supporting information

Supplementary Table 1. Primers used in this study.

Target gene	Primer name	Sequence (5'-3') <sup>a</sup>	Purpose		
<i>Bchxt8</i>	LZ213	GGAAGAGACAACGCCAAGAAC	Quantitative RT-PCR		
	LZ214	CTCATGATCAAACACCTTATCTC			
	LZ209	ACATTTTGTGATTTGGTCGATG			
	LZ210	GAGCACTATGCGACGCAGAAG			
	LZ207	CATTCCCAACTGGTATTGGTAAC			
	LZ208	GGAAATAGTGACTACTACGTTT			
	LZ103	CCCAGGATGTAGAAAGCAGTG			
	LZ104	TTTCAGGACTGTCTCAACTC			
	<i>Bchxt13</i>	LZ197 (5.1)		GTCTTGGAAAAATGTGGAGAG	Gene knockout
		LZ198 (5.2)		TTTTCGCTTCGTGATGAACAAC	
LZ199 (5.3)		GGGTACCGAGCTCGAAITCCATCTGTCTATCACACCAGCATC			
LZ200 (3.3)		CTCGGCGCCGGAAGCTTCTCGTGAAATGCATTGCAAC			
LZ201 (3.2)		TTTCCTTCAATAACAATCAAGTCC			
LZ202 (3.1)		GCAATCGACTTGAGATACAGAC			
LZ203		GTGGGATTGAGTCAACAGATG			
LZ204		CCAAAGGTCCCATGCAGTTG			
LZ187 (5.1)		GAAGAATTTATCCAGCATTGAAG			
LZ188 (5.2)		AAGATTTGGTGAACCATCAAC			
<i>Bchxt15</i>	LZ189 (5.3)	GGGTACCGAGCTCGAATTTCCGAAAGAGTAACGATCCCCTATG	Gene knockout		
	LZ190 (3.3)	CTCGGCGCCGGAAGCTTGGAAATGGGTGTATGGTCCCTTC			
	LZ191 (3.2)	AATAAATGGCAGGAAGTTCAGAG			
	LZ192 (3.1)	ATTAACGTTCCAGAAGATTGAG			
	LZ193	GTTCAAAGTCTTAGCCACAG			
	LZ194	TACAGTACCATAGATACCAGTAG			
	HPH cassette	20 (cassette-5)		GAATTCGAGCTCGGTACCCGGGGGA	
		21 (cassette-3)		CAAGCTTCGGCGGCCGAG	
		22 (screen-3)		GTAACCATGCATGGTTGCCT	
		23 (screen-5)		GGGTACCGAGCTCGAATTC	

<i>Bchxt13</i>	LZ205	GGGACAAGTTTGTACAAAAAAGCAGGCTGTAGAGGTAATGGTTGATATTCTAG	Subcellular localization
	LZ241	GCTTTCACCTTTGGAAACCATGATATCAACCTGATCTGCACCTTTATCATG	
<i>Bchxt15</i>	LZ195	GGGACAAGTTTGTACAAAAAAGCAGGCTGCCCGTTCCGCAATTGAGGAAG	
	LZ239	GCTTTCACCTTTGGAAACCATGATATCGGTAATCTTTTCAGGACTGTC	
<i>Bciga1</i>	LZ240	GACAGTCTGAAAAGAGTACCGATATCATGGTTTCCAAGGTGAAGAGC	
	LZ242	CATGATAAAGGTGCAGATCAGGTTGATATCATGGTTTCCAAGGTGAAGAGC	
	LZ245	GGGACCACCTTTGTACAAGAAAGCTGGGTCTAAGCGGCCGCTTTGTAAAG	

<sup>a</sup> The *atfB1* and *atfB2* sites are indicated in italic, respectively.



# CHAPTER 6

Pectate-induced gene expression in *Botrytis cinerea* and the identification and functional analysis of *cis*-regulatory D-galacturonic acid responsive elements

Lisha Zhang, Joost Stassen, Sayantani Chatterjee, Maxim Cornelissen, Jan A. L. van Kan

## Abstract

The fungal plant pathogen *Botrytis cinerea* produces a spectrum of cell wall degrading enzymes for the decomposition of host cell wall polysaccharides and the consumption of the monosaccharides that are released. Especially pectin is an abundant cell wall component, and the decomposition of pectin by *B. cinerea* has been extensively studied. An effective concerted action of the appropriate pectin depolymerising enzymes, monosaccharide transporters and catabolic enzymes is important for complete D-galacturonic acid utilization by *B. cinerea*. In this study, we performed RNA sequencing to compare genome-wide transcriptional profiles in *B. cinerea* grown in media containing glucose and pectate as sole carbon source. Transcript levels of 32 genes that are induced by pectate were further examined in cultures grown on six different monosaccharides, by means of quantitative RT-PCR, leading to the identification of 8 genes that are specifically induced by D-galacturonic acid. Conserved sequence motifs were identified in the promoters of genes involved in pectate decomposition and D-galacturonic acid utilization. The role of these motifs in regulating D-galacturonic acid-induced expression was functionally analysed in the promoter of the *Bclga1* gene, which encodes one of the key enzymes in the D-galacturonic acid catabolic pathway. Regulation by D-galacturonic acid required the presence of sequences with a conserved motif, designated, GAE1 and a binding site for the pH-dependent transcriptional regulator PacC.

## Introduction

The plant cell wall is the first barrier to pathogen invasion, and consists mainly of polysaccharides that form a complex three-dimensional network together with lignin and proteins. The main components of plant cell wall polysaccharides are cellulose, hemicellulose, and pectin. The ability to decompose complex plant cell wall polysaccharides is an important aspect of the lifestyle of fungal pathogens. Necrotrophic fungal plant pathogens secrete large amounts of enzymes to decompose plant cell wall polysaccharides in order to facilitate the penetration, the subsequent maceration and the acquisition of carbon from decomposed plant tissues (Amselem et al., 2011). Hemibiotrophic pathogens also produce polysaccharide decomposing enzymes during the late, necrotizing phase of infection (Gan et al., 2013; King et al., 2011; O'Connell et al., 2012). By contrast, many biotrophic pathogens and symbionts have a markedly lower content of enzymes for cell wall decomposition in their genome (Baxter et al., 2010; Duplessis et al., 2011; Martin et al., 2010), presumably to reduce the damage to the host and avoid the plant defence responses triggered by the release of cell wall fragments.

*Botrytis cinerea* is a necrotrophic fungal plant pathogen infecting more than 200 host plants and causing severe economic damage to crops worldwide (Dean et al., 2012; Williamson et al., 2007). *B. cinerea* secretes large amounts of cell wall degrading enzymes for host tissue decomposition and nutrient acquisition. The preference for infection of pectin-rich plants and tissues (ten Have et al., 2002) suggests that effective pectin degradation is important for virulence of *B. cinerea*. The genome of *B. cinerea* encodes 118 Carbohydrate Active enZymes (CAZymes, [www.cazy.org](http://www.cazy.org)) (Cantarel et al., 2009) associated with plant cell wall decomposition, of which a large proportion is involved in the decomposition of pectin (Amselem et al., 2011). The pectin degrading capacity of *B. cinerea* and the saprotroph *Aspergillus niger* is similar. These two unrelated fungi are not only similar in the number of enzymes in pectin-related CAZY families that are encoded in their genomes, but also in the ratio between pectin degrading lyases versus hydrolases (Amselem et al., 2011).

Several *B. cinerea* pectin degrading enzyme activities have been detected during host infection, including pectin and pectate lyases, pectin methylesterase (PMEs), exopolygalacturonases (exo-PGs), and endo-polygalacturonases (endo-PGs) (Cabanne and Doneche, 2002; Kars et al., 2005b; Kars and van Kan, 2004; Rha et al., 2001; ten Have et al., 2001). The importance of several pectinases for virulence of *B. cinerea* was investigated by targeted mutagenesis in endo-PG genes and PME genes. Knockout mutants  $\Delta Bcpg1$  and  $\Delta Bcpg2$  were reduced in virulence by 25% and > 50%, respectively (Kars et al., 2005a; ten Have et al., 1998). A  $\Delta Bcpe1$  mutant in one *B. cinerea* strain showed reduction in

virulence (Valette-Collet et al., 2003); in a different strain, however, mutants in the same *Bcpme1* gene or the *Bcpme2* gene, or even  $\Delta Bcpme1/\Delta Bcpme2$  double knockout mutants, were not altered in virulence (Kars et al., 2005b). However, there is still a number of pectinolytic genes that remain to be functionally analysed.

The monosaccharide D-galacturonic acid is the most abundant component of pectic polysaccharides (Caffall and Mohnen, 2009; Mohnen, 2008) and is the final product released from pectin degradation. The D-galacturonic acid catabolic pathway is conserved in many filamentous fungi (Martens-Uzunova and Schaap, 2008; Richard and Hilditch, 2009). The pathway has been genetically and biochemically characterized in *B. cinerea*, and consists of three catalytic steps involving four genes: *Bcgar1*, *Bcgar2*, *Bclgd1*, and *Bclga1* (Zhang et al., 2011). Their transcript levels were induced substantially when the fungus was cultured in media containing D-galacturonic acid, pectate or pectin as the sole carbon source (Zhang et al., 2011). Knockout mutants in each step of the four genes ( $\Delta Bcgar1/\Delta Bcgar2$ ,  $\Delta Bclgd1$ , and  $\Delta Bclga1$ ) were affected in growth on D-galacturonic acid, pectate, or pectin as the sole carbon source (Zhang et al., 2011), and in virulence on *Nicotiana benthamiana* and *Arabidopsis thaliana* leaves (Zhang and van Kan, 2013).

Collectively, the functional analyses on the *B. cinerea* endo-PG genes and the D-galacturonic acid catabolic pathway genes indicate that a concerted action of the appropriate pectin depolymerising enzymes and catabolic enzymes is important for complete D-galacturonic acid utilization by *B. cinerea*. Previous studies showed that several genes involved in pectin decomposition and D-galacturonic acid catabolism are induced *in vitro* by D-galacturonic acid and are expressed at high levels during infection in the stage of lesion expansion, when plant cell wall degradation occurs (Wubben et al., 2000; Zhang et al., 2011; Zhang and van Kan, 2013). Co-expression of these genes suggests that a central regulatory mechanism is present in *B. cinerea*.

Current knowledge of the regulation of pectinolytic genes and D-galacturonic acid catabolic genes in fungi is limited. Several studies showed that D-galacturonic acid is an inducer for some pectinolytic genes and D-galacturonic acid catabolic genes (Martens-Uzunova and Schaap, 2008; Martens-Uzunova et al., 2006; Mojzita et al., 2010; Wubben et al., 2000; Zhang et al., 2011; Zhang and van Kan, 2013). A conserved element (TTGGNGG) was identified in the bidirectional promoter region shared between the D-galacturonic acid reductase and 2-keto-3-deoxy-L-galactonate aldolase genes from 18 fungal species, including *B. cinerea* (Martens-Uzunova and Schaap, 2008). This conserved element is also present in the promoters of several pectin degrading enzymes in *A. niger* (Martens-Uzunova and Schaap, 2008). However, the function of this element in regulation by D-galacturonic acid remains to be characterised.

In order to get further insight into the *B. cinerea* genes that participate in pectin decomposition and D-galacturonic acid utilization, we have exploited the next generation RNA-sequencing (RNA-seq) technology (Wang et al., 2009) to perform a genome-wide transcriptome analysis in *B. cinerea* grown in media containing either glucose or pectate as sole carbon sources. We identified a set of genes that are significantly altered in gene expression. Promoter sequences of these genes were analysed to identify conserved motifs that may act as *cis*-regulatory elements in the regulation of pectate decomposition and D-galacturonic acid utilization. The promoter of the *Bclga1* gene was functionally analysed by fusing various promoter constructs to a reporter gene and monitoring reporter activity in the presence of D-galacturonic acid.

## Results

### Pectate-induced gene expression in *Botrytis cinerea*

To study the transcriptome of *Botrytis cinerea* during degradation of pectic polymers and D-galacturonic acid utilization, RNA-seq was performed and the transcriptome profiles were compared between cultures containing glucose and sodium polygalacturonate (pectate) as sole carbon source. Cultures were grown in glucose-containing medium overnight and transferred to fresh medium with either glucose or pectate, and sampled at 6 h after transfer. RNA was isolated from three independent cultures in each condition. One sample of each condition was used for RNA-seq and the other two were used for quantitative RT-PCR (qRT-PCR) validation. A total of 6,800,254 and 6,462,333 read pairs were obtained from glucose- and pectate-containing cultures, respectively, of which 90.3% and 91.6% could be mapped to *B. cinerea* genome version 2 (Staats and van Kan, 2012). The number of fragments per kilobase of transcript per million reads mapped (FPKM) was determined for the 10,345 predicted genes as released with *B. cinerea* genome version 2 (Staats and van Kan, 2012), supplemented with two manually annotated gene models representing genes known to be involved in D-galacturonic acid utilization, *Bcpg2* and *Bcpme1* (Valette-Collet et al., 2003; Wubben et al., 1999). Of these 10,347 genes, 7,602 (73.5%) and 7,556 (73.0%) genes had an FPKM value > 1 in glucose- and pectate-containing culture, respectively. The transcript level of 32 genes was significantly ( $q < 0.05$ ) up-regulated ( $\log_2 > 2$ ) in pectate-containing culture compared to the glucose-containing culture (Table 1). The transcript levels of these 32 genes were further determined by qRT-PCR, and indeed showed strong induction in pectate-containing culture as compared to the glucose-containing culture, with the exception of B0510\_9368 (Table 1). For 23 of the 31 genes, the induction folds as determined by RNA-seq and by qRT-PCR, on independent

biological samples, were in very good agreement (the difference between the  $\log_2$  values for a given sample was  $< 1$ ).

In order to examine the expression of pectinolytic genes in the presence of pectate, we generated a list of CAZymes with substrate specificity for pectic compounds, and listed their expression values (Table S1). Among the 42 pectin-specific CAZyme encoding genes in the *B. cinerea* genome, 14 genes were expressed at least 2-fold higher in pectate as compared to glucose (with a minimum FPKM value of 1 in at least one of the samples), comprising genes encoding enzymes assigned to 6 CAZY families: GH28, GH78, GH105, GH115, CE8 and PL1.

### **Differential gene expression in cultures containing different monosaccharides**

Pectate that was used as an inducer in the cultures used for the RNAseq studies is a linear, unbranched polygalacturonate of 99% purity. We presumed that instead of the polymer itself, the D-galacturonate monosaccharide released from the polymer would act as the inducer of gene expression. To investigate whether the 31 pectate-induced genes are specifically up-regulated in the presence of D-galacturonate or may also be up-regulated by other cell wall-related monosaccharides, their transcript levels were determined by qRT-PCR in cultures containing glucose, D-galacturonic acid, arabinose, rhamnose, galactose, or xylose as the sole carbon source, respectively. Cultures were pre-grown in glucose-containing medium and transferred to fresh medium with the different carbon sources, and sampled at 3 h after transfer. The 31 pectate-induced genes could be divided into three groups based on expression profiles: (1) genes of which transcript levels were up-regulated in D-galacturonic acid-containing culture compared to glucose-containing culture, and at least 2-fold higher as compared to cultures containing other monosaccharides. This group comprises genes involved in D-galacturonic acid catabolism (*Bcgar2* (B0510\_551) and *Bclga1* (B0510\_552; (Zhang et al., 2011)), pectin hydrolysis (endo-polygalacturonase gene *Bcpg2* and exo-polygalacturonase gene B0510\_2787), as well as members of the major facilitator superfamily (B0510\_3996, encoding hexose transporter BcHXT15 (Dulermo et al., 2009) and B0510\_978, encoding a putative sugar:H<sup>+</sup> symporter), and two additional genes: B0510\_4887, encoding a putative alcohol dehydrogenase and B0510\_171, encoding a secreted protein (Figure 1); (2) genes of which transcript levels, as compared to that in glucose-containing culture, were not only induced by D-galacturonic acid, but also by other monosaccharide(s) to different extents (Figure S1A); (3) genes of which transcript levels were not induced by D-galacturonic acid, as compared to glucose (Figure S1B).

**Table 1.** Up-regulated genes in pectate-containing culture and conserved sequences in their promoter regions.

B0510_V2_ID	RNAseq		qRT-PCR		Gene annotation	Gene name	Motif occurrence relative to translation start site												
	Pectate		log2(P/G)				1	2	3	4	5	6	7	8					
	Glucose	Pectate	log2(P/G)	log2(P/G)															
B0510_171	3.835	551.495	7.168	3.645															
B0510_9316	0.416	51.167	6.943	7.060															
B0510_1685	0.353	24.443	6.113	2.897	putative catalase														
B0510_4051	0.845	32.466	5.263	3.265	putative oxidoreductase														
B0510_8116	3.322	120.367	5.179	4.215	putative cytochrome P450														
B0510_9368	0.274	7.552	4.785	0.281	putative NADH-dependent flavin oxidoreductase														
B0510_4887	21.112	570.923	4.757	4.228	putative alcohol dehydrogenase														
B0510_1156	5.126	123.397	4.589	3.662															
B0510_7189	0.218	4.705	4.432	2.470	putative amino acid transporter														
B0510_552	15.675	335.766	4.421	4.204	2-keto-3-deoxy-L-galactonate aldolase	<i>Bcgn1</i>													
B0510_551	4.601	88.782	4.270	3.942	D-galacturonic acid reductase	<i>Bcgn2</i>													
B0510_3593	9.214	173.838	4.238	4.752	putative secreted metalloproteinase														
B0510_1684	0.401	6.639	4.050	2.935	putative GMC oxidoreductase														
B0510_8767	1.366	21.445	3.973	3.177	putative serine protease														
B0510_3095	21.446	320.265	3.900	2.543	oxaloacetate acetylhydrolase														
B0510_5927	1.419	20.225	3.833	3.177	putative ABC transporter														
B0510_9071	2.245	30.329	3.756	4.370															
B0510_8243	52.529	652.423	3.635	3.027															
B0510_9363	4.646	56.496	3.604	3.032															
B0510_3901	0.574	6.492	3.499	4.172	putative beta-1,3 exoglucanase														
B0510_3996	2.111	23.421	3.472	3.437	hexose transporter 15	<i>Bcxt15</i>													
B0510_2787	15.396	167.685	3.445	5.326	putative exo-polygalacturonase														
B0510_8492	5.687	60.226	3.405	3.240															
BcPG2	31.347	327.904	3.387	3.360		<i>Bcpg2</i>													
B0510_7215	77.831	748.277	3.265	3.192															

## Chapter 6

B0510_10339	18.008	172.491	3.260	5.515	putative carboxypeptidase S1	-929
B0510_978	1.460	13.979	3.259	3.895	putative sugar:H+ symporter	-893
B0510_8954	6.244	57.579	3.205	2.758		-688
B0510_6060	13.058	119.954	3.199	2.188		-874
B0510_6786	4.028	32.653	3.019	4.002	putative tripeptidyl peptidase	-542
B0510_1079	38.662	298.206	2.947	3.035		-210
B0510_3706	186.182	1359.410	2.868	3.554		-462

\* 6 overlapping matches

The *Bclgd1* gene, encoding the enzyme involved in the second step of D-galacturonic acid catabolism, and previously shown to be induced in media containing pectic carbon sources (Zhang et al., 2011), was not represented in the above list of 31 pectate-induced genes, because the relative expression did not reach a statistically significant threshold. We used qRT-PCR to also determine the transcript levels of *Bclgd1* in cultures containing glucose, D-galacturonic acid, arabinose, rhamnose, galactose, or xylose as the sole carbon source. The data showed that *Bclgd1* was specifically up-regulated (over 30-fold) in the D-galacturonic acid-containing culture (Figure 1).

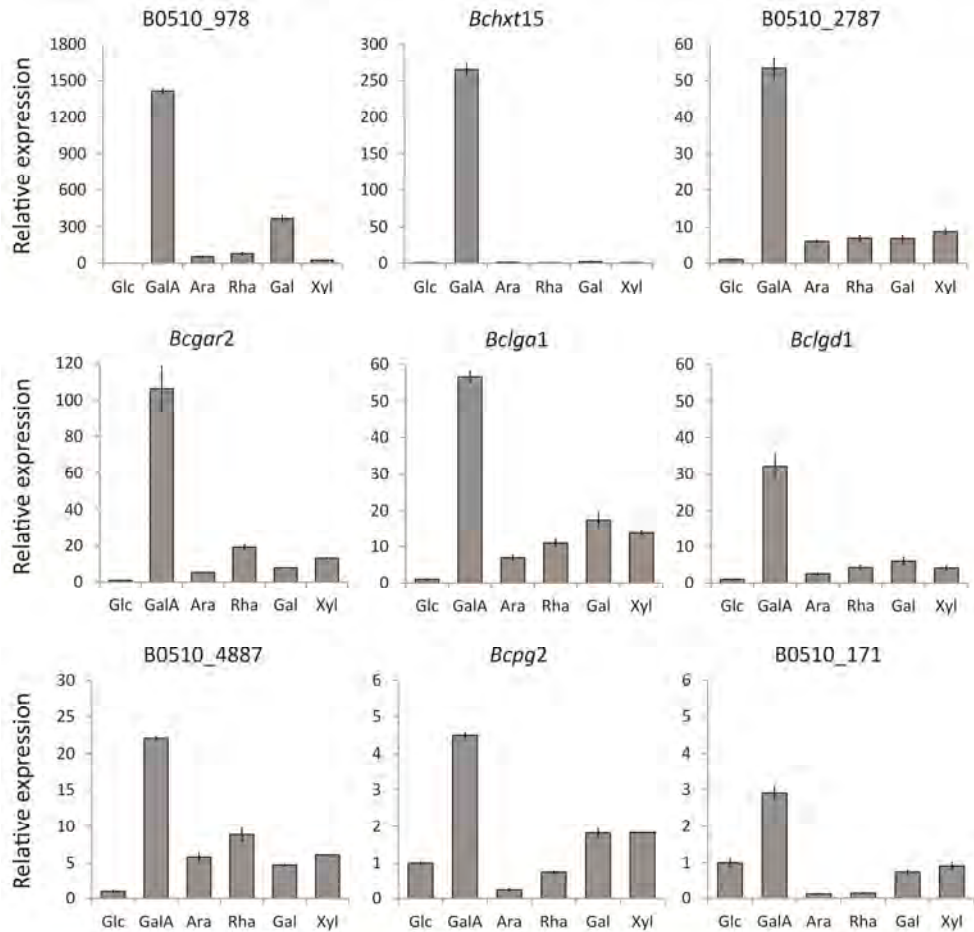


**Figure 1.** Relative gene transcript levels in *Botrytis cinerea* when grown on different carbon sources (Glc, glucose; GalA, D-galacturonic acid; Ara, arabinose; Rha, rhamnose; Gal, galactose; Xyl, xylose) as assessed by quantitative RT-PCR. Cultures were sampled for RNA extraction at 3 h after transfer from a pre-culture with glucose as carbon source. mRNA levels of candidate genes were normalized to the levels of the constitutive reference gene *Bcrp15* and calibrated to the levels obtained in a glucose-containing culture (set as 1), according to the  $2^{-\Delta\Delta Ct}$  method. Data are represented as means  $\pm$  standard deviation from one biological repeat with three technical replicates.

### ***Cis*-regulatory elements present in the promoters of D-galacturonic acid-up-regulated genes**

To identify potential transcriptional regulatory elements involved in gene activation by D-galacturonic acid, the promoters of 8 genes that were up-regulated specifically in the presence of D-galacturonic acid ( $\log_2$  ratio of the value in D-galacturonic acid as compared to any other tested sugar is over 2) were used for *cis*-regulatory element analysis. The promoter regions of these 8 genes (1 kb upstream of the translation start codon, or up to the boundaries of the coding sequence of the neighbouring gene, whichever was shortest) were used to construct position-specific scoring matrices (PSSMs) of 5 to 20-nucleotide motifs based on the alignment of at most a single occurrence of the motif in each input sequence. To avoid a bias for the overlapping part of the 1 kb upstream sequences of the *Bcgar2* and *Bclga1* genes (which are located in a bidirectional gene cluster with 1.7 kb shared promoter region), the entire sequence between these two genes was provided as a single promoter sequence. Eight candidate elements were identified at an e-value below  $1e5$  (Figure 2), which include motifs that encompass consensus sequences of binding motifs for the transcriptional regulators CreA (5'-SYGGRG-3') (Cubero and Scazzocchio, 1994) and PacC (5'-GCCARG-3') (Tilburn et al., 1995). The coordinates of the motifs in relation to the translation start site of each gene are listed in Table 1.

The consensus motif sequence 5'-CCNCCAA-3' (hereafter designated GAE1) identified by Martens-Uzunova and Schaap (2008), present in the promoters of gene clusters orthologous to the *B. cinerea Bcgar2-Bclga1* cluster in many filamentous fungi, is contained in the motif with the lowest e-value, and was found in all 7 promoter regions provided. In addition to the 8 genes used for motif finding, the GAE1 motif was also found in the promoter regions of the significantly up-regulated genes B0510\_171 and B0510\_3593 ( $p < 1e-5$ ) (Table 1), as well as in 8 genes for which RNA-seq data provided evidence for up-regulation in pectate-containing medium ( $\log_2 > 2$  and FPKM  $> 1$  in the pectate culture sample), albeit with non-significant  $q$  value ( $q > 0.05$ ; Table S2). In total, the GAE1 motif occurs 327 times in the promoters of 323 genes in the entire *B. cinerea* genome ( $p < 0.05$ ), among which there are three pectinolytic genes (Table S1).

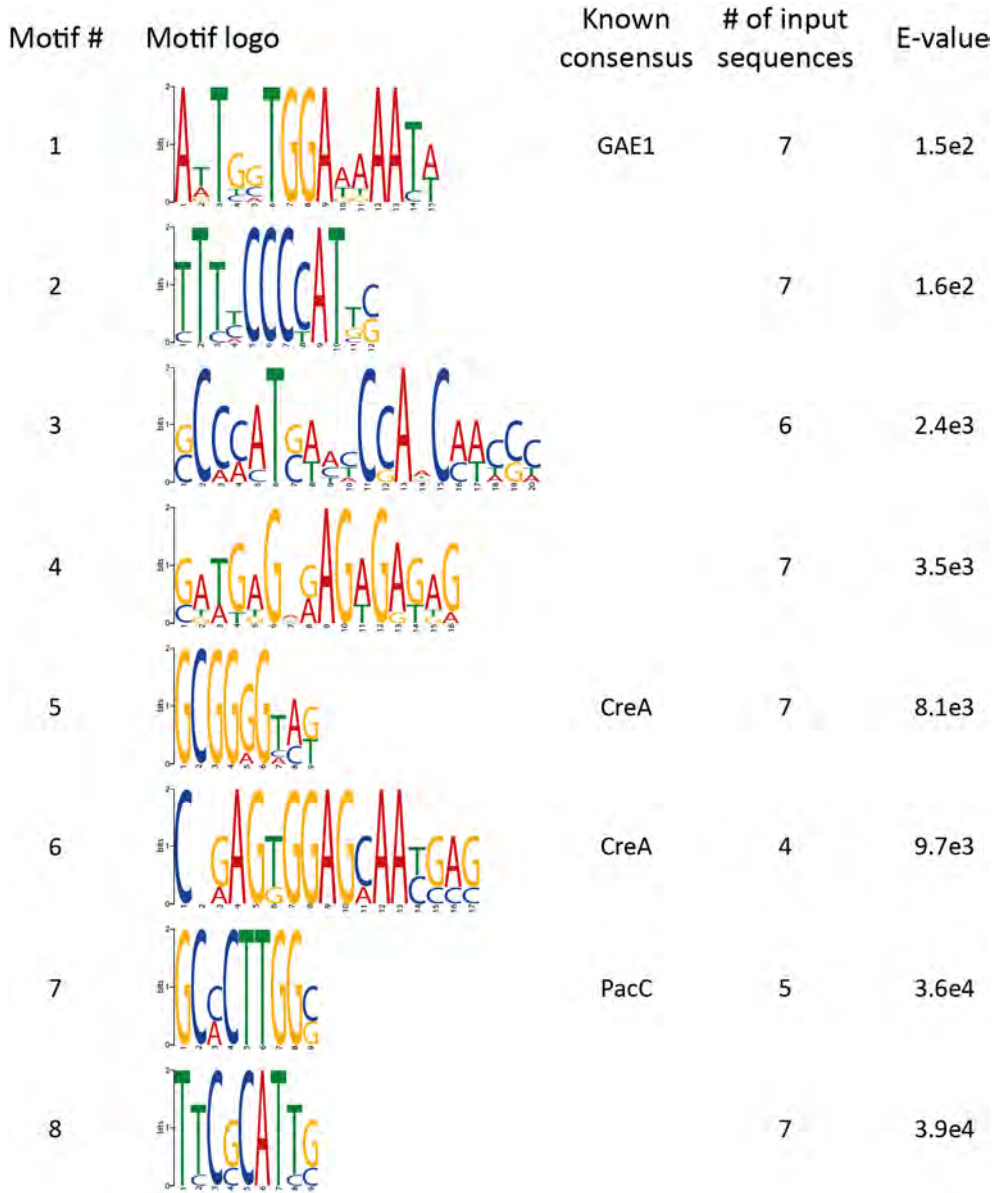


**Figure 2.** Conserved sequence motifs in the promoters of genes in *Botrytis cinerea* which are specifically up-regulated in D-galacturonic acid. The motifs are displayed as sequence logos. # of input sequences represents the number of sequences in the input set containing the motif. E-value relates the statistical significance of the motif.

### Functional analysis of the *cis*-regulatory elements

Besides the predicted conserved GAE1 motif, there are 8 CreA binding motifs (Cubero and Scazzocchio, 1994) and one PacC binding motif (Tilburn et al., 1995) in the promoter region of the *Bcgar2-Bclga1* gene cluster. The motifs 2, 3 and 4 (Figure 2) are each present once around positions -1000, -800 and -26, relative to the start of the *Bclga1* coding sequence. To determine the contribution of these elements to the induction of gene expression by D-galacturonic acid, the full-length (FL) promoter region of this gene cluster (in the direction for *Bclga1* expression) was fused with a codon-optimised *gfp* gene and a set of promoter deletion constructs was generated in which different combinations of motifs were removed (Del1-8) (Figure 3A). The FL and deletion constructs were transformed into wild-type *B. cinerea* strain B05.10 and for each construct, up to 10 transformants were verified for proper integration of the construct and propagated for reporter gene analysis. The conidia of transformants were germinated in the presence of glucose or D-galacturonic acid for 20 h and hyphae of the germlings were subsequently examined by epifluorescence microscopy. As shown in Figure 3, GFP fluorescence with the FL promoter was observed in the presence of D-galacturonic acid but not in glucose. GFP fluorescence of transformants with promoter deletion constructs Del1, Del2, and Del7 was the same as that with the FL promoter in D-galacturonic acid, whereas no GFP fluorescence was detected with the all other promoter deletion constructs. None of the transformants (either with the FL promoter or the deletion constructs) showed any GFP fluorescence when grown in glucose.

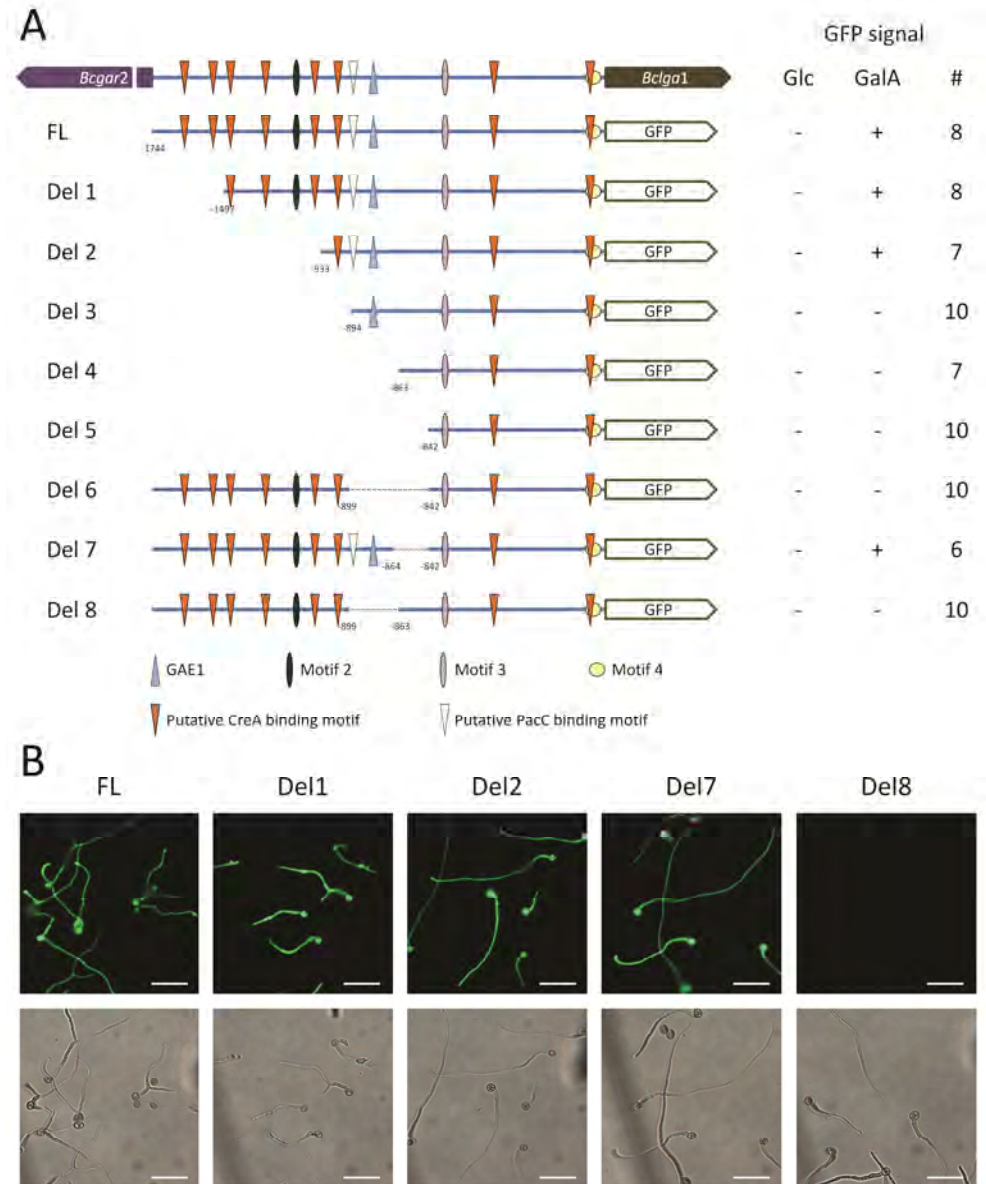


**Figure 3.** Functional analysis in *Botrytis cinerea* of the *cis*-regulatory elements in the promoter region of the *Bcgar2-Bclga1* gene cluster. A, a set of unidirectional (for *Bclga1* expression) promoter fragments with various deletions was fused to *gfp* reporter gene and transformed into *B. cinerea* wild-type strain. Deletion constructs were named sequentially from Del1 to Del8. The predicted regulatory elements are indicated at the bottom. + and – indicate the presence or absence of GFP fluorescence in *B. cinerea* transformants that were germinated in medium with glucose (Glc) or D-galacturonic acid (GalA) for 20 h. # indicates the number of independent transformants analysed for each construct. B, fluorescence microscopic images (top) and light microscope images (bottom) of *B. cinerea* transformants that were germinated in medium with D-galacturonic acid for 20 h. Scale bar = 50  $\mu$ m.

## Discussion

In this study, RNA-seq technology was applied to genome-wide transcriptome analysis in *B. cinerea* grown in media containing glucose or pectate as sole carbon source. 32 genes in *B. cinerea* were identified that are significantly up-regulated when grown on pectate as compared to glucose. Furthermore, the transcript levels of these genes were verified by qRT-PCR with two additional biological repeats. The data obtained by qRT-PCR were strongly correlated with the data from the RNA-seq experiments. Of the initially identified 32 pectate-induced genes, 31 were indeed highly up-regulated in pectate with a  $\log_2$  ratio higher than 2. For 23 of the 31 genes, the RNA-seq and qRT-PCR data (on independent biological samples) showed less than 2-fold difference in the induction ratios, indicating that RNA-seq is a suitable method for quantifying gene expression, even when performed on a single biological sample. *Bcgar2*, *Bclgd1* and *Bclga1* encode enzymes involved in the three catalytic steps of D-galacturonic acid catabolism (Zhang et al., 2011). The up-regulation of expression of *Bcgar2* and *Bclga1* found in our RNA-seq analysis was in agreement with qRT-PCR data obtained before (Zhang et al., 2011). The transcript levels of *Bclgd1* were also highly induced by pectate (Zhang et al., 2011), but this gene was not among the 31 up-regulated genes, because it was not statistically significant at the threshold of  $q < 0.05$  (*Bclgd1*:  $\log_2 = 2.4$ ,  $q = 0.159$ ). In addition, the *Bchxt15* gene, encoding a putative D-galacturonic acid transporter (Chapter 5), was significantly up-regulated in the RNA-seq experiment. Growth of  $\Delta Bchxt15$  mutants on D-galacturonic acid was not different from the wild-type strain (Chapter 5), indicating that other hexose transporters also contribute to D-galacturonic acid uptake. Indeed, the RNA-seq data revealed that another putative sugar:H<sup>+</sup> symporter gene, B0510\_978, was highly up-regulated by pectate. qRT-PCR analysis demonstrated that both *Bchxt15* and B0510\_978 were specifically up-regulated by D-galacturonic acid compared to glucose, with ~560-fold and ~1400-fold respectively. The expression data suggest that B0510\_978 might play a prominent role in D-galacturonic acid uptake. Further studies with knockout mutants of the B0510\_978 gene in the wild-type strain and in a  $\Delta Bchxt15$  mutant background could shed more light on its function in D-galacturonic acid uptake.

Pectate is a linear polymer of D-galacturonic acid and it is plausible to assume that pectate hydrolysis, by a mixture of endo-PGs and exo-PGs, would provide D-galacturonic acid for fungal growth over a fair period of time, until the substrate would be entirely degraded. On the other hand, if *B. cinerea* would be provided with D-galacturonic acid monosaccharide as sole carbon source, this would lead to a short, transient burst of expression of genes involved in D-galacturonic acid utilization which would fade out as soon as the bulk of monosaccharide would be absorbed from the medium. In order to

mimic gene expression during the degradation of pectate in plant tissue and the subsequent utilization of the released monosaccharides, we decided to choose pectate as the carbon source for RNA-seq analysis. We anticipated that the induction of gene expression in pectate-containing medium is likely mediated by the monosaccharides released upon hydrolysis. This would imply that genes that are inducible during growth on pectate should also be induced during growth on D-galacturonic acid. Unexpectedly, qRT-PCR analysis demonstrated that ~50% of the 31 pectate-up-regulated genes were not induced by D-galacturonic acid. It should be noted that the samples for RNA-seq were prepared at 6 h after transfer to pectate, whereas the samples for qRT-PCR were prepared at 3 h after transfer to the monosaccharide. It is possible that 3 h was not sufficient to induce the transcript levels of these genes. Previous studies showed that the transcript levels of D-galacturonic acid catabolic genes were higher at 3 h after transfer than at 9 h after transfer in medium with D-galacturonic acid or pectate as the carbon source (Zhang et al., 2011), probably because the carbon sources were already depleted at 9 h. Further transcript analysis with more time points will allow to compare the expression profiles of genes in D-galacturonic acid and pectate in more detail. Also, the ambient pH was different in the D-galacturonic acid-containing culture (adjusted to pH 5.6 with sodium hydroxide) and pectate-containing culture (pH 7.0), and this may also have affected the expression profiles. It has been reported that the transcript levels of several *B. cinerea* genes are modulated by ambient pH, including genes encoding proteases and cell wall degrading enzymes (Billon-Grand et al., 2012; Rolland et al., 2009). B0510\_3593 and B0510\_10339, both encoding secreted proteases, and B0510\_3901, encoding a beta-1,3-exoglucanase, were up-regulated in the presence of pectate (pH 7.0) but not D-galacturonic acid (pH 5.6), suggesting that ambient pH may have affected the expression of these genes.

The GAE1 element is not only present in the promoters of all eight genes specifically induced by D-galacturonic acid- and of several pectinolytic genes of *B. cinerea*, but also in the promoters of several co-expressed pectinolytic genes of *Aspergillus niger* and in gene clusters orthologous to the *B. cinerea Bcgar2-Bclga1* cluster in many filamentous fungi (Martens-Uzunova and Schaap, 2008). This suggests that the GAE1 motif is part of a conserved regulatory system for pectin degradation and D-galacturonic acid utilization in different fungi. Functional analysis of the regulatory elements in the promoter region of the *Bcgar2-Bclga1* gene cluster suggests that the promoter region containing the GAE1 element and the PacC binding motif is essential for the induction of gene expression by D-galacturonic acid. These sequences are in very close proximity, only 15 nucleotides apart. Constructs Del2 and Del3 differ only in the presence of one CreA binding motif and the PacC binding motif, while fluorescence was only observed in Del2-containing

transformants, but not in Del3-containing transformants. This result shows that the PacC binding motif is essential, while the GAE1 motif alone is insufficient for D-galacturonate-induced expression. Comparison of the results for constructs Del8 and FL suggest that only 35 nucleotides (between coordinates -899 and -863) are essential for D-galacturonate-induced expression. Additional promoter deletion constructs will need to be designed to further dissect the sequences that are important in regulation.

In summary, a set of genes was identified in *B. cinerea* of which the transcript levels were specifically induced by D-galacturonic acid. These genes encode proteins involved in pectin degradation, monosaccharide uptake and D-galacturonic acid catabolism, suggesting the existence of an efficient, co-regulated D-galacturonic acid utilization network in *B. cinerea*. The promoters of these co-expressed genes share certain *cis*-regulatory elements and are therefore potentially regulated by a set of common transcription factors. It has been reported that in *Aspergillus* species, several transcription factors that are involved in plant cell wall polysaccharide degradation and in the catabolism of the derived monosaccharides are induced by the corresponding monosaccharide (Battaglia et al., 2011; Gruben, 2012). For example, RhaR regulates the expression of genes related to rhamnose utilization and its expression is induced by rhamnose (Gruben, 2012). However, the list of *B. cinerea* genes that are significantly up-regulated by pectate does not include any gene encoding a putative transcription factor or DNA-binding protein. One possible explanation is that the transcript levels of transcriptional regulator genes increase fast (reaching a peak at an early time point) and subsequently decrease rapidly, such that induction cannot be detected at 6 h after transfer from glucose to pectate. Alternatively, the transcriptional regulator might be present in an inactive form, and activated in the presence of D-galacturonic acid to promote target gene expression. Other experimental approaches, such as a DNA-protein pull-down combined with mass spectrometry analysis, may allow to identify the transcription factor(s) binding to crucial *cis*-regulatory elements allowing a better understanding of the regulatory network of *B. cinerea* for pectin degradation and D-galacturonic acid utilization.

## Materials and methods

### Fungal strains and growth conditions

*Botrytis cinerea* wild-type strain B05.10 and strains transformed with *Bcgar2-Bclga1* promoter deletion constructs used in this study were routinely grown on Malt Extract Agar (Oxoid, Basingstoke, UK; 50 g/L) in the dark at 20 °C for 3-4 days. The plates were placed for one night under near-UV light (350–400 nm) to promote sporulation, and were subsequently returned to darkness. Conidia were harvested 4-7 days later in 10–20 mL of water, and the suspension was filtered over glass wool to remove mycelium fragments. The conidia suspension was centrifuged at 1200 rpm for 5 min. The supernatant was discarded and the conidia in the pellet were resuspended at the desired density.

### RNA extraction

The conidia of the wild-type strain B05.10 were incubated in Gamborg's B5 liquid culture supplemented with 10 mM (NH<sub>4</sub>)H<sub>2</sub>PO<sub>4</sub> and 50 mM glucose at 20 °C, 150 rpm. After 16 h of growth, the mycelium was harvested and transferred into fresh Gamborg's B5 medium supplemented with 10 mM (NH<sub>4</sub>)H<sub>2</sub>PO<sub>4</sub> and a carbon source. For the cultures used for RNA-seq analysis, either 50 mM glucose or 0.5% sodium polygalacturonate (pectate) was added; mycelium was harvested from these cultures at 6 h post transfer and freeze-dried. For the cultures used for quantitative RT-PCR, either glucose, D-galacturonic acid, L-arabinose, L-rhamnose, D-galactose, or L-xylose was added at 50 mM final concentration; mycelium was harvested from these cultures at 3 h post transfer and freeze-dried.

Total RNA was isolated using the Nucleospin<sup>®</sup> RNA plant kit (Machery-Nagl, Düren, Germany), according to the manufacturer's instructions. First strand cDNA was synthesized from 1 µg total RNA with SuperScript<sup>®</sup> III Reverse Transcriptase (Invitrogen) according to the manufacturer's instructions.

### RNA-sequencing and data analysis

Twenty micrograms of total RNA for each RNA sample were prepared as described above. cDNA synthesis, library preparation and Illumina sequencing (100 bp paired-end reads) were performed at Beijing Genome Institute (BGI, Hong Kong). The obtained Illumina RNA-seq reads were trimmed to remove the first 12 nucleotides using fastx trimmer ([http://hannonlab.cshl.edu/fastx\\_toolkit/](http://hannonlab.cshl.edu/fastx_toolkit/)) and mapped to annotated genes on version 2 of the *B. cinerea* genome (Staats and van Kan, 2012) using Tophat (version 2.0.6) with default settings (Trapnell et al., 2009). Differentially expressed genes were then determined using Cuffdiff (version 2.0.2) with default settings and cut-offs (Trapnell et al., 2013).

### Quantitative RT-PCR

Quantitative RT-PCR was performed using an ABI7300 PCR machine (Applied Biosystems, Foster City, U.S.A.) in combination with the qPCR SensiMix kit (BioLine, London, U.K.). The primers to detect the transcripts of *B. cinerea* genes are listed in Table S3. Real-time PCR conditions were as follows: an initial 95 °C denaturation step for 10 min followed by denaturation for 15 s at 95 °C and annealing/extension for 45 s at 60 °C for 40 cycles. The data were analysed on the 7300 System SDS software (Applied Biosystems, Foster City, U.S.A.). The transcript levels of target genes were normalized to the transcript levels of the constitutively expressed gene *Bcrp15* and calibrated to the levels observed in glucose culture (set as 1), according to the  $2^{-\Delta\Delta Ct}$  method.

### Conserved motif elements finding

Conserved motif elements were predicted by MEME (Bailey and Elkan, 1994) with minimum size 5 nucleotides, maximum size 20 nucleotides, zero or one occurrence per sequence, using the promoter regions of 8 D-galacturonic acid up-regulated genes as training set. The occurrence of motifs in the promoter regions was performed by the scanning for matches to the position-specific scoring matrices (PSSMs) describing the motif with PoSSuM search (Beckstette et al., 2009).

### Plasmid construction and *B. cinerea* transformation

In order to study the regulation of the promoter of the *Bcgar2-Bclga1* gene cluster in *B. cinerea*, a yeast recombination-based cloning vector pNDH-GFP was generated as described previously (Figure S2) (Schumacher, 2012). The full-length promoter region of *Bcgar2-Bclga1* and a series of promoter deletions were amplified from genomic DNA using primers listed in Table S4. The amplified promoter regions, together with *NcoI*-linearized pNDH-GFP, were co-transformed into the uracil-auxotrophic yeast strain FY834 (Winston et al., 1995), as described by Schumacher (2012). The transformants were confirmed by PCR with primers LZ182/183 and plasmids were isolated with Zymoprep yeast plasmid miniprep kit I (Zymo research) according to the manufacturer's instructions. Plasmids were then transformed into competent *Escherichia coli* DH5 $\alpha$  cells to increase the DNA yield. The resulting plasmids were checked by sequencing (Macrogen) and subsequently transformed into *B. cinerea* wild-type strain B05.10 by protoplast transformation (Kars et al., 2005b). The hygromycin-resistant transformants were checked by PCR for the presence of the *hph* gene with primers LZ92/93 and up to 10 independent transformants of each construct were used for analysis of GFP fluorescence.

### **Microscopic analysis**

Conidia of the strains containing different promoter constructs were incubated on glass slides with Gamborg's B5 liquid medium supplemented with 10 mM  $(\text{NH}_4)_2\text{H}_2\text{PO}_4$  and 50 mM of glucose or D-galacturonic acid as the carbon source at 20 °C. After 20 h incubation, the slides were covered with cover slips and observed under a Nikon Eclipse 90i epifluorescence microscope (Nikon, Badhoevedorp, the Netherlands) or light microscopy. GFP fluorescence was visualized by using a GFP-B filter cube (EX460-500, DM 505, BA510-560). The NIS-Elements software package was used to analyze digital pictures.

### **Supporting information**

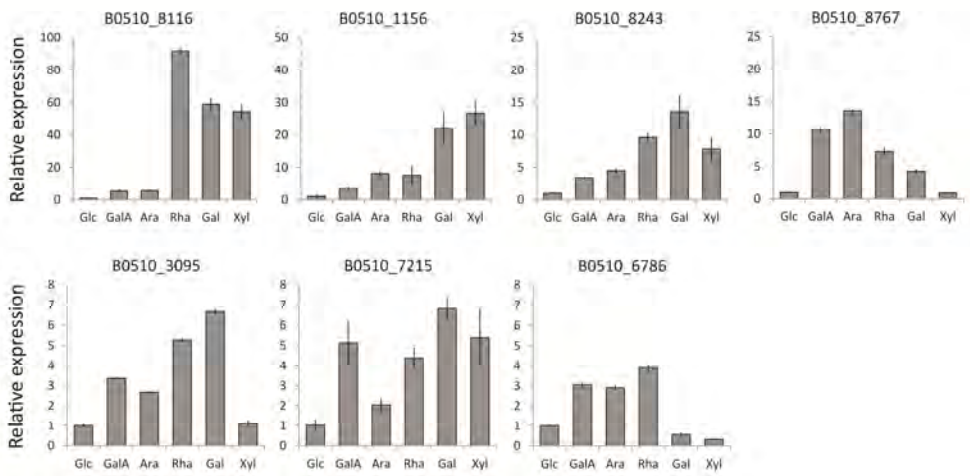
Supplementary Figures S1, S2 and Supplementary Tables S1, S2, S3, S4.

### **Acknowledgements**

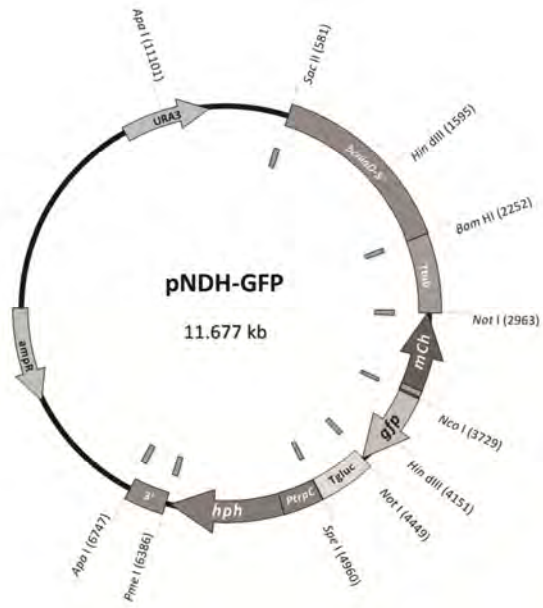
The authors are grateful to Pierre de Wit (Wageningen University, Laboratory of Phytopathology) for critical reading of the manuscript. The authors acknowledge funding by the Foundation Technological Top Institute Green Genetics (Project 2CC035RP) and the Netherlands Graduate School Experimental Plant Sciences.

Supporting information

A







Supplementary Figure 2. pNDH-GFP vector map.

**Supplementary Table 1.** Pectinolytic genes present in the *Botrytis cinerea* genome.

B0510_V2_ID	Glucose	Pectate	log2(P/G)	<i>q</i> -value	CAZY category	Gene annotation	Gene name	1	2	3	4	5	6	7	8
B0510_10150T1	0.1	1.6	3.463	0.422	GH28	endo-xylogalacturonan hydrolase						-553			
B0510_2787T1	15.4	167.7	3.445	0.006	GH28	exo-polygalacturonase		-344	-115	-197	-268	-240	-368	-71	
BcPG2	31.3	327.9	3.387	0.007	GH28	endo-polygalacturonase	Bcpg2								
B0510_3256T1	1	5.2	2.371	0.348	GH28	endo-polygalacturonase	Bcpg6		-514	-423	-58	-701	-450		
B0510_980T1	0.3	0.9	1.811	1.000	GH28	polygalacturonase									
B0510_1497T1	12.1	32.9	1.446	0.517	GH28	exo-polygalacturonase									
B0510_3088T1	0.9	2.4	1.367	0.682	GH28	rhamnogalacturonase									
B0510_9132T1	0.2	0.5	1.005	1.000	GH28	polygalacturonase			-115					-60	
B0510_1717T1	0.6	1.2	1.005	1.000	GH28	endo-rhamnogalacturonase									
B0510_5913T1	1.9	3	0.616	0.874	GH28	rhamnogalacturonase	rhamnogalacturonase A		-66						
B0510_5388T1	9342	11524	0.303	0.959	GH28	endo-polygalacturonase	Bcpg1								
B0510_9022T1	4.2	4.9	0.214	0.974	GH28	polygalacturonase									
B0510_5605T1	0	0.7	-	1.000	GH28	rhamnogalacturonan a-L-rhamnopyranohydrolase									
B0510_536T1	0	0	0.000	1.000	GH28	endo-polygalacturonase	Bcpg4								
B0510_972T1	0	0	0.000	1.000	GH28	endo-polygalacturonase	Bcpg5		-162						
B0510_8304T1	5.8	5.4	-0.103	0.993	GH28	exo-polygalacturonase							-434		
B0510_2072T1	33.6	22	-0.610	0.851	GH28	endo-polygalacturonase	Bcpg3								
B0510_4838T1	0.6	0.1	-1.997	1.000	GH28	rhamnogalacturonase									
B0510_8894T1	1.5	3.2	1.122	0.715	GH78	a-L-rhamnosidase									
B0510_9604T1	6.5	8.9	0.449	0.910	GH78	a-L-rhamnosidase									-753
B0510_4600T1	0.2	0.2	0.008	1.000	GH78	a-L-rhamnosidase									
B0510_9440T1	0.4	0.4	-0.255	1.000	GH78	a-L-rhamnosidase			-292						
B0510_9568T1	1.3	1	-0.333	1.000	GH78	a-L-rhamnosidase			-45						
B0510_10160T1	1.9	1.4	-0.467	0.919	GH78	a-L-rhamnosidase									

B0510_5846T1	0.1	0	-	1.000	GH78	a-L-rhamnosidase			
B0510_7636T1	0.7	0	-	1.000	GH78	a-L-rhamnosidase			
B0510_9131T1	0	0	0.000	1.000	GH88	d-4,5-unsaturated b-glucuronyl hydrolase			
B0510_3902T1	2	4.2	1.061	0.756	GH105	rhamnogalacturonyl hydrolase			
B0510_9011T1	2.8	6.1	1.124	0.675	GH115	xylogalacturonase			
B0510_344T1	12.8	31	1.280	0.593	CE8	pectin methylesterase	Bcpme2		
BcPME1	82.7	181.2	1.132	0.675	CE8	pectin methylesterase	Bcpme1	-102	
B0510_10151T1	0.8	1.5	1.001	1.000	CE8	pectin methylesterase			-258
B0510_230T1	5.9	11.2	0.920	0.772	CE8	pectin methylesterase			
B0510_5387T1	54.5	66.7	0.293	0.945	CE8	pectin methylesterase			
B0510_10061T1	54.6	340.7	2.642	0.091	PL1	pectin/pectate lyase			
B0510_6513T1	10.9	18.9	0.789	0.798	PL1	pectin/pectate lyase			-649
B0510_5319T1	2.3	2.3	0.001	1.000	PL1	pectin/pectate lyase			
B0510_27T1	0	0.4	-	1.000	PL1	pectin/pectate lyase			-118
B0510_161T1	0	0.8	-	1.000	PL1	pectin/pectate lyase			
B0510_10108T1	24	6.9	-1.800	0.390	PL1	pectin/pectate lyase			
B0510_7357T1	0.3	0.9	1.580	1.000	PL3	pectate lyase			-579
B0510_4894T1	2.3	1.4	-0.699	0.871	PL3	pectate lyase			

Pectate-induced gene expression and *cis*-regulatory elements

**Supplementary Table 2.** Motifs present in the promoters of genes which are up-regulated in pectate with  $\log_2 > 2$  and FPKM  $> 1$ .

Gene ID	Glucose	Pectate	log2(G/P)	q_value	Motif occurrence relative to translation start site								
					1	2	3	4	5	6	7	8	
B0510_9321	0	17.247	+	0.291									
B0510_847	0	10.626	+	0.473									
B0510_1769	0	7.584	+	0.519	-431								
B0510_8943	0	6.790	+	0.675			-827	-424	-559				
B0510_4442	0	5.399	+	0.675			-224		-944				
B0510_805	0	5.399	+	0.675									
B0510_9317	0	5.027	+	0.247									
B0510_7071	0	5.017	+	0.473									
B0510_8156	0	4.680	+	0.473									
B0510_6151	0	4.476	+	0.675					-710				
									-712				
									-716				
									-718				
B0510_6688	0	4.476	+	0.675									
B0510_6620	0	4.307	+	0.451				-565					
B0510_9073	0	3.942	+	0.306									
B0510_8397	0	3.763	+	0.519					-979				
B0510_2281	0	3.646	+	0.586					-619				
									-621				
									-625				
									-772				
B0510_7392	0	3.561	+	0.675									
B0510_961	0	3.547	+	0.451									
B0510_6229	0	3.336	+	0.401						-300			
B0510_8737	0	3.134	+	0.675						-716			
B0510_10031	0	2.930	+	0.586									
B0510_10076	0	2.775	+	0.586				-772		-941			
B0510_1086	0	2.656	+	0.675									
B0510_2981	0	2.656	+	0.675									
B0510_2332	0	2.499	+	0.473									
B0510_4148	0	2.411	+	0.675									
B0510_8603	0	2.411	+	0.675									
B0510_4226	0	2.394	+	0.586									
B0510_9230	0	2.305	+	0.675									
B0510_3355	0	2.287	+	0.310								-680	
B0510_898	0	2.167	+	0.324									
B0510_7757	0	2.057	+	0.369									
B0510_760	0.505147	16.479	5.02777	0.099			-447						
B0510_9315	0.082749	2.578	4.96109	0.110									
B0510_161	0.193018	4.055	4.39303	0.222									
B0510_8117	1.28588	24.025	4.22371	0.066				-545				-504	
B0510_571	0.131669	2.251	4.0953	0.083									

## Chapter 6

B0510_8090	0.974393	13.256	3.76596	0.070		
B0510_9074	0.420173	5.273	3.6495	0.054		
B0510_5161	9.04469	108.640	3.58634	0.390		
B0510_2829	0.667777	7.873	3.55939	0.401		
B0510_5870	0.329131	3.854	3.5497	0.106		
B0510_2703	1.75597	18.509	3.39789	0.066		-406
B0510_3161	0.271986	2.713	3.31824	0.452		-814
B0510_2678	2.74592	25.834	3.23392	0.190		
B0510_9765	1.0326	9.244	3.16221	0.211		-117
B0510_4415	1.13556	9.750	3.10197	0.085		
B0510_8225	1.42541	11.812	3.05075	0.095		
B0510_356	0.467527	3.870	3.04937	0.185		
B0510_3094	2.7207	21.978	3.01398	0.064		
B0510_9487	1.54029	12.364	3.00489	0.054		
B0510_4253	0.276816	2.220	3.00377	0.350		
B0510_4480	0.27342	2.182	2.99623	0.526		
B0510_8009	0.597224	4.761	2.99482	0.351		
B0510_986	12.0469	90.565	2.91029	0.074	-951	-406
B0510_5582	0.313652	2.357	2.90963	0.376		
B0510_5394	0.504295	3.775	2.9043	0.377		
B0510_6851	4.54339	33.987	2.90316	0.233		-6
B0510_4622	2.89946	20.654	2.83259	0.313		
B0510_1267	0.881412	6.193	2.81271	0.144		
B0510_8053	0.968327	6.748	2.80084	0.324		
B0510_6922	0.43703	3.032	2.7945	0.586		-274
B0510_263	4.60295	31.900	2.79294	0.052		
B0510_572	0.344937	2.386	2.79048	0.151		
B0510_7044	0.823742	5.668	2.78254	0.175		-33
B0510_9005	164.604	1127.320	2.77583	0.055		
B0510_7045	5.98364	40.636	2.76366	0.066		
B0510_10107	1.06581	7.220	2.7601	0.586	-708	
B0510_2377	94.5399	636.038	2.75012	0.070		
B0510_6269	0.657354	4.380	2.73622	0.348		-75
B0510_662	1.54308	10.267	2.73406	0.129	-964	
B0510_2634	1.11394	7.379	2.72775	0.348		
B0510_3012	0.374873	2.438	2.70147	0.440		
B0510_3371	70.7604	454.457	2.68313	0.091		-678
B0510_10061	54.5672	340.720	2.64248	0.091		
B0510_1920	2.65035	16.395	2.62896	0.177		-483
B0510_1335	35.0757	213.752	2.60739	0.129		
B0510_1601	31.4767	191.417	2.60436	0.120		
B0510_8047	2.50934	14.968	2.57646	0.250		
B0510_1974	3.16594	18.816	2.57126	0.250		
B0510_9472	0.559668	3.313	2.56533	0.636	-148	-161

Pectate-induced gene expression and *cis*-regulatory elements

B0510_4222	19.4185	114.390	2.55846	0.091	-696					
B0510_8146	0.481883	2.825	2.55135	0.284	-148					
B0510_7089	0.626028	3.618	2.5307	0.249						
B0510_3112	1.19286	6.887	2.52952	0.190						
B0510_4766	622.814	3570.970	2.51944	0.179						
B0510_4635	7.81764	44.646	2.51373	0.104						
B0510_7380	2.82466	16.072	2.50837	0.190				-870		
B0510_7497	32.2155	182.485	2.50195	0.115						
B0510_10179	3.46272	19.508	2.49411	0.189				-92		
B0510_8534	6.18222	34.618	2.48532	0.210						
B0510_8006	32.368	180.713	2.48106	0.139						
B0510_9362	23.798	132.734	2.47963	0.139						
B0510_4642	3.43828	19.174	2.4794	0.266						
B0510_5201	10.9964	61.172	2.47583	0.113				-829		
B0510_4050	2.07997	11.554	2.47373	0.339						
B0510_3478	3.05809	16.326	2.41644	0.291				-773		
B0510_3330	0.638468	3.404	2.41465	0.444						
B0510_9042	15.0723	80.324	2.41393	0.152						
B0510_10077	85.4803	452.033	2.40277	0.143				-408		
B0510_780	41.9201	221.269	2.40009	0.159	-283	-366	-371 -561 -569 -577	-62 -66	-308	-916
B0510_5061	6.5151	34.364	2.39902	0.156						
B0510_882	2.93036	15.415	2.39517	0.255						-74
B0510_556	1.40478	7.334	2.38422	0.395				-28		
B0510_2586	2.56483	13.344	2.37923	0.451				-728		-685
B0510_4299	26.9433	139.725	2.37459	0.150						
B0510_3256	1.00477	5.199	2.37138	0.348						
B0510_9070	5.71558	29.360	2.36088	0.294						-164
B0510_7220	12.3815	62.293	2.33088	0.168						
B0510_1948	0.410483	2.052	2.32196	0.541						
B0510_634	3.55129	17.704	2.3177	0.190						
B0510_3926	7.2976	36.378	2.31759	0.176						
B0510_1854	2.28806	11.280	2.30162	0.423				-783		
B0510_565	0.605407	2.981	2.29978	0.685						
B0510_6828	15.497	76.262	2.29898	0.213						
B0510_5408	1.48895	7.293	2.29215	0.549						
B0510_9261	0.884096	4.307	2.28453	0.688						
B0510_1346	40.204	194.961	2.27778	0.190						
B0510_3291	0.806069	3.876	2.26553	0.401						
B0510_687	5.32028	25.339	2.25179	0.224						
B0510_8195	2.9928	14.252	2.25158	0.567				-637 -643		
B0510_4925	1.90495	9.065	2.25056	0.307				-369		

## Chapter 6

B0510_1260	20.1765	95.946	2.24955	0.202	
B0510_8529	379.472	1797.530	2.24395	0.195	
B0510_4142	20.3662	96.302	2.24139	0.241	
B0510_3641	9.25031	43.511	2.23381	0.211	
B0510_8592	30.7009	143.946	2.22918	0.202	
B0510_1582	3.59137	16.678	2.21537	0.259	
B0510_24	729.753	3372.430	2.20831	0.215	-734
B0510_8905	0.542809	2.506	2.20708	0.422	
B0510_3760	263.529	1193.870	2.17961	0.313	
B0510_202	67.2549	304.273	2.17766	0.222	
B0510_3644	4.03035	18.087	2.16599	0.277	
B0510_4359	53.1567	238.464	2.16545	0.233	-355
B0510_6083	13.3901	60.007	2.16396	0.255	
B0510_8682	20.8736	93.149	2.15786	0.286	
B0510_9597	1.06202	4.720	2.15187	0.593	
B0510_5181	11.9674	52.656	2.13749	0.255	
B0510_509	1.23668	5.433	2.13519	0.451	-177 -849
B0510_8666	32.4779	142.571	2.13415	0.241	
B0510_3467	102.305	447.110	2.12775	0.291	
B0510_6519	4.55707	19.839	2.12218	0.405	
B0510_9256	55.9285	243.103	2.11991	0.279	-978
B0510_3106	6.41871	27.707	2.10991	0.310	-201
B0510_5358	20.3936	88.010	2.10956	0.291	
B0510_6645	1.60218	6.902	2.10689	0.369	-146
B0510_6227	3.92406	16.760	2.09463	0.291	
B0510_6075	5.89842	25.125	2.09073	0.281	
B0510_7937	35.92	152.330	2.08434	0.348	
B0510_223	1.65878	7.014	2.08017	0.350	-353
B0510_10180	1.91219	8.080	2.07916	0.350	-982
B0510_2897	10.0731	42.278	2.06938	0.284	
B0510_4579	1514.08	6340.290	2.0661	0.350	
B0510_956	7.26488	30.405	2.06531	0.369	
B0510_9741	123.675	517.451	2.06487	0.294	-178
B0510_5366	15.474	64.657	2.06296	0.263	
B0510_7379	39.2905	164.061	2.06198	0.264	
B0510_2019	7.87028	32.790	2.05877	0.367	
B0510_8523	2.91895	12.154	2.05793	0.313	-314
B0510_1761	1.8782	7.793	2.05292	0.451	-710
B0510_2325	34.7605	144.045	2.051	0.270	
B0510_5933	122.804	504.326	2.038	0.291	
B0510_3707	58.6897	240.794	2.03662	0.293	
B0510_3171	45.5707	186.874	2.03588	0.284	
B0510_9524	96.4246	395.112	2.03479	0.289	-256

## Pectate-induced gene expression and *cis*-regulatory elements

B0510_1494	22.9426	93.726	2.03042	0.286	
B0510_4022	119.513	485.891	2.02347	0.284	
B0510_5764	16.1573	65.430	2.01776	0.327	
B0510_6478	6.65947	26.828	2.01027	0.399	-124
B0510_8438	0.974055	3.906	2.00373	0.451	
B0510_7108	66.8656	268.121	2.00355	0.291	-445
B0510_5939	0.531567	2.129	2.0016	0.575	
B0510_10364	76.8871	307.777	2.00107	0.294	

**Supplementary Table 3.** Primers used for quantitative RT-PCR.

Primer No.	Target gene	Sequence (5'-3')
LZ322	B0510_171 F	TGTTGGTAGCGCAACTGTCAG
LZ323	B0510_171 R	CATAGTCGGTGAACATTGCTC
LZ324	B0510_9316 F	CGAGGATGCTGTATGTTTTGAC
LZ325	B0510_9316 R	CTCACTCTTCTCACTCCAAC
LZ328	B0510_1685 F	TCTAGGAAAACAGGAAGGTCAG
LZ329	B0510_1685 R	CCTTCTAACTCTCTCATGCTTG
LZ268	B0510_4051 F	GAGATTATGGGAGATTGATCTTC
LZ269	B0510_4051 R	ACATGAAGATCCAATTCCAAG
LZ326	B0510_8116 F	TCATACCAGGTGGCTCGACAG
LZ327	B0510_8116 R	TCTTTCGGGTCTCCATTGATC
LZ270	B0510_9368 F	ATGGCTCATCTAGGTGGGATC
LZ271	B0510_9368 R	ACTTCTTTCAATTTGTCGCCTTG
LZ272	B0510_4887 F	CAGCGTATAGTCCTTTGGTCAG
LZ273	B0510_4887 R	TAGCATGGGTCTCGAAATAGC
LZ274	B0510_1156 F	GGTCAACTATTCGCCTCCATC
LZ275	B0510_1156 R	CCATCACAGCAGAAGCCACAC
LZ276	B0510_7189 F	CTTGCGGTAGTAAACGTCTTTG
LZ277	B0510_7189 R	CGACAAGGTAGACATTGAGAG
LZ39	B0510_552 F	CAAGGTTTGGGAATTGTACAGAG
LZ40	B0510_552 R	GTATCCTCCATATCCATAGTAGC
LZ278	B0510_551 F	CGACACATCCTTCGATTCCCTC
LZ279	B0510_551 R	TTACGTTCAATAGCGTAGAGAG
LZ280	B0510_3593 F	TTCAACTCACGTATCTCCAAGC
LZ281	B0510_3593 R	AACCAGGTGGTGAAGTAATCGG
LZ284	B0510_1684 F	TCGCCTCGGGAATCCATCG
LZ285	B0510_1684 R	ATCAGCACCCCTTTCAGCAAC
LZ286	B0510_8767 F	TTCTAAGTTCCTGGATCGGTTC
LZ287	B0510_8767 R	ACAACGGCAGCTGGGGTTGAC
LZ288	B0510_3095 F	GTTACGGTGGCCCTCTCATC
LZ289	B0510_3095 R	GTAGTACTCCTCTGCTGGAAC
LZ290	B0510_5927 F	TTCAGAAAGAGACTACACTTGCG
LZ291	B0510_5927 R	TCACCAGTCTTGCCGGTCTTG
LZ292	B0510_9071 F	GAGTATGGTAAGGTGATTCTTGC
LZ293	B0510_9071 R	CATATACCCACGGAAAGAAGTC
LZ294	B0510_8243 F	CCAGTTGAACCTCTCATCTACC
LZ295	B0510_8243 R	TCAGTCTCCTTCTCCACCTTG
LZ296	B0510_9363 F	CATGCACTTCTAGGAGGCATAG
LZ297	B0510_9363 R	CTCATTCCACTGATACCATGTC
LZ298	B0510_3901 F	TACCACAACCTACAACAGCAAC
LZ299	B0510_3901 R	CCATCCATATCAATCATACTTTCC
LZ300	B0510_3996 F	CGCCTCTACTCAATGGTTGTG
LZ301	B0510_3996 R	CTTCCAAAGTCTTGCCCTTCG

Pectate-induced gene expression and *cis*-regulatory elements

LZ302	B0510_2787 F	GCTCATTGCGAGGACTTTCAC
LZ303	B0510_2787 R	TAATCGTTCATTACACAAGTG
LZ304	B0510_8492 F	CATTGGTGGAACACCGACTC
LZ305	B0510_8492 R	AGCTCGAGGTGTATCATAGTC
LZ68	BcPG2 F	GGAAGTGCCACTTTTGTTAC
LZ69	BcPG2 R	TCCATCCCACCATCTTGCTC
LZ306	B0510_7215 F	TTATGGTGACAAGGCACTCGAC
LZ307	B0510_7215 R	TCTGCTTCTCATACAATCCTCTG
LZ308	B0510_10339 F	TGCCACTGGAGATGATTCAAGG
LZ309	B0510_10339 R	AAAGCGGTGGAGCTAGCGTAG
LZ310	B0510_978 F	GGCCAAGTGCAGTTTCTACAC
LZ311	B0510_978 R	AACATGGTTTACGCCTCCGAAG
LZ312	B0510_8954 F	TCATCTTCTATTGTGGGATCATC
LZ313	B0510_8954 R	ATCCATAAGCATCCCTTGAAC
LZ314	B0510_6060 F	CTGCGGATTATGAACATCACAAG
LZ315	B0510_6060 R	TTCGTGGCGATCTGCTGCTAC
LZ316	B0510_6786 F	TACTTTCTGGAAGTACGCGATC
LZ317	B0510_6786 R	TGAGTAGAGCCAAGGGTTGAG
LZ318	B0510_1079 F	CAAGGGTCTGGGAGTGTAGAG
LZ319	B0510_1079 R	GGAGGGGAATAACAACATTGTTC
LZ320	B0510_3706 F	ATCCTCAAAATCCTAAGCATCAC
LZ321	B0510_3706 R	TCTCATAACATCATTAAACCAGATC
LZ37	<i>Bclgd1</i> F	TGGTCATGGCATGACTTTCAC
LZ38	<i>Bclgd1</i> R	GTTGCGAATCGGAAACGAGATA

**Supplementary Table 4.** Primers used for generating promoter constructs.

Primer No.	Target gene	Sequence (5'-3')	Description
LZ174	FL F	GATTACTACCTCGCCCTTGCTTACCATCGATGATGTTGAAATGTTATTGAA	
LZ147	FL R	TGAAAAGCTCTTACCCTTGGAAACCATGTGTATGATTATATGTATGTAGATG	
LZ253	Del1 F	GATTACTACCTCGCCCTTGCTTACCATCTATCGGTGTTTCGGCTGCTT	With LZ147 to amplify Del1 fragment
LZ254	Del2 F	GATTACTACCTCGCCCTTGCTTACCATCTCAAATGGCCACAACCTCTAC	With LZ147 to amplify Del2 fragment
LZ148	Del3 F	GATTACTACCTCGCCCTTGCTTACCATCATCAGAAAAGCTTATGGTGGAAAAAT	With LZ147 to amplify Del3 fragment
LZ149	Del4 F	GATTACTACCTCGCCCTTGCTTACCATCCAGCTTCAACGACACTCAGA	With LZ147 to amplify Del4 fragment
LZ150	Del5 F	GATTACTACCTCGCCCTTGCTTACCATCATGTTGAATCGACAATTTTAGTCC	With LZ147 to amplify Del5 fragment
LZ154	Del6 F	CTTACCCACGCCCTTGGATGTTGAATCGACAATTTTAGTCC	With LZ147 to amplify Del6-3' fragment
LZ155	Del6 R	GGACTAAAATTTGTCGATTCAAACATCCAAGGGCGTGGGTAGAG	With LZ174 to amplify Del6-5' fragment
LZ156	Del7 F	GAAAGCTTATTTGGTGGAAAAATAGTTATGTTGAATCGACAATTTTAGTCC	With LZ147 to amplify Del7-3' fragment
LZ157	Del7 R	GGACTAAAATTTGTCGATTCAAACATAACTATTTTTCCACCAATAAGCTTTC	With LZ174 to amplify Del7-5' fragment
LZ184	Del8 F	CTTACCCACGCCCTTGGTCCAGCTTCAACGACACTCAGA	With LZ147 to amplify Del8-3' fragment
LZ185	Del8 R	TCTGAGTGTGTTGAAGCTGGACCAAGGCGTGGGGTAGAG	With LZ174 to amplify Del8-5' fragment
LZ182	pNDH-GFP F	GTTTTCCAGTCACGACCCCTTAATCTCATGAACTCCCTTG	
LZ183	pNDH-GFP R	CAGGAAACAGCTATGACCCTCTCCGCTGACTGAGAAC	
LZ92	HPH F	GGTTCGGGTAGGGTTGTTT	
LZ93	HPH R	GTGTAATTGACCGAATTCCTTGC	

# CHAPTER 7

General discussion



The plant pathogenic fungus *Botrytis cinerea* predominantly infects pectin-rich plant species and tissues. Effective pectin degradation thus is important for virulence of *B. cinerea*. The experimental results presented in this thesis provide more insights into the role of pectin degradation by *B. cinerea*. On the one hand, we report a novel feature of *B. cinerea* endo-polygalacturonases (BcPGs) that act as microbe-associated molecular patterns (MAMPs) and describe the identification of the receptor complex in *Arabidopsis thaliana* that is required for the responsiveness to BcPGs. On the other hand, we discuss the role of pectinases and D-galacturonic acid catabolism in virulence of *B. cinerea*. We subsequently discuss the co-regulation of genes involved in pectin degradation, D-galacturonic acid uptake and catabolism and propose a model for this concerted action.

### **Novel features of endo-polygalacturonases in plant-pathogen interactions**

BcPGs are not only important virulence factors, but are also able to induce necrotic responses when infiltrated in leaves of several plant species (Kars et al., 2005a). The data presented in chapter 2 demonstrate that fungal endo-PGs (including BcPGs) may act as MAMPs. This observation is analogous to reports on the ethylene-inducing xylanase (EIX) from the saprotrophic fungus *Trichoderma* and *B. cinerea* xylanase xyn11A (Enkerli et al., 1999; Furman-Matarasso et al., 1999; Noda et al., 2010), which are both able to cause a necrotic response in tobacco and tomato. Both for the *B. cinerea* endo-PGs and the *Trichoderma* and *B. cinerea* xylanases, catalytically inactive proteins were equally able to induce a necrotic response, indicating that it is the protein that is recognized, rather than hydrolytic products of cell wall polymers also known as damage-associated molecular patterns (DAMPs).

For bacterial MAMPs such as flagellin and EF-Tu, the full-blown plant responses can be triggered by an oligopeptide that contains the epitope determining structure, presumably perceived as a linear peptide stretch. Also in the *Trichoderma* EIX, a pentapeptide epitope has been identified as an essential component for induction of the hypersensitive response (HR) (Rotblat et al., 2002). Among fungal endo-PGs, an 11-amino acid sequence is present as the longest conserved linear stretch. Unfortunately, a synthetic peptide of 22 amino acids, comprising these 11 amino acid residues was not capable of inducing necrosis. This observation does not necessarily exclude the importance of this sequence as an epitope for recognition. Possibly the 3-dimensional structure of the synthetic peptide differs from the structure present in the native protein, or the peptide is unstable and degraded by plant proteases after infiltration in the plant. Notably, the corresponding region in the sequence of *A. thaliana* endo-PGs contains at position 1 a proline residue instead of glycine. The proline most likely alters the 3-dimensional structure of plant endo-PGs, which would enable them to escape recognition by the plant itself. Further studies

are required to elucidate which amino acid motifs in fungal endo-PGs are crucial for inducing necrosis.

Plants perceive potential microbial invaders by using pattern recognition receptors (PRRs) that recognize MAMPs. As described in chapter 2, we studied the natural variation of *A. thaliana* accessions in responsiveness to BcPGs, and found among others that accession Col-0 is responsive to BcPGs, whereas accession Br-0 is not responsive. Molecular identification and functional characterization demonstrated that the gene *RBPG1*, encoding an LRR-RLP, determines responsiveness to BcPGs in Col-0. *RBPG1* is one member of a family of four RLP-encoding genes (*RLP39*, *RLP40*, *RLP41* and *RBPG1*) that occur in a cluster within this region of the Col-0 genome. Accession Br-0 contains only two RLP-encoding genes (*rbpg1-1* and *rbpg1-2*) in this region. Although *RLP39*, *rbpg1-2* as well as *RBPG1* were able to form a complex with BcPG3, only *RBPG1* is responsive and able to induce necrosis. This situation is analogous to the tomato LRR-RLPs LeEix1 and LeEix2, encoded by two paralogous genes from a gene cluster, that act as receptors for EIX. Both receptors are able to bind EIX, whereas only LeEix2 mediates necrotic responses (Ron and Avni, 2004). Further studies demonstrated that LeEix1, but not LeEix2 interacts with tomato BAK1 in a ligand-independent manner, and the LeEIX1-BAK1 interaction is required for the ability of LeEix1 to attenuate the signalling of LeEix2 (Bar et al., 2010). *RBPG1*, however, does not form a complex with BAK1 in the co-immunoprecipitation assay. We demonstrate that a different LRR-RLK, named SOBIR1 (Gao et al., 2009), is an interactor of *RBPG1* and this interaction is required for the induction of necrosis upon application of BcPG3. *RBPG1* and *rbpg1-2* were also able to form a complex with SOBIR1. Further studies are required to investigate whether other (as yet unknown) components in the complex have the ability to bind *RBPG1* to determine specificity.

HR-associated cell death usually enhances susceptibility of plants to *B. cinerea* (Govrin and Levine, 2000). However, we demonstrate that *RBPG1* has no effect on susceptibility nor on disease resistance against *B. cinerea*. The full lesion development of *B. cinerea* on *A. thaliana* leaves occurs within 3 days post inoculation, whereas the response of *A. thaliana* to BcPG proteins is visible 3 days after infiltration. This suggests that the necrotic response is possibly too slow to have any impact on the infection by *B. cinerea*. Furthermore, *RBPG1* does not contribute to disease resistance to other microbial pathogens like *Hyaloperonospora arabidopsidis*, *Phytophthora capsici* and *Pseudomonas syringae* pv. tomato DC3000, probably because *RBPG1* does not recognize the endo-PGs produced by these pathogens, due to the lack of the conserved epitope fpg11. The role of *RBPG1* in disease resistance to other pathogens that contain the epitope fpg11 in their endo-PGs (e. g. *Colletotrichum higginsianum*) is not known yet and requires future studies.

## The role of pectinases in virulence of *Botrytis cinerea*

The *B. cinerea* genome contains six genes encoding endo-PGs (Wubben et al., 1999). All gene family members are differentially expressed *in planta* (ten Have et al., 2001; Zhang and van Kan, unpublished). *Bcpg1* is expressed in all tissues tested although differences in transcript levels occur. *Bcpg2* is expressed early in the infection of tomato, broad bean, and courgette, but not in tobacco, *A. thaliana*, and apple. *Bcpg3* and *Bcpg5* are mainly expressed in apple fruit tissue, in agreement with the *in vitro* inducibility of *Bcpg3* at low pH and of *Bcpg5* by apple pectin. *Bcpg4* and *Bcpg6* are mostly expressed in late stages of infection, when extensive tissue maceration occurs, in agreement with *in vitro* inducibility of *Bcpg4* and *Bcpg6* by D-galacturonic acid.

BcPG1 seems to be universally required for full virulence. Knockout mutants in the *Bcpg1* gene were reduced in virulence on tomato leaves, tomato fruit, apple fruit (ten Have et al., 1998), as well as on leaves of broad bean (ten Have and van Kan, unpublished), *Nicotiana benthamiana* and *A. thaliana* (Zhang and van Kan, unpublished). This can be explained by the constitutive expression of *Bcpg1* *in planta* (ten Have et al., 2001) and the observation that the BcPG1 protein is abundant in *B. cinerea* secretomes in different media (Espino et al., 2010; Shah et al., 2009a). Mutants in the *Bcpg2* gene were reduced in virulence on tomato as well as broad bean leaves (Kars et al., 2005a), but not on *N. benthamiana* leaves and *A. thaliana* leaves (Zhang and van Kan, unpublished). This is consistent with the observation that expression of *Bcpg2* can be detected in tomato leaves but not in *N. benthamiana* and *A. thaliana* leaves. Individual knockout mutants in *Bcpg3*, *Bcpg4*, *Bcpg5*, and *Bcpg6* have been generated, but all of them displayed similar virulence as the wild-type strain on tomato, broad bean (Kars, 2007) and *N. benthamiana* leaves (Zhang and van Kan, unpublished). The targeted mutation studies have indicated that none of the single *Bcpg* genes is absolutely essential for penetration and host colonization. This is likely due to overlapping activities of the individual enzymes, resulting in functional redundancy. In view of the partial reduction in virulence of single *Bcpg1* and single *Bcpg2* mutants, it was of interest to generate double knockout mutants in both *Bcpg1* and *Bcpg2*, and check whether a further reduction of virulence could be obtained. These double mutants, however, were still virulent on tomato and *N. benthamiana* (Zhang and van Kan, unpublished). Silencing or deletion of multiple *Bcpg* genes would be required to investigate functional overlap among BcPG isozymes in more detail.

Besides endo-PGs, the joint action of other pectinases may also be important for successful infection. RNA-seq analyses revealed that the transcript levels of genes encoding an exo-polygalacturonase (exo-PG) and two pectin/pectate lyases were abundant during infection on tomato (Zhang and van Kan, unpublished). Deletion of these

candidate genes, possibly in combination with the endo-PG genes, would be required to study their contribution to virulence of *B. cinerea*.

### **The role of D-galacturonic acid uptake and utilization in virulence of *Botrytis cinerea***

The monosaccharide D-galacturonic acid is the ultimate hydrolytic product released by the joint action of endo-PGs and exo-PGs. In view of the large amount of carbon deposited in host cell walls, and the high proportion of pectin in these walls, D-galacturonic acid may constitute an important carbon supply for nutrition of *B. cinerea* when it colonizes and grows inside a host. Several genes involved in pectin decomposition and D-galacturonic acid catabolism are induced *in vitro* by D-galacturonic acid (Wubben et al., 2000; Zhang et al., 2011, Chapter 3), as is the expression of the putative D-galacturonic acid transporters (Chapter 5 and 6). Furthermore, most of these genes are expressed at higher levels during infection in the stage of lesion expansion, when host tissue decomposition occurs at high rates (Wubben et al., 2000; Zhang et al., 2011, Chapter 3). These observations collectively are indicative of a continuous release, uptake and consumption of D-galacturonic acid during infection.

The individual knockout mutants in the putative D-galacturonic acid transporters *Bchxt13* and *Bchxt15* displayed normal growth on D-galacturonic acid (Chapter 5), suggesting that the hexose uptake system in  $\Delta Bchxt13$  and  $\Delta Bchxt15$  mutants provides sufficient D-galacturonic acid for growth to the same extent as the wild-type strain. The expression analysis described in Chapter 6 identified another putative hexose transporter that was up-regulated even stronger than *Bchxt15*. Generating knockout mutants in this gene needs to be performed to investigate its possible function in D-galacturonic acid uptake.

Once D-galacturonic acid is taken up by the fungus, there should be a catabolic pathway in place to consume it. As in many other ascomycetes (Martens-Uzunova and Schaap, 2008), the D-galacturonic acid catabolic pathway in *B. cinerea* consists of three catalytic steps converting D-galacturonic acid to pyruvate and L-glyceraldehyde. The pathway involves two non-homologous galacturonate reductase genes (*Bcgar1* and *Bcgar2*), a galactonate dehydratase gene (*Bclgd1*), and a 2-keto-3-deoxy-L-galactonate aldolase gene (*Bclga1*) (Zhang et al., 2011, Chapter 3). The transcript levels of all these genes were induced substantially when the fungus was cultured in media containing D-galacturonic acid, pectate, or pectin as the sole carbon source. Deletion of these four genes in *B. cinerea*, either separately or in combinations, affected growth on D-galacturonic acid or pectic substrates (pectate, apple pectin, and citrus pectin) as the sole carbon source. The extent of growth reduction of the mutants on pectic substrates was correlated with the

proportion of D-galacturonic acid content in the substrate. Growth of the mutants on apple pectin (containing only 61% D-galacturonic acid) was better than on citrus pectin (containing 78% D-galacturonic acid), while growth on sodium pectate (containing > 99% D-galacturonic acid) was negligible (Zhang et al., 2011, Chapter 3).

The deletion of these four genes in *B. cinerea* did not affect virulence on tomato leaves, apples, and peppers (Zhang et al., 2011, Chapter 3), but reduced virulence on *N. benthamiana* and *A. thaliana* leaves (Zhang and van Kan, 2013, Chapter 4). The extent of reduction in virulence of mutants in the D-galacturonic acid catabolic pathway was correlated with the content of D-galacturonic acid in the cell wall of the host plants tested. This suggested that D-galacturonic acid released from pectin in plant cell walls makes up an important part of the nutrition of *B. cinerea*. However, more detailed studies revealed that the *B. cinerea* mutants were retarded in growth due to inhibitory activity by catabolic pathway intermediates that accumulate in the D-galacturonic acid catabolic mutants (Zhang and van Kan, 2013, Chapter 4). However, it is not possible to directly test the growth inhibitory activity of the intermediates, since they are not commercially available.

The D-galacturonic acid catabolic pathway has also been characterized in *Aspergillus niger* and *Hypocrea jecorina* (Martens-Uzunova and Schaap, 2008; Richard and Hilditch, 2009). However, in these fungi there is no growth inhibition by catabolic pathway intermediates (Kuivanen et al., 2012; Wiebe et al., 2010). The degradation of intermediate 2-keto-3-deoxy-L-galactonate was observed in *A. niger* and *H. jecorina* mutant cultures (Wiebe et al., 2010), suggesting that these fungi possess an enzyme activity that converts the compound into an, as yet unknown, metabolite that is no longer inhibitory, whereas such an enzyme is less effective or missing in *B. cinerea*. Alternatively, the intermediates might not be toxic to the fungus. But it might be possible that through another enzymatic reaction, the intermediates are converted into toxic products, which are produced in *B. cinerea* but not in *A. niger* and *H. jecorina*. However, the exact physiological causes that determine growth inhibition remain to be resolved.

Collectively, the functional analyses on the *Bcpg* genes and the D-galacturonic acid catabolic pathway genes indicate that *B. cinerea* secretes endo-PGs primarily for the purpose of pectin decomposition, which facilitates the penetration and colonization of host tissues. However, our data suggest that the pectin breakdown products might contribute only little to the increase in fungal growth and biomass production.

## **Transcription factors regulating cell wall degrading enzymes in *Botrytis cinerea***

The full consumption of available carbon sources by *B. cinerea* requires a concerted action of the appropriate depolymerising enzymes, monosaccharide transporters and catabolic enzymes. The expression of the genes encoding these enzymes were up-regulated in medium containing D-galacturonic acid, including *Bcgar2*, *Bclga1* (Zhang et al., 2011, Chapter 3), *Bcpg2*, B0510\_2787 (encoding an exo-PG), *Bchxt15* (Chapter 5) and B0510\_978 (encoding a putative sugar:H<sup>+</sup> symporter) (Chapter 6). The co-expression pattern of these genes suggests the presence of common *cis*-regulatory elements in their promoter regions, which mediate their regulation by (a) common transcription factor(s).

Conserved motifs are indeed present in the promoters of several pectinolytic genes and D-galacturonic acid catabolic genes in *B. cinerea* (Chapter 6). Functional analysis of regulatory elements present in the promoter region of *Bclga1* suggests that a sequence stretch of 35 nucleotides encompassing the PacC binding site and GAE1 motif are required for the up-regulation by D-galacturonic acid (Chapter 6). Further experiments need to be performed to assign the key sequence for regulation and to identify D-galacturonic acid-responsive transcription factor(s) that operate in regulating the pectinolytic complex of *B. cinerea*. Two potential mechanisms of gene activation may be considered (Figure 1B and 1C). Firstly, the transcription factor regulating pectinolytic genes might be present in an inactive form in *B. cinerea* in the absence of D-galacturonic acid, either in the cytoplasm or in the nucleus. The extracellular decomposition of pectin and subsequent uptake of D-galacturonic acid by the fungus leads to elevated levels of D-galacturonic acid in the cytoplasm. D-galacturonic acid might, directly or indirectly, activate the transcriptional regulator leading to its ability to promote transcription of pectinolytic genes (Figure 1B). An alternative mechanism that might be operating is that the transcription factor which regulates the co-expression of pectinolytic genes in *B. cinerea* is not expressed in the absence of D-galacturonic acid. The presence of D-galacturonic acid, either at the hyphal periphery or at low levels inside the cytoplasm might, through an unknown regulatory mechanism, induce expression of the D-galacturonic acid-responsive transcription factor(s) in an active form (Figure 1C). Both regulatory mechanisms are, at this point in time, hypothetical and will require further study.

## **Conclusions and perspectives**

Plant cell walls are complex chemical structures. Many fungi, including plant pathogens have the genetic potential to decompose cell walls by means of concerted actions of different enzymes (CAZymes). The degradation of plant cell wall polysaccharides releases

monosaccharides that can be used by fungi for growth. Genome sequences of plant pathogenic fungi have provided insights into the cell wall decomposing potential of fungi. Some of these enzymes are being exploited for industrial application, to decompose organic matter and release useful breakdown products. *B. cinerea* is not only a pathogenic fungus of great economic relevance (Dean et al., 2012), but also serves as a good exemplary case to illustrate various aspects of plant cell wall decomposition by (pathogenic) fungi.

Figure 1 illustrates our current view of the different steps of pectin decomposition and monosaccharide consumption by *B. cinerea*. One endo-PG (BcPG1) and as yet functionally uncharacterized exo-PG and pectin/pectate lyase are constitutively expressed and secreted to the hyphal periphery. These enzymes serve as pioneers to explore the environment (Figure 1A). When a pectic substrate is present in the vicinity of hyphae, it is cleaved by the concerted action of these hydrolases. This cleavage will release monosaccharides that are taken up into the hyphae by a (possibly ligand-specific) monosaccharide transporter protein, expressed at low basal level. Accumulation of D-galacturonate monosaccharide in the fungal cytoplasm is evidence for the presence of a pectic substrate in the environment and acts as a signal to boost the decomposing machinery for this particular polysaccharide. The presence of the monosaccharide activates a transcriptional regulator (Figures 1B and 1C), which induces the coordinated transcription of three distinct groups of genes, encoding additional secreted depolymerising enzymes, transporter proteins and monosaccharide catabolic enzymes, which collectively facilitate the complete degradation and consumption of pectin (Figure 1D).

Many conceptual features and steps that are illustrated in Figure 1 for the decomposition of pectin by *B. cinerea* (degradation by concerted actions of endo- and exo-hydrolases; uptake of monosaccharides by plasma membrane transporters; entry of the monosaccharide into the catabolic pathway; co-regulation of genes involved in degradation of one particular type of cell wall polysaccharide) may also be operational in other fungi, and may be valid for decomposition of other plant cell wall polysaccharides as well. Different levels of complexity may be observed and connections are likely to exist between pathways involved in decomposing the different types of plant cell wall polysaccharides. The insights into the components and the regulation of the plant cell wall decomposing machinery in *B. cinerea* may provide new leads for designing a rational control strategy for this devastating pathogen. Interfering with the plant cell wall decomposing machinery of *B. cinerea* will lead to reduced host tissue decomposition and delayed outgrowth of the fungus, eventually causing a significant reduction in host damage.

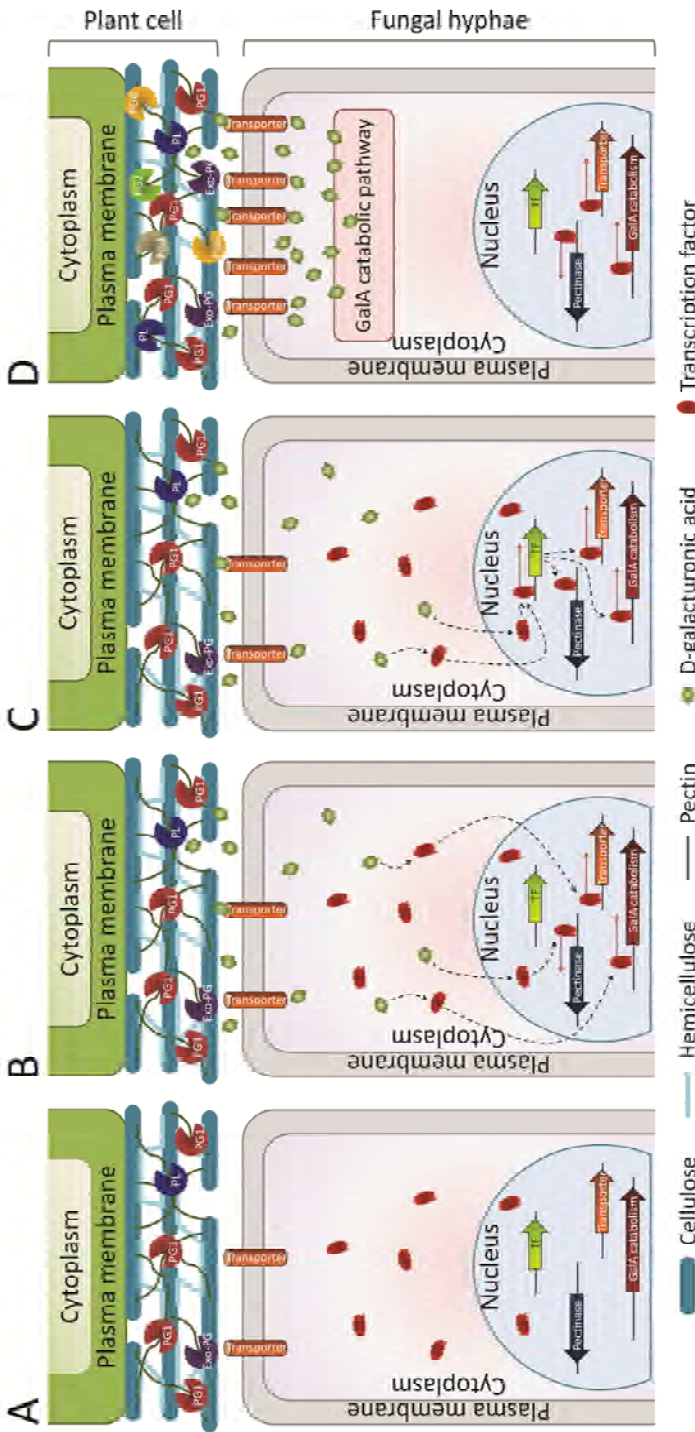


**Figure 1.** Schematic illustration of pectin decomposition and D-galacturonic acid (GaIA) consumption in *Botrytis cinerea*. Initial pectin decomposition by concerted action of endo-PG (PG1), exo-PG and pectin/pectate lyase (PL) and uptake of released GaIA by plasma membrane-associated transporters (A). The elevated levels of GaIA in the cytoplasm either directly activate transcription factor(s) (TF(s)) which could be present in the cytoplasm/ nucleus (B), or firstly induce the expression of the GaIA-responsive TF(s) (C). Subsequently, the activated TF(s) co-regulate the expression of genes encoding additional pectinases (e.g. exo-PG, PL, PG2, PG4, and PG6), transporters, and GaIA catabolic enzymes (D).

## References

- Adie, B. A., et al., 2007. ABA is an essential signal for plant resistance to pathogens affecting JA biosynthesis and the activation of defenses in Arabidopsis. *Plant Cell*. 19, 1665-1681.
- Aguero, C. B., et al., 2005. Evaluation of tolerance to Pierce's disease and *Botrytis* in transgenic plants of *Vitis vinifera* L. expressing the pear *PGIP* gene. *Mol Plant Pathol*. 6, 43-51.
- Amselem, J., et al., 2011. Genomic analysis of the necrotrophic fungal pathogens *Sclerotinia sclerotiorum* and *Botrytis cinerea*. *PLoS Genet*. 7, e1002230.
- Armand, S., et al., 2000. The active site topology of *Aspergillus niger* endopolygalacturonase II as studied by site-directed mutagenesis. *J Biol Chem*. 275, 691-696.
- Aro, N., et al., 2005. Transcriptional regulation of plant cell wall degradation by filamentous fungi. *FEMS Microbiol Rev*. 29, 719-739.
- Bailey, T. L., Elkan, C., 1994. Fitting a mixture model by expectation maximization to discover motifs in biopolymers. *Proc Int Conf Intell Syst Mol Biol*. 2, 28-36.
- Bar, M., et al., 2010. BAK1 is required for the attenuation of ethylene-inducing xylanase (Eix)-induced defense responses by the decoy receptor LeEix1. *Plant J*. 63, 791-800.
- Battaglia, E., et al., 2011. Analysis of regulation of pentose utilisation in *Aspergillus niger* reveals evolutionary adaptations in Eurotiales. *Stud Mycol*. 69, 31-38.
- Baxter, L., et al., 2010. Signatures of adaptation to obligate biotrophy in the *Hyaloperonospora arabidopsidis* genome. *Science*. 330, 1549-1551.
- Beckstette, M., et al., 2009. Significant speed up of database searches with HMMs by search space reduction with PSSM family models. *Bioinformatics*. 25, 3251-3258.
- Billon-Grand, G., et al., 2012. pH modulation differs during sunflower cotyledon colonization by the two closely related necrotrophic fungi *Botrytis cinerea* and *Sclerotinia sclerotiorum*. *Mol Plant Pathol*. 13, 568-578.
- Blumenkranz, N., Asboe-Hansen, G., 1973. New method for quantitative determination of uronic acids. *Anal Biochem*. 54, 484-489.
- Boller, T., Felix, G., 2009. A renaissance of elicitors: perception of microbe-associated molecular patterns and danger signals by pattern-recognition receptors. *Annu Rev Plant Biol*. 60, 379-406.
- Böttcher, C., et al., 2009. The multifunctional enzyme CYP71B15 (PHYTOALEXIN DEFICIENT3) converts cysteine-indole-3-acetonitrile to camalexin in the indole-3-acetonitrile metabolic network of *Arabidopsis thaliana*. *Plant Cell*. 21, 1830-1845.
- Boudart, G., et al., 2003. Elicitor activity of a fungal endopolygalacturonase in tobacco requires a functional catalytic site and cell wall localization. *Plant Physiol*. 131, 93-101.
- Bouton, S., et al., 2002. QUASIMODO1 encodes a putative membrane-bound glycosyltransferase required for normal pectin synthesis and cell adhesion in Arabidopsis. *Plant Cell*. 14, 2577-2590.
- Brito, N., et al., 2006. The endo-beta-1,4-xylanase xyn11A is required for virulence in *Botrytis cinerea*. *Mol Plant Microbe Interact*. 19, 25-32.
- Brunner, F., et al., 2002. Pep-13, a plant defense-inducing pathogen-associated pattern from *Phytophthora* transglutaminases. *EMBO J*. 21, 6681-6688.
- Brutus, A., et al., 2010. A domain swap approach reveals a role of the plant wall-associated kinase 1 (WAK1) as a receptor of oligogalacturonides. *Proc Natl Acad Sci U S A*. 107, 9452-9457.
- Buchanan, C. L., et al., 1999. An extremely thermostable aldolase from *Sulfolobus solfataricus* with specificity for non-phosphorylated substrates. *Biochem J*. 343 Pt 3, 563-570.

## References

- Cabanne, C., Doneche, B., 2002. Purification and characterization of two isozymes of polygalacturonase from *Botrytis cinerea*. Effect of calcium ions on polygalacturonase activity. *Microbiol Res.* 157, 183-189.
- Cabral, A., et al., 2011. Identification of *Hyaloperonospora arabidopsidis* transcript sequences expressed during infection reveals isolate-specific effectors. *PLoS One.* 6, e19328.
- Cabrera, J. C., et al., 2008. Egg box conformation of oligogalacturonides: the time-dependent stabilization of the elicitor-active conformation increases its biological activity. *Glycobiology.* 18, 473-482.
- Caffall, K. H., Mohnen, D., 2009. The structure, function, and biosynthesis of plant cell wall pectic polysaccharides. *Carbohydr Res.* 344, 1879-1900.
- Cantarel, B. L., et al., 2009. The Carbohydrate-Active EnZymes database (CAZy): an expert resource for Glycogenomics. *Nucleic Acids Res.* 37, D233-D238.
- Cao, H., et al., 1994. Characterization of an Arabidopsis mutant that is nonresponsive to inducers of systemic acquired resistance. *Plant Cell.* 6, 1583-1592.
- Cao, J., et al., 2011. Whole-genome sequencing of multiple *Arabidopsis thaliana* populations. *Nat Genet.* 43, 956-963.
- Chaparro-Garcia, A., et al., 2011. The receptor-like kinase SERK3/BAK1 is required for basal resistance against the late blight pathogen *Phytophthora infestans* in *Nicotiana benthamiana*. *PLoS One.* 6, e16608.
- Chinchilla, D., et al., 2006. The Arabidopsis receptor kinase FLS2 binds flg22 and determines the specificity of flagellin perception. *Plant Cell.* 18, 465-476.
- Chinchilla, D., et al., 2009. One for all: the receptor-associated kinase BAK1. *Trends Plant Sci.* 14, 535-541.
- Chinchilla, D., et al., 2007. A flagellin-induced complex of the receptor FLS2 and BAK1 initiates plant defence. *Nature.* 448, 497-500.
- Choquer, M., et al., 2007. *Botrytis cinerea* virulence factors: new insights into a necrotrophic and polyphageous pathogen. *FEMS Microbiol Lett.* 277, 1-10.
- Churchill, G. A., Doerge, R. W., 1994. Empirical threshold values for quantitative trait mapping. *Genetics.* 138, 963-971.
- Clough, S. J., Bent, A. F., 1998. Floral dip: a simplified method for *Agrobacterium*-mediated transformation of *Arabidopsis thaliana*. *Plant J.* 16, 735-743.
- Cosgrove, D. J., 2001. Plant cell walls: wall-associated kinases and cell expansion. *Curr Biol.* 11, R558-R559.
- Cubero, B., Scazzocchio, C., 1994. Two different, adjacent and divergent zinc finger binding sites are necessary for CREA-mediated carbon catabolite repression in the proline gene cluster of *Aspergillus nidulans*. *EMBO J.* 13, 407-415.
- Curtis, M. D., Grossniklaus, U., 2003. A gateway cloning vector set for high-throughput functional analysis of genes in *planta*. *Plant Physiol.* 133, 462-469.
- Curvers, K., et al., 2010. Abscisic acid deficiency causes changes in cuticle permeability and pectin composition that influence tomato resistance to *Botrytis cinerea*. *Plant Physiol.* 154, 847-860.
- D'Ovidio, R., et al., 2004. Polygalacturonases, polygalacturonase-inhibiting proteins and pectic oligomers in plant-pathogen interactions. *Biochim Biophys Acta.* 1696, 237-244.
- De Lorenzo, G., et al., 2001. The role of polygalacturonase-inhibiting proteins (PGIPs) in defense against pathogenic fungi. *Annu Rev Phytopathol.* 39, 313-335.
- Dean, R., et al., 2012. The Top 10 fungal pathogens in molecular plant pathology. *Mol Plant Pathol.* 13, 414-430.

- Decreux, A., et al., 2006. *In vitro* characterization of the homogalacturonan-binding domain of the wall-associated kinase WAK1 using site-directed mutagenesis. *Phytochemistry*. 67, 1068-1079.
- Delaney, T. P., et al., 1994. A central role of salicylic Acid in plant disease resistance. *Science*. 266, 1247-1250.
- Denoux, C., et al., 2008. Activation of defense response pathways by OGs and Flg22 elicitors in *Arabidopsis* seedlings. *Mol Plant*. 1, 423-445.
- Dewey, F. M., et al., 2008. Quantification of *Botrytis* and laccase in winegrapes. *Am J Enol Vitic*. 59, 47-54.
- Doehlemann, G., et al., 2005. Molecular and functional characterization of a fructose specific transporter from the gray mold fungus *Botrytis cinerea*. *Fungal Genet Biol*. 42, 601-610.
- Dulermo, T., et al., 2010. Novel insights into mannitol metabolism in the fungal plant pathogen *Botrytis cinerea*. *Biochem J*. 427, 323-332.
- Dulermo, T., et al., 2009. Dynamic carbon transfer during pathogenesis of sunflower by the necrotrophic fungus *Botrytis cinerea*: from plant hexoses to mannitol. *New Phytol*. 183, 1149-1162.
- Duplessis, S., et al., 2011. *Melampsora larici-populina* transcript profiling during germination and timecourse infection of poplar leaves reveals dynamic expression patterns associated with virulence and biotrophy. *Mol Plant Microbe Interact*. 24, 808-818.
- Englyst, H. N., Cummings, J. H., 1984. Simplified method for the measurement of total non-starch polysaccharides by gas-liquid chromatography of constituent sugars as alditol acetates. *Analyst*. 109, 937-942.
- Enkerli, J., et al., 1999. The enzymatic activity of fungal xylanase is not necessary for its elicitor activity. *Plant Physiol*. 121, 391-397.
- Espino, J. J., et al., 2005. *Botrytis cinerea* endo-beta-1,4-glucanase *Cel5A* is expressed during infection but is not required for pathogenesis. *Physiol Mol Plant Pathol*. 66, 213-221.
- Espino, J. J., et al., 2010. The *Botrytis cinerea* early secretome. *Proteomics*. 10, 3020-3034.
- Federici, L., et al., 2006. Polygalacturonase inhibiting proteins: players in plant innate immunity? *Trends Plant Sci*. 11, 65-70.
- Felix, G., et al., 1999. Plants have a sensitive perception system for the most conserved domain of bacterial flagellin. *Plant J*. 18, 265-276.
- Fernandez-Acero, F. J., et al., 2010. 2-DE proteomic approach to the *Botrytis cinerea* secretome induced with different carbon sources and plant-based elicitors. *Proteomics*. 10, 2270-2280.
- Ferrari, S., et al., 2006. Antisense expression of the *Arabidopsis thaliana* *AtPGIP1* gene reduces polygalacturonase-inhibiting protein accumulation and enhances susceptibility to *Botrytis cinerea*. *Mol Plant Microbe Interact*. 19, 931-936.
- Ferrari, S., et al., 2003a. *Arabidopsis* local resistance to *Botrytis cinerea* involves salicylic acid and camalexin and requires EDS4 and PAD2, but not SID2, EDS5 or PAD4. *Plant J*. 35, 193-205.
- Ferrari, S., et al., 2003b. Tandemly duplicated *Arabidopsis* genes that encode polygalacturonase-inhibiting proteins are regulated coordinately by different signal transduction pathways in response to fungal infection. *Plant Cell*. 15, 93-106.
- Fischer-Parton, S., et al., 2000. Confocal microscopy of FM4-64 as a tool for analysing endocytosis and vesicle trafficking in living fungal hyphae. *J Microsc*. 198, 246-259.
- Fisher, M. C., et al., 2012. Emerging fungal threats to animal, plant and ecosystem health. *Nature*. 484, 186-194.
- Flors, V., et al., 2008. Interplay between JA, SA and ABA signalling during basal and induced resistance against *Pseudomonas syringae* and *Alternaria brassicicola*. *Plant J*. 54, 81-92.

## References

- Furman-Matarasso, N., et al., 1999. A point mutation in the ethylene-inducing xylanase elicitor inhibits the beta-1-4-endoxylanase activity but not the elicitation activity. *Plant Physiol.* 121, 345-351.
- Galletti, R., et al., 2008. The AtrbohD-mediated oxidative burst elicited by oligogalacturonides in *Arabidopsis* is dispensable for the activation of defense responses effective against *Botrytis cinerea*. *Plant Physiol.* 148, 1695-1706.
- Gan, P., et al., 2013. Comparative genomic and transcriptomic analyses reveal the hemibiotrophic stage shift of *Colletotrichum* fungi. *New Phytol.* 197, 1236-1249.
- Gao, M., et al., 2009. Regulation of cell death and innate immunity by two receptor-like kinases in *Arabidopsis*. *Cell Host Microbe.* 6, 34-44.
- Garcia-Andrade, J., et al., 2011. *Arabidopsis* ocp3 mutant reveals a mechanism linking ABA and JA to pathogen-induced callose deposition. *Plant J.* 67, 783-794.
- Gomez-Gomez, L., Boller, T., 2000. FLS2: an LRR receptor-like kinase involved in the perception of the bacterial elicitor flagellin in *Arabidopsis*. *Mol Cell.* 5, 1003-1011.
- Govrin, E. M., Levine, A., 2000. The hypersensitive response facilitates plant infection by the necrotrophic pathogen *Botrytis cinerea*. *Curr Biol.* 10, 751-757.
- Greeff, C., et al., 2012. Receptor-like kinase complexes in plant innate immunity. *Front Plant Sci.* 3, 209.
- Gruben, B. S., 2012. Novel transcriptional activators of *Aspergillus* involved in plant biomass utilization. PhD thesis, Utrecht University, Microbiology.
- Harholt, J., et al., 2006. ARABINAN DEFICIENT 1 is a putative arabinosyltransferase involved in biosynthesis of pectic arabinan in *Arabidopsis*. *Plant Physiol.* 140, 49-58.
- Hauser, M. T., et al., 2001. Trichome distribution in *Arabidopsis thaliana* and its close relative *Arabidopsis lyrata*: molecular analysis of the candidate gene GLABROUS1. *Mol Biol Evol.* 18, 1754-1763.
- Heese, A., et al., 2007. The receptor-like kinase SERK3/BAK1 is a central regulator of innate immunity in plants. *Proc Natl Acad Sci U S A.* 104, 12217-12222.
- Hematy, K., et al., 2009. Host-pathogen warfare at the plant cell wall. *Curr Opin Plant Biol.* 12, 406-413.
- Hickey, P. C., et al., 2004. Live-cell imaging of filamentous fungi using vital fluorescent dyes and confocal microscopy. *Methods in Microbiology.* 34, 63-88.
- Hilditch, S., et al., 2007. The missing link in the fungal D-galacturonate pathway: identification of the L-threo-3-deoxy-hexulose aldolase. *J Biol Chem.* 282, 26195-26201.
- Hilz, H., et al., 2005. Cell wall polysaccharides in black currants and bilberries-characterisation in berries, juice, and press cake. *Carbohydr. Polym.* 59, 477-488.
- Holub, E. B., et al., 1994. Phenotypic and genotypic characterization of interactions between isolates of *Peronospora parasitica* and accessions of *Arabidopsis thaliana*. *Mol Plant Microbe Interact.* 7, 223-239.
- Hondmann, D. H., et al., 1991. Glycerol catabolism in *Aspergillus nidulans*. *J Gen Microbiol.* 137, 629-636.
- Hückelhoven, R., 2007. Cell wall-associated mechanisms of disease resistance and susceptibility. *Annu Rev Phytopathol.* 45, 101-127.
- Huitema, E., et al., 2011. A straightforward protocol for electro-transformation of *Phytophthora capsici* zoospores. *Methods Mol Biol.* 712, 129-135.
- Isshiki, A., et al., 2001. Endopolygalacturonase is essential for citrus black rot caused by *Alternaria citri* but not brown spot caused by *Alternaria alternata*. *Mol Plant Microbe Interact.* 14, 749-757.

- Jacobs, A. K., et al., 2003. An Arabidopsis callose synthase, GSL5, is required for wound and papillary callose formation. *Plant Cell*. 15, 2503-2513.
- Janni, M., et al., 2008. The expression of a bean PGIP in transgenic wheat confers increased resistance to the fungal pathogen *Bipolaris sorokiniana*. *Mol Plant Microbe Interact*. 21, 171-177.
- Jolie, R. P., et al., 2010. Pectin methylesterase and its proteinaceous inhibitor: a review. *Carbohydr Res*. 345, 2583-2595.
- Jones, J. D., Dangl, J. L., 2006. The plant immune system. *Nature*. 444, 323-329.
- Joubert, D. A., et al., 2007. A polygalacturonase-inhibiting protein from grapevine reduces the symptoms of the endopolygalacturonase BcPG2 from *Botrytis cinerea* in *Nicotiana benthamiana* leaves without any evidence for *in vitro* interaction. *Mol Plant Microbe Interact*. 20, 392-402.
- Juge, N., 2006. Plant protein inhibitors of cell wall degrading enzymes. *Trends Plant Sci*. 11, 359-367.
- Kämper, J., et al., 2006. Insights from the genome of the biotrophic fungal plant pathogen *Ustilago maydis*. *Nature*. 444, 97-101.
- Kars, I., 2007. The role of pectin degradation in pathogenesis of *Botrytis cinerea*. PhD thesis, Wageningen University, Phytopathology.
- Kars, I., et al., 2005a. Necrotizing activity of five *Botrytis cinerea* endopolygalacturonases produced in *Pichia pastoris*. *Plant J*. 43, 213-225.
- Kars, I., et al., 2005b. Functional analysis of *Botrytis cinerea* pectin methylesterase genes by PCR-based targeted mutagenesis: *Bcpme1* and *Bcpme2* are dispensable for virulence of strain B05.10. *Mol Plant Pathol*. 6, 641-652.
- Kars, I., van Kan, J. A. L., 2004. Extracellular enzymes and metabolites involved in pathogenesis of *Botrytis*. *Botrytis: biology, pathology and control* (Y. Elad, B. Williamson, P. Tudzynski and N. Delen, eds.) Kluwer Academic Publishers, The Netherlands. 99-118.
- Kester, H. C., Visser, J., 1990. Purification and characterization of polygalacturonases produced by the hyphal fungus *Aspergillus niger*. *Biotechnol Appl Biochem*. 12, 150-60.
- Kim, H., Woloshuk, C. P., 2011. Functional characterization of fst1 in *Fusarium verticillioides* during colonization of maize kernels. *Mol Plant Microbe Interact*. 24, 18-24.
- King, B. C., et al., 2011. Arsenal of plant cell wall degrading enzymes reflects host preference among plant pathogenic fungi. *Biotechnol Biofuels*. 4, 4.
- Kintner, P. K., Vanburen, J. P., 1982. Carbohydrate interference and its correction in pectin analysis using the m-hydroxydiphenyl method. *J Food Sci*. 47, 756-759.
- Koeck, M., et al., 2011. The role of effectors of biotrophic and hemibiotrophic fungi in infection. *Cell Microbiol*. 13, 1849-1857.
- Kohorn, B. D., et al., 2009. Pectin activation of MAP kinase and gene expression is WAK2 dependent. *Plant J*. 60, 974-982.
- Kohorn, B. D., Kohorn, S. L., 2012. The cell wall-associated kinases, WAKs, as pectin receptors. *Front Plant Sci*. 3, 88.
- Krampe, S., Boles, E., 2002. Starvation-induced degradation of yeast hexose transporter Hxt7p is dependent on endocytosis, autophagy and the terminal sequences of the permease. *FEBS Lett*. 513, 193-196.
- Kravtchenko, T. P., et al., 1992. Analytical comparison of three industrial pectin preparations. *Carbohydr Polym*. 18, 17-25.
- Kuivanen, J., et al., 2012. Engineering filamentous fungi for conversion of d-galacturonic acid to L-galactonic acid. *Appl Environ Microbiol*. 78, 8676-8683.
- Kunze, G., et al., 2004. The N terminus of bacterial elongation factor Tu elicits innate immunity in Arabidopsis plants. *Plant Cell*. 16, 3496-3507.

## References

- Kuorelahti, S., et al., 2006. L-galactonate dehydratase is part of the fungal path for D-galacturonic acid catabolism. *Mol Microbiol.* 61, 1060-1068.
- Kuorelahti, S., et al., 2005. Identification in the mold *Hypocrea jecorina* of the first fungal D-galacturonic acid reductase. *Biochemistry.* 44, 11234-11240.
- Lamb, C., Dixon, R. A., 1997. The oxidative burst in plant disease resistance. *Annu Rev Plant Physiol Plant Mol Biol.* 48, 251-275.
- Langmead, B., Salzberg, S. L., 2012. Fast gapped-read alignment with Bowtie 2. *Nat Methods.* 9, 357-359.
- Li, H., et al., 2009. The Sequence Alignment/Map format and SAMtools. *Bioinformatics.* 25, 2078-2079.
- Li, J., et al., 2002. BAK1, an Arabidopsis LRR receptor-like protein kinase, interacts with BRI1 and modulates brassinosteroid signaling. *Cell.* 110, 213-222.
- Liebrand, T. W., et al., 2012. Endoplasmic reticulum-quality control chaperones facilitate the biogenesis of Cf receptor-like proteins involved in pathogen resistance of tomato. *Plant Physiol.* 159, 1819-1833.
- Liebrand, T. W., et al., 2013. The receptor-like kinase SOBIR1/EVR interacts with receptor-like proteins in plant immunity against fungal infection. submitted.
- Liepins, J., et al., 2006. Enzymes for the NADPH-dependent reduction of dihydroxyacetone and D-glyceraldehyde and L-glyceraldehyde in the mould *Hypocrea jecorina*. *Febs J.* 273, 4229-4235.
- Lingner, U., et al., 2011. Hexose transporters of a hemibiotrophic plant pathogen: functional variations and regulatory differences at different stages of infection. *J Biol Chem.* 286, 20913-20922.
- Manfredini, C., et al., 2005. Polygalacturonase-inhibiting protein 2 of *Phaseolus vulgaris* inhibits BcPG1, a polygalacturonase of *Botrytis cinerea* important for pathogenicity, and protects transgenic plants from infection. *Physiol Mol Plant Pathol.* 67, 108-115.
- Marger, M. D., Saier, M. H., 1993. A major superfamily of transmembrane facilitators that catalyze uniport, symport and antiport. *Trends Biochem Sci.* 18, 13-20.
- Martens-Uzunova, E. S., Schaap, P. J., 2008. An evolutionary conserved d-galacturonic acid metabolic pathway operates across filamentous fungi capable of pectin degradation. *Fungal Genet Biol.* 45, 1449-1457.
- Martens-Uzunova, E. S., et al., 2006. A new group of exo-acting family 28 glycoside hydrolases of *Aspergillus niger* that are involved in pectin degradation. *Biochem J.* 400, 43-52.
- Martin, F., et al., 2011. Sequencing the fungal tree of life. *New Phytol.* 190, 818-821.
- Martin, F., et al., 2010. Perigord black truffle genome uncovers evolutionary origins and mechanisms of symbiosis. *Nature.* 464, 1033-1038.
- Meyer, U., Dewey, F., 2000. Efficacy of different immunogens for raising monoclonal antibodies to *Botrytis cinerea*. *Mycol Res.* 104, 979-987.
- Mohnen, D., 2008. Pectin structure and biosynthesis. *Curr Opin Plant Biol.* 11, 266-277.
- Mojzita, D., et al., 2010. Metabolic engineering of fungal strains for conversion of D-galacturonate to meso-galactarate. *Appl Environ Microbiol.* 76, 169-175.
- Monaghan, J., Zipfel, C., 2012. Plant pattern recognition receptor complexes at the plasma membrane. *Curr Opin Plant Biol.* 15, 349-357.
- Nakagawa, T., et al., 2007. Development of series of gateway binary vectors, pGWBs, for realizing efficient construction of fusion genes for plant transformation. *J Biosci Bioeng.* 104, 34-41.
- Nam, K. H., Li, J., 2002. BRI1/BAK1, a receptor kinase pair mediating brassinosteroid signaling. *Cell.* 110, 203-212.

- Nishimura, M. T., et al., 2003. Loss of a callose synthase results in salicylic acid-dependent disease resistance. *Science*. 301, 969-972.
- Nishiyama, Y., et al., 2002. Crystal structure and hydrogen-bonding system in cellulose Ibeta from synchrotron X-ray and neutron fiber diffraction. *J Am Chem Soc*. 124, 9074-9082.
- Noda, J., et al., 2010. The *Botrytis cinerea* xylanase Xyn11A contributes to virulence with its necrotizing activity, not with its catalytic activity. *BMC Plant Biol*. 10, 38.
- O'Connell, R. J., et al., 2012. Lifestyle transitions in plant pathogenic *Colletotrichum* fungi deciphered by genome and transcriptome analyses. *Nat Genet*. 44, 1060-1065.
- Oeser, B., et al., 2002. Polygalacturonase is a pathogenicity factor in the *Claviceps purpurea/rye* interaction. *Fungal Genet Biol*. 36, 176-186.
- Ogawa, M., et al., 2009. ARABIDOPSIS DEHISCENCE ZONE POLYGALACTURONASE1 (ADPG1), ADPG2, and QUARTET2 are polygalacturonases required for cell separation during reproductive development in Arabidopsis. *Plant Cell*. 21, 216-233.
- Ozcan, S., Johnston, M., 1999. Function and regulation of yeast hexose transporters. *Microbiol Mol Biol Rev*. 63, 554-569.
- Pao, S. S., et al., 1998. Major facilitator superfamily. *Microbiol Mol Biol Rev*. 62, 1-34.
- Paper, J. M., et al., 2007. Comparative proteomics of extracellular proteins *in vitro* and *in planta* from the pathogenic fungus *Fusarium graminearum*. *Proteomics*. 7, 3171-3183.
- Penninckx, I. A., et al., 1996. Pathogen-induced systemic activation of a plant defensin gene in Arabidopsis follows a salicylic acid-independent pathway. *Plant Cell*. 8, 2309-2323.
- Penninckx, I. A., et al., 1998. Concomitant activation of jasmonate and ethylene response pathways is required for induction of a plant defensin gene in Arabidopsis. *Plant Cell*. 10, 2103-2113.
- Phalip, V., et al., 2009. Plant cell wall degradation with a powerful *Fusarium graminearum* enzymatic arsenal. *J Microbiol Biotechnol*. 19, 573-581.
- Poinsot, B., et al., 2003. The endopolygalacturonase 1 from *Botrytis cinerea* activates grapevine defense reactions unrelated to its enzymatic activity. *Mol Plant Microbe Interact*. 16, 553-564.
- Powell, A. L., et al., 2000. Transgenic expression of pear PGIP in tomato limits fungal colonization. *Mol Plant Microbe Interact*. 13, 942-950.
- Raiola, A., et al., 2011. Pectin methylesterase is induced in Arabidopsis upon infection and is necessary for a successful colonization by necrotrophic pathogens. *Mol Plant Microbe Interact*. 24, 432-440.
- Rasul, S., et al., 2012. Nitric oxide production mediates oligogalacturonide-triggered immunity and resistance to *Botrytis cinerea* in *Arabidopsis thaliana*. *Plant Cell Environ*. 35, 1483-1499.
- Rha, E., et al., 2001. Expression of exo-polygalacturonases in *Botrytis cinerea*. *FEMS Microbiol Lett*. 201, 105-109.
- Richard, P., Hilditch, S., 2009. D-galacturonic acid catabolism in microorganisms and its biotechnological relevance. *Appl Microbiol Biotechnol*. 82, 597-604.
- Rolland, S., et al., 2009. pH controls both transcription and post-translational processing of the protease BcACP1 in the phytopathogenic fungus *Botrytis cinerea*. *Microbiology*. 155, 2097-2105.
- Ron, M., Avni, A., 2004. The receptor for the fungal elicitor ethylene-inducing xylanase is a member of a resistance-like gene family in tomato. *Plant Cell*. 16, 1604-1615.
- Rotblat, B., et al., 2002. Identification of an essential component of the elicitation active site of the EIX protein elicitor. *Plant J*. 32, 1049-1055.
- Roux, M., et al., 2011. The Arabidopsis leucine-rich repeat receptor-like kinases BAK1/SERK3 and BKK1/SERK4 are required for innate immunity to hemibiotrophic and biotrophic pathogens. *Plant Cell*. 23, 2440-2455.

## References

- Rui, O., Hahn, M., 2007. The *Botrytis cinerea* hexokinase, Hxk1, but not the glucokinase, Glk1, is required for normal growth and sugar metabolism, and for pathogenicity on fruits. *Microbiology*. 153, 2791-2802.
- Scheller, H. V., Ulvskov, P., 2010. Hemicelluloses. *Annu Rev Plant Biol*. 61, 263-289.
- Schols, H. A., et al., 2009. Revealing pectin's structure. *Pectins and pectinases* (H.A. Schols, R. G. F. Visser, and A. G.J. Voragen, eds) Wageningen Academic Publishers, The Netherlands. 19-34.
- Schumacher, J., 2012. Tools for *Botrytis cinerea*: New expression vectors make the gray mold fungus more accessible to cell biology approaches. *Fungal Genet Biol*. 49, 483-497.
- Sealy-Lewis, H. M., Fairhurst, V., 1992. An NADP(+)-dependent glycerol dehydrogenase in *Aspergillus nidulans* is inducible by D-galacturonate. *Curr Genet*. 22, 293-296.
- Shah, P., et al., 2009a. Comparative proteomic analysis of *Botrytis cinerea* secretome. *J Proteome Res*. 8, 1123-1130.
- Shah, P., et al., 2009b. A proteomic study of pectin-degrading enzymes secreted by *Botrytis cinerea* grown in liquid culture. *Proteomics*. 9, 3126-3135.
- Shieh, M. T., et al., 1997. Molecular genetic evidence for the involvement of a specific polygalacturonase, P2c, in the invasion and spread of *Aspergillus flavus* in cotton bolls. *Appl Environ Microbiol*. 63, 3548-3552.
- Souffriau, B., et al., 2012. Evidence for rapid uptake of D-galacturonic acid in the yeast *Saccharomyces cerevisiae* by a channel-type transport system. *FEBS Lett*. 586, 2494-2499.
- Spanu, P. D., et al., 2010. Genome expansion and gene loss in powdery mildew fungi reveal tradeoffs in extreme parasitism. *Science*. 330, 1543-1546.
- Staats, M., van Kan, J. A. L., 2012. Genome update of *Botrytis cinerea* strains B05.10 and T4. *Eukaryot Cell*. 11, 1413-1414.
- Stam, P., 1993. Construction of integrated genetic-linkage maps by means of a new computer package - Joinmap. *Plant J*. 3, 739-744.
- Tamura, K., et al., 2007. MEGA4: Molecular Evolutionary Genetics Analysis (MEGA) software version 4.0. *Mol Biol Evol*. 24, 1596-1599.
- ten Have, A., et al., 2001. *Botrytis cinerea* endopolygalacturonase genes are differentially expressed in various plant tissues. *Fungal Genet Biol*. 33, 97-105.
- ten Have, A., et al., 1998. The endopolygalacturonase gene *Bcpg1* is required for full virulence of *Botrytis cinerea*. *Mol Plant Microbe Interact*. 11, 1009-1016.
- ten Have, A., et al., 2002. The contribution of the cell wall degrading enzymes to pathogenesis of fungal plant pathogens. *The Mycota XI, Agricultural applications* (F. Kempken, ed.) Springer-Verlag, Germany. 341-358.
- Thomma, B. P., et al., 1998. Separate jasmonate-dependent and salicylate-dependent defense-response pathways in *Arabidopsis* are essential for resistance to distinct microbial pathogens. *Proc Natl Acad Sci U S A*. 95, 15107-15111.
- Tilburn, J., et al., 1995. The *Aspergillus* PacC zinc finger transcription factor mediates regulation of both acid- and alkaline-expressed genes by ambient pH. *EMBO J*. 14, 779-790.
- Torres, M. A., et al., 2005. Pathogen-induced, NADPH oxidase-derived reactive oxygen intermediates suppress spread of cell death in *Arabidopsis thaliana*. *Nat Genet*. 37, 1130-1134.
- Trapnell, C., et al., 2013. Differential analysis of gene regulation at transcript resolution with RNA-seq. *Nat Biotechnol*. 31, 46-53.
- Trapnell, C., et al., 2009. TopHat: discovering splice junctions with RNA-Seq. *Bioinformatics*. 25, 1105-1111.
- Uitzetter, J. H., et al., 1986. Characterization of *Aspergillus nidulans* mutants in carbon metabolism isolated after D-galacturonate enrichment. *J Gen Microbiol*. 132, 1167-1172.

- Valette-Collet, O., et al., 2003. Disruption of *Botrytis cinerea* pectin methylesterase gene *Bcpme1* reduces virulence on several host plants. *Mol Plant Microbe Interact.* 16, 360-367.
- van Baarlen, P., et al., 2007. Histochemical and genetic analysis of host and non-host interactions of *Arabidopsis* with three *Botrytis* species: an important role for cell death control. *Mol Plant Pathol.* 8, 41-54.
- van Damme, M., et al., 2005. Identification of *Arabidopsis* loci required for susceptibility to the downy mildew pathogen *Hyaloperonospora parasitica*. *Mol Plant Microbe Interact.* 18, 583-592.
- van den Brink, J., de Vries, R. P., 2011. Fungal enzyme sets for plant polysaccharide degradation. *Appl Microbiol Biotechnol.* 91, 1477-1492.
- van Kan, J. A. L., 2006. Licensed to kill: the lifestyle of a necrotrophic plant pathogen. *Trends Plant Sci.* 11, 247-253.
- van Kan, J. A. L., et al., 1997. Cutinase A of *Botrytis cinerea* is expressed, but not essential, during penetration of gerbera and tomato. *Mol Plant Microbe Interact.* 10, 30-38.
- van Ooijen, J. W., et al., 2002. MapQTL® Version 4.0, Software for the calculation of QTL positions on genetic maps. Plant Research International, Wageningen, The Netherlands.
- van Ooijen, J. W., Voorrips, R. E., 2001. Joinmap® 3.0, Software for the calculation of genetic linkage maps. Plant Research International, Wageningen, The Netherlands.
- van Suylekom, D., et al., 2007. Degradation of the hexose transporter Hxt5p in *Saccharomyces cerevisiae*. *Biol Cell.* 99, 13-23.
- Verhoeff, K., et al., 1988. Changes in pH and the production of organic-acids during colonization of tomato petioles by *Botrytis cinerea*. *J Phytopathology.* 122, 327-336.
- Visser, J., et al., 1988. Glycerol uptake mutants of the hyphal fungus *Aspergillus nidulans*. *J Gen Microbiol.* 134, 655-659.
- Voegelé, R. T., et al., 2001. The role of haustoria in sugar supply during infection of broad bean by the rust fungus *Uromyces fabae*. *Proc Natl Acad Sci U S A.* 98, 8133-8138.
- Volpi, C., et al., 2011. The ectopic expression of a pectin methyl esterase inhibitor increases pectin methyl esterification and limits fungal diseases in wheat. *Mol Plant Microbe Interact.* 24, 1012-1019.
- Voragen, A. G. J., et al., 1986. Determination of the degree of methylation and acetylation of pectins by h.p.l.c. *Food Hydrocolloids.* 1, 65-70.
- Vorwerk, S., et al., 2004. The role of plant cell wall polysaccharide composition in disease resistance. *Trends Plant Sci.* 9, 203-209.
- Vos, P., et al., 1995. AFLP: a new technique for DNA fingerprinting. *Nucleic Acids Res.* 23, 4407-4414.
- Wagner, T. A., Kohorn, B. D., 2001. Wall-associated kinases are expressed throughout plant development and are required for cell expansion. *Plant Cell.* 13, 303-318.
- Wang, G., et al., 2008. A genome-wide functional investigation into the roles of receptor-like proteins in *Arabidopsis*. *Plant Physiol.* 147, 503-517.
- Wang, S., et al., 2006. Windows QTL Cartographer 2.5. Department of statistics, North Carolina State University, Raleigh, NC., <http://statgen.ncsu.edu/qtlcart/WQTLCart.htm>.
- Wang, Y., et al., 2011. Comparative secretome investigation of *Magnaporthe oryzae* proteins responsive to nitrogen starvation. *J Proteome Res.* 10, 3136-3148.
- Wang, Z., et al., 2009. RNA-Seq: a revolutionary tool for transcriptomics. *Nat Rev Genet.* 10, 57-63.
- Wei, H., et al., 2004. A putative high affinity hexose transporter, hxtA, of *Aspergillus nidulans* is induced in vegetative hyphae upon starvation and in ascogenous hyphae during cleistothecium formation. *Fungal Genet Biol.* 41, 148-156.
- Wiebe, M. G., et al., 2010. Bioconversion of D-galacturonate to keto-deoxy-L-galactonate (3-deoxy-L-threo-hex-2-ulosonate) using filamentous fungi. *BMC Biotechnol.* 10, 63.

## References

- Wieczorke, R., et al., 1999. Concurrent knock-out of at least 20 transporter genes is required to block uptake of hexoses in *Saccharomyces cerevisiae*. *FEBS Lett.* 464, 123-128.
- Williamson, B., et al., 2007. *Botrytis cinerea*: the cause of grey mould disease. *Mol Plant Pathol.* 8, 561-580.
- Winston, F., et al., 1995. Construction of a set of convenient *Saccharomyces cerevisiae* strains that are isogenic to S288C. *Yeast.* 11, 53-55.
- Wubben, J. P., et al., 1999. Cloning and partial characterization of endopolygalacturonase genes from *Botrytis cinerea*. *Appl Environ Microbiol.* 65, 1596-1602.
- Wubben, J. P., et al., 2000. Regulation of endopolygalacturonase gene expression in *Botrytis cinerea* by galacturonic acid, ambient pH and carbon catabolite repression. *Curr Genet.* 37, 152-157.
- Yajima, W., Kav, N. N., 2006. The proteome of the phytopathogenic fungus *Sclerotinia sclerotiorum*. *Proteomics.* 6, 5995-6007.
- Yang, F., et al., 2011. Secretomics identifies *Fusarium graminearum* proteins involved in the interaction with barley and wheat. *Mol Plant Pathol.* 13, 445-453.
- Zabackis, E., et al., 1995. Characterization of the cell-wall polysaccharides of *Arabidopsis thaliana* leaves. *Plant Physiol.* 107, 1129-1138.
- Zandleven, J., et al., 2007. Xylogalacturonan exists in cell walls from various tissues of *Arabidopsis thaliana*. *Phytochemistry.* 68, 1219-1226.
- Zerbino, D. R., Birney, E., 2008. Velvet: algorithms for de novo short read assembly using de Bruijn graphs. *Genome Res.* 18, 821-829.
- Zhang, L., et al., 2011. The D-galacturonic acid catabolic pathway in *Botrytis cinerea*. *Fungal Genet Biol.* 48, 990-997.
- Zhang, L., van Kan, J. A. L., 2013. *Botrytis cinerea* mutants deficient in d-galacturonic acid catabolism have a perturbed virulence on *Nicotiana benthamiana* and *Arabidopsis*, but not on tomato. *Mol Plant Pathol.* 14, 19-29.
- Zhou, N., et al., 1999. *Arabidopsis* PAD3, a gene required for camalexin biosynthesis, encodes a putative cytochrome P450 monooxygenase. *Plant Cell.* 11, 2419-2428.
- Zipfel, C., et al., 2006. Perception of the bacterial PAMP EF-Tu by the receptor EFR restricts *Agrobacterium*-mediated transformation. *Cell.* 125, 749-760.

## Summary

The necrotrophic fungal plant pathogen *Botrytis cinerea* is able to infect over 200 host plants and cause severe damage to crops, both pre- and post-harvest. *B. cinerea* often penetrates host leaf tissue at the anticlinal cell wall and subsequently grows into and through the middle lamella, which consists mostly of low-methylesterified pectin. Effective pectin degradation thus is important for virulence of *B. cinerea*. **Chapter 1** describes the chemical structures of plant cell wall polysaccharides, the cell wall-associated mechanisms that confer resistance against pathogens, and the microbial enzymes involved in cell wall decomposition. It then discusses the plant cell wall degrading enzymes of pathogenic fungi and illustrates with case studies the process of pectin decomposition by *B. cinerea*.

**Chapter 2** describes the molecular identification and functional characterization of a novel MAMP receptor RBPG1, a Leucine-Rich Repeat Receptor-Like Protein (LRR-RLP), that recognizes fungal endo-polygalacturonases (endo-PGs), in particular the *B. cinerea* protein BcPG3. Infiltration of the BcPG3 protein into *Arabidopsis thaliana* accession Col-0 induced a necrotic response. Heat-inactivated protein and a catalytically inactive mutant protein retained the ability to induce necrosis. An 11-amino acid peptide stretch was identified that is conserved among many fungal but not plant endo-PGs. A synthetic peptide comprising this sequence was unable to induce necrosis. A map-based cloning strategy, combined with comparative and functional genomics, led to the identification of the *RBPG1* gene, which is required for responsiveness of *A. thaliana* to the BcPG3 protein. Co-immunoprecipitation experiments demonstrated that RBPG1 and BcPG3 form a complex in *Nicotiana benthamiana*, which also involves the *A. thaliana* LRR-RLK SOBIR1. The *sobir1* mutant plants no longer respond to BcPG3. Furthermore, overexpression of RBPG1 in the BcPG3-non-responsive accession Br-0 did not enhance resistance to a number of microbial pathogens.

**Chapter 3** describes the functional, biochemical and genetic characterization of the D-galacturonic acid catabolic pathway in *B. cinerea*. The *B. cinerea* genome contains two non-homologous galacturonate reductase genes (*Bcgar1* and *Bcgar2*), a galactonate dehydratase gene (*Bclgd1*), and a 2-keto-3-deoxy-L-galactonate aldolase gene (*Bclga1*). Targeted gene replacement of all four genes in *B. cinerea*, either separately or in combinations, yielded mutants that were affected in growth on D-galacturonic acid, pectate, or pectin as the sole carbon source. The extent of growth reduction of the mutants on pectic substrates was positively correlated to the proportion of D-galacturonic acid present in the pectic substrate. The virulence of these mutants on different host plants is discussed in **Chapter 4**. These mutants showed reduced virulence on *N. benthamiana* and *A. thaliana* leaves, but not on tomato leaves. The cell walls of *N. benthamiana* and *A. thaliana* leaves have a higher D-galacturonic acid content as compared to tomato. Additional *in vitro* growth assays with the knockout mutants suggested that the reduced virulence of D-galacturonic acid catabolism-deficient mutants on *N. benthamiana* and *A. thaliana* is not only due to the inability of the

## Summary

mutants to utilize an abundant carbon source as nutrient, but also due to the growth inhibition by catabolic intermediates.

In **Chapter 5**, the functional characterization of two putative D-galacturonic acid transporters is presented. *Bchxt15* is highly and specifically induced by D-galacturonic acid, whereas *Bchxt13* is highly expressed in the presence of all carbon sources tested except for glucose. Subcellular localization of BcHXT13-GFP and BcHXT15-GFP fusion proteins expressed under their native promoter suggests that the fusion proteins are localized in plasma membranes and intracellular vesicles. Knockout mutants in the *Bchxt13* and *Bchxt15* genes, respectively, were neither affected in their growth on D-galacturonic acid as the sole carbon source, nor in their virulence on tomato and *N. benthamiana* leaves.

**Chapter 6** describes the genome-wide transcriptome analysis in *B. cinerea* grown in media containing glucose and pectate as sole carbon sources. Genes were identified that are significantly altered in their expression during growth on these two carbon sources. Conserved sequence motifs were identified in the promoters of genes involved in pectate decomposition and D-galacturonic acid utilization. The role of these motifs in regulating D-galacturonic acid-induced expression was functionally analysed in the promoter of the *Bclga1* gene, which encodes one of the key enzymes in the D-galacturonic acid catabolic pathway. The regulation by D-galacturonic acid required the presence of sequences encompassing the GAE1 motif and a binding motif for the pH-dependent transcriptional regulator PacC.

**Chapter 7** provides a general discussion of the results presented in this thesis. A model of the concerted action of pectin degradation and subsequent monosaccharide consumption and co-regulation of gene expression is proposed.

## Samenvatting

De necrotrofe plantenpathogene schimmel *Botrytis cinerea* is in staat om meer dan 200 waardplanten te infecteren, en veroorzaakt ernstige schade in land- en tuinbouwgewassen en producten, zowel voor als na de oogst. *B. cinerea* dringt plantenweefsels meestal binnen via de anticlinale celwand van epidermiscellen en groeit vervolgens in en dóór de middenlamel, die vooral bestaat uit pectine met een lage methyl-veresteringsgraad. Effectieve pectine afbraak is daarom belangrijk voor de virulentie van *B. cinerea*. **Hoofdstuk 1** beschrijft de chemische structuren van plantencelwand polysaccharides, de celwand- geassocieerde mechanismen die een plant resistent maken tegen pathogenen, en de groepen van microbiële enzymen die zijn betrokken bij celwandafbraak. Vervolgens worden de plantencelwand-afbrekende enzymen van plantenpathogene schimmels in detail besproken en worden voorbeelden gegeven van enzymen die *B. cinerea* gebruikt bij pectine afbraak.

**Hoofdstuk 2** beschrijft de moleculaire identificatie en functionele analyse van een nieuwe MAMP receptor RBPG1, een leucine-rijk receptor-eiwit (LRR-RLP), dat endo-polygalacturonases (endo-PGs) van schimmels herkent, en met name het *B. cinerea* eiwit BcPG3. Injectie van het BcPG3 eiwit in *Arabidopsis thaliana* genotype Col-0 induceert een necrotische reactie. Ook hitte-geïnactiveerd BcPG3 eiwit en een katalytisch inactief mutant BcPG3 eiwit induceren necrose. Een peptide fragment van 11 aminozuren is aanwezig in een groot aantal schimmel endo-PGs, maar niet in endo-PGs van planten. Een synthetisch peptide dat deze schimmel-specifieke sequentie bevat, induceert geen necrose. Met een kloneringsstrategie gebaseerd op genetische kartering, vergelijkende genomanalyse en een functionele analyse werd uiteindelijk het *RBPG1* gen geïdentificeerd. Aanwezigheid van het RBPG1 receptor eiwit is vereist in *A. thaliana* om het BcPG3 eiwit te herkennen. Door middel van co-immunoprecipitatie experimenten werd aangetoond dat RBPG1 en BcPG3 een eiwitcomplex vormen in *Nicotiana benthamiana*, en in het complex is ook het *A. thaliana* LRR-RLK eiwit SOBIR1 aanwezig. *A. thaliana* planten met een mutatie in *SOBIR1* vertoonden geen necrotische reactie meer na injectie van BcPG3. Overexpressie van RBPG1 in het BcPG3-ongevoelige *A. thaliana* genotype Br-0 leidde niet tot verhoogde ziekteresistentie tegen microbiële pathogenen.

**Hoofdstuk 3** beschrijft de functionele, biochemische en genetische karakterisering van de catabole afbraakroute voor D-galacturonzuur in *B. cinerea*. In het *B. cinerea* genoom zijn twee niet-homologe galacturonaat reductase genen (*Bcgar1* en *Bcgar2*), een galactonaat dehydratase gen (*Bclgd1*), en een 2-keto-3-deoxy-L-galactonaat aldolase gen (*Bclga1*) aanwezig. Gerichte uitschakeling van alle vier de genen in *B. cinerea*, ieder apart of in combinaties, leverde mutanten op die waren verstoord in hun groei op D-galacturonzuur, pectaat of pectine als enige koolstofbron. De mate van groeireductie van de mutanten op pectine-achtige substraten vertoonde een positieve correlatie met het gehalte aan D-galacturonzuur in het substraat. De virulentie van deze mutanten op verschillende waardplanten wordt beschreven

## Samenvatting

in **Hoofdstuk 4**. De mutanten waren minder virulent op bladeren van *N. benthamiana* en *A. thaliana*, maar niet op die van tomaat. De celwanden van bladeren van *N. benthamiana* en *A. thaliana* bevatten een hoger gehalte aan D-galacturonzuur dan bladeren van tomaat. Aanvullende *in vitro* groeiproeven toonden aan dat de verminderde virulentie van deze *B. cinerea* mutanten in de D-galacturonzuur catabole route op *N. benthamiana* en *A. thaliana* niet uitsluitend werd veroorzaakt door het feit dat ze zich niet kunnen voeden met deze in overvloed aanwezige koolstofbron, maar dat er ook groeiremming optreedt door intermediaire metabolieten van de D-galacturonzuur afbraakroute.

In **Hoofdstuk 5** wordt de functionele analyse beschreven van twee mogelijke membraantransporters die betrokken zijn bij opname van D-galacturonzuur. *Bchxt15* wordt sterk en specifiek geïnduceerd door D-galacturonzuur, terwijl *Bchxt13* hoog tot expressie komt in aanwezigheid van alle koolstofbronnen die werden getest, behalve glucose. Om de subcellulaire lokalisatie te bepalen van BcHXT13-GFP en BcHXT15-GFP fusie eiwitten, werden hun genen onder eigen promotor tot expressie gebracht, en werd aangetoond dat de fusie eiwitten aanwezig zijn in plasma membranen en in intracellulaire blaasjes. Mutanten in de genen *Bchxt13* en *Bchxt15* waren niet te onderscheiden van wild type wat betreft hun groei op D-galacturonzuur als enige koolstofbron, en virulentie op tomaat en op *N. benthamiana* bladeren.

**Hoofdstuk 6** beschrijft een genoom-brede transcriptoom analyse in *B. cinerea* die is opgekweekt in medium met glucose of pectaat als enige koolstofbron. Er werden genen geïdentificeerd die significant hoger tot expressie kwamen tijdens groei in pectaat dan in medium zonder pectaat. Geconserveerde DNA sequentie motieven zijn aanwezig in de promotor gebieden van genen die zijn betrokken bij pectaat afbraak en de groei op D-galacturonzuur. De rol van deze sequentie motieven in de regulatie van genexpressie door D-galacturonzuur werd bestudeerd door fragmenten van de promotor van het *Bclga1* gen, dat codeert voor een van de enzymen in de catabole route voor D-galacturonzuur, te fuseren aan GFP. De regulatie door D-galacturonzuur vereiste de aanwezigheid van een zogenaamd 'GAE1 motief' en het bindingsmotief voor de pH-afhankelijke transcriptionele regulator PacC.

**Hoofdstuk 7** bevat een algemene discussie van de resultaten in dit proefschrift. Een model wordt gepresenteerd dat beschrijft hoe een gezamenlijke actie van meerdere genen en enzymen leidt tot een effectieve pectine afbraak, gevolgd door opname en consumptie van de vrijgekomen monosaccharides en hoe dit proces gereguleerd wordt op gen- en enzym-niveau.

## Acknowledgements

I came to the Netherlands on February 2nd, 2009 to start my PhD research. After 4 years and 5 months, I am very pleased with the completion of my PhD thesis. During these years, I got help and support from many people both for my research and for my living. Here I would like to take this opportunity to express my appreciation to all these people.

First of all, I would like to express my sincere gratitude to my co-promoter and supervisor Dr. Jan van Kan for your trust and for offering me the PhD position. You provided me excellent guidance and so many constructive suggestions during my work and writing. With your kind supervision, I could always raise my own scientific questions and follow them up confidently. After meaningful discussions with you I got past many tough situations during the work. I am also very happy to have had opportunities by your recommendation to assist courses, supervise students in the lab and collaborate with excellent research groups for my project. I benefited a lot from all these activities.

I am grateful to my promoter Prof. Pierre de Wit. Thanks for the annual discussion on my research progress and for offering constructive comments on the thesis writing.

I am grateful to my external supervisor Dr. Guido van den Ackerveken. Thanks for offering generous help to my work including experimental materials and discussion on the research progress.

I thank Prof. Francine Govers for recommending me for this project. Without your trust, I could not have had the opportunity to be a PhD candidate, and to enjoy the nice time in the Netherlands with Chenlei.

I thank Prof. Zhengguang Zhang (张正光), for supervising my MSc thesis and for giving me technical training, with which I could quickly get used to a new fungal research system in the Netherlands. I thank Prof. Yuanchao Wang (王源超) and Dr. Yuling Bai (白玉玲) for giving me positive comments in an interview in Nanjing during my application for the PhD position.

I am very happy to have worked with all the colleagues in the laboratory of Phytopathology, in which I experienced a welcoming and inspiring atmosphere. I thank all of you, especially Joost Stassen, Ronnie de Jonge and Luigi Faino for the help with bioinformatic analysis; Harrold van de Burg, Thomas Liebrand, Dirk Jan Valkenburg, Guodong Wang (王国栋) and Zhao Zhang (张钊) for the help with experiments and materials; Ali Ormel for the great help with all kinds of paperwork; the students, Panagiota Tagkalaki, Devlin Tjoitang, Harry Thiewes, Shamsun Nahar, Pol Rey Serra, Maxim

## Acknowledgements

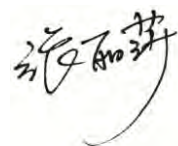
Cornelissen and Sayantani Chatterjee, for their contribution to my PhD project and for sharing with me cultures and stories from different countries and places.

I also received a lot of technical support from people outside the laboratory of Phytopathology and I gratefully acknowledge Yvonne Westphal and Henk Schols for providing facilities, advice and assistance to determine the plant cell wall composition, Joyce Elberse for assistance with the plant disease assays and Julia Schumacher for providing experimental materials.

It was a great honour to be offered a scholarship for Outstanding Self-financed Students Abroad from the China Scholarship Council. I felt very fortunate to receive this award in the Chinese embassy in the Netherlands and got encouragement from Ambassador Jun Zhang (张军), Counsellor Qingchao Fang (方庆朝) and Secretary Lei Xia (夏磊).

It was really a great pleasure to make many friends in Wageningen. With all of you, Chenlei and I had a very colourful and enjoyable time. I want to first thank Shutong Wang (王树桐), Ningwen Zhang (张凝文), Ke Lin (林柯), Na Li (李娜) and Wei Liu (刘巍) for kindly sub-renting us nice apartments, with which we could build up a very warm and comfortable home. I thank Chunxu Song (宋春旭), Wei Qin (覃伟), Xu Cheng (程旭), Yanru Song (宋彦儒), Feng Zhu (朱峰) and Minghui Fei (费明慧) for sharing all kinds of living experience in the Netherlands, fascinating and unforgettable journeys in Europe, and for helping organizing everything around the thesis ceremony. I thank Lisong Ma (马利松), Fang Xu (徐方), Ke Peng (彭珂), Fengfeng Wang (王枫枫), Chunhui Zhou (周春晖), Yuanchuan Zhang (张源川) and Xin Li (李歆) for sharing with us their personal stories, which benefited our living, studying and working. I thank Yan Wang (王燕), Yu Du (杜羽), Miao Han (韩淼), Guozhi Bi (毕国志) and Yin Song (宋银) for many warm and delicious dinners. I thank Ting Hieng Ming (陈贤明), Ya-Fen Lin (林雅芬), Qing Liu (刘庆), Ting Yang (杨婷), Wei Song (宋伟), Ying Zhang (张莹), Chunting Lang (郎春婷), Weicong Qi (戚维聪), Xi Chen (陈曦), Lemeng Dong (董乐萌), Juan Du (杜鹃), Chunzhao Zhao (赵春钊), Junyou Wang (王俊友), Lijin Tian (田利金), Hui Li (李慧) and many other people for introducing me to all kinds of scientific knowledge.

Finally, I express my deepest gratitude to my family for their full support and understanding, especially to my dear husband, Chenlei Hua (华辰雷), for your endless love, support and patience.



## Curriculum vitae



Lisha Zhang was born on December 23rd, 1982 in Baoding, China. She has attended a bachelor study in biological sciences at Hebei University (Baoding, China) in 2001. After graduation in 2005, she was enrolled in a master programme in Nanjing Agricultural University (Nanjing, China) under the supervision of Prof. Zhengguang Zhang. In 2008, she obtained her MSc degree with a thesis entitled 'Cloning and functional analysis of hexose kinase and inhibitor of apoptosis protein in *Magnaporthe grisea*'. From 2009 to 2013, she conducted her PhD research in the laboratory of Phytopathology at Wageningen University (Wageningen, The Netherlands). She worked on pectin degradation by *Botrytis cinerea* described in this thesis under the supervision of Dr. J.A.L. van Kan.

## Publications

**Zhang, L.**, Hua, C., Stassen, J., Chatterjee, S., Cornelissen, M., van Kan, J.A.L. D-galacturonic acid utilization by *Botrytis cinerea*. In preparation.

**Zhang, L.**, Kars, I., Wagemakers, L., Liebrand, T.W.H., Tagkalaki, P., Tioitang, D., Essenstam, B., Elberse, J., van den Ackerveken, G., and van Kan, J.A.L. Fungal endo-polygalacturonases are recognized as MAMPs in Arabidopsis by the Receptor-Like Protein RBPG1. In preparation.

Nafisi, M.\* , Stranne, M.\* , **Zhang, L.\***, Bromley, J., van Kan, J.A.L., and Sakuragi, Y. Roles of arabinan and its degradation enzyme in plant-microbe interaction: arabinan is required for the full defence capacity in *Arabidopsis thaliana* and the endo-arabinanase BcARA1 is a novel virulence factor of *Botrytis cinerea*. In preparation.

**Zhang, L.**, and van Kan, J.A.L. The contribution of cell wall degrading enzymes to virulence of fungal plant pathogen. In: Kempken, F. (Ed.), The Mycota XI (2nd Edition), Agricultural Applications. Springer-Verlag, Berlin, in press.

**Zhang, L.** and van Kan, J.A.L. (2013) *Botrytis cinerea* mutants deficient in D-galacturonic acid catabolism have a perturbed virulence on *Nicotiana benthamiana* and Arabidopsis, but not on tomato. Mol. Plant Pathol. 14, 19-29.

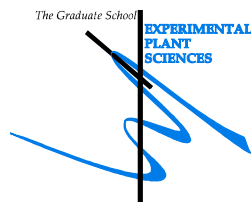
**Zhang, L.**, Thiewes, H. and van Kan, J.A.L. (2011) The D-galacturonic acid catabolic pathway in *Botrytis cinerea*. Fungal Genet. Biol. 48, 990-997.

**Zhang, L.**, Lv, R., Dou, X., Qi, Z., Hua, C., Zhang, H., Wang, Z., Zheng, X. and Zhang, Z. (2011) The function of MoGlc1 in integration of glucose and ammonium utilization in *Magnaporthe oryzae*. PLoS One. 6, e22809.

Gan, Y., **Zhang, L.**, Zhang, Z., Dong, S., Li, J., Wang, Y. and Zheng, X. (2008) The LCB<sub>2</sub> subunit of the sphingolipid biosynthesis enzyme serine palmitoyltransferase can function as an attenuator of the hypersensitive response and Bax-induced cell death. New Phytol. 181, 127-146.

\*Those authors contributed equally.

**Education Statement of the Graduate School**  
**Experimental Plant Sciences**



**Issued to:** Lisha Zhang  
**Date:** 5 June 2013  
**Group:** Phytopathology, Wageningen University and Research Centre

<b>1) Start-up phase</b>	<u>date</u>
▶ <b>First presentation of your project</b> Cloning and functional analysis of the Arabidopsis rbgp1 locus conferring resistance to <i>Botrytis cinerea</i> endopolygalacturonases	Oct 23, 2009
▶ <b>Writing a review or book chapter</b> Pectin as a barrier and nutrient source for fungal plant pathogens. Kempken, Frank (Ed), The Mycota XI (2nd Edition), 2013 (July)	Feb 2012
▶ <b>MSc courses</b> Genomics (ABG30306)	Jan-Feb 2010
▶ <b>Laboratory use of isotopes</b>	

*Subtotal Start-up Phase* **12,5 credits\***

<b>2) Scientific Exposure</b>	<u>date</u>
▶ <b>EPS PhD student days</b> EPS PhD student day 2012 4th European Plant Science Retreat, John Innes Centre, Norwich, UK	Nov 30, 2012 Aug 15-17, 2012
▶ <b>EPS theme symposia</b> EPS Theme 2 'Interactions between Plants and Biotic Agents', Utrecht University EPS Theme 2 symposium and Willie Commelin Scholten Day, University of Amsterdam EPS Theme 2 symposium and Willie Commelin Scholten Day, Wageningen University EPS Theme 2 symposium and Willie Commelin Scholten Day, Utrecht University	Jan 15, 2010 Feb 03, 2011 Feb 10, 2012 Jan 24, 2013
▶ <b>NWO Lunteren days and other National Platforms</b> NWO-ALW meeting 'Experimental Plant Sciences', Lunteren, The Netherlands ALW Platform Molecular Genetics Annual Meeting, Lunteren, The Netherlands NWO-ALW meeting 'Experimental Plant Sciences', Lunteren, The Netherlands ALW Platform Molecular Genetics Annual Meeting, Lunteren, The Netherlands NWO-ALW meeting 'Experimental Plant Sciences', Lunteren, The Netherlands	Apr 06-07, 2009 Oct 15-16, 2009 Apr 19-20, 2010 Oct 14-15, 2010 Apr 04-05, 2011 Apr 02-03, 2012 Apr 22-23, 2013
▶ <b>Seminars (series), workshops and symposia</b> Seminar Dr. Rays H.Y. Jiang Plant Sciences Seminar Prof. Olaf van Kooten and Prof. Jack Leunissen Plant Sciences Seminar Prof. Pierre de Wit and Prof. Fred van Eeuwijk Seminar Prof. Richard Oliver Seminar Prof. Nick Panopoulos Seminar Dr. Laurent Zimmerli Plant Sciences Seminar Prof. Holger Meinke and Prof. Paul Struik Plant Sciences Seminar Prof. Louise Vet and Prof. Just Vlak Seminar Prof. Naoto Sibuya Seminar Prof. David Baulcombe Seminar Dr. Kirsten Bomblies Seminar Dr. Rosie Bradshaw Symposium "Ecology and Experimental Plant sciences 2" Mini-symposium 'Intraspecific Pathogen Variation - Implications and Opportunities' EPS Flying Seminar Dr. Detlef Weigel	Jun 10, 2009 Oct 13, 2009 Nov 10, 2009 Nov 20, 2009 Jan 11, 2010 Jan 25, 2010 Apr 13, 2010 May 11, 2010 Sep 09, 2010 Sep 27, 2010 Nov 18, 2010 Aug 04, 2011 Sep 22, 2009 Jan 22, 2013 Feb 27, 2013
▶ <b>International symposia and congresses</b> The 10th European Conference on Fungal Genetics, Noordwijkerhout, The Netherlands XV International Botrytis symposium, Cadiz, Spain Botrytis-Sclerotinia Post-Genome Workshop, Lyon, France	Mar 29-Apr 01, 2010 May 30-Jun 04, 2010 Sep 15-17, 2011
▶ <b>Presentations</b> The 10th European Conference on Fungal Genetics (poster) NWO-ALW meeting 'Experimental Plant Sciences' (poster) XV International Botrytis symposium (oral + poster) ALW Platform Molecular Genetics Annual Meeting (oral) Botrytis-Sclerotinia Post-Genome Workshop, Lyon, France (oral) Networking event of TTI Green Genetics (poster) EPS Theme 2 symposium and Willie Commelin Scholten Day (oral) Botrytis Workshop, Münster, Germany (oral) NWO-ALW meeting 'Experimental Plant Sciences' (oral)	Mar 29-Apr 01, 2010 Apr 19-20, 2010 May 30-Jun 04, 2010 Oct 15, 2010 Sep 15-17, 2011 Sep 22, 2011 Feb 10, 2012 Oct 15, 2012 Apr 22-23, 2013
▶ <b>IAB interview</b>	Feb 18, 2011
▶ <b>Excursions</b>	

*Subtotal Scientific Exposure* **21,5 credits\***

**CONTINUED ON NEXT PAGE**

<b>3) In-Depth Studies</b> ▶ <b>EPS courses or other PhD courses</b> Environmental signaling, Utrecht VLAG course Glycosciences Autumn School "Host-Microbe Interactomics" ▶ <b>Journal club</b> ▶ <b>Individual research training</b> Food chemistry (cell wall analysis), Wageningen University, Netherlands	<u>date</u>  Aug 24-26, 2009 May 17-20, 2010 Nov 01-03, 2011  Apr 04-08, 2011
---	---

*Subtotal In-Depth Studies*

*4,5 credits\**

<b>4) Personal development</b> ▶ <b>Skill training courses</b> English TOEFL training Techniques for Writing and Presenting a Scientific Paper Networking event of TTI Green Genetics Networking event of TTI Green Genetics CBSG Matchmaking event ▶ <b>Organisation of PhD students day, course or conference</b> ▶ <b>Membership of Board, Committee or PhD council</b>	<u>date</u>  2009 Dec 13-16, 2011 Sep 22, 2011 Sep 19, 2012 Oct 18, 2012
--	--

*Subtotal Personal Development*

*3,1 credits\**

<b>TOTAL NUMBER OF CREDIT POINTS*</b>	<b>41.6</b>
---------------------------------------	-------------

Herewith the Graduate School declares that the PhD candidate has complied with the educational requirements set by the Educational Committee of EPS which comprises of a minimum total of 30 ECTS credits

*\* A credit represents a normative study load of 28 hours of study.*



This research was conducted in the Laboratory of Phytopathology of Wageningen University and was financially supported by the graduate school Experimental Plant Sciences (EPS) and the Technological Top Institute Green Genetics (TTI-GG).

Cover & Layout by: Lisha Zhang

Printed by: Proefschriftmaken.nl || Uitgeverij BOXPress